United States
Environmental Protection
Agency

Acid Rain Division
(6204J)
Washington, D.C. 20460

EPA/430/R-97-013
February 1997

EPA

Flow Reference Method Testing and Analysis: Wind Tunnel Experimental Results

Volume 1

Flow Reference Method Testing and Analysis

Wind Tunnel Experimental Results

Prepared for

U.S. Environmental Protection Agency
Acid Rain Division, 6204J
401 M Street, SW
Washington, DC 20460

Contract No. 68-D2-0168
Work Assignment 5C-01

Prepared by

The Cadmus Group, Inc.
1920 Highway 54, Suite 100
Durham, NC 27713

February, 1997

ACKNOWLEDGMENTS

The principal authors of this report were Dr. Arthur Werner, Ms. Penelope Kellar, and Mr. Scott Shanklin of The Cadmus Group, Inc. Dr. Elliott Lieberman and Mr. John Schakenbach of the U.S. Environmental Protection Agency provided continuing guidance throughout this project and the preparation of this report. Dr. William Warren-Hicks and Ms. Jie Tao of The Cadmus Group, Inc., provided the statistical design and data analysis assistance. Mr. Gene Fax of Cadmus provided constructive review on this report. Experiments were conducted in North Carolina State University's (NCSU) Merrill Subsonic Wind Tunnel under the critical supervision of Dr. John Perkins, in the NCSU Department of Mechanical and Aerospace Engineering. Dr. Perkins was assisted by Mr. Kraig Marquis and Mr. Eric Thirolle (Cadmus), Mr. Ed. Baker (NCSU), and Mr. Keith Hazel (Climax Engineering). Mrs. Blanche Dean of Cadmus provided production assistance.

TABLE OF CONTENTS

Page

VOLUME 1

1.0 INTRODUCTION 1–1
- 1.1 PURPOSE OF PROGRAM 1–1
- 1.2 GOALS OF THE WIND TUNNEL TESTS 1–1
- 1.3 DESCRIPTION OF WIND TUNNEL 1–2
- 1.4 DESCRIPTION OF TEST PROBES 1–4
- 1.5 DOCUMENT PURPOSE AND ORGANIZATION 1–9

2.0 OVERVIEW OF DATA COLLECTION, HANDLING, AND QUALITY ASSURANCE 2–1
- 2.1 OVERVIEW OF FLOW MEASUREMENT PROCEDURES 2–1
- 2.2 YAW ALIGNING AND VELOCITY MEASUREMENT PROCEDURES 2–3
- 2.3 DATA ACQUISITION, HANDLING, AND QUALITY ASSURANCE 2–7
- 2.4 STUDY TO DETERMINE APPROPRIATE SAMPLE SIZE 2–8
- 2.5 CALIBRATION OF PROBES 2–9

3.0 MODIFIED KIEL PROBE EXPERIMENTS 3–1
- 3.1 COMPARISON OF WAKE PORTS AND FECHHEIMER PORTS IN DETERMINING YAW NULL 3–1
- 3.2 SENSITIVITY AND ACCURACY OF STATIC PRESSURE DETERMINATIONS USING THE WAKE PORTS 3–2
- 3.3 CONCLUSIONS 3–5

4.0 STANDARD CALIBRATION COEFFICIENTS AND VARIABILITY WITH VELOCITY FOR 2D PROBES 4–1
- 4.1 TEST PROCEDURES 4–1
- 4.2 CALIBRATION COEFFICIENTS 4–1
- 4.3 VARIATION WITH VELOCITY 4–1
- 4.4 CONCLUSIONS 4–3

5.0 PITCH ANGLE EFFECTS ON VELOCITY MEASUREMENTS PERFORMED WITH 2D PROBES 5–1
- 5.1 TEST PROCEDURES 5–1
- 5.2 SENSITIVITY OF CALIBRATION COEFFICIENTS TO PITCH ANGLE 5–1
- 5.3 PITCH ANGLE EFFECTS ON VELOCITY DETERMINATIONS 5–2
- 5.4 CONCLUSIONS 5–7

6.0 ACCURACY OF YAW ANGLE MEASUREMENTS AND EFFECT ON VELOCITY MEASUREMENT 6–1
- 6.1 TEST PROCEDURES 6–1
- 6.2 ACCURACY OF YAW ANGLE DETERMINATIONS AND VELOCITY DETERMINATIONS 6–1

TABLE OF CONTENTS
(continued)

Page

6.3 FLOW MEASUREMENT ERROR DUE TO YAW NULL MISALIGNMENT FOR THE AUTOPROBE TYPE S 6–3
6.4 CONCLUSIONS 6–6

7.0 CALIBRATION CURVES AND ACCURACY OF VELOCITY DETERMINATIONS FOR 3D PROBES 7–1
7.1 TEST PROCEDURES 7–1
7.2 CALIBRATION CURVES 7–2
7.3 ACCURACY OF VELOCITY DETERMINATIONS 7–3
7.4 ACCURACY OF PITCH ANGLE DETERMINATIONS 7–9
7.5 CONCLUSIONS 7–9

8.0 ENTRY WALL EFFECTS ON YAW NULLING 8–1
8.1 TEST PROCEDURES 8–1
8.2 RESULTS OF ENTRY WALL EFFECTS TESTS 8–1
8.3 CONCLUSIONS 8–4

9.0 CONCLUSIONS AND RECOMMENDED FOLLOW-UP 9–1

VOLUME 2
Appendix A—Study to Determine Sample Size A-1
Appendix B—Study of Entry Wall Effects on Yaw Nulling B-1
Appendix C—Raw Data C-1
Appendix D—Data Disks D-1

LIST OF FIGURES

		Page
Figure 1-1	Schematic (top view) of the Merrill Subsonic Wind Tunnel Facility located at North Carolina State University in Raleigh	1-3
Figure 1-2	Schematic of modified Kiel probe (MK1)	1-5
Figure 1-3	Autoprobe positioned for insertion into the wind tunnel	1-6
Figure 1-4	Front and side views of spherical probe	1-7
Figure 1-5	Top, side, and cross-sectional views of DAT probe	1-7
Figure 2-1	Magnehelic meters used to measure differential pressures (P_1-P_2, P_2-P_3, P_4-P_5) across various ports of test probes	2-4
Figure 2-2	Schematic (overhead perspective) showing positive and negative pitch angle and yaw angle orientation of flow probe with respect to test port for wind tunnel and flow directions	2-5
Figure 3-1	ΔP_w and ΔP_f vs. Yaw Angle: Modified Kiel - Wake Port 1 - Velocity = 30 fps	3-6
Figure 3-2	ΔP_w and ΔP_f vs. Yaw Angle: Modified Kiel - Wake Port 1 - Velocity = 60 fps	3-7
Figure 3-3	ΔP_w and ΔP_f vs. Yaw Angle: Modified Kiel - Wake Port 1 - Velocity = 90 fps	3-8
Figure 3-4	ΔP_w and ΔP_f vs. Yaw Angle: Modified Kiel - Wake Port 4 - Velocity = 30 fps	3-9
Figure 3-5	ΔP_w and ΔP_f vs. Yaw Angle: Modified Kiel - Wake Port 4 - Velocity = 60 fps	3-10
Figure 3-6	ΔP_w and ΔP_f vs. Yaw Angle: Modified Kiel - Wake Port 4 - Velocity = 90 fps	3-11
Figure 3-7	Probe: Modified Kiel MK1 - Wake Port Calibration Coefficients - Wake Port 1	3-12
Figure 3-8	Probe: Modified Kiel MK1 - Wake Port Calibration Coefficients - Wake Port 2	3-13

LIST OF FIGURES
(continued)

		Page
Figure 3-9	Probe: Modified Kiel MK1 - Wake Port Calibration Coefficients - Wake Port 3	3-14
Figure 3-10	Probe: Modified Kiel MK1 - Wake Port Calibration Coefficients - Wake Port 4	3-15
Figure 3-11	Probe: Modified Kiel With Thermocouple - MK2 - Wake Port Calibration Coefficients - Wake Port 4	3-16
Figure 3-12	Probe: 3/8" Type S-1- Calibration Coefficients	3-17
Figure 3-13	Probe: 3/8" Type S-2 - Calibration Coefficients	3-18
Figure 3-14	Probe: 3/8: Type S-3 - Calibration Coefficients	3-19
Figure 3-15	Probe: Modified Kiel - MK1 - Wake Port Calibration Coefficients - Wake Port 1	3-20
Figure 3-16	Probe: Modified Kiel - MK1 - Wake Port Calibration Coefficients - Wake Port 2	3-21
Figure 3-17	Probe: Modified Kiel - MK1 - Wake Port Calibration Coefficients - Wake Port 3	3-22
Figure 3-18	Probe: Modified Kiel - MK1 - Wake Port Calibration Coefficients - Wake Port 4	3-23
Figure 3-19	Probe Modified Kiel with Thermocouple - MK2 - Wake Port Calibration Coefficients - Wake Port 4	3-24
Figure 3-20	Probe: 3/8" Type S-1- Calibration Coefficients	3-25
Figure 3-21	Probe: 3/8" Type S-2 - Calibration Coefficients	3-26
Figure 3-22	Probe: 3/8" Type S-3 - Calibration Coefficients	3-27
Figure 3-23	Probe: Modified Kiel -MK1 - Calibration Coefficients Wake Port 1	3-28
Figure 3-24	Probe: Modified Kiel -MK1 - Calibration Coefficients Wake Port 3	3-29

LIST OF FIGURES
(continued)

		Page
Figure 3-25	Probe: Modified Kiel -MK1 - Calibration Coefficients Wake Port 4	3-30
Figure 3-26	Probe Modified Kiel with Thermocouple - MK2 - Calibration Coefficients - Wake Port 4	3-31
Figure 3-27	Probe: 3/8" Type S-1 - Calibration Coefficients	3-32
Figure 4-1	Probe: 3/8" Type S-1 - Calibration Coefficients	4-5
Figure 4-2	Probe: 3/8" Type S-2 - Calibration Coefficients	4-6
Figure 4-3	Probe: 3/8" Type S-3 - Calibration Coefficients	4-7
Figure 4-4	Probe: Modified Kiel With Thermocouple - MK2 - Wake Port Calibration Coefficients (Wake Port = 4)	4-8
Figure 4-5	Probe: Modified S - USS-1 - Calibration Coefficients	4-9
Figure 4-6	Probe: Modified S - USS-2 - Calibration Coefficients	4-10
Figure 4-7	Probe: Modified S - USS-3 - Calibration Coefficients	4-11
Figure 4-8	Probe: Autoprobe - Type S - Calibration Coefficients	4-12
Figure 4-9	Probe: Autoprobe - Modified S - Calibration Coefficients	4-13
Figure 4-10	Probe: French Probe - F2 - Calibration Coefficients	4-14
Figure 5-1	Probe: 3/8" Type S - S-1 - Calibration Coefficient vs. Pitch Angle	5-9
Figure 5-2	Probe: Modified S - USS-1 - Calibration Coefficient vs. Pitch Angle	5-10
Figure 5-3	Probe: Modified S - USS-3 - Calibration Coefficient vs. Pitch Angle	5-11
Figure 5-4	Probe: Autoprobe - Type S - Calibration Coefficient vs. Pitch Angle	5-12
Figure 5-5	Probe: Autoprobe - Modified S - Calibration Coefficient vs. Pitch Angle	5-13
Figure 5-6	Probe: French Probe - F-2 - Calibration Coefficient vs. Pitch Angle	5-14

LIST OF FIGURES
(continued)

		Page
Figure 5-7	Percent Deviation of Measured Velocity from Axial Velocity vs. Pitch Angle at 30 fps	5-15
Figure 5-8	Percent Deviation of Measured Velocity from Axial Velocity vs. Pitch Angle at 60 fps	5-16
Figure 5-9	Percent Deviation of Measured Velocity from Axial Velocity vs. Pitch Angle at 90 fps	5-17
Figure 6-1	Probe: Modified Kiel Probe with Thermocouple - MK2 Theta Null Deviation from the True Yaw Null	6-7
Figure 6-2	Probe: 3/8" Type S - S1 Theta Null Deviation from the True Yaw Null	6-8
Figure 6-3	Probe: Modified S - USS-1 Theta Null Deviation from the True Yaw Null	6-9
Figure 6-4	Probe: Modified S -USS-3 Theta Null Deviation from the True Yaw Null	6-10
Figure 6-5	Probe: Autoprobe Type S Theta Null Deviation from the True Yaw Null	6-11
Figure 6-6	Probe: Autoprobe Mod S Theta Null Deviation from the True Yaw Null	6-12
Figure 6-7	Probe: Spherical MS5 - 2 Theta Null Deviation from the True Yaw Null	6-13
Figure 6-8	Probe: DAT - 3D-1 Theta Null Deviation from the True Yaw Null	6-14
Figure 6-9	Probe: DAT - 3D-2 Theta Null Deviation from the True Yaw Null	6-15
Figure 6-10	Probe: DAT - 3D-3 Theta Null Deviation from the True Yaw Null	6-16
Figure 6-11	C_p vs. Yaw Angle	6-17

LIST OF FIGURES
(continued)

		Page
Figure 6-12	Flow Measurement Error from Yaw Error	6-18
Figure 7-1	Probe: DAT 3D-1 - F1 vs. pitch angle	7-13
Figure 7-2	Probe: DAT 3D-1 - F2 vs. pitch angle	7-14
Figure 7-3	Probe: DAT 3D-2 - F1 vs. pitch angle	7-15
Figure 7-4	Probe: DAT 3D-2 - F2 vs. pitch angle	7-16
Figure 7-5	Probe: DAT 3D-3 - F1 vs. pitch angle	7-17
Figure 7-6	Probe: DAT 3D-3 - F2 vs. pitch angle	7-18
Figure 7-7	Probe: Spherical MS5-2 - F1 vs. pitch angle	7-19
Figure 7-8	Probe: Spherical MS5-2 - F2 vs. pitch angle	7-20
Figure 7-9	Probe: DAT 3D-1 - F1 vs. pitch angle	7-21
Figure 7-10	Probe: DAT 3D-1 - F2 vs. pitch angle	7-22
Figure 7-11	Probe: DAT 3D-2 - F1 vs. pitch angle	7-23
Figure 7-12	Probe: DAT 3D-2 - F2 vs. pitch angle	7-24
Figure 7-13	Probe: DAT 3D-3 -F1 vs. pitch angle	7-25
Figure 7-14	Probe: DAT 3D-3 - F2 vs. pitch angle	7-26
Figure 7-15	Probe: Spherical MS5-2 - F1 vs. pitch angle	7-27
Figure 7-16	Probe: Spherical MS5-2 - F2 vs. pitch angle	7-28
Figure 8-1	Flow pattern at yaw angle of -45°	8-3
Figure 8-2	Flow pattern at yaw angle of +20°	8-3
Figure 8-3	Manual S-type: yaw/wall effect - 60 fps, 0 pitch, 1-42" from wall	8-7
Figure 8-4	Manual S-type: yaw/wall effect - 60 fps, 0 pitch, 1" from wall	8-8

LIST OF FIGURES
(continued)

		Page
Figure 8-5	Manual S-type: yaw/wall effect - 60 fps, 0 pitch, 3" from wall	8-9
Figure 8-6	Manual S-type: yaw/wall effect - 60 fps, 0 pitch, 6" from wall	8-10
Figure 8-7	Manual S-type: yaw/wall effect - 60 fps, 0 pitch, 9" from wall	8-11
Figure 8-8	Manual S-type: yaw/wall effect - 60 fps, 0 pitch, 12" from wall	8-12
Figure 8-9	Manual S-type: yaw/wall effect - 60 fps, 0 pitch, 42" from wall	8-13
Figure 8-10	Autoprobe S-type: yaw/wall effect - 60 fps, 0 pitch, -10° to + 10°	8-14
Figure 8-11	Autoprobe S-type: yaw/wall effect - 60 fps, 0 pitch, 165° to 185°	8-15
Figure 8-12	Autoprobe S-type: yaw/wall effect - 60 fps, 0 pitch, -50° to +200°	8-16
Figure 8-13	Autoprobe S-type: yaw/wall effect - 60 fps, +10 pitch, -10° to + 10°	8-17
Figure 8-14	Autoprobe S-type: yaw/wall effect - 60 fps, +10 pitch, 165° to 185°	8-18
Figure 8-15	Autoprobe S-type: yaw/wall effect - 60 fps, +10 pitch, -50° to +200°	8-19
Figure 8-16	Autoprobe S-type: yaw/wall effect - 60 fps, -10 pitch, -10° to + 10°	8-20
Figure 8-17	Autoprobe S-type: yaw/wall effect - 60 fps, -10 pitch, 165° to 185°	8-21
Figure 8-18	Autoprobe S-type: yaw/wall effect - 60 fps, -10 pitch, -50° to +200°	8-22
Figure 8-19	Mod Kiel w/therm.: Yaw/wall effect - 60 fps, 1" from wall	8-23
Figure 8-20	Mod Kiel w/therm.: Yaw/wall effect - 60 fps, 5" from wall	8-24
Figure 8-21	Spherical probe: yaw/wall effect - 60 fps, 4" from wall	8-25
Figure 8-22	DAT probe: yaw/wall effect - 60 fps, 3" from wall	8-26

LIST OF TABLES

		Page
Table 1-1	Probes Calibrated and Tested in NCSU Wind Tunnel	1-8
Table 3-1	ΔP as a Function of Yaw Angle for Wake Ports 1 and 4 of the Modified Kiel Probe Prototype	3-2
Table 3-2	Calibration Coefficients Across Pitch Angles for Various Wake Ports of the Modified Kiel Probe Prototypes (MK1 and MK2) and for the Type S (S-1) Probe at 0° Yaw	3-5
Table 4-1	Calibration Coefficients Obtained for 2D Probes at Specific Velocities	4-2
Table 4-2	Variability of Calibration Coefficients Across Velocities for 2D Probes Determined at Pitch Angle 0°	4-3
Table 5-1	Sensitivity of C_p to Pitch Angle for 2D Probes	5-2
Table 5-2	Axial Velocity Evaluation for 2D Probes	5-4
Table 5-3	Maximum Percent Deviation of Measured Velocity from Axial Velocity Across All Velocities at Zero Yaw	5-6
Table 5-4	Maximum Percent Deviation of Measured Velocity from Axial Velocity Across 60 and 90 fps at Zero Yaw	5-6
Table 6-1	Summary of Yaw Angle Accuracy and Effect on Velocity Determination	6-2
Table 6-2	Yaw Angle Error Detailed Data	6-3
Table 7-1	DAT Probe (3D-1) Velocity Accuracy	7-5
Table 7-2	DAT Probe (3D-2) Velocity Accuracy	7-6
Table 7-3	DAT Probe (3D-3) Velocity Accuracy	7-7
Table 7-4	Spherical Probe (MS5-2) Velocity Accuracy	7-8
Table 7-5	3D Probe Pitch Angle Accuracy	7-10
Table 7-6	Summary of 3D Probes Velocity Accuracy Results	7-11
Table 8–1	Summary Table of the Effect of Distance from Wall Entry on the Number of Yaw Nulls Observed	8-4

1.0 INTRODUCTION

1.1 PURPOSE OF PROGRAM

Electric utilities have recently expressed concerns that continuous emission monitoring systems (CEMS) installed to comply with regulations implemented under the U.S. Environmental Protection Agency's (EPA) Acid Rain Program report higher heat input and SO_2 emissions values than are estimated using conventional (input/output and output loss) methods. The basis of the concern is that EPA's reference method for volumetric flow determination (Test Method 2)[1] may overestimate flow rate, which could result in overestimates of sulfur dioxide emissions and heat input.

To address this concern, EPA has begun an experimental field project with The Cadmus Group, Inc., to assess Test Method 2 and compare its results with those obtained using alternative methods of measuring volumetric flow. During the next year, EPA will work with Cadmus to design, coordinate, and report on a multi-laboratory field study of Test Method 2. The study will address several major questions. First, what is the accuracy and variability of the reference method? Next, how do reference method measurements compare with other measurements of flow, particularly in situations experiencing significant off-axial flow? Finally, do the field results indicate that the procedures for Test Method 2 require improvements, and if so, in what regard?

As a preliminary step toward evaluating the test method, EPA asked Cadmus to perform wind tunnel tests of flow measurement probes that are either approved or under consideration for use with Test Method 2. Under EPA direction, Cadmus designed these tests and conducted them in the Merrill Subsonic Wind Tunnel at North Carolina State University (NCSU) in Raleigh. The wind tunnel tests were designed to evaluate how accurately various probes can measure angles and velocity of flow under prescribed conditions and, additionally, to calibrate the probes for use in planned multi-laboratory field experiments. To provide a basis for selecting probes for the field test, the wind tunnel testing was performed over a range of velocity, pitch, and yaw settings approximating the conditions encountered at actual utility sites.

1.2 GOALS OF THE WIND TUNNEL TESTS

The wind tunnel tests were originally designed to achieve five principal goals: (1) evaluate a prototype modified Kiel probe; (2) determine the minimum sample size required for subsequent experiments; (3) evaluate the accuracy of yaw angle nulling procedures and velocity determinations by various two-dimensional (2D) and three-dimensional (3D) probes; (4) determine pitch angle and velocity measurement accuracy for selected 3D probes; and (5) calibrate probes that will be used in the field study. During the course of the wind tunnel study, a sixth objective was added as a result of preliminary findings revealed in a related flow study conducted by the Electric Power Research Institute (EPRI). This objective was to examine what effect, if any, proximity of the probe tip to the wind tunnel entry wall had on determining yaw null. A more detailed summary of the wind tunnel study goals follows.

---

[1] 40 CFR Ch. 1 (7-1-92 Edition), Pt. 60, App. A, Method 2—Determination of Stack Gas Velocity and Volumetric Flow Rate (Type S Pitot Tube), pgs. 691-709 (hereinafter referred to as Method 2).

- ***Modified Kiel Probe Evaluation.*** Using the Kiel/cylinder pitot static probe constructed and tested by Mitchell, et al.[2] in the late 1970s as the basis, a standard Kiel probe was modified by adding four candidate wake ports and two Fechheimer ports to produce a prototype for testing in the NCSU wind tunnel. The tests were designed to determine whether the alternative probe was sufficiently promising to warrant further consideration for use under Test Method 2. If so, additional wind tunnel testing would be conducted to collect data for use in finalizing the probe's design prior to field testing.

- ***Required Sample Size Determination.*** Early in the wind tunnel testing, an experiment was conducted to determine the minimum number of replicates required for each subsequent test. A 3/8-inch Type S probe was used in this experiment.

- ***Yaw Angle and Axial Flow Accuracy Determination.*** Evaluating the accuracy of flow angle determinations using various probe types was the third goal of the wind tunnel experimentation. Flow angles were determined using procedures prescribed for the specific type of probe under evaluation. All probes were tested to examine accuracy of yaw angle determination, as well as accuracy of yaw-corrected velocity measurements.

- ***Determination of Pitch Angle and Velocity Pressure Accuracy for 3D Probes.*** Determining pitch angle accuracy and velocity pressure accuracy using DAT and spherical probes was the fourth goal of the wind tunnel testing.

- ***Probe Calibration.*** Calibrating each probe to be used in the field study was an important goal of the wind tunnel testing. For the 2D probes, single calibration factors at 0° yaw and 0° pitch were derived. Calibration curves as specified in draft Method 2F[3] were derived for the DAT and spherical probes.

- ***Examination of Wall Effects on Yaw Null Determination.*** A recent EPRI study indicated that multiple yaw nulls were located in yaw-angle scans when a Type S probe was placed near the wall entry point. Therefore, a study to evaluate how proximity of the probe tip to the wind tunnel entry wall affects the ability to identify yaw null was added as an objective of this study.

1.3 DESCRIPTION OF WIND TUNNEL

The Merrill Subsonic Wind Tunnel (Figure 1–1), where these experiments were conducted during the summer of 1996, is a continuous flow, single-return tunnel with a test section vented to the atmosphere. The test section is 45 inches wide, 32 inches high, and 46 inches long in the flow direction. Wind tunnel speeds ranging from 10 to approximately 120 feet per second (fps) are controlled by a variable-pitch fan driven by a 50-hp constant-speed motor. Vanes located in each

---

[2] Mitchell, W.J., B.E. Blagun, D.E. Johnson, and M.R. Midgett. 1979. *Angular Flow Insensitive Pitot Tube for Use with Standard Stack Testing Equipment.* U.S. Environmental Protection Agency, Office of Research and Development, EPA-600/4-79-00.

[3] U.S. Environmental Protection Agency Method 2F—Determination of Stack Gas Velocity and Volumetric Flow Rate (Three-dimensional Pitot Tube). Draft, June 30, 1993 (hereinafter referred to as Method 2F).

corner of the tunnel reduce losses in total pressure and prevent flow separation from the tunnel walls. Three screens and one honeycomb section are located just upstream of the entrance cone to the test section to reduce turbulence and eliminate tunnel surge.

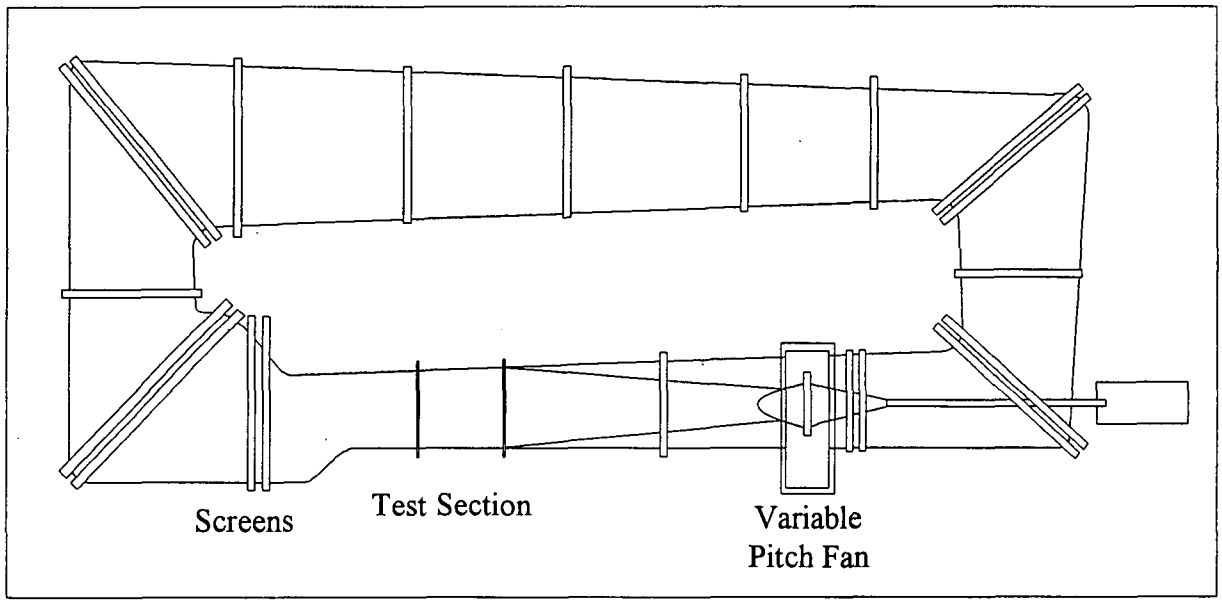

Figure 1-1. Schematic (top view) of the Merrill Subsonic Wind Tunnel Facility located at North Carolina State University in Raleigh.

Well suited for probe calibration, the wind tunnel maintains steady, low-turbulence, uniform flow in the test section, which is large enough to avoid flow disturbance by the presence of the probe. Wind tunnel calibration has shown that the velocity profile is constant to within less than 1% in a 6-inch cube located in the center of the test section, where all measurements for these experiments, except for the entry wall effects, were made.

The actual wind tunnel velocity during each test is measured using an elliptical-nose, standard pitot-static tube manufactured by Airflow Developments Limited, High Wycombe, England. Widely regarded as the best available, this standard probe is the only one recommended for use without individual calibration and has a pitot coefficient of unity. All test probes were calibrated against this standard tube.

A digital inclinometer is used to measure angles of rotation with respect to the wind tunnel longitudinal axis (yaw angle) to a visually estimated accuracy of $\pm 0.1°$. The tunnel also has an installed device, termed a "pitch board" (see Section 2.1), that allows the pitot tube to be rotated in the flow direction (pitch angle) to a visually estimated accuracy of $\pm 0.5°$.

Gas temperature, used in calculating gas velocity, is measured using a standard chrome-alumel thermocouple, mounted inside the wind tunnel test section. A digital readout of the temperature is displayed on the outside wall of the tunnel. Because the test section is vented, the barometric

pressure[4] in the room is equal to the pressure in the wind tunnel test section. This pressure is measured using a standard mercury-filled barometer (manufactured by Central Scientific Company, Chicago, Illinois) that can be read with a visually estimated accuracy of 0.005 inches of mercury.

1.4 DESCRIPTION OF TEST PROBES

Probes selected for the wind tunnel experiments included those considered most likely to be tested in the field either because (1) they have been used historically for field testing or (2) earlier wind tunnel or field tests have demonstrated the probes' ability to measure both velocity and angle of flow. These highest-priority probes included three types of 2D probes (three manual probes and two "Autoprobes") and two types of 3D probes:

2D Probes

Modified Kiel (prototype)
Type S
Modified S
Autoprobe with Type S probe
Autoprobe with Modified S probe

3D Probes

DAT
Spherical

The modified Kiel probe is shown schematically in Figure 1–2. Figure 1-3 is a photograph of the Autoprobe being inserted into the wind tunnel. The spherical and DAT probes are shown schematically in Figures 1–4 and 1-5, respectively.

Initial plans called for testing of two additional probes—the French and Loop S—if sufficient time were available. Of these, only the French probe—a cylindrical probe with a single impact port—was tested, however, and testing was limited to calibration and determination of pitch angle accuracy. The Loop S probe was not tested because the wind tunnel entry port would have required modification to accommodate the probe head.

Two-dimensional probes are used to measure stack velocity pressure and can be used to determine yaw angle. In Mitchell's study, the ability of the modified Kiel probe to measure total flow was unaffected by yaw and pitch angles of up to ±30°. The wake port on the probe was found to have some ability to measure yaw angle and to accurately measure static pressure. The prototype Kiel probe tested in this study, shown in Figure 1–2, is a standard Kiel probe to which four candidate wake ports and two Fechheimer ports were added. The four wake port holes are offset 180° from the Kiel's impact port and are located 1.375, 2.125, 2.875, and 3.625 inches down the probe shaft from the center of the impact port. The impact port in the probe's venturi head is 1/8 inch in diameter, each wake port is 3/32 inches in diameter, and each Fechheimer port is 1/8 inch in diameter. Each Fechheimer port is offset 30° from, and is located 2.375 inches down the probe shaft from, the center of the impact port. The modified Kiel probe was also fitted with a mock "thermocouple"—a stainless

[4] Barometric pressure is synonymous with ambient pressure.

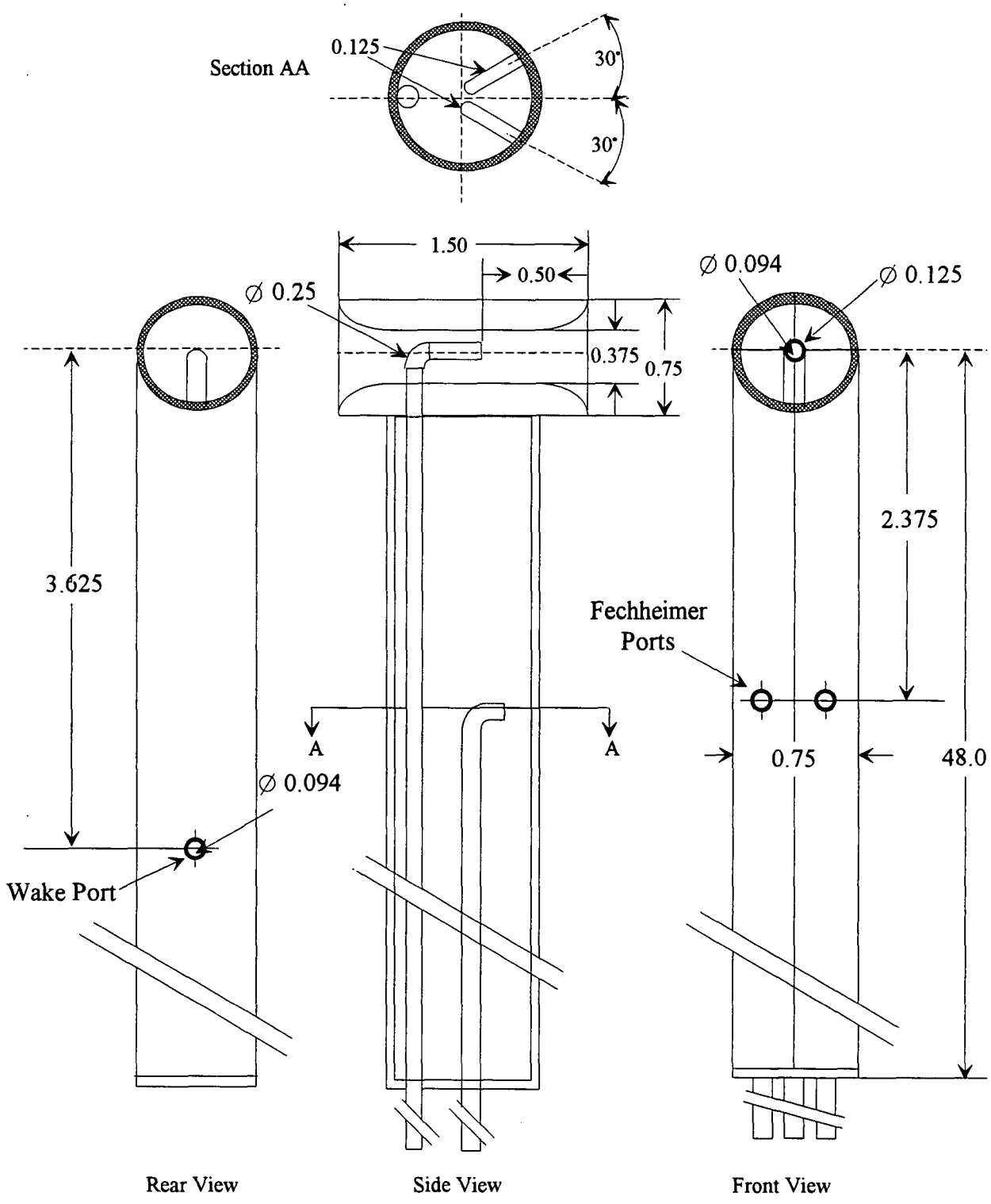

Figure 1-2. Schematic of modified Kiel probe (MK1).

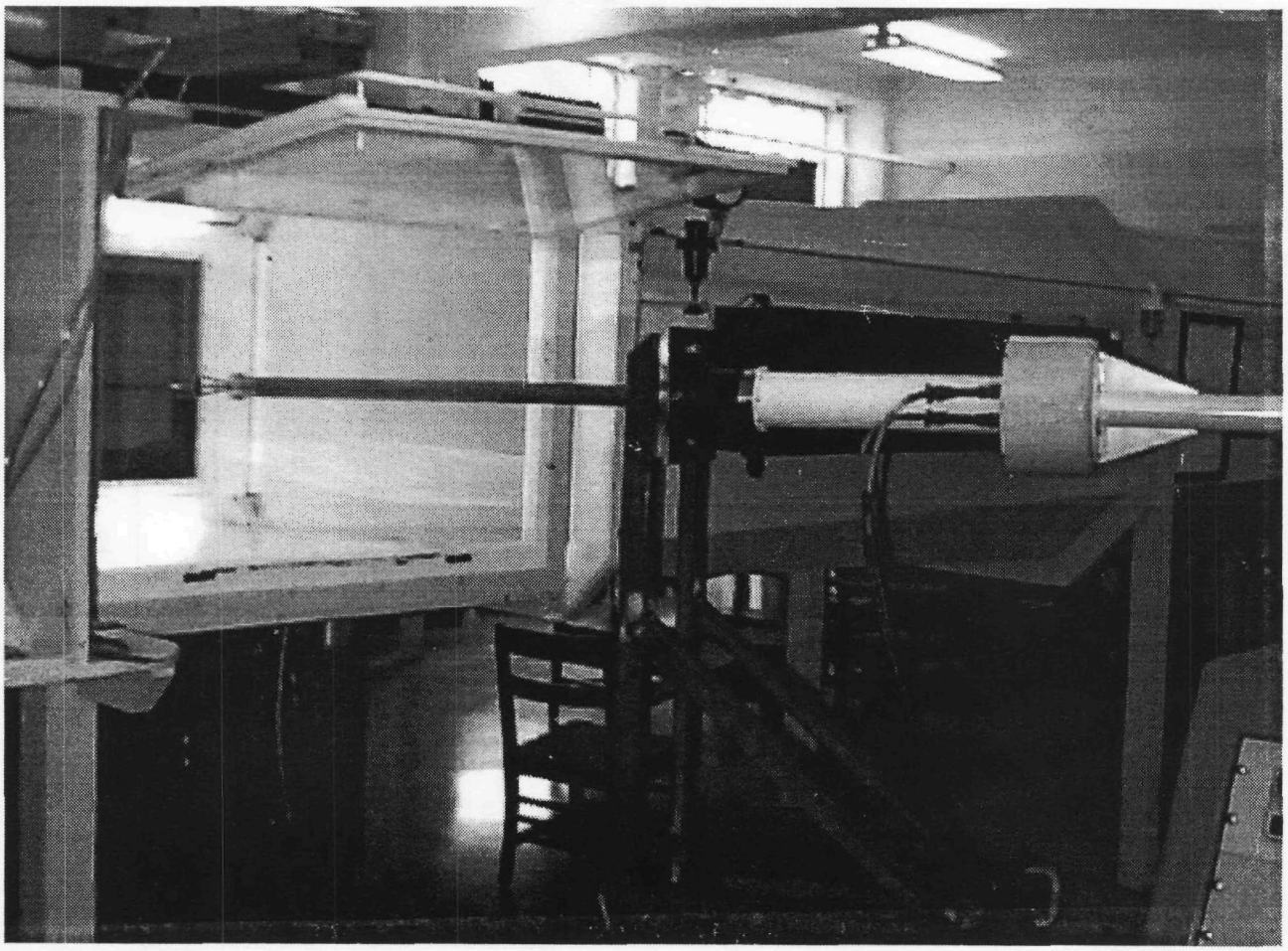

Figure 1-3. Autoprobe positioned for insertion into the wind tunnel.

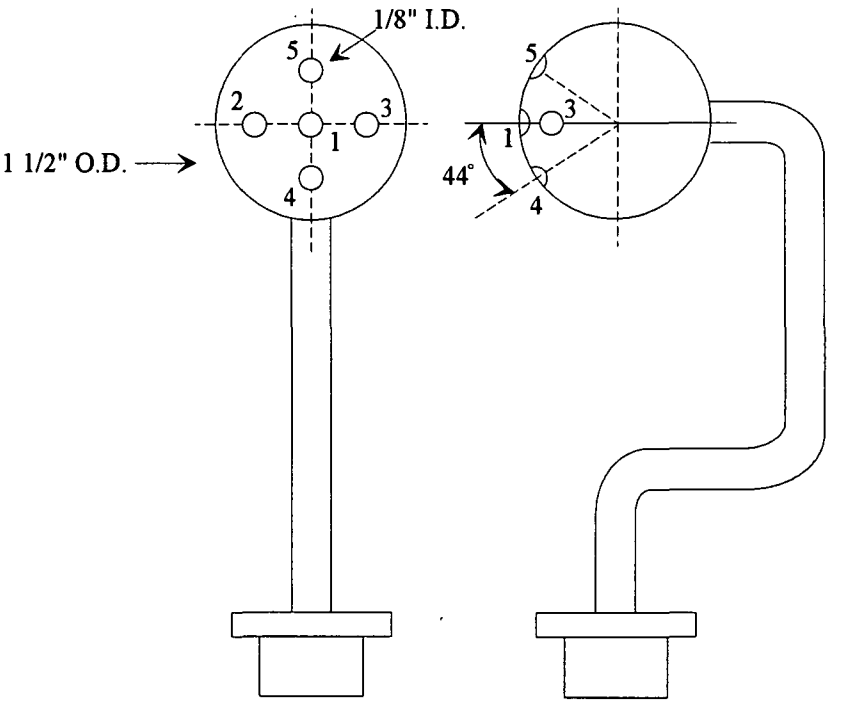

Figure 1-4. Front and side views of spherical probe.

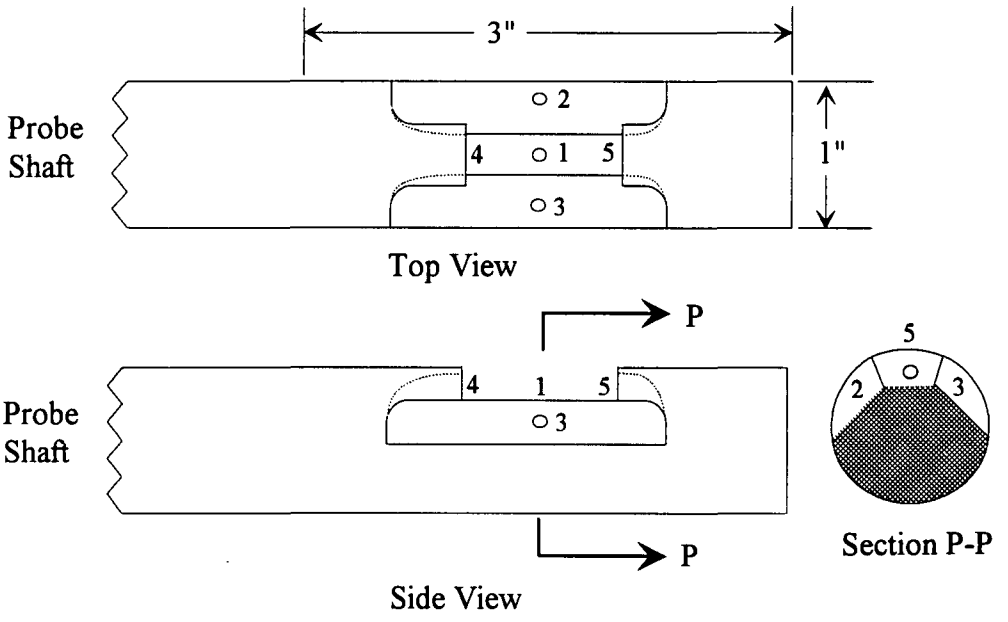

Figure 1-5. Top, side, and cross-sectional views of DAT probe.

steel wire approximately 3 inches in length attached to the top of the probe near the Kiel head to simulate the presence of a thermocouple. Also tested were three 3/8-inch diameter Method 2 Type S pitot tubes, which are the probes most commonly used in flow measurements. Three 3/8-inch diameter "modified S" probes, which have wider orifice separations than standard Type S probes, were also included in the testing.

Three-dimensional probes are used to provide measurements of pressure, pitch angle, and yaw angle of the velocity vector, which are used to calculate axial velocity. For these experiments, three DAT probes and one spherical probe were tested.

Table 1-1 shows the candidate probes for testing in EPA's planned multi-laboratory field study. Also shown are their key physical dimensions and the experiments performed on the probes in the NCSU wind tunnel.

Table 1-1. Probes Calibrated and Tested in NCSU Wind Tunnel

Probe		Probe Characteristics			Test	
Type	ID	Outside Diameter (in.)	Measurement Port Diameter (in.)	Length (ft)	Yaw Nulling	Calibration
Modified Kiel Prototype	MK-1 [a]	3/4	3/32	4	X	X
	MK-2 [a]	3/4	3/32	4	X	X
Type S	3/8S-1	3/8	b	10	X	X
	3/8S-2	3/8	b	10		X
	3/8S-3	3/8	b	10		X
Modified Type S	USS-1	3/8	1/4	10	X	X
	USS-2	3/8	1/4	10		X
	USS-3	3/8	1/4	10	X	X
Autoprobe Type S	AS	3/8	b	4	X	X
Autoprobe Modified S	AMS	3/8	1/4	4	X	X
French	F-2	3/4	c	6		X
Spherical	MS5-2	1-1/2	1/8	7	X	X
DAT	3D-1	1	d	10	X	X
	3D-2	1	d	10	X	X
	3D-3	1	d	10	X	X

[a] MK-1 is the modified Kiel probe; MK-2 is the modified Kiel probe with a mock "thermocouple" added. See section 2.
[b] Elliptical ports 15/32" x 9/32"
[c] Conical impact port—5/16" leading edge tapered to 3/16" orifice; wake port—3/16"
[d] Ports P1, P2, and P3—1/8"; Ports P4 and P5—3/32"

1.5 DOCUMENT PURPOSE AND ORGANIZATION

This document presents the results of several experiments conducted at the NCSU Merrill Subsonic Wind Tunnel during the summer of 1996. The results are being used to help design the field testing phase of EPA's collaborative flow study, which, as currently planned, will be conducted at utility boilers having distinct stack flow characteristics. The results of the modified Kiel probe experiments presented in this report were used to refine the design of that probe. Results of the tests performed on the other probes, along with the calibration coefficients, are also being used to develop the experimental design for the field study.

Section 2.1 of this document describes the general test procedures used in the wind tunnel experiments, including the procedures for yaw nulling and for pitch angle determination. The procedures used in acquiring and handling the data and the steps taken to ensure data quality during both the testing and data analysis phases of the project are presented in Section 2.2. Section 2.3 discusses the steps implemented to determine the minimum number of replicates required for each experiment on each probe (based on the 3/8-inch Type S probe). Procedures used for calibrating probes are described in Section 2.4.

Sections 3 through 8 present the procedures, results, and conclusions specific to each experiment conducted in the wind tunnel. Section 3 presents and discusses the experiments performed on the modified Kiel probe, including a comparison of the wake ports and Fechheimer ports in determining yaw null and an analysis of the sensitivity and accuracy of static pressure determinations using the wake ports. Section 4 describes the derivation of the calibration coefficients for the 2D probes and their variability with velocity. Pitch angle effects on velocity measurements made with the 2D probes are discussed in Section 5 (including the sensitivity of the calibration coefficients to pitch angle and how pitch angle influences velocity determination). Section 6 examines the accuracy of yaw angle measurements and the effects of yaw angle on velocity measurements. Section 7 presents and discusses calibration curves for the 3D probes and the accuracy of the velocity and pitch angle measurements obtained with each of these probes. The results of the experiments performed to examine how the determination of yaw null is influenced by a probe's proximity to the tunnel wall are presented and discussed in Section 8. Overall conclusions and recommendations for follow-up study are presented in the final section, Section 9. Three appendices accompany this report: Appendix A presents and analyzes the experiment conducted to determine the minimum sample size required; Appendix B contains additional plots of the wall-effect experiments; Appendix C contains the raw experimental data for the results discussed in this report and Appendix D contains the raw data on 3 ½ inch floppy diskettes.

2.0 OVERVIEW OF DATA COLLECTION, HANDLING, AND QUALITY ASSURANCE

2.1 OVERVIEW OF FLOW MEASUREMENT PROCEDURES

Volumetric flow is calculated as the product of the average axial flow velocity and the cross-sectional area of a stack or duct at the measurement location. The accuracy of this calculation depends on the accuracy of the individual velocity measurements and on the accuracy of the measurement of the cross-sectional area at the test location. This study focuses on the accuracy of measuring axial velocity.

EPA Test Method 2 (Determination of Stack Gas Velocity and Volumetric Flow Rate) is based on the differential pressure measurement technique first developed by Henri Pitot in 1732. The total pressure of a fluid in motion is the sum of static pressure and dynamic pressure. Static pressure is due to the random motion of molecules vibrating with thermal energy, transferring momentum from molecule to molecule and to surrounding surfaces. Static pressure is the pressure one would feel if one were moving along with the stream. The static pressure of a gas is determined by its temperature and density. Dynamic pressure is proportional to the square of the velocity and the gas density; density is, in turn, proportional to molecular weight. The velocity of a moving stream can be calculated from the following equation:

$$V = \sqrt{2R}\sqrt{(P_t - P_s)}\sqrt{\frac{T}{P_s M}} \qquad \textbf{(Eq. 2.1)}$$

where:

V	=	flow velocity
R	=	the gas constant
P_t	=	total pressure
P_s	=	the static pressure of the gas
P_t-P_s	=	dynamic or differential pressure
T	=	absolute temperature
M	=	molecular weight of the gas

Thus, the temperature, static pressure, and molecular weight of the effluent stream and the difference between the total and static pressure must be measured to calculate velocity.

When a pitot probe is placed into a moving gas stream, the impact opening of the probe will experience the total pressure of the system. Static pressure must be measured at a point where the flow is undisturbed. Many velocity probes do not sense the true static pressure directly; instead, for various design reasons, they sense a pressure related to it. A probe-specific calibration factor C_p is introduced to account for this difference. Incorporating C_p into Equation 2.1 provides the final equation as applied in Test Method 2:

$$V = K_p C_p \left(\sqrt{\Delta P}\right) \sqrt{\frac{T}{P_s M}} \qquad \textbf{(Eq. 2.2)}$$

where

K_p = 85.49 = pitot tube constant to calculate velocity in fps
ΔP = $P_t - P_s$

A well constructed standard, or "L-shaped", pitot tube can have a calibration coefficient of unity, indicating that the probe measures true total and static pressures. Unfortunately, the standard pitot-static probe is rarely suitable for repeated use in hostile environments such as power-plant stacks. Because of its robust design, the probe most commonly used for Test Method 2 is the Stausscheibe, or "Type S" probe. The static port of the Type S probe is located on the back side of the probe, where the pressure is significantly affected by flow over the probe head. C_p values for Type S pitot tubes therefore generally range from about 0.80 to 0.86. Other types of probes have different C_p values, depending on probe shape and static port placement.

The NCSU wind tunnel is vented to the atmosphere; thus, static pressure is equal to barometric or ambient pressure. The gas is air, and the molecular weight is 28.97 lb/mole. Thus, Equation 2.2 can be simplified to yield Equation 2.3, as follows:

$$V = 15.9\, C_p \sqrt{\frac{\Delta P\left(T_F + 460\right)}{P_{bar}}} \qquad \textbf{(Eq. 2.3)}$$

where

15.9 = scale factor to calculate velocity in fps
ΔP = differential pressure in inches of water
T_F = temperature in °F
P_{bar} = barometric pressure in inches of mercury

Equation 2.3 can be rearranged to calculate ΔP:

$$\Delta P = \frac{P_{bar} V^2}{252.8\, C_p^2 \left(T_F + 460\right)} \qquad \textbf{(Eq. 2.4)}$$

For the experiments conducted in this study, wind tunnel velocities were set by adjusting the blade pitch of a variable-pitch, constant-RPM (revolutions per minute) fan (see Figure 1–1) until the desired ΔP (calculated by setting the nominal velocity in Equation 2.4) is reached. The ΔP in the wind tunnel was measured with the standard pitot-static tube (which has a C_p of 1) described in Section 1. This

pitot tube was inserted through an opening in the top of the wind tunnel and then lowered into position in the center of the test section. Temperature was taken with a standard chrome-alumel thermocouple mounted inside the wind tunnel test section, and barometric pressure was read using a standard mercury-filled barometer located outside the tunnel in the laboratory.

The pressure drop between two points in the nozzle section of the tunnel was continuously monitored by an electronic pressure transducer. The signal from the transducer (in millivolts) was displayed continuously by a digital readout near the tunnel. The signal from the transducer was read and recorded when the velocity was set using the standard pitot tube. To maintain a constant pressure drop in the tunnel, the fan blade pitch was adjusted until a constant reading from the electronic transducer was obtained.

Test probes were secured to portable floor stands and then leveled with an inclinometer. Desired yaw angles were also established with the use of an inclinometer. Each test probe was connected to a series of magnehelic differential pressure gauges with brass fittings and 1/8-inch tubing (Figure 2–1). Pressure differences (in inches of H_2O) were read directly from these gauges. Desired pitch angles were determined using a board located just under the opening to the test port (illustrated in Figure 2–2). Pitch angles were changed by rotating the probe stands until the probe was in line with the desired angle delineated on the pitch board.

Leak checks were performed on the probes before they were inserted into the wind tunnel. Each probe pressure line was connected through a tee to a common pressure vessel and the appropriate magnehelic gauge port. After sealing each probe pressure orifice with tape, the vessel was pressurized and the magnehelic gauges were read. After several minutes, the gauges were re-read; the probes were assumed leak-free if none of the readings changed. The potential for leaks was also monitored during the test by observing the magnehelic gauges. Following completion of successful leak checks, the probes were inserted through the test port and the probe tips positioned at the center of the wind tunnel (approximately 22.5 inches from the inner wall).

2.2 YAW ALIGNING AND VELOCITY MEASUREMENT PROCEDURES

Procedures for yaw nulling and measuring velocity are summarized, by probe, in the following four subsections.

2.2.1 Modified Kiel Probe

Two alternative procedures were tested to evaluate the accuracy of yaw angle determinations with the modified Kiel probe. In the first procedure, the probe was rotated so that the wake port was at a yaw angle of -15° relative to the flow as read by the digital inclinometer. The wake port pressure minus the Kiel impact port pressure (ΔP_W) was read and recorded. This procedure was repeated at yaw angles of -10°, -5°, 0°, 5°, 10°, and 15°. ΔP_W vs. yaw angle was plotted to determine the position of the probe at which the yaw angle would be zero (i.e., the yaw null position).

The second procedure evaluated the yaw-angle accuracy obtained using the Fechheimer ports. To do this, the Kiel impact port was oriented into the direction of flow. The probe was rotated so that the impact port was at a yaw angle of -15° to the flow as read by the digital inclinometer. The pressure difference across the Fechheimer ports (ΔP_F) was read and recorded. This procedure was

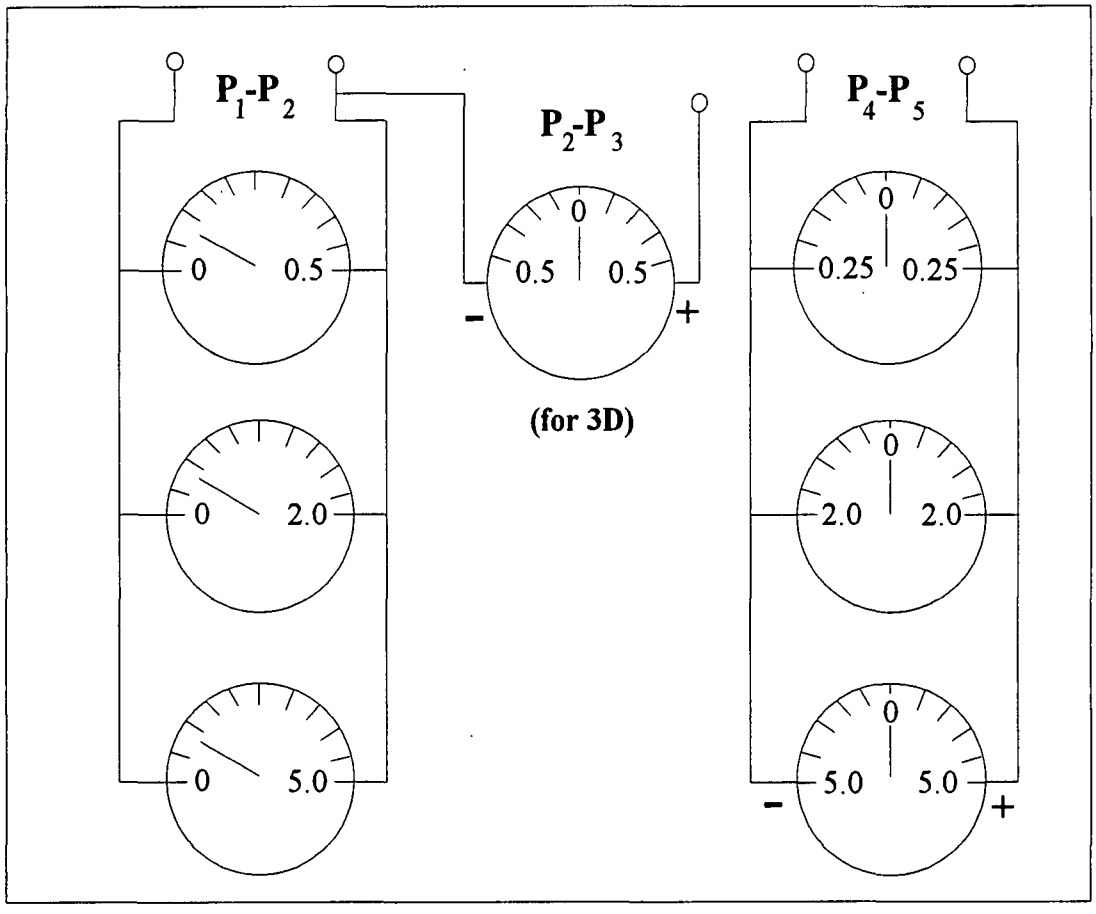

Figure 2-1. Magnehelic meters used to measure differential pressures (P_1-P_2, P_2-P_3, P_4-P_5) across various ports of test probes.

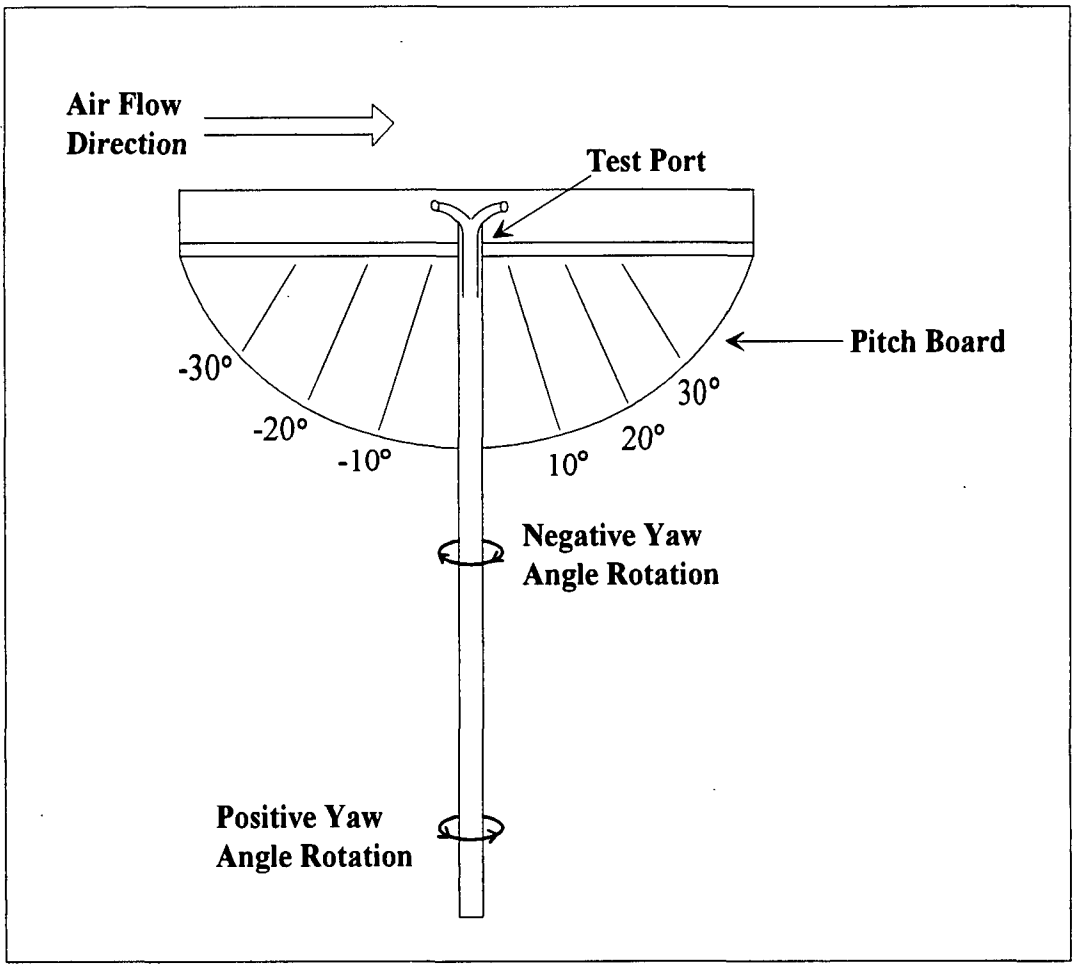

Figure 2-2. Schematic (overhead perspective) showing positive and negative pitch angle and yaw angle orientation of flow probe with respect to test port for wind tunnel and flow directions.

repeated at yaw angles of -10°, -5°, 0°, 5°, 10°, and 15°. ΔP_F vs. yaw angle was plotted to determine the angle θ_y at which $\Delta P_F = 0$. .

When the Fechheimer ports were used for yaw nulling (see, e.g., Section 3), the impact port was aligned with the flow and rotated until $\Delta P_F = 0$. The yaw null angle, θ_y, relative to the axis of the duct was then determined with the use of the digital inclinometer. The ΔP between the impact and wake ports was used to determine velocity in the direction of flow. Velocity was multiplied by $\cos\theta_y$ to determine axial flow.

2.2.2 Type S, Modified S, and French Probes

Yaw angles for the Type S and modified S probes were determined by rotating the probes until a null reading was obtained. The probe was then rotated 90° from the null to position the impact port of the pitot head directly into the flow. Using the digital inclinometer, yaw angle was then determined from the angle between the pitot tube and the axis of the duct or stack. The differential pressure and temperature readings were then recorded. The velocity component in the direction of stack gas flow (i.e., total velocity) was calculated using Equation 2.3. The yaw-corrected axial component of velocity was determined by multiplying the total velocity by $\cos\theta_y$. Insufficient information was available to the experimenters to develop a yaw nulling procedure for the French probe. For this probe, the pitot tube was inserted into the tunnel with the impact port pointed into the flow (i.e., a nominal yaw angle of zero between the impact port and the axis of flow).

2.2.3 Autoprobe Type S and Modified S

With the Autoprobe, probe rotation is accomplished by a computer-controlled stepper motor and notched-belt drive. The Autoprobe locates the null angle by (1) rotating the probe by coarse increments to locate an approximate null, (2) then rotating by finer increments through the approximate null to verify and improve the approximate null value, and (3) performing a linear regression to find the most probable null angle. Yaw null values are displayed on the computer monitor and can be saved in a file. Once the yaw angle has been determined, the probe is rotated 90° to determine the ΔP for the velocity measurement. The axial velocity was calculated by multiplying the measured impact velocity by $\cos\theta_y$.

2.2.4 DAT and Spherical Probes

The five ports on the sensing heads of the DAT and spherical probes are numbered 1 through 5 (see Figures 1-4 and 1-5), and the pressures measured at each port are referred to as P_1, P_2, P_3, P_4, and P_5. Ports P_2 and P_3 are located symmetrically on either side of impact pressure port P_1. These 3D probes were yaw nulled by rotating the probe until a zero differential pressure between ports P_2 and P_3 was obtained. The yaw angle was then determined with the use of the digital inclinometer that had been set to zero on the axis of the wind tunnel. Clockwise rotation of the probe was considered positive, and counter-clockwise rotation, negative.

The pressure differential between P_4 and P_5 is a function of pitch angle and gas stream velocity. The pitch angle, θ_p, is obtained from a calibration curve that plots the ratio $F_1 = (P_4-P_5)/(P_1-P_2)$ vs. pitch angle. Flow toward the tester ($P_4>P_5$) is considered positive, and flow away from the tester ($P_5>P_4$) is considered negative. The probe's calibration curve also provides 3D pitot calibration coefficients,

$F_2 = C_{ps}[(P_t-P_s)/(P_1-P_2)]^{½}$, as a function of pitch angle, θ_p. (In this case, the standard pitot-static tube is used, so $C_{ps} = 1$.) Axial velocity is obtained from θ_y, θ_p, F_2, $P_1 - P_2$, temperature, and barometric pressure (see Section 7, Equations 7.3 and 7.4).

2.3 DATA ACQUISITION, HANDLING, AND QUALITY ASSURANCE

Cadmus developed extensive data-handling and chain-of-custody procedures to ensure that high-quality information was used in the data analyses. In addition, quality checks of the data recording procedures, data base handling procedures, and computer code were conducted throughout this study. General data handling procedures are outlined below.

In the wind tunnel laboratory, data associated with all manual probes (i.e., all probes except the Autoprobe) were recorded on standardized data collection forms. The data collection forms were developed to ensure that a consistent and complete set of information was recorded for each run of a specific experiment. Information that uniquely identified each run was recorded on the data collection form. These data included date, probe type, probe ID, nominal velocity, pitch angle, yaw angle, repetition number, and (for entry wall effects experiments) distance from the wall. For the Autoprobe, this information was recorded in a laboratory notebook and in the electronic file containing the Autoprobe readings (including run number and count time). This procedure enabled the Autoprobe electronic data to be associated readily with the information contained in the laboratory notebook to ensure that the electronic data could be identified.

Completed data sheets and floppy disks were transferred from the wind tunnel to the Cadmus office in Durham, North Carolina, for quality assurance and analysis, and a hard copy of the information was retained by the NCSU principal investigator. The information was duplicated, and copies of the data sheets, laboratory notebook, and floppy disks were stored outside of the Cadmus office.

For the manual probes, data from the data recording sheets were entered into an ASCII file. The ASCII computer files were checked by two independent observers to ensure the data were transferred without error. The data were plotted and outliers identified. The outlier data were again checked to verify they were not the result of a data transfer error. Suspect data were also examined by NCSU researchers to determine whether either an experimental error or a transcription error could have occurred. If explainable errors were identified, the data were marked and corrections made, if appropriate.

Autoprobe data useful for the analyses were extracted from the electronic file using a computer program written by Cadmus. The computer code was independently checked to ensure that the proper fields were extracted from the original file. The Autoprobe data and manual probe data were stored in SAS® data sets for analysis. Autoprobe data were transferred to spreadsheet software files for analyses and plotting.

All SAS® code used to plot or analyze the data were checked by an independent programmer to ensure no programming errors had occurred. In addition, the resulting plots and analysis outputs were examined for validity. When suspect information was found, the computer code and associated data were again examined to ensure accuracy.

2.4 STUDY TO DETERMINE MINIMUM SAMPLE SIZE

Early in the wind tunnel experimental program, a study was performed to establish the number of replicates required for evaluating accuracy of the yaw angle, calibration coefficient, and velocity. The experimental design and detailed results are presented in Appendix A. A 3/8–inch Type S pitot tube was tested at

- velocities of 30, 60, and 90 fps;
- pitch angles from -20° to 20° in 10° increments; and
- yaw angles from -15° to 15° in 5° increments.

Eight replicate measurements were taken.

The Type S probe was used in the pilot test because its measurement variance was expected to be representative of the probes involved in this study. ΔP for both the Type S and standard pitot tubes was measured to calculate the calibration coefficient, C_p, using the following equation:

$$C_p = \sqrt{\frac{\Delta P_P}{\Delta P_s}} \qquad \textbf{(Eq. 2.5)}$$

where,

ΔP_P = differential pressure for the standard pitot tube, and
ΔP_s = differential pressure for the Type S pitot tube.

The equation for estimating sample size is

$$n = \frac{Z_{\alpha/2}^2 \, \sigma_d^2}{E^2}, \qquad \textbf{(Eq. 2.6)}$$

where,

n = estimated sample size;
$Z_{\alpha/2}$ = Z statistic that indicates the confidence desired (e.g., 90% or 95%) in the measured calibration coefficient;
σ_d^2 = variance in the calibration coefficient estimates (calculated as sample variance using the eight replicates); and
E = level of error (e.g., 20% or 10%) in the average calibration coefficient estimation that is acceptable.

For example, a sample size can be estimated that allows us to be 95% confident that the measured C_p is within 5% of the true mean C_p. Sample sizes were calculated for selected values of Z (80%, 90%, 95%) and E (20%, 10%, 5%). Calculated sample sizes were then examined at different velocities, pitch angles, and yaw angles. The results of the study (see Appendix A) indicate that the

variability in the calibration coefficients is very small over all velocities, pitch angles, and yaw angles. When averaged across the tested yaw angles, fewer than three replicates for each experiment were sufficient to achieve less than 5% error in the results with 99% confidence. Therefore, to be conservative, the number of replicates for all experiments was fixed at three (with the exception of one modified S probe calibration, for which measurements were conducted in duplicate).

2.5 CALIBRATIONS OF PROBES

Two general calibration procedures were used, depending on the type of probe. Each probe to be tested in the field was calibrated according to the following procedures at three velocities: 30, 60, and 90 fps. The modified Kiel and Type S probes were also calibrated at velocities of 40, 50, 70, and 80 fps.

2.5.1 Single Calibration Factors

Single calibration factors at yaw and pitch angles of 0° were derived for the modified Kiel, Type S, modified S, French, Autoprobe Type S, and Autoprobe modified S probes. The standard pitot-static tube was inserted into the wind tunnel so that the port used for determining total pressure was located in the center of the wind tunnel test section; the wind tunnel speed was initially set to an approximate, desired velocity (usually 30, 60, or 90 fps). The true wind tunnel speed was then calculated using the ΔP_P for the standard pitot-static tube and the gas temperature and barometric pressure (see Equations 2.3 and 2.4). The standard pitot tube was then withdrawn from the wind tunnel test section and the test probe was inserted at an orientation of 0° pitch and 0° yaw. The ΔP between the impact and static ports of the test probe was then measured.

This procedure was repeated for each 2D probe at each test velocity. This procedure was also used to evaluate the effect of pitch angle on the calibration coefficient, by repeating this process at pitch angles between ±30° pitch in 10° increments (including 5° and -5°).

2.5.2 DAT and Spherical Probe Calibration Curves

For the DAT and spherical probes, calibration curves were derived as specified in draft Method 2F for velocities of 30, 60, and 90 fps. Calibration of 3D probes involves generating two types of calibration curves. The first curve is obtained by plotting the ratio F_1 of the ΔP across the fourth and fifth ports, P_4-P_5, to the ΔP across the first and second ports, P_1-P_2 [or , $F_1 = (P_4-P_5)/(P_1-P_2)$] against known pitch angles. The second curve is constructed by plotting the 3D pitot coefficient, F_2, against known pitch angles; F_2 is equivalent to $C_{ps}[(P_t-P_s)/(P_1-P_2)]^{½}$ where C_{ps} is the standard pitot tube coefficient (=1 for the standard pitot tube used in these experiments) and P_t-P_s is the differential pressure across the ports of the standard pitot tube.

The calibration procedure began by inserting the standard pitot-static tube into the wind tunnel so that the total pressure port was located in the center of the wind tunnel test section. The wind tunnel speed was set using the ΔP_P for the standard pitot-static tube and the gas temperature and barometric pressure. The standard pitot tube was then withdrawn from the wind tunnel test section, and the 3D test probe was inserted in its place.

Consistent with draft Method 2F, the 3D probes were first checked to ensure that they were actually pointing directly into the flow. (The Method 2F calibration procedure requires flow direction to be

axial.) Probes were yaw nulled by inserting the probe head into the center of the wind tunnel and rotating the probe until the digital inclinometer read 0°. At that point, the 3D probe was properly aligned and ready for calibration.

Using the digital inclinometer, pitch angles were established to within ±0.5°. With the 3D probe oriented at 0° pitch and yaw nulled, readings of P_1-P_2 and P_4-P_5 were taken. These steps were repeated for each pitch angle (-30, -20, -15, -10, -5, 0, 5, 10, 15, 20, 30°), and the calibrations were performed at 30, 60, and 90 fps. The F_1 and F_2 ratios obtained for each pitch angle in the three flow ranges were averaged, and the average values were plotted against pitch angle. A smooth line was then drawn through the data points. For each calculated F_1 value at each velocity, the angles and the corresponding F_2 values were determined from the smoothed calibration curve; differences from the actual measured angles and F_2 values were then determined. For F_1, Method 2F requires that the difference at each comparison be within ±2° for angles between 0° and 40°. For F_2 values, the difference must not exceed ±3.0% of the F_2 ratio at the same pitch angle. If these criteria cannot be met, the applicability of the calibration curve should be limited to a finite velocity range over which measurements within the specifications can be obtained.

3.0 MODIFIED KIEL PROBE EXPERIMENTS

The wind tunnel tests of the prototype Kiel probe were designed to:

- evaluate the sensitivity and accuracy of yaw angle determinations using the wake ports,
- evaluate the sensitivity and accuracy of yaw angle determinations using the Fechheimer ports,
- evaluate the sensitivity and accuracy of static pressure determinations using the wake ports,
- evaluate the sensitivity and accuracy of static pressure determinations at different pitch angles,
- determine whether the addition of a thermocouple would affect probe performance, and
- obtain a calibration coefficient.

3.1 COMPARISON OF WAKE PORTS AND FECHHEIMER PORTS IN DETERMINING YAW NULL

3.1.1 Test Procedures

Experiments were conducted at velocities of 30, 60, and 90 fps to evaluate the sensitivity and accuracy of yaw angle determinations using the wake ports and Fechheimer ports. In this experiment, the yaw angle sensitivities of wake port 1 (closest to the Kiel head) and wake port 4 (farthest from the Kiel head) were tested. The angular sensitivity of wake port 1 was determined using the following procedure. All wake ports except wake port 1 were covered with tape, and wake port 1 was oriented into the direction of flow. With the aid of a digital inclinometer, the probe was rotated so that the wake port was positioned at a yaw angle of -15° relative to the flow. The difference between the wake port pressure and the Kiel head pressure (ΔP_W) was read and recorded. This procedure was repeated at yaw angles of -10°, -5°, 0°, 5°, 10°, and 15°. ΔP_W vs. yaw angle was plotted for all three velocities. The entire procedure was repeated for wake port 4. No difference was observed between wake ports 1 and 4; therefore, wake ports 2 and 3 were not tested.

To evaluate the Fechheimer ports, the Kiel head port was oriented into the direction of flow. The probe was rotated so that the Kiel port was at a yaw angle of -15° to the flow as measured by the digital inclinometer. The pressure difference across the Fechheimer ports (ΔP_F) was read and recorded. This procedure was repeated at yaw angles of -10°, -5°, 0°, 5°, 10°, and 15°. ΔP_F vs. yaw angle was plotted for all three velocities. The entire procedure was repeated for wake port 4.

3.1.2 Yaw Nulling Results

Figures 3-1 through 3-6 present the results of the yaw angle sensitivity and accuracy tests. Each figure is a plot of ΔP_W and ΔP_F vs. yaw angle for a specific wake port and velocity (30, 60 or 90 fps). In all six plots, ΔP_W is approximately constant with yaw angle from -15° to 15°. This observation demonstrates that the wake port cannot be used to find the zero yaw angle (yaw null). Alternatively, at five of the six tested velocities, ΔP_F is shown to be a strong monotonic function of yaw angle and equals zero when yaw angle equals zero. Even in Figure 3-4 (wake port 4, velocity 30 fps) where ΔP_F vs. yaw angle is not monotonic, ΔP_F is zero only at the point where yaw angle equals zero. (The anomalous, non-monotonic behavior shown in this figure was repeatable but cannot be explained readily.)

The data shown in these plots are summarized in Table 3-1. Over the range in yaw angles of -15° to 15°, the largest variation in ΔP_W is 0.15 inches of water for wake port 1 and 0.05 for wake port 4. By contrast, the average slope of the ΔP_F vs. yaw angle plot is 0.13 inches/degree at 90 fps and 0.05 inches/degree at 60 fps (see also Figures 3-2, 3-3, 3-5, and 3-6). At 30 fps, ΔP_F changes by about 1.5 inches between yaw angles of -5° and 5°.

Table 3-1. ΔP as a Function of Yaw Angle for Wake Ports 1 and 4 of the Modified Kiel Probe Prototype

Differential Pressure[a]	Velocity (fps)	Yaw Angle (°)						
		-15	-10	-5	0.00	5	10	15
ΔP_{FW1}	30	-0.20	-0.15	-0.07	-0.002	0.07	0.12	0.19
	60	-0.90	-0.60	-0.30	-0.01	0.23	0.50	0.74
	90	-1.90	-1.40	-0.70	-0.10	0.50	1.30	1.95
ΔP_{W1}	30	0.34	0.34	0.34	0.34	0.34	0.35	0.35
	60	1.50	1.50	1.47	1.45	1.50	1.50	1.50
	90	3.20	3.20	3.20	3.15	3.30	3.30	3.35
ΔP_{FW4}	30	-0.20	-0.17	-0.85	-0.01	0.70	0.12	0.12
	60	-0.90	-0.65	-0.35	-0.02	0.28	0.53	0.71
	90	-2.00	-1.40	-0.70	0.00	0.60	1.30	1.95
ΔP_{W4}	30	0.31	0.33	0.33	0.33	0.33	0.33	0.33
	60	1.43	1.44	1.44	1.40	1.45	1.44	1.42
	90	3.20	3.23	3.25	3.20	3.20	3.21	3.20

[a] Nomenclature for this table:
ΔP_{FW1} = ΔP_F with wake port 1 open
ΔP_{W1} = ΔP_W between Kiel probe head and wake port 1
ΔP_{FW4} = ΔP_F with wake port 4 open
ΔP_{W4} = ΔP_W between Kiel probe head and wake port 4

3.2 Sensitivity and Accuracy of Static Pressure Determinations Using the Wake Ports

3.2.1 Test Procedures

After determining that the Fechheimer ports can be used for yaw nulling (see Section 3.1), a series of tests was conducted to evaluate the feasibility of using a wake port as the static pressure port for the Kiel probe across a range of pitch angles. To help assess the performance of the modified Kiel probe, the sensitivity and accuracy of pressure drop measurements made with the Kiel probe were compared to measurements of ΔP made with the standard Type S probe at similar velocities and pitch angles.

In these experiments, the modified Kiel probe (labeled MK1) was yaw nulled using the Fech-heimer ports, and ΔP_W was measured at pitch angles between -30° and 30° in 10° increments (but including -5° and 5°) at three velocities (30, 60 and 90 fps). Complete data sets were col-lected using wake ports 1, 3, and 4. Data for wake port 2 were collected only at 0°. At each measured point, ΔP_W, ΔP_P

(the pressure differential across the standard pitot tube), yaw angle as measured by the digital inclinometer, pitch angle, and temperature were recorded. The Type S probe was yaw nulled using the procedure described in Section 2.1.1, and ΔP, ΔP_P, yaw angle, pitch angle, and temperature were recorded. Three replicates of the S probe measurements were taken.

After the initial tests demonstrated that the modified Kiel probe could be used to measure static pressure and find a yaw null, a stainless steel wire—intended to mimic a thermocouple—was added to the probe (see Section 1.4) to determine whether a temperature-reading device added to the Kiel probe would affect probe performance. This modified prototype Kiel probe was identified as MK2. Only wake port 4 on the MK2 probe was tested. For MK2 only, additional sampling was conducted at 25, 28, 32, and 35 fps.

For each combination of pitch angle, velocity, and wake port, the calibration coefficient was calculated as:

$$C_{pw} = \sqrt{\frac{\Delta P_P}{\Delta P_W}} \qquad \textbf{(Eq. 3.1)}$$

where

ΔP_w = difference between wake port pressure and Kiel head pressure

C_{pw}, calculated at zero pitch and yaw, was plotted against velocity in the range of 30 to 90 fps in 10 fps increments. These plots were created for all four wake ports of the original probe (MK1), for wake port 4 of MK2, and for the three replicate Type S probes.

3.2.2 Results of Wake Port Evaluation

Figures 3–7 through 3–10 are plots of C_{pw} vs. velocity over the velocity range 30 to 90 fps for wake ports 1-4 for probe MK1. Three measurements were taken at each velocity. A line connects the means of each set of three measurements taken at each velocity and the bands show maxima and minima at each velocity. For each wake port, the means of C_{pw} between 40 and 90 fps are constant to within 0.02; however, C_{pw} increases by at least 0.03 as velocity decreases from 40 to 30 fps. Figure 3–11 is a plot of C_{pw} vs. velocity for MK2 with additional C_{pw} determinations at velocities of 25, 28, 32, and 35 fps. The behavior of this probe at velocities less than 40 fps markedly differs from the behavior at velocities greater than 40 fps, in that C_{pw} oscillates over a 0.03 range between 40 and 25 fps.

Similar plots for the three Type S probes are shown in Figures 3–12 through 3–14. The mean calibration coefficient, C_p, for each probe varies by 0.025 and 0.030 from 40 to 90 fps, with a minimum value at 40 fps and maximum value at 90 fps (but the curves are not monotonic in this range). For all three Type S probes, C_p increases by about 0.015 between 40 and 30 fps, but the value of C_p in this range is always less than the value of C_p at 90 fps. This increase at the low end of the velocity range is about half of the increase observed for the Kiel probes.

Figures 3–15 through 3–19 show curves fitted to the C_{pw} vs. velocity data over the range of 40 to 90 fps for the Kiel probe. (Velocity data at 30 fps were not used because of the apparent instability of the C_{pw} measurements below 40 fps noted above.) Data are fit with both a regression line having slope = 0 (assuming C_{pw} is independent of velocity) and an unconstrained regression line. Clearly, little difference between the horizontal and unconstrained fits is evident. Over the velocity range between 40 and 90 fps, the two regression lines for C_{pw} differ, at most, by less than 1%. Therefore, using a constant calibration factor for any of the wake ports in this velocity range is reasonable. These velocity-independent calibration coefficients, 0.737 and 0.742 for wake port 4 on probes MK1 and MK2, respectively, differ by less than 1%, and in both cases the mean square error (MSE) is less than $1x10^{-4}$ (see Figures 3-18 and 3-19). This comparison demonstrates that the addition of a thermocouple to the modified Kiel probe would not measurably affect the calibration coefficient at zero pitch and zero yaw.

Figures 3–20 through 3–22 show similar curve fits to the C_p vs. velocity data for the three Type S probes over the velocity range from 30 to 90 fps. Regressions constructed with slope = 0 (C_p constrained to be velocity-independent) for these probes yield calibration coefficients of 0.829, 0.832, and 0.828, all within less than 1% of each other. Similar to the results for the Kiel probe, mean square errors for these fits were around $1x10^{-4}$.

To determine the robustness of the modified Kiel probe with respect to pitch angle, ΔP_w was measured at pitch angles between -30° and 30° at constant velocity (30, 60, and 90 fps) for wake ports 1, 3, and 4. Figure 3–23 is a plot of C_{pw} vs. pitch angle at velocities of 30, 60, and 90 fps for wake port 1 of probe MK1. Figures 3–24 and 3–25 are similar plots for wake ports 3 and 4 of probe MK1. Figure 3–26 shows C_{pw} vs. pitch angle for wake port 4 of probe MK2. For comparison, Figure 3–27 plots C_p vs. pitch angle for one of the Type S probes (Probe S-1) at the same three velocities.

Figure 3–23 demonstrates that C_{pw} for wake port 1 depends strongly on pitch angle at all three velocities and that the dependence on pitch is similar at all three velocities. Figure 3–24 shows that the dependence of C_{pw} on pitch angle is much reduced for wake port 3 when compared to wake port 1. Figures 3–25 and 3–26 show that for wake port 4 the C_{pw} vs. pitch angle curve for wake port 4 on both MK1 and MK2 is relatively flat and that the "thermocouple" does not affect this pitch angle independence. For wake ports 1 and 3, C_{pw} varies linearly between pitch angles of -20° and 20° and remains unchanged between -30° and -20° and between 20° and 30°. The dependence of C_p on pitch angle is similar at each tested velocity.

Table 3–2 quantitatively summarizes the stability of the calibration coefficients across pitch angles for the modified Kiel probes and the Type S probe. The table lists the range of calibration coefficients for each wake port and the Type S probe at each velocity across the range of pitch angles. The stability of the modified Kiel probe with respect to pitch angle improves markedly as the location of the wake port is moved farther from the Kiel head. The Type S probe is more sensitive to changes in pitch angle than any Kiel probe configuration, with changes in C_p ranging from 26.52% to 29.51% over the measured pitch-angle range. The largest change in C_p for the Type S probe occurs at pitch angles beyond ±20°. In the range of -20° to 20°, the pitch sensitivity of the Type S probe ranges

from 6.10% to 9.00% (see Figure 3-27), similar to the sensitivity of the modified Kiel probe with wake port 3, which ranges from 7.49% to 9.91% (see Figure 3-25).

Table 3-2. Calibration Coefficients Across Pitch Angles[a] for Various Wake Ports of the Modified Kiel Probe Prototypes (MK1 and MK2)[b] and for the Type S (S-1) Probe at 0° Yaw

	Velocity (fps)														
	30					60					90				
	MK1			MK2		MK1			MK2		MK1			MK2	
	W1[d]	W3	W4	W4	Type S	W1	W3	W4	W4	Type S	W1	W3	W4	W4	Type S
Minimum	0.71	0.77	0.76	0.75	0.84	0.67	0.72	0.74	0.72	0.80	0.67	0.72	0.73	0.72	0.79
Mean[c]	0.78	0.80	0.78	0.78	0.90	0.75	0.75	0.75	0.75	0.86	0.76	0.75	0.75	0.75	0.87
Maximum	0.86	0.84	0.81	0.80	1.06	0.82	0.78	0.77	0.76	1.03	0.82	0.78	0.76	0.76	1.03
Range	0.14	0.08	0.06	0.05	0.22	0.15	0.06	0.03	0.05	0.23	0.15	0.05	0.03	0.05	0.23
% Change[e]	20.03	9.91	7.55	6.01	26.52[f]	21.64	8.09	3.94	6.03	29.43[g]	22.26	7.49	3.96	6.28	29.51[h]

[a] Pitch angles from -30° to 30°

[b] MK1 is the modified Kiel probe prototype; MK2 is the modified Kiel probe prototype with mock thermocouple

[c] Average of three replicates

[d] W1 = Wake Port 1
W3 = Wake Port 3
W4 = Wake Port 4

[e] $$\%\ change\ in\ C_{pw} = \frac{\left|\max C_{pw} - \min C_{pw}\right|}{\min C_{pw}}\ 100$$

[f] % change = 6.10% between -20° and +20°

[g] % change = 7.80% between -20° and +20°

[h] % change = 9.00% between -20° and +20°

3.3 CONCLUSIONS

The test results described in this section lead to the following conclusions regarding the prototype modified Kiel probe:

- Wake ports are too insensitive to be used for yaw nulling.
- Fechheimer ports can be used to yaw null with an accuracy of better than 1° at velocities between 40 and 90 fps and at all pitch angles in the range ±30°.
- At pitch and yaw angles equal to zero, a wake port placed between 1-3/8 inches and 3-5/8 inches from the Kiel head can be used to measure static pressure. For velocities between 40 and 90 fps, each port can be used to derive a constant calibration coefficient.
- For a wake port located 3-5/8 inches from the Kiel port, pressure drop measured by the probe is independent of pitch angle in the range ±30°; for wake ports placed closer to the Kiel head, measured pressure drop is dependent on pitch angle.
- Thus, the modified Kiel probe using wake port 4 can be used to determine total stack flow and yaw angle in the velocity range 40 to 90 fps for pitch angles in the range ±30°. The probe cannot be used to determine pitch angle.

Figure 3-1. Delta Pw and Delta Pf vs. Yaw Angle:
Modified Kiel - Wake Port 1 - 30 fps

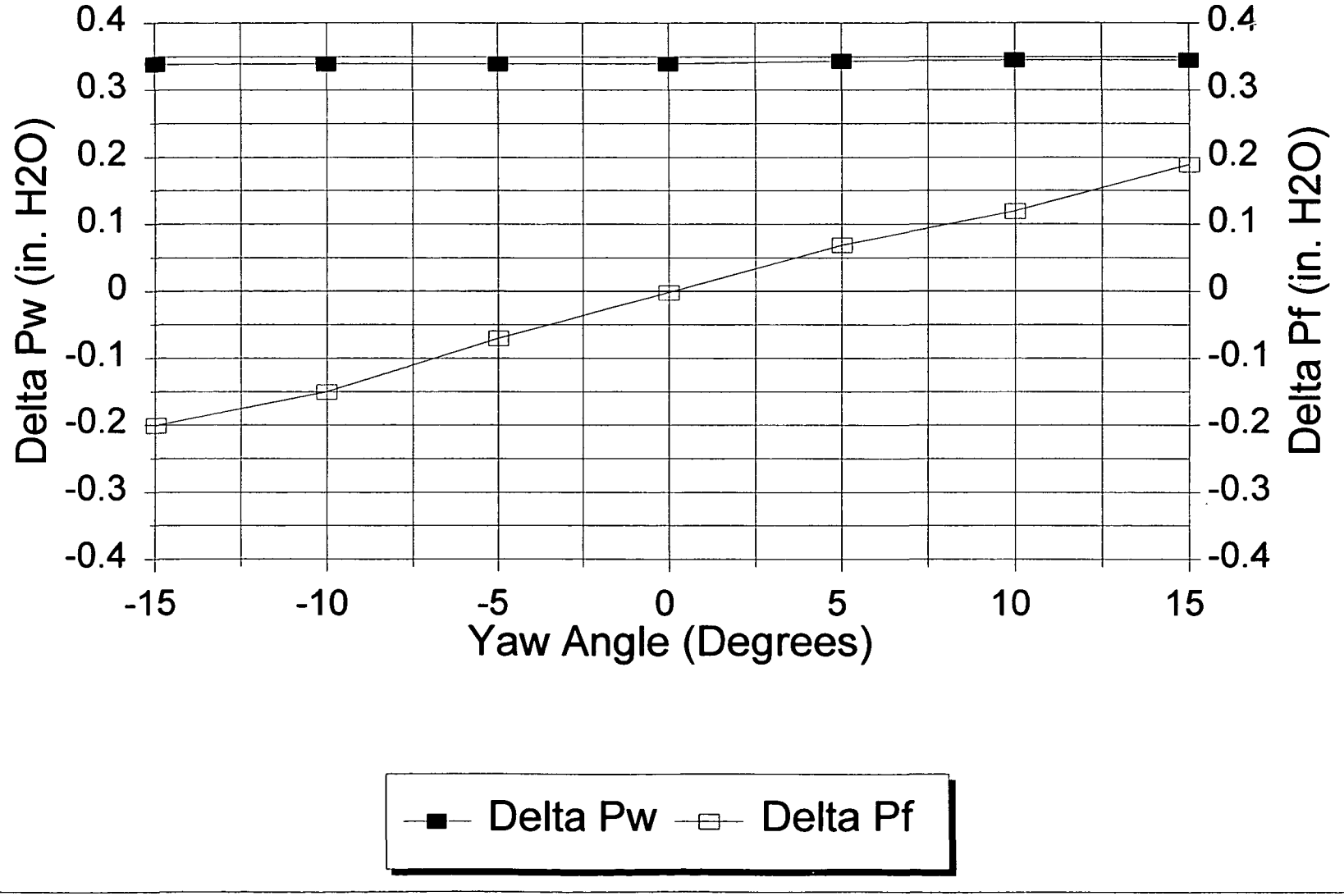

Figure 3-2. Delta Pw and Delta Pf vs. Yaw Angle:
Modified Kiel - Wake Port 1 - 60 fps

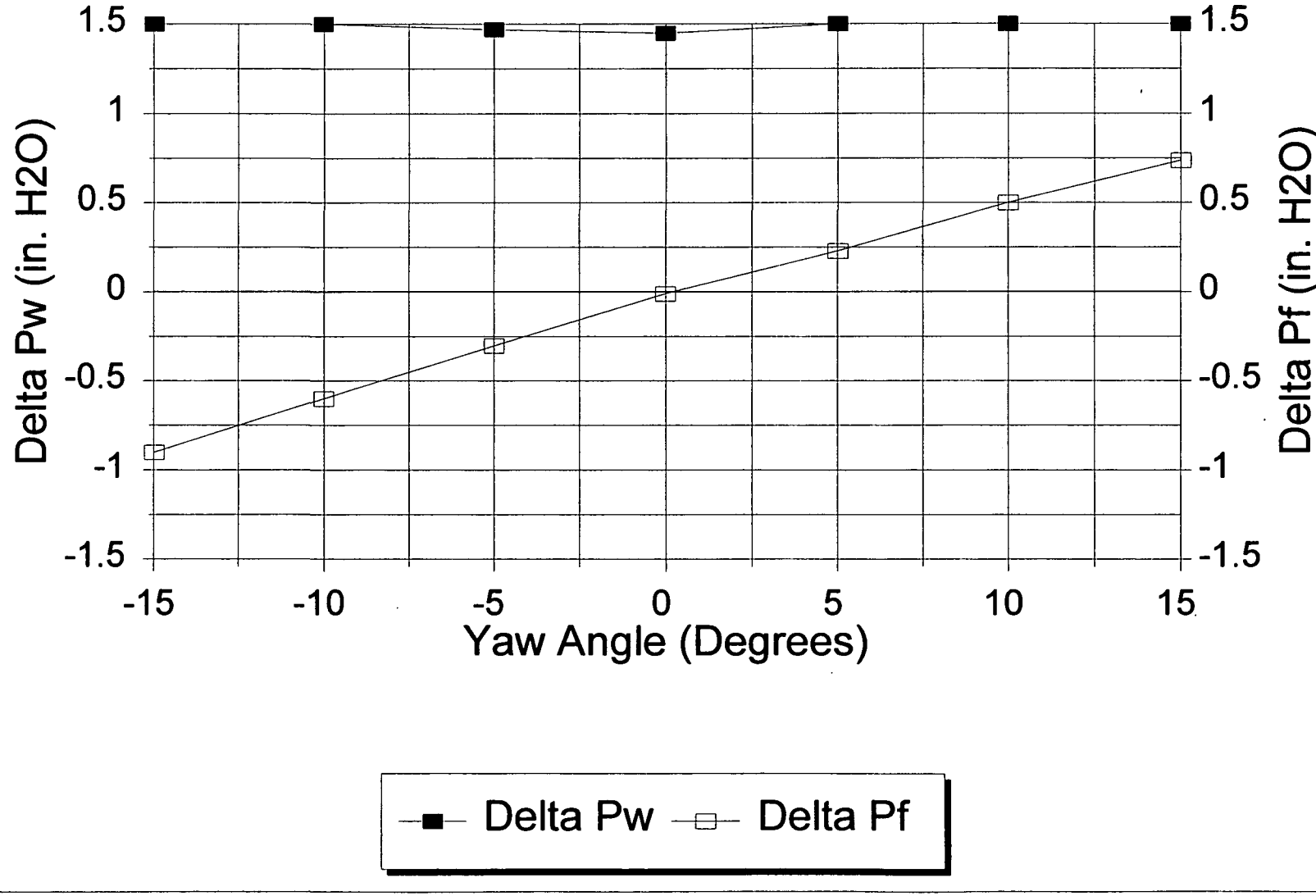

Figure 3-3. Delta Pw and Delta Pf vs. Yaw Angle:
Modified Kiel - Wake Port 1 - 90 fps

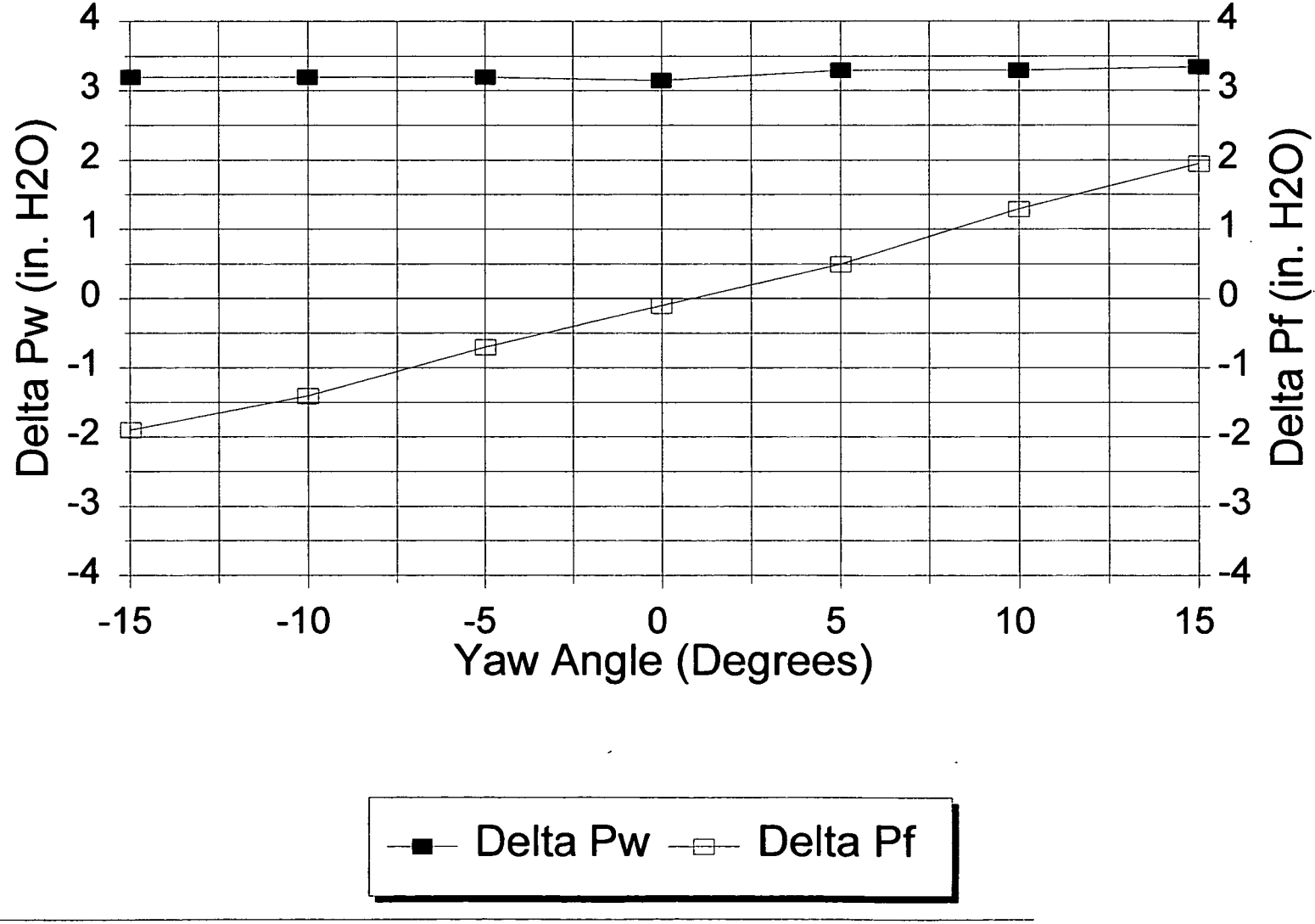

Figure 3-4. Delta Pw and Delta Pf vs. Yaw Angle:
Modified Kiel - Wake Port 4 - 30 fps

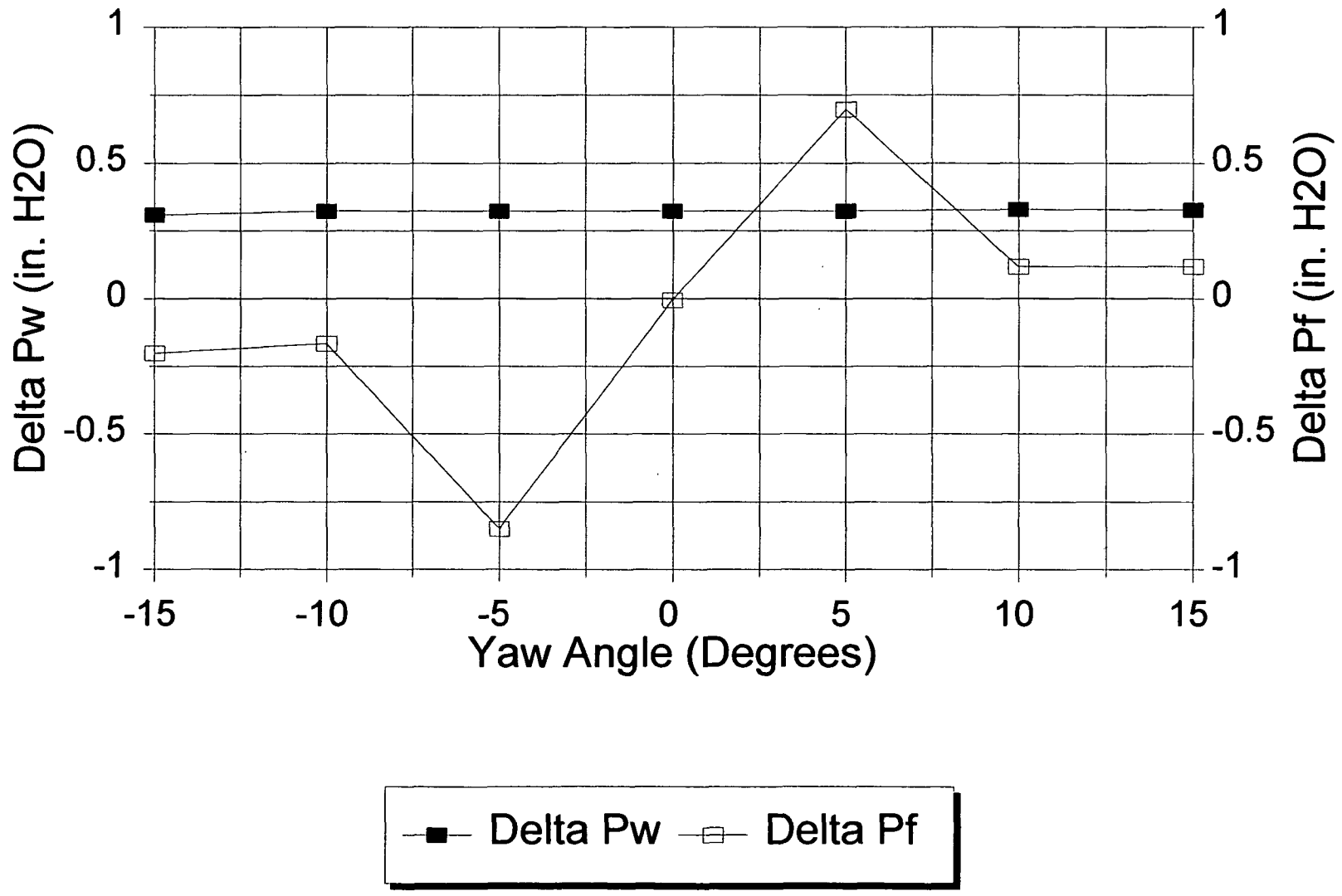

Figure 3-5. Delta Pw and Delta Pf vs. Yaw Angle:
Modified Kiel - Wake Port 4 - 60 fps

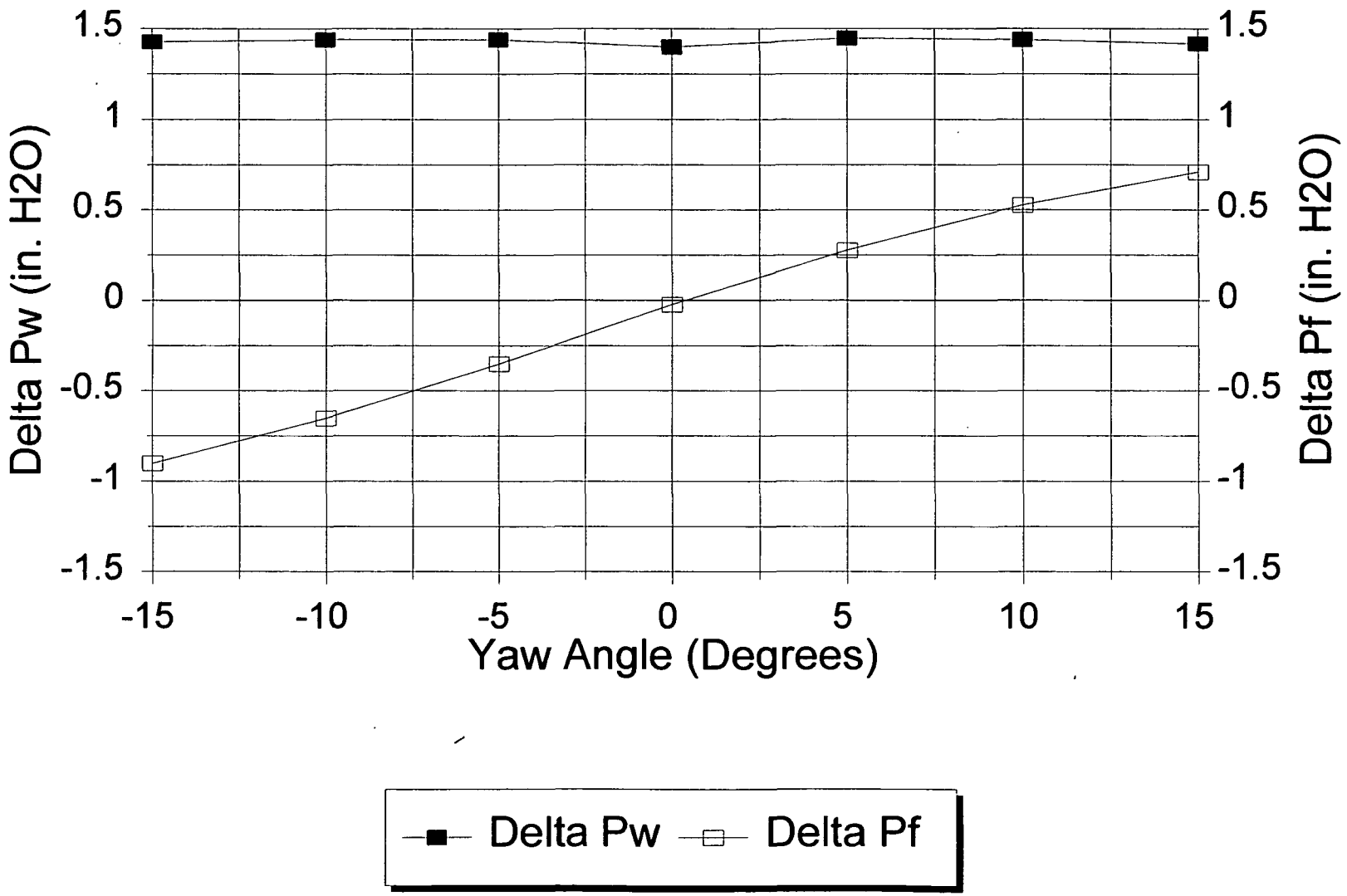

Figure 3-6. Delta Pw and Delta Pf vs. Yaw Angle:
Modified Kiel - Wake Port 4 - 90 fps

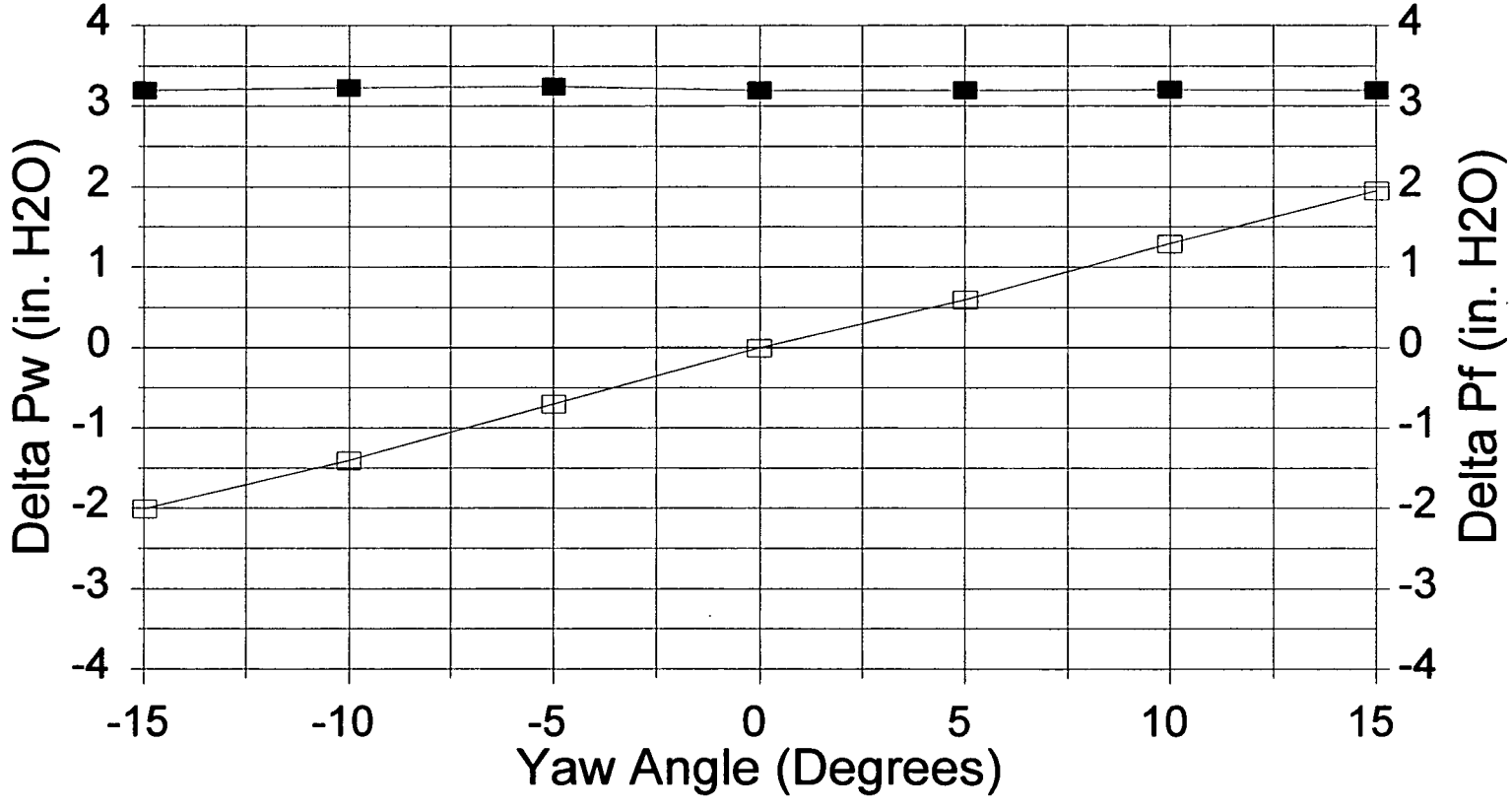

Figure 3-7. Probe: Modified Kiel - MK1

Wake Port Calibration Coefficients

Wake Port=1

Pitch=0, Yaw=0

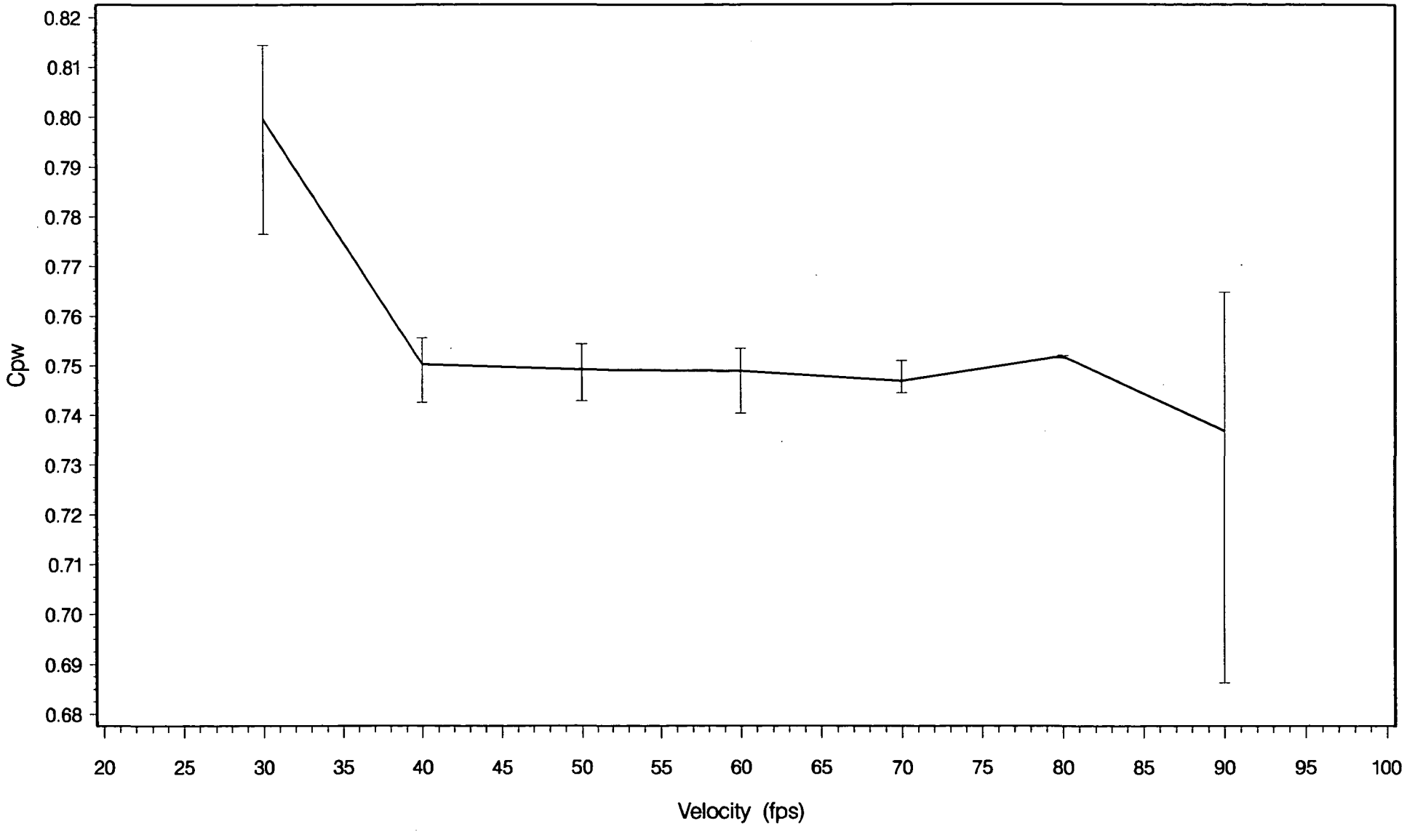

Bands Indicate the Minimum and Maximum Values

c:flow\statpres\mk1stata.dat; c:\sas\mk1plot4.sas

Figure 3-8. Probe: Modified Kiel - MK1

Wake Port Calibration Coefficients

Wake Port = 2

Pitch = 0, Yaw = 0

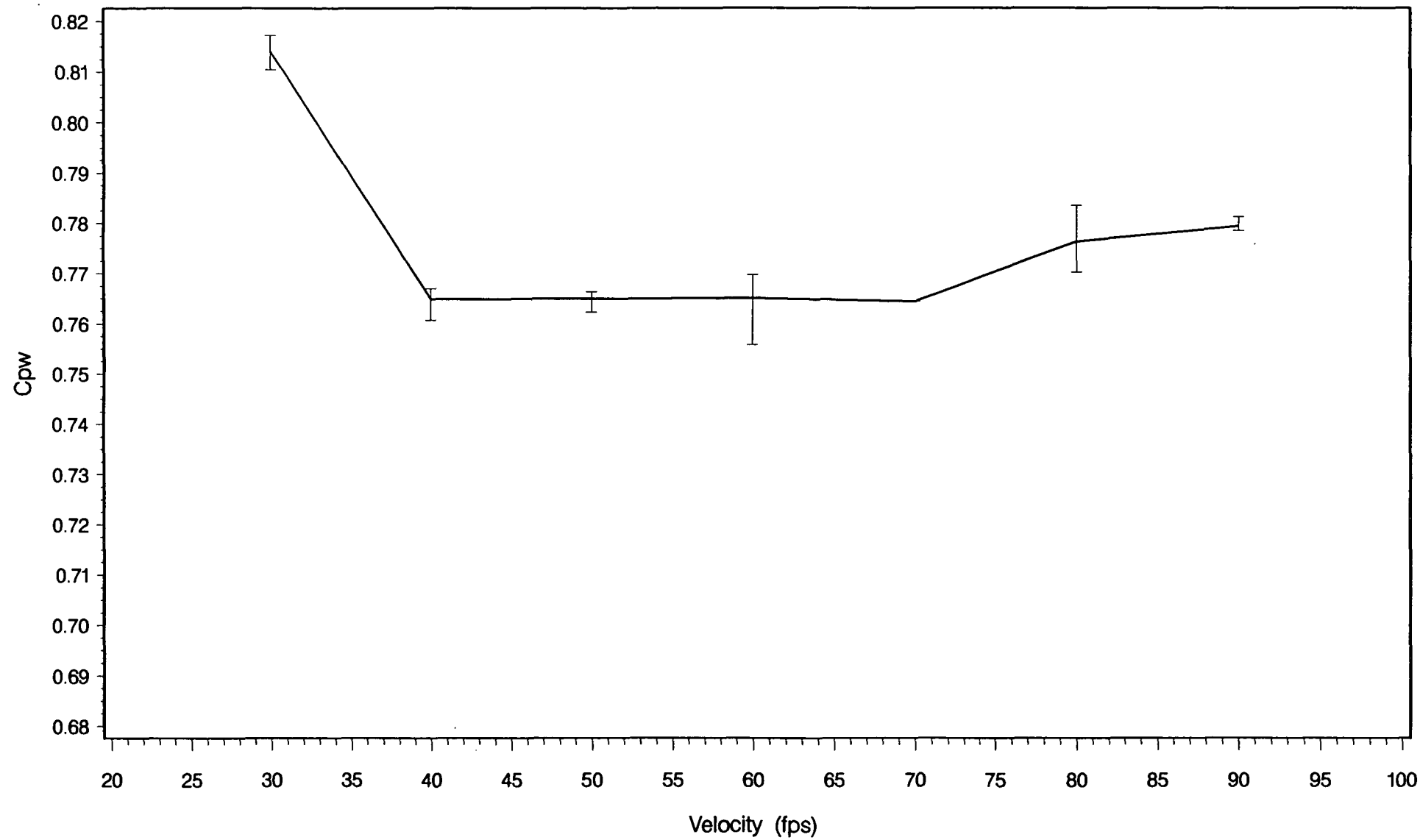

Bands Indicate the Minimum and Maximum Values

c:flow\statpres\mk1stata.dat; c:\sas\mk1plot4.sas

Figure 3−9. Probe: Modified Kiel − MK1

Wake Port Calibration Coefficients

Wake Port = 3

Pitch = 0, Yaw = 0

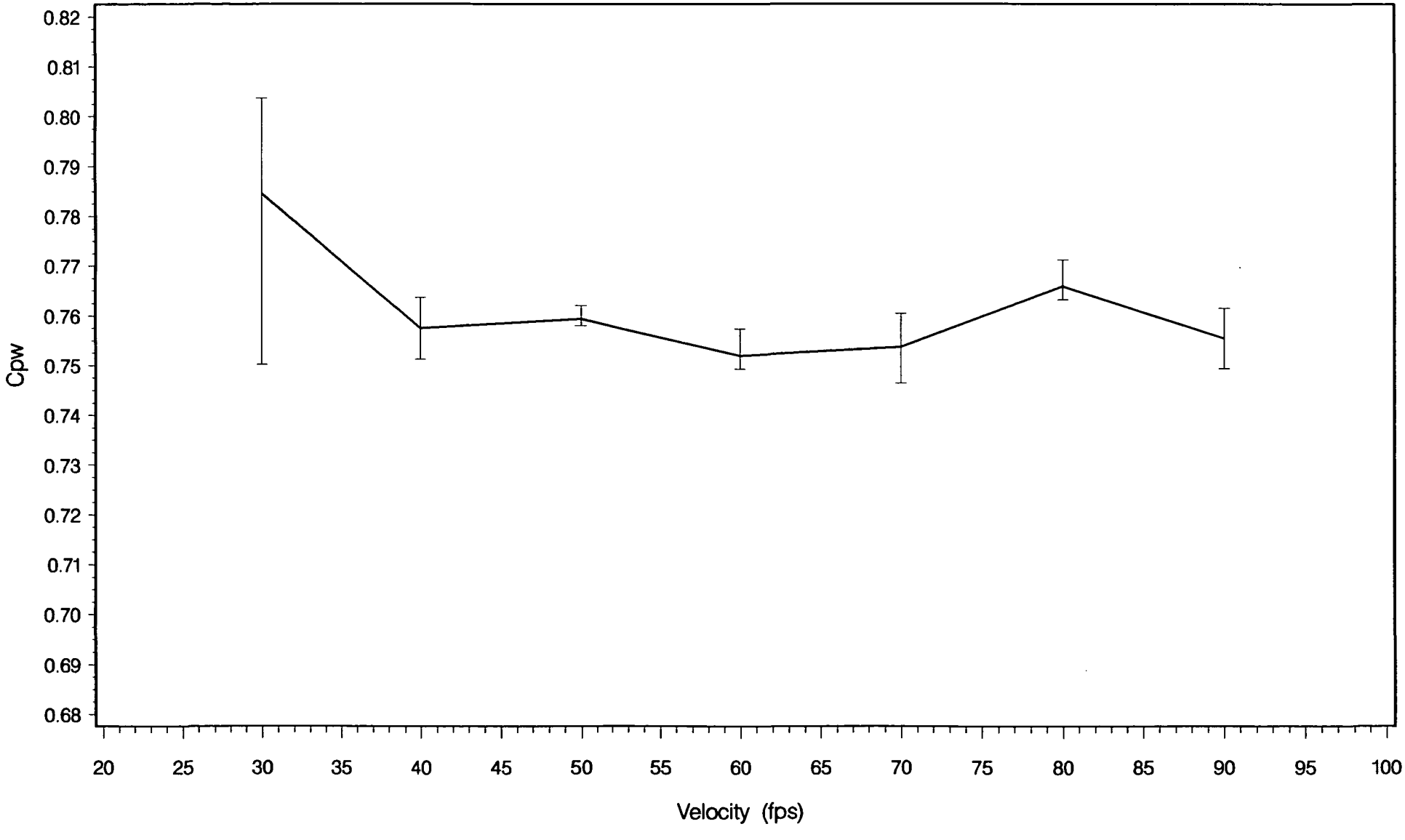

Bands Indicate the Minimum and Maximum Values

c:flow\statpres\mk1stata.dat; c:\sas\mk1plot4.sas

Figure 3-10. Probe: Modified Kiel - MK1

Wake Port Calibration Coefficients

Wake Port = 4

Pitch = 0, Yaw = 0

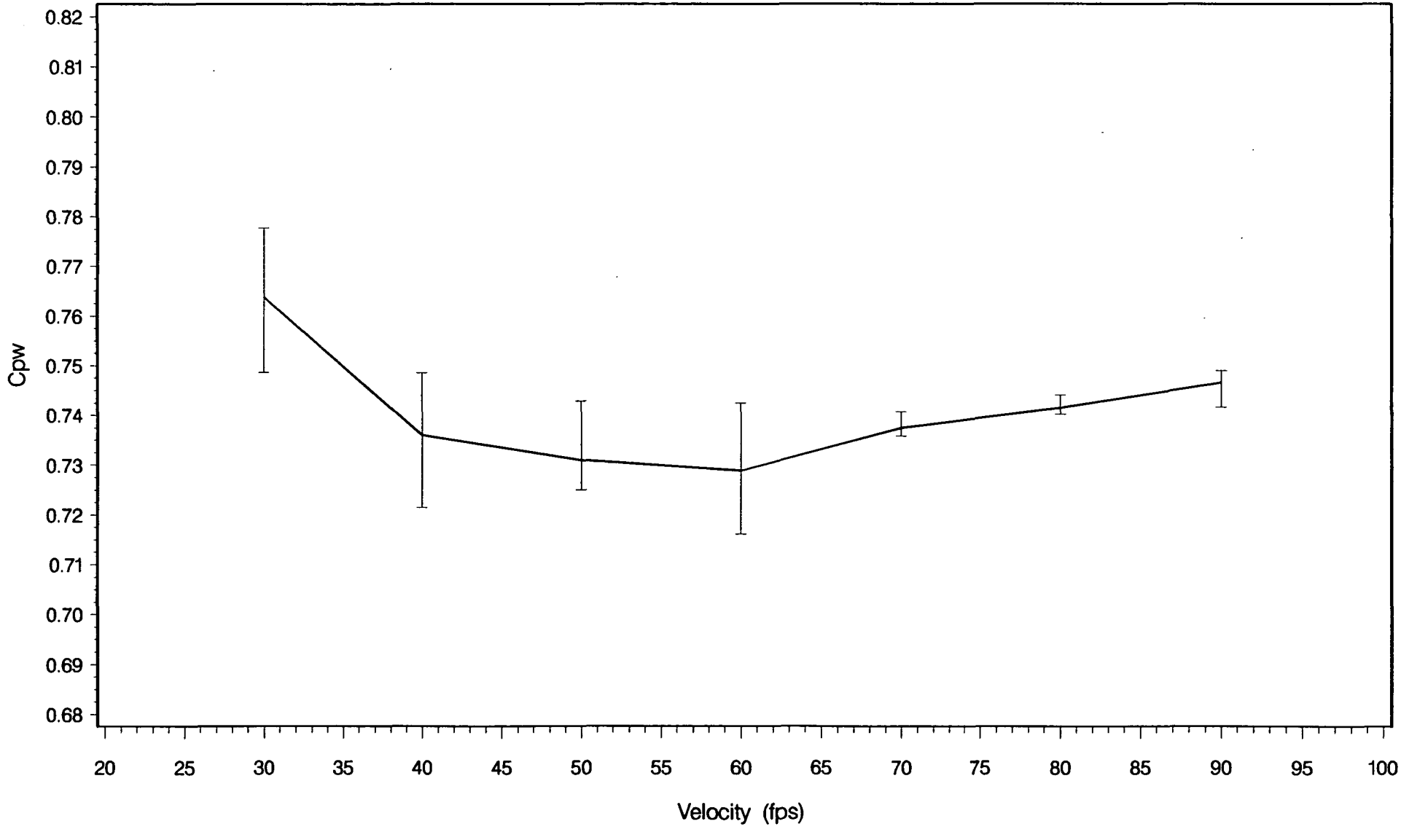

Bands Indicate the Minimum and Maximum Values

c:flow\statpres\mk1stata.dat; c:\sas\mk1plot4.sas

Figure 3-11. Probe: Modified Kiel With Thermocouple-MK2

Wake Port Calibration Coefficients

Wake Port = 4

Pitch = 0, Yaw = 0

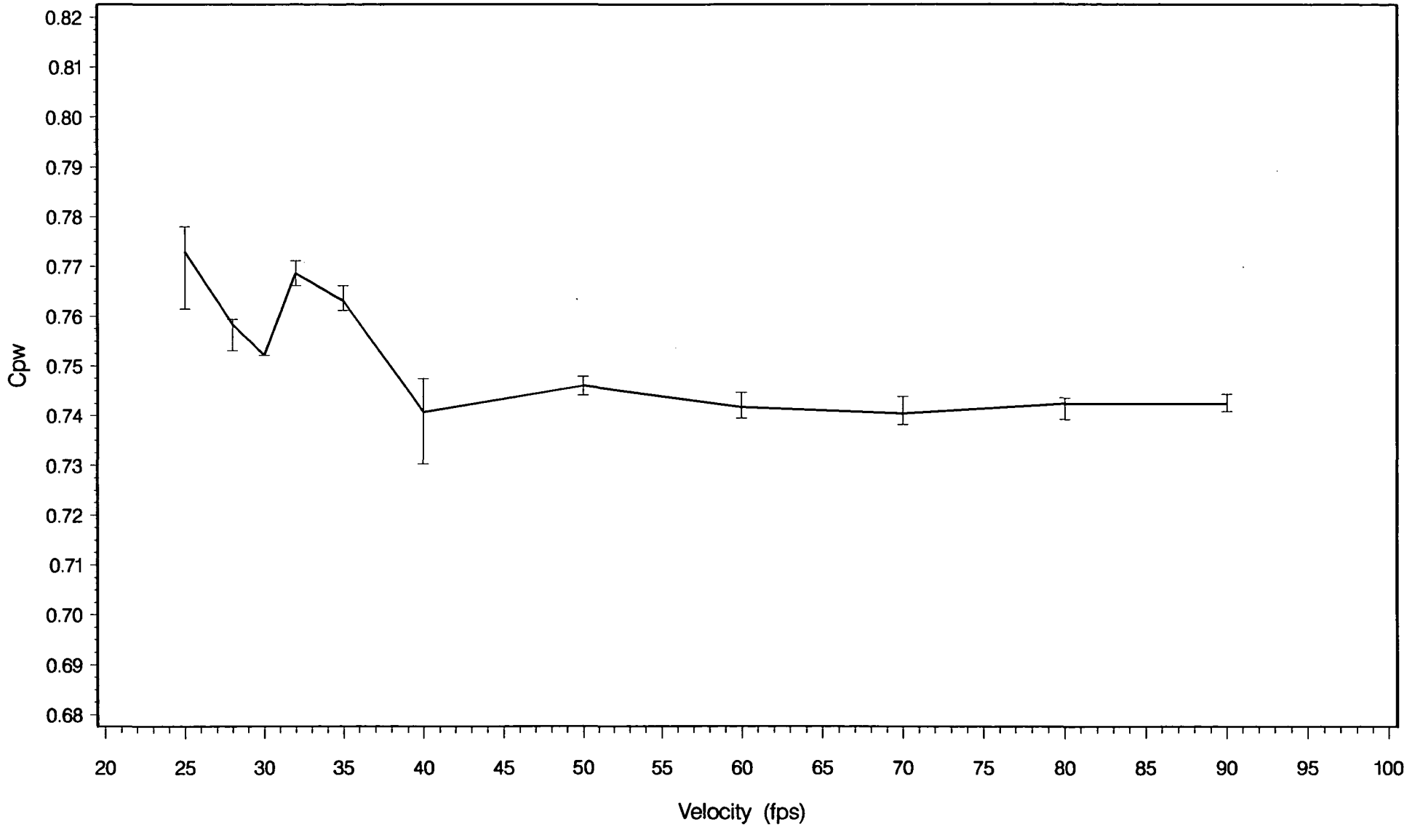

Bands Indicate the Minimum and Maximum Values

mk2cala.dat mk2plot1.sas

Figure 3-12. Probe: 3/8" Type S-1

Calibration Coefficients

Pitch = 0, Yaw = 0

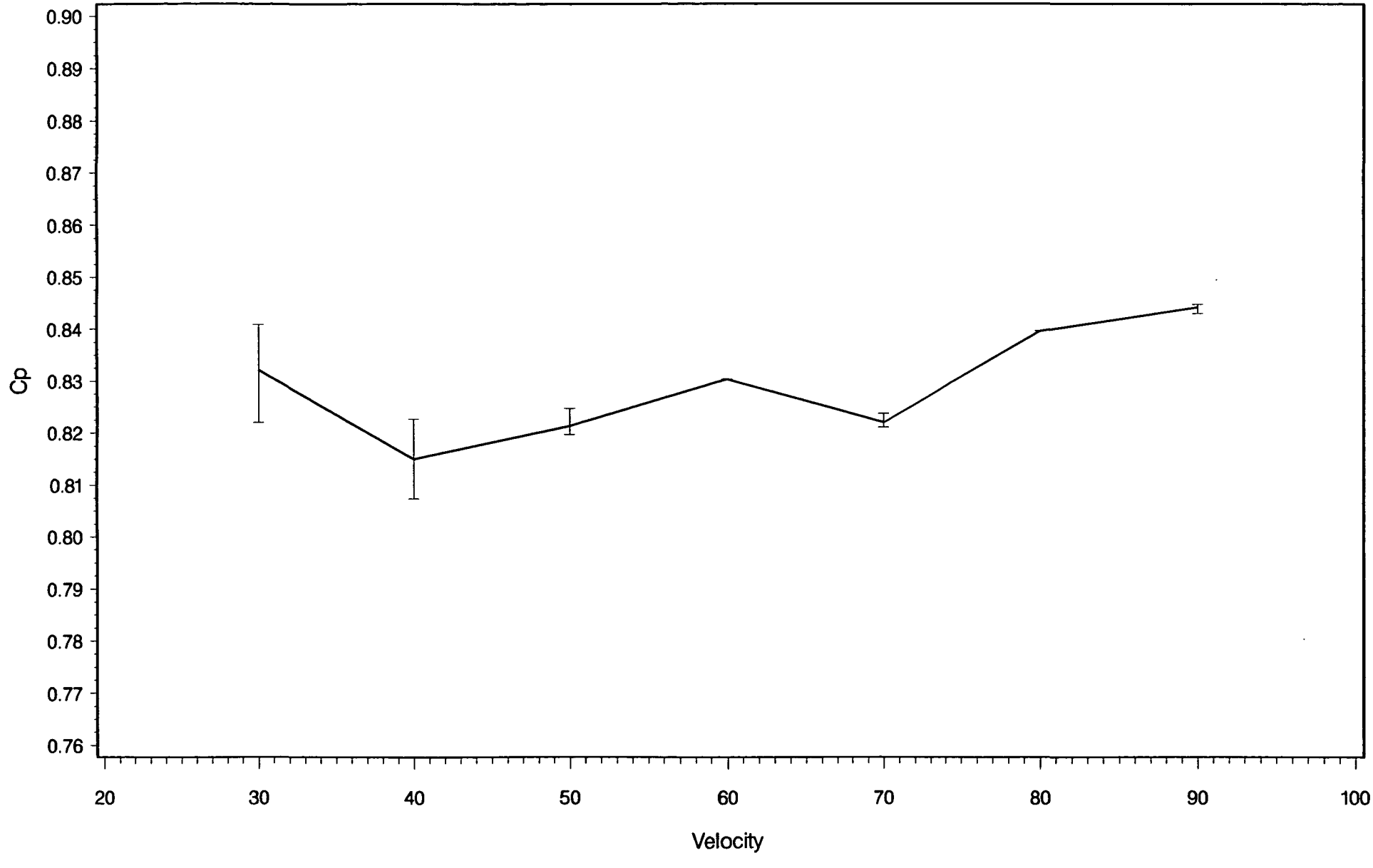

Bands Indicate the Minimum and Maximum Values

3-81cal2.dat 3-81c2pl.sas

Figure 3-13. Probe: 3/8" Type S-2

Calibration Coefficients

Pitch = 0, Yaw = 0

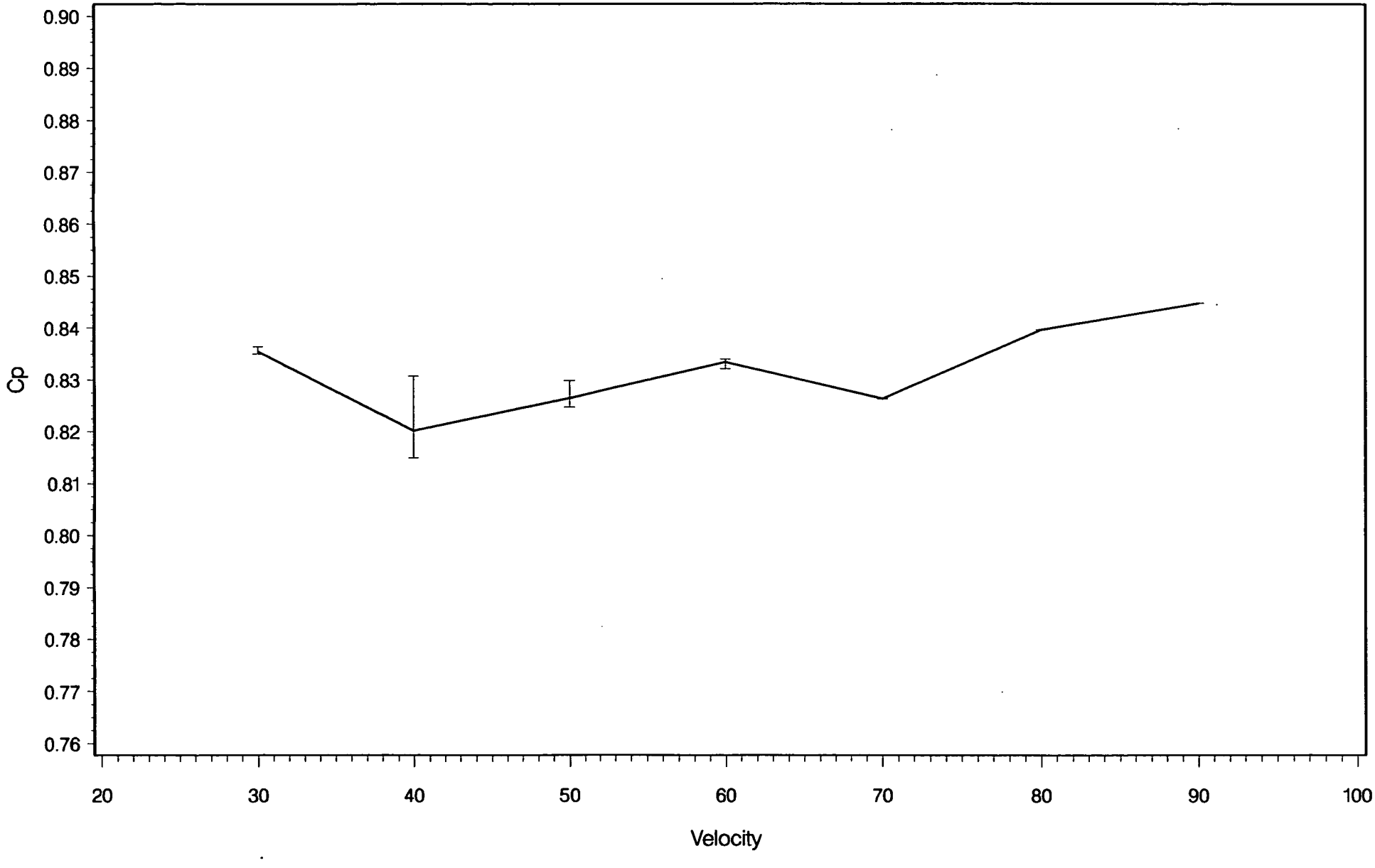

Bands Indicate the Minimum and Maximum Values

3-82cal2.dat 3-82c2pl.sas

Figure 3-14. Probe: 3/8" Type S-3

Calibration Coefficients

Pitch = 0, Yaw = 0

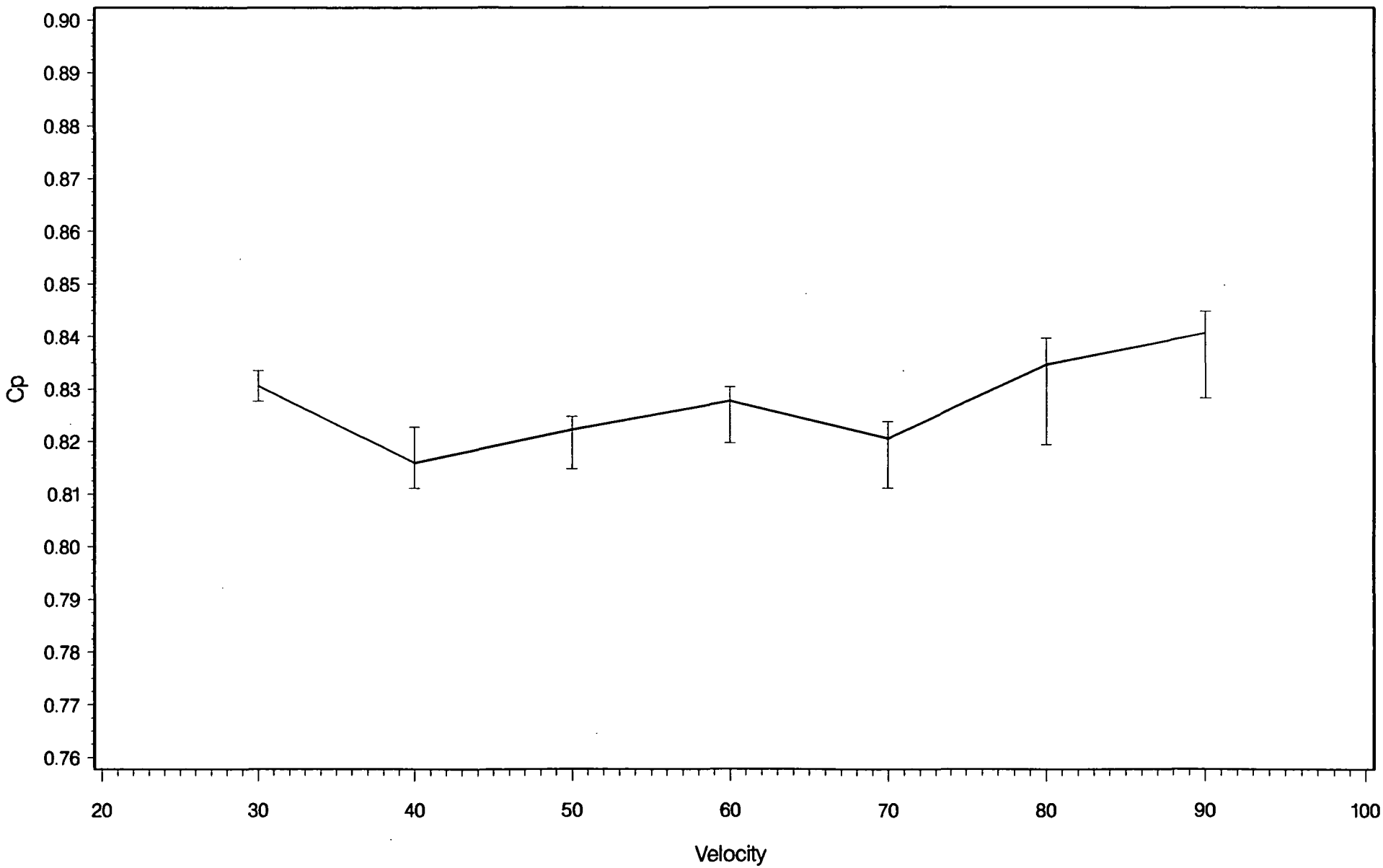

Bands Indicate the Minimum and Maximum Values

3-83cal2.dat 3-83c2pl.sas

Figure 3-15. Probe: Modified Kiel – MK1

Wake Port Calibration Coefficient

Wake Port=1

Pitch=0, Yaw=0

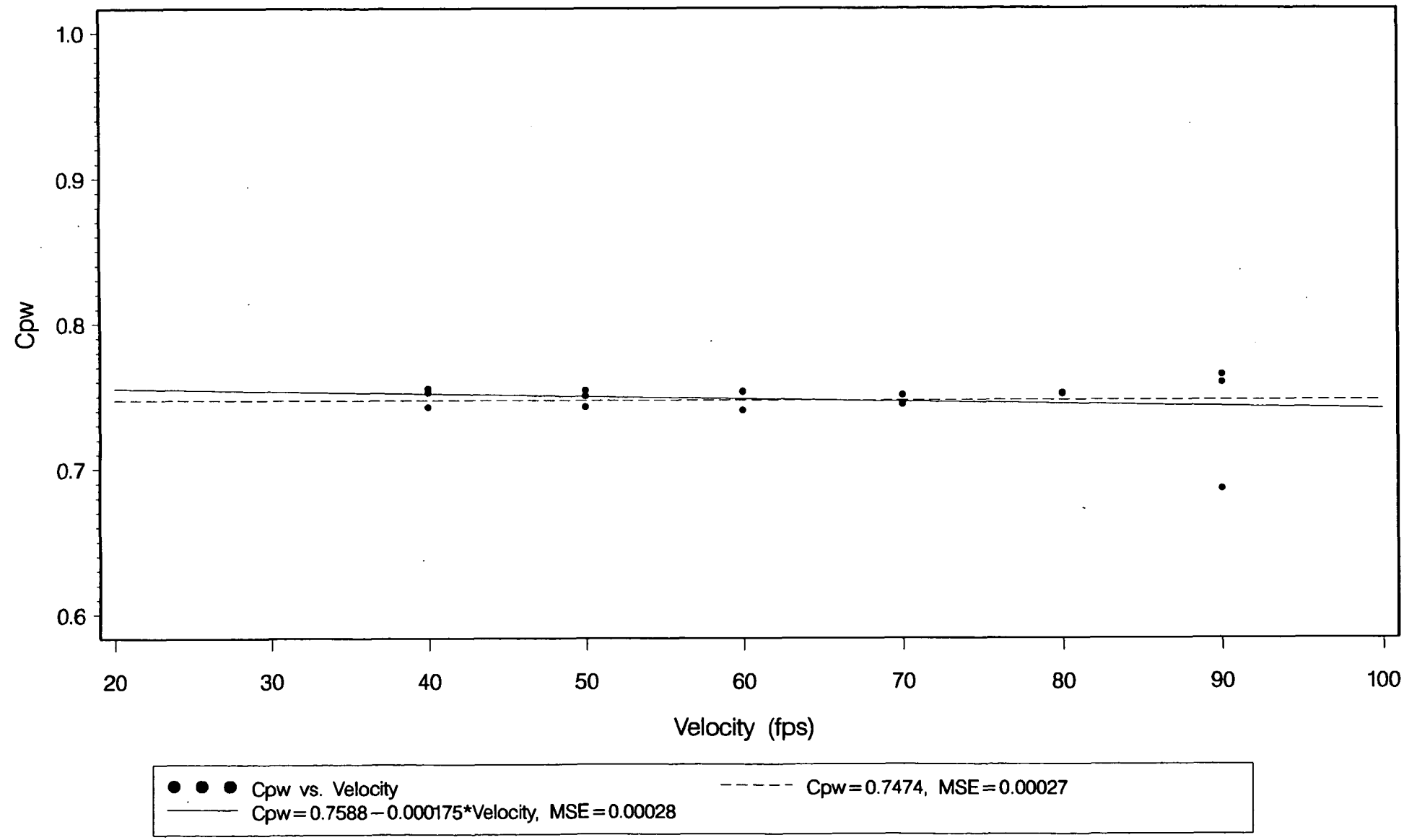

mk1stata.sd2]:regavg.sas

Figure 3−16. Probe: Modified Kiel − MK1

Wake Port Calibration Coefficient

Wake Port = 2

Pitch = 0, Yaw = 0

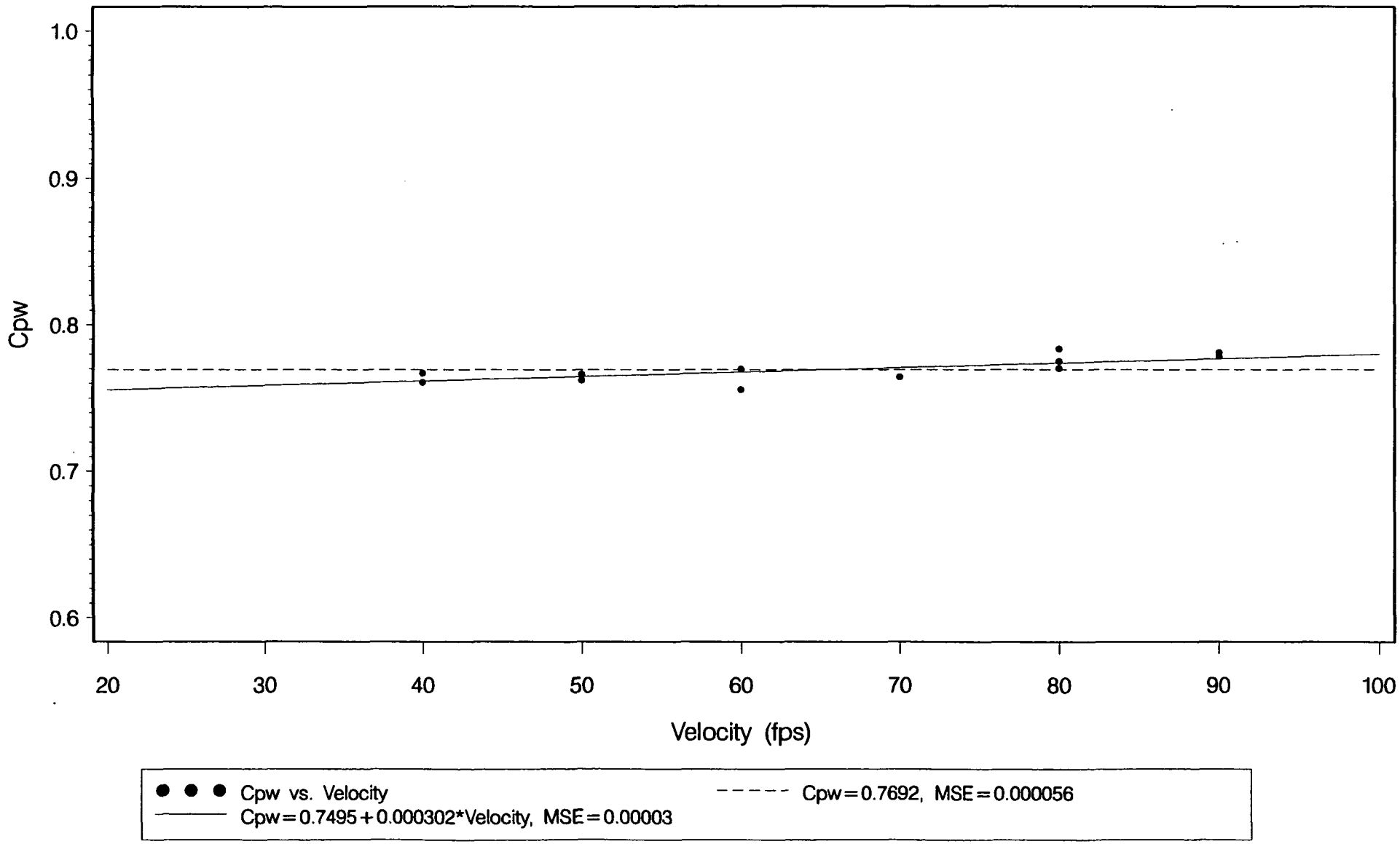

mk1stata.sd2 j:regavg.sas

Figure 3-17. Probe: Modified Kiel - MK1

Wake Port Calibration Coefficient

Wake Port = 3

Pitch = 0, Yaw = 0

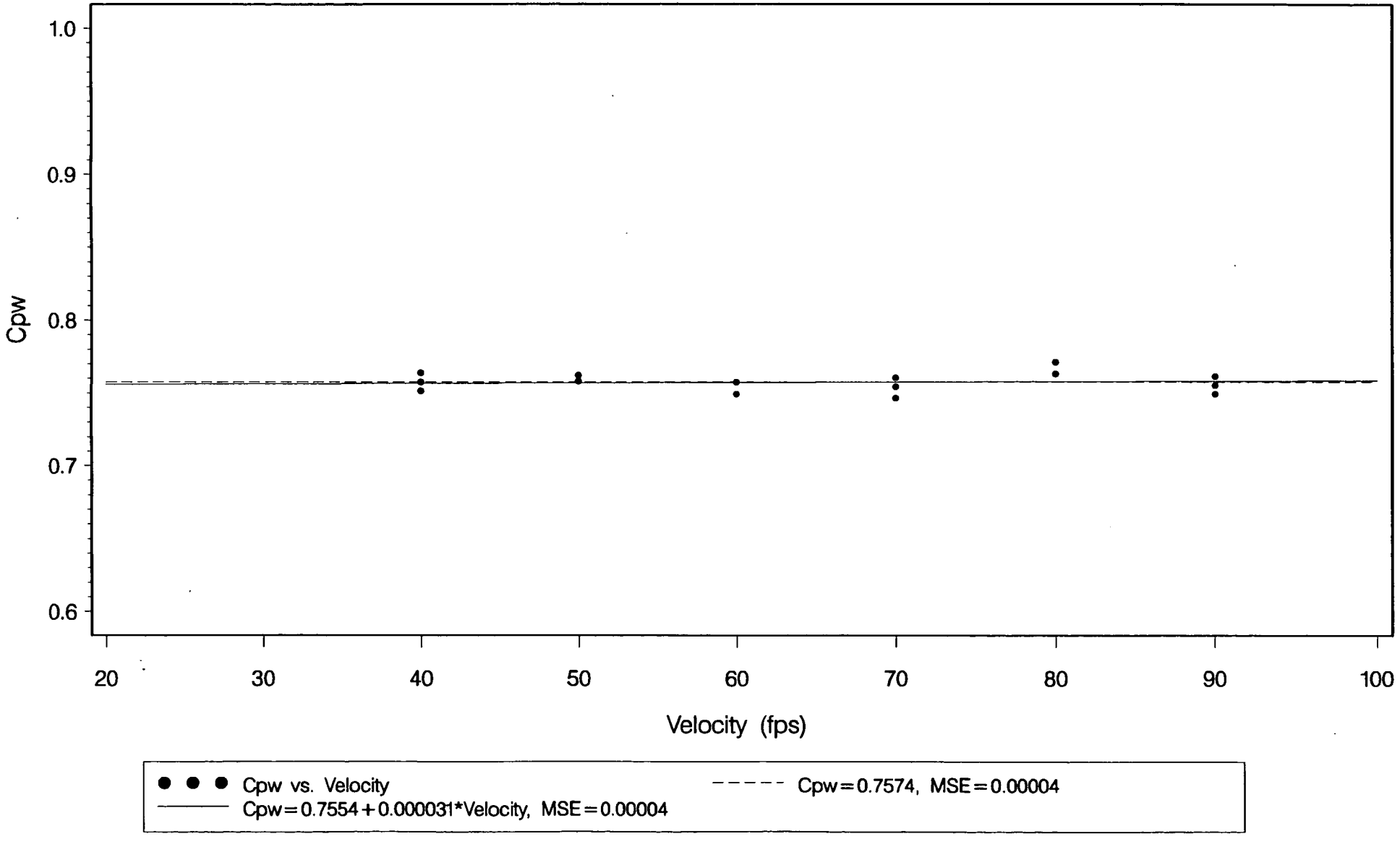

mk1stata.sd2]:regavg.sas

Figure 3–18. Probe: Modified Kiel – MK1

Wake Port Calibration Coefficient

Wake Port = 4

Pitch = 0, Yaw = 0

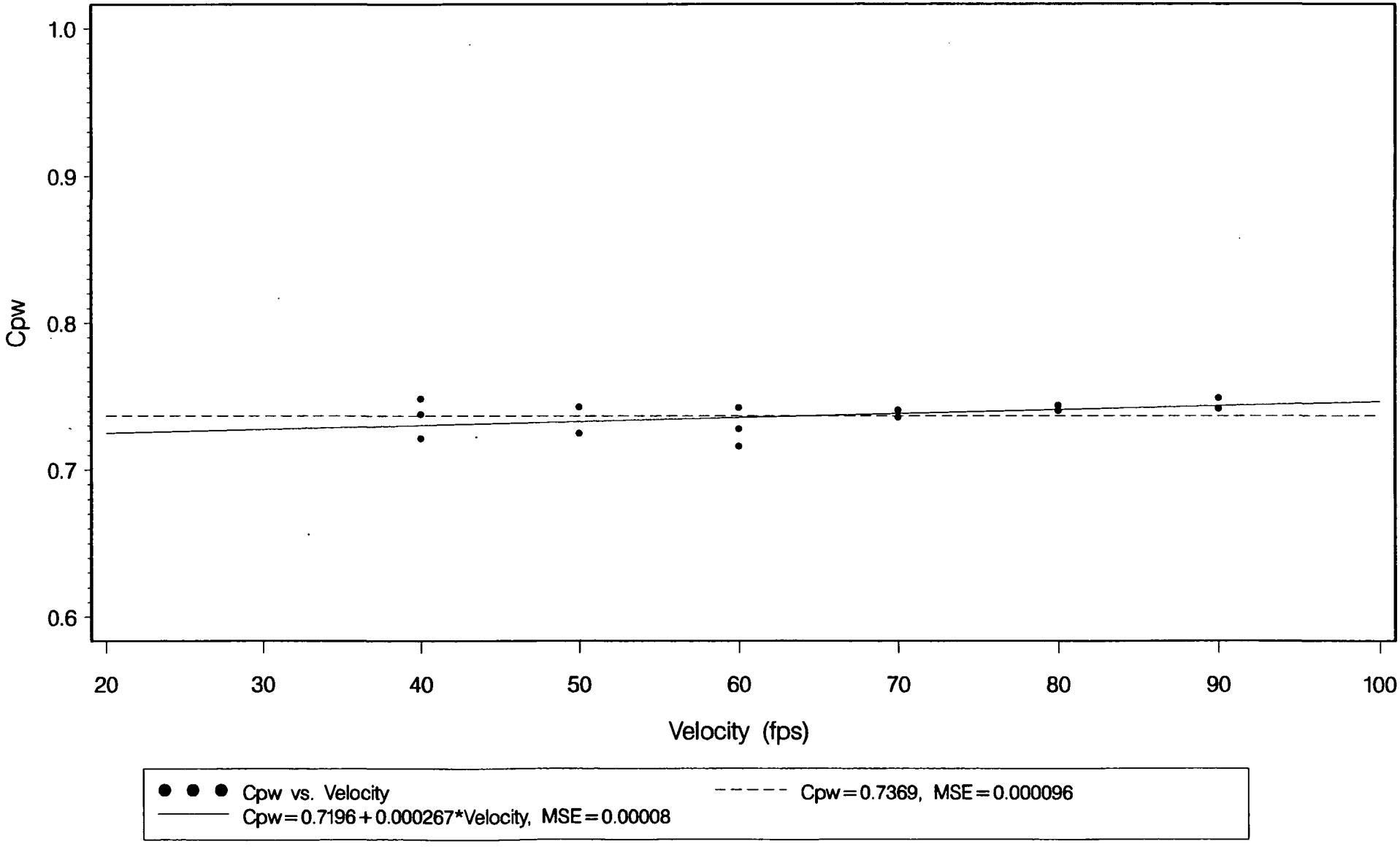

mk1stata.sd2 j:regavg.sas

Figure 3-19. Probe: Modified Kiel With Thermocouple - MK2

Wake Port Calibration Coefficient

Wake Port = 4

Pitch = 0, Yaw = 0

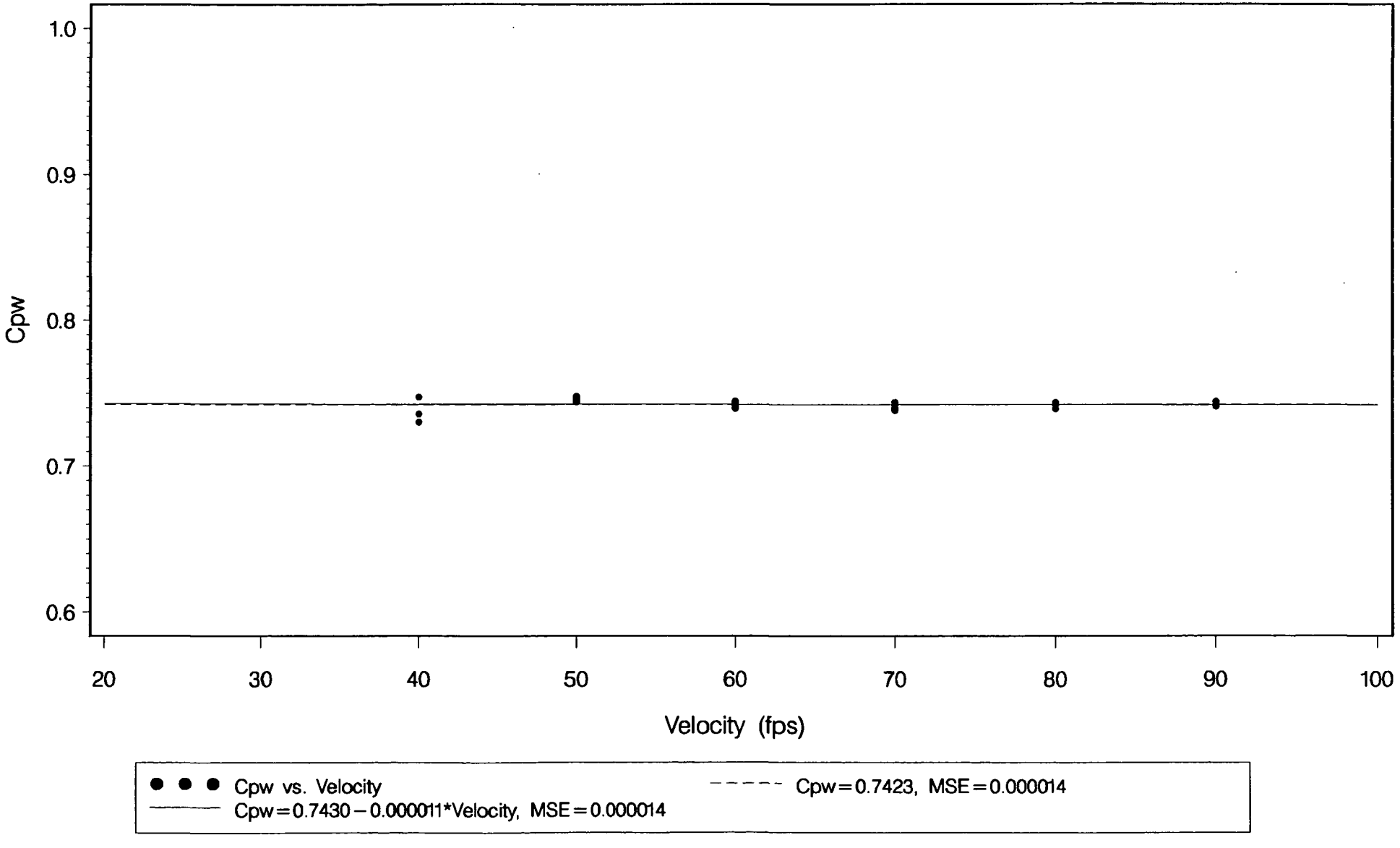

mk2cala.sd2]:regavg.sas

Figure 3-20. Probe: 3/8" Type S-1

Calibration Coefficient

Pitch = 0, Yaw = 0

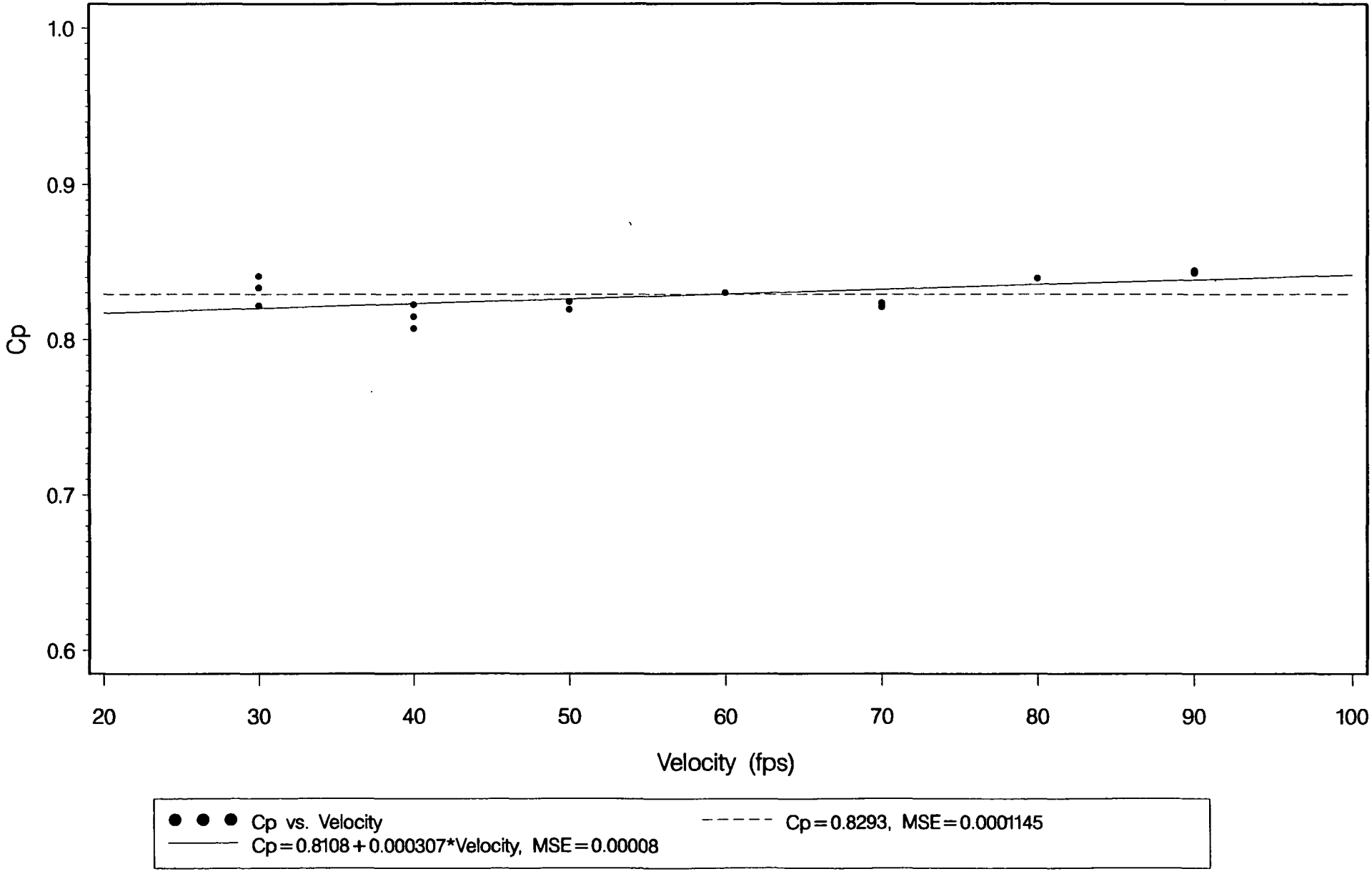

cal2_381.sd2 j:regavg.sas

Fgure 3−21. Probe: 3/8" Type S−2

Calibration Coefficient

Pitch = 0, Yaw = 0

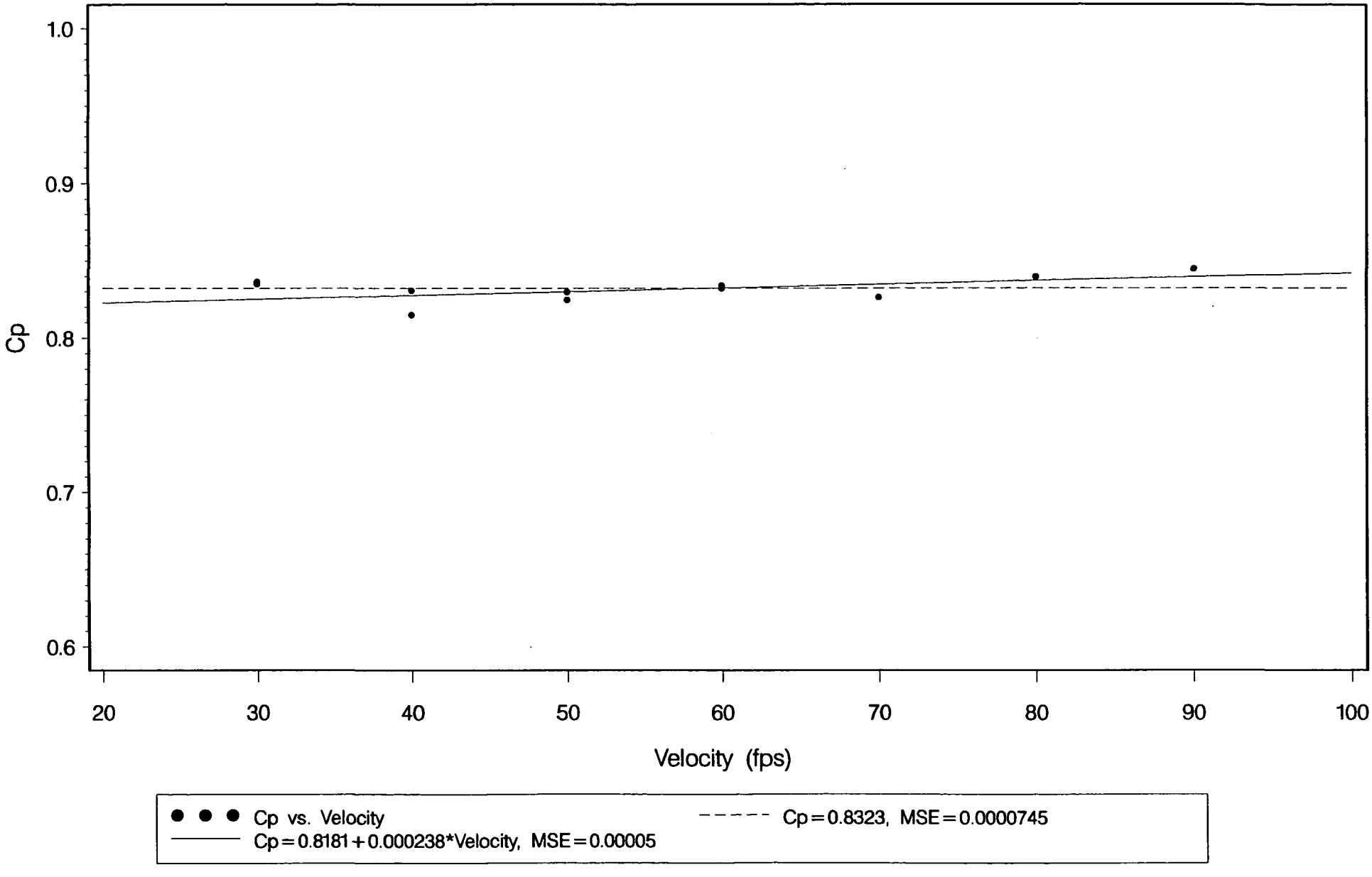

cal2_382.sd2 j:regavg.sas

Figure 3-22. Probe: 3/8" Type S-3

Calibration Coefficient

Pitch = 0, Yaw = 0

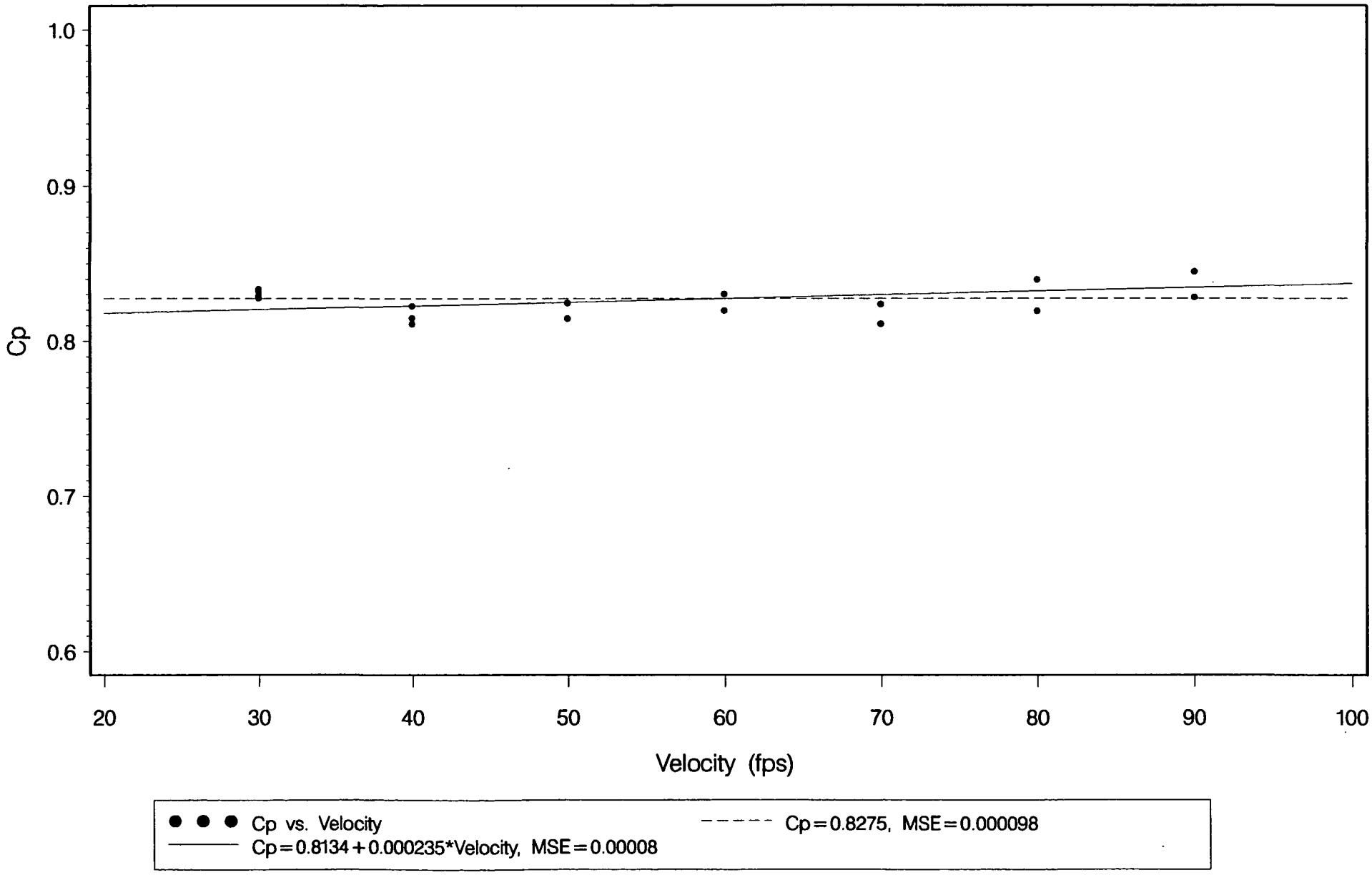

cal2_383.sd2 j:regavg.sas

Figure 3-23. Probe: Modified Kiel - MK1

Calibration Coefficients

Wake Port=1

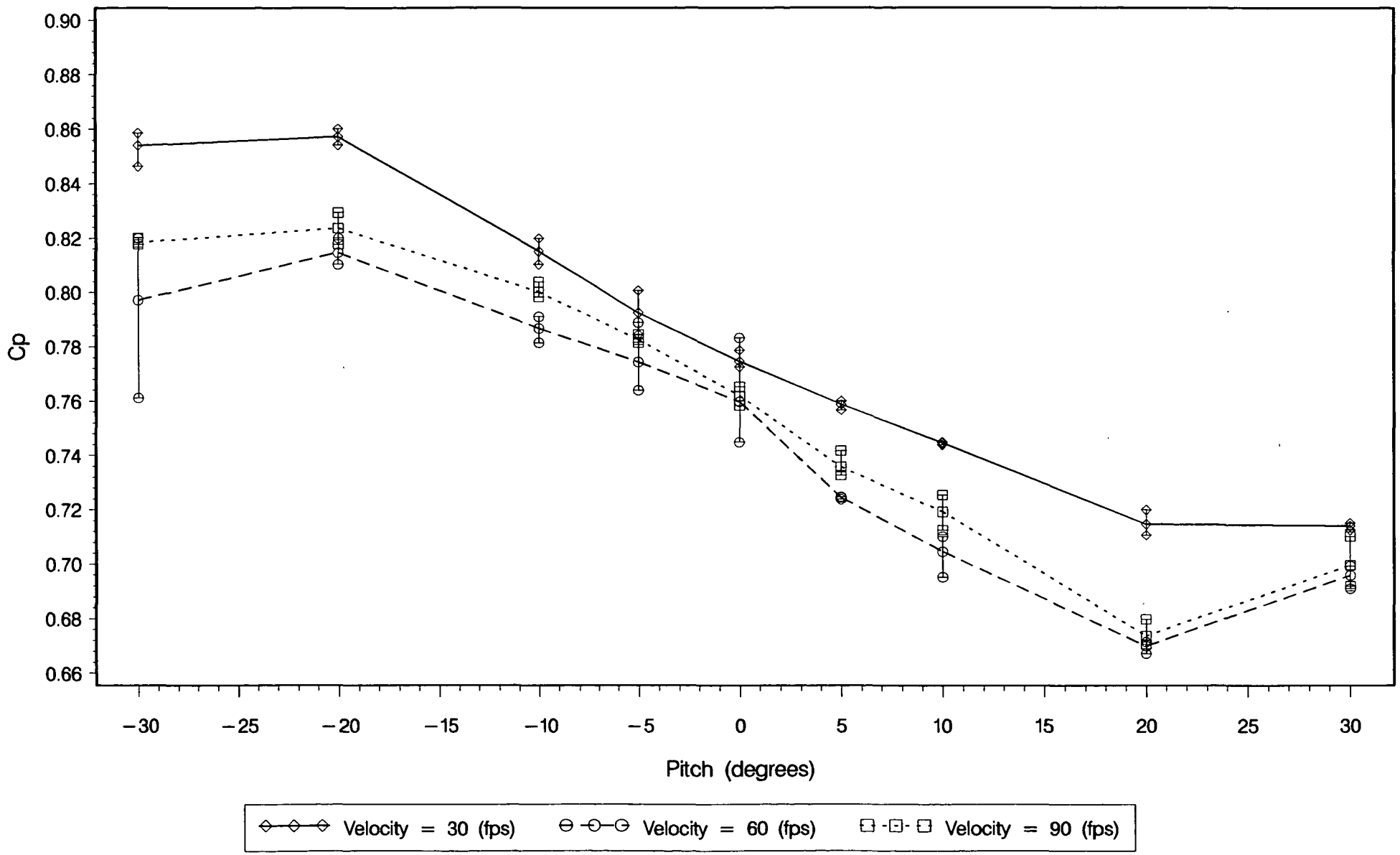

Bands Indicate the Minimum and Maximum Values

\statpres\mk1statc.dat mk1cpl02.sas

Figure 3−24. Probe: Modified Kiel − MK1

Calibration Coefficients

Wake Port = 3

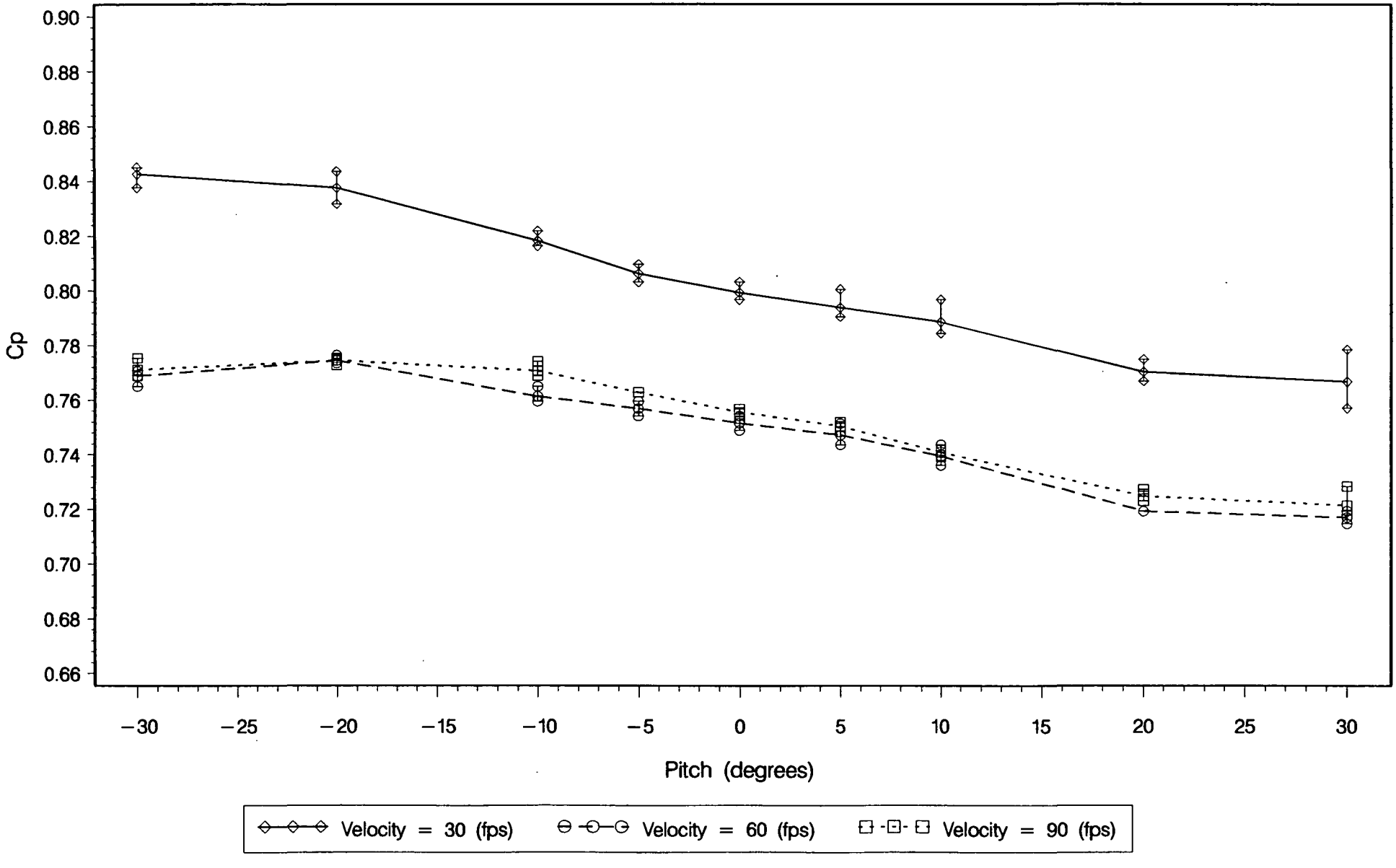

Bands Indicate the Minimum and Maximum Values
\statpres\mk1statc.dat mk1cpl02.sas

Figure 3−25. Probe: Modified Kiel − MK1

Calibration Coefficients

Wake Port = 4

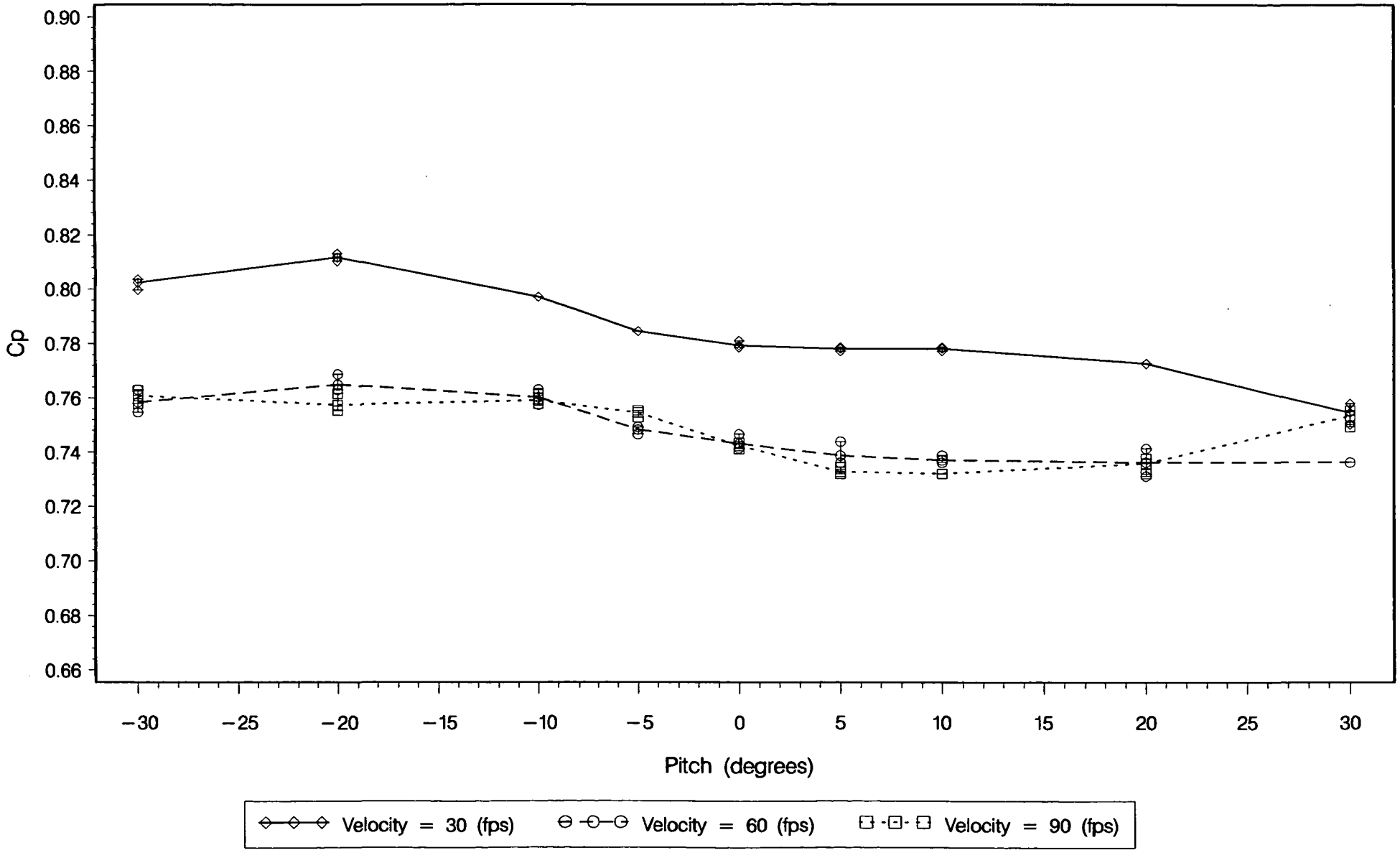

Bands Indicate the Minimum and Maximum Values

\statpres\mk1statc.dat mk1cpl02.sas

Figure 3-26. Probe: Modified Kiel With Thermocouple-MK2

Calibration Coefficients

Wake Port = 4

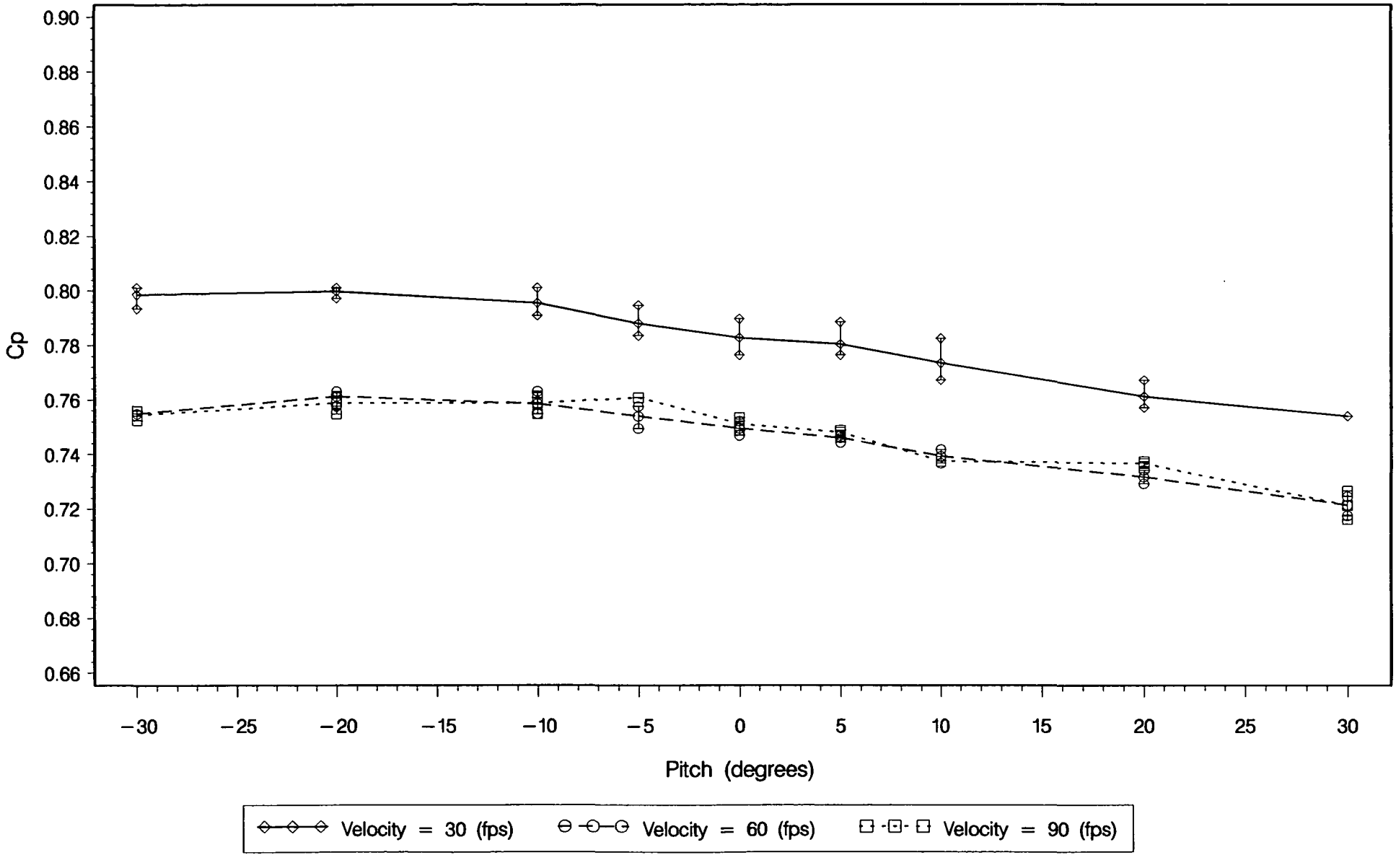

Bands Indicate the Minimum and Maximum Values
\statpres\mk2stat.dat mk2stp02.sas

Figure 3-27. Probe: 3/8" Type S-1

Calibration Coefficients

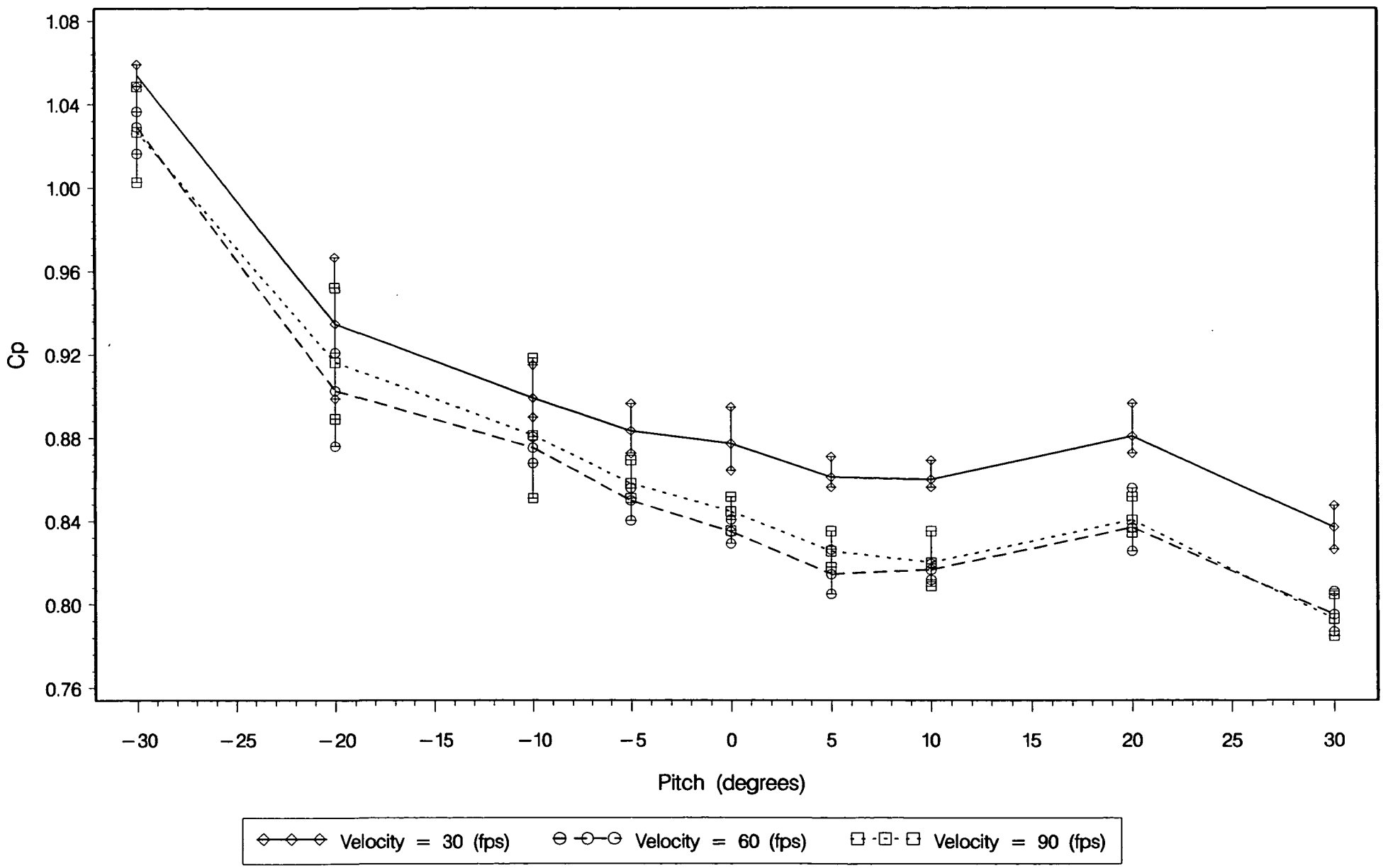

Bands Indicate the Minimum and Maximum Values
318s1ang.dat 38s1pl08.sas

4.0 STANDARD CALIBRATION COEFFICIENTS AND VARIABILITY WITH VELOCITY FOR 2D PROBES

4.1 TEST PROCEDURES

All 2D probes tested were calibrated at zero pitch and yaw angles to derive standard (Method 2) calibration coefficients. The procedure is similar to that specified in EPA Reference Method 2 for a Type S pitot tube. Method 2 calls for averaging three replicate calibrations at a velocity of 50 fps and states that the resulting calibration coefficient will generally be valid to within ±3% above velocities of 17 fps. Alternatively, probes may be calibrated at a minimum of four velocities between 10 and 83 fps.

In the calibrations conducted for these studies, the probes were not yaw nulled. The three modified S probes, the French probe, and the Autoprobe Type S and modified S were calibrated in triplicate at velocities of 30, 60, and 90 fps. The three manual Type S probes were calibrated in triplicate at 30, 40, 50, 60, 70, 80, and 90 fps. For the modified Kiel probe, discussed in Section 3, the calibration coefficient became unstable at velocities less than 40 fps. Thus, for the purpose of standard calibration, only data collected at 40, 50, 60, 70, 80, and 90 fps are used, with the understanding that the calibration coefficient so derived is not valid below 40 fps.

4.2 CALIBRATION COEFFICIENTS

Figures 4–1 through 4–10 are plots of C_p vs. velocity for each probe calibrated during these tests. The vertical bar at each velocity denotes the range of the three replicates, and the solid line connects the means of C_p at each velocity. Table 4-1 shows the mean and range of the calibration coefficients for each probe at each velocity setting. Also shown is the range as a percent of the mean value. The largest range around any point for either Autoprobe is less than 0.37% of the mean C_p. For all other probes, except one of the manual modified S probes, the largest range around any point in the calibration curve is less than 2.43% of the mean C_p. The ranges around the mean C_p values for the modified S probe USS-1 are between 3.30 and 3.93%.

4.3 VARIATION WITH VELOCITY

Table 4–2 summarizes across all velocities the data collected during the calibration coefficient determinations. All reported results, except the coefficients of variation, are derived from the means of the three data points shown in the plots. The coefficients of variation are derived from the individual, unaveraged C_p values. The table lists velocity ranges and specific velocities over which each probe was calibrated, the mean C_p over the velocity range, the minimum and maximum values of C_p over the velocity range, the coefficient of variation, and the sample size used to calculate the coefficient of variation. For all probes except the modified S probes, the coefficient of variation is 1.29% or less. The largest coefficients of variation are 3.06% and 3.59%, both for modified S probes.

Table 4-1. Calibration Coefficients Obtained for 2D Probes at Specific Velocities (Pitch Angle = 0°, Yaw Angle = 0°)

Probe Type	Probe ID	Cp [a]	Velocity (in fps)							% Change in Mean C_p Across All Velocities [b]
			30	40	50	60	70	80	90	
Type S	3/8 S-1	Mean	0.832	0.815	0.821	0.830	0.822	0.840	0.844	3.56
		Range	0.019	0.015	0.005	0.00	0.003	0.00	0.002	
		% of Mean	2.27	1.89	0.61	0.00	0.31	0.00	0.20	
	3/8 S-2	Mean	0.835	0.820	0.826	0.833	0.826	0.840	0.845	3.06
		Range	0.001	0.016	0.005	0.002	0.00	0.00	0.00	
		% of Mean	0.18	1.93	0.62	0.22	0.00	0.00	0.00	
	3/8 S-3	Mean	0.831	0.816	0.822	0.828	0.821	0.835	0.841	3.05
		Range	0.006	0.012	0.010	0.011	0.013	0.020	0.016	
		% of Mean	0.70	1.42	1.22	1.28	1.54	2.43	1.95	
Modified Kiel	MK2-WP4	Mean	0.752	0.741	0.746	0.742	0.740	0.742	0.742	1.62
		Range	0.00	0.017	0.004	0.005	0.006	0.004	0.003	
		% of Mean	0.00	2.32	0.51	0.70	0.76	0.58	0.46	
Modified S	USS-1	Mean	0.939	—	—	0.886	—	—	0.878	6.95
		Range	0.037	—	—	0.029	—	—	0.030	
		% of Mean	3.93	—	—	3.30	—	—	3.39	
	USS-2 [c]	Mean	0.863	—	—	0.858	—	—	0.838	2.98
		Range	0.010	—	—	0.008	—	—	0.00	
		% of Mean	1.15	—	—	0.94	—	—	0.00	
	USS-3	Mean	0.914	—	—	0.853	—	—	0.875	7.15
		Range	0.004	—	—	0.00	—	—	0.00	
		% of Mean	0.42	—	—	0.00	—	—	0.00	
French	F-2	Mean	0.740	—	—	0.760	—	—	0.755	2.70
		Range	0.008	—	—	0.014	—	—	0.004	
		% of Mean	1.12	—	—	1.82	—	—	0.48	
Auto Type S	AS	Mean	0.814	—	—	0.802	—	—	0.804	1.50
		Range	0.001	—	—	0.00	—	—	0.00	
		% of Mean	0.10	—	—	0.02	—	—	0.17	
Auto Modified S	AMS	Mean	0.864	—	—	0.852	—	—	0.850	1.65
		Range	0.001	—	—	0.003	—	—	0.001	
		% of Mean	0.12	—	—	0.37	—	—	0.15	

[a] Values for "% of mean" may not agree with those obtained by dividing the value for "Range" by the value for "Mean" due to rounding. Range and Mean values were rounded to three significant digits, and values for % of Mean were calculated from values with more than three significant digits.

[b] $$\begin{pmatrix} \textit{Percent Change} \\ \textit{in Mean } C_p \\ \textit{Across Velocities} \end{pmatrix} = \frac{\max\limits_{v=30..90fps} \{Mean\ C_p^v\} - \min\limits_{v=30..90fps} \{Mean\ C_p^v\}}{\min\limits_{v=30..90fps} \{Mean\ C_p^v\}} 100$$

[c] Based on duplicate measurements at each velocity; measurements for all other probes based on three or more measurements at each velocity.

Table 4-2. Variability of Calibration Coefficients Across Velocities for 2D Probes Determined at Pitch Angle 0°

Probe Type	Probe ID	Velocities (fps)	Statistics of C_p[a]			Coefficient of Variation (%)[b]	Sample Size
			Min.	Mean	Max.		
Type S	3/8 S-1	30-90[c]	0.815	0.829	0.844	1.29	21
	3/8 S-2	30-90[c]	0.820	0.832	0.845	1.04	21
	3/8 S-3	30-90[c]	0.816	0.827	0.841	1.20	28
Modified Kiel	MK2-WP4	40-90[d]	0.740	0.742	0.746	0.50	36
Modified S	USS-1	30,60,90	0.878	0.901	0.939	3.59	9
	USS-2	30,60,90	0.838	0853	0.863	1.45	6
	USS-3	30,60,90	0.853	0.881	0.914	3.06	9
French	F-2	30,60,90	0.740	0.752	0.760	1.22	9
Auto Type S	AS	30,60,90	0.802	0.807	0.814	0.71	9
Auto Modified S	AMS	30,60,90	0.850	0.855	0.864	0.79	9

[a] These statistics were calculated using the mean values of C_p at each velocity.
[b] Coefficient of variation = (standard deviation/mean) x 100.
[c] Velocity = 30, 40, 50, 60, 70, 80, and 90 fps.
[d] Velocity = 40, 50, 60, 70, 80, and 90 fps.

4.4 CONCLUSIONS

The data presented in this section support the following findings:

- Except for one manual modified S probe, the range of variation in any single-velocity calibration is less than or equal to 2.43% of the mean C_p value. The range of variation in the single-velocity calibration of one modified S probe is higher (from 3.30 to 3.93%). For the Autoprobes, the range is less than or equal to 0.37% of the mean C_p value.

- For the three modified S probes, the maximum percentage changes in mean C_p over the range of tested velocities are 7.15, 6.95, and 2.98%. For all other probes, the percentage change in mean C_p over the range of tested velocities is 3.56% or less. (See last column in Table 4-1.)

- Except for the manual modified S probes, the coefficient of variation with respect to velocity over the range 30 to 90 fps (40 to 90 fps for the modified Kiel probe) is 1.29% or less.

These findings point to the following conclusions:

- For all probes except the manual modified S, variability in the calibration coefficients derived at individual velocity settings was low. The variability was especially low for the Autoprobes.

- As reflected in the percentage change in mean C_p and in the low coefficients of variation, the calibration coefficients for all the tested 2D probes, except for the modified S probes, are stable in the 30 to 90 fps range (40 to 90 fps for the modified Kiel probe).

- Across all velocities, the greatest variation in calibration coefficients was exhibited by the manual modified S probes, reaching as high as 7.15% across the tested range. It may be advisable to require this probe to be calibrated at a wind tunnel velocity close to the prevailing velocity where the probe will be used.

- The modified Kiel probe should not be used at velocities less than 40 fps because its calibration coefficient appears to be very sensitive to velocity changes below this level. This specific velocity cutoff applies only to the modified Kiel probe dimensions tested here; modified Kiel probes of the same design but with a different diameter and port sizes may have different velocity cutoffs.

Figure 4-1. Probe: 3/8" Type S-1

Calibration Coefficients

Pitch = 0, Yaw = 0

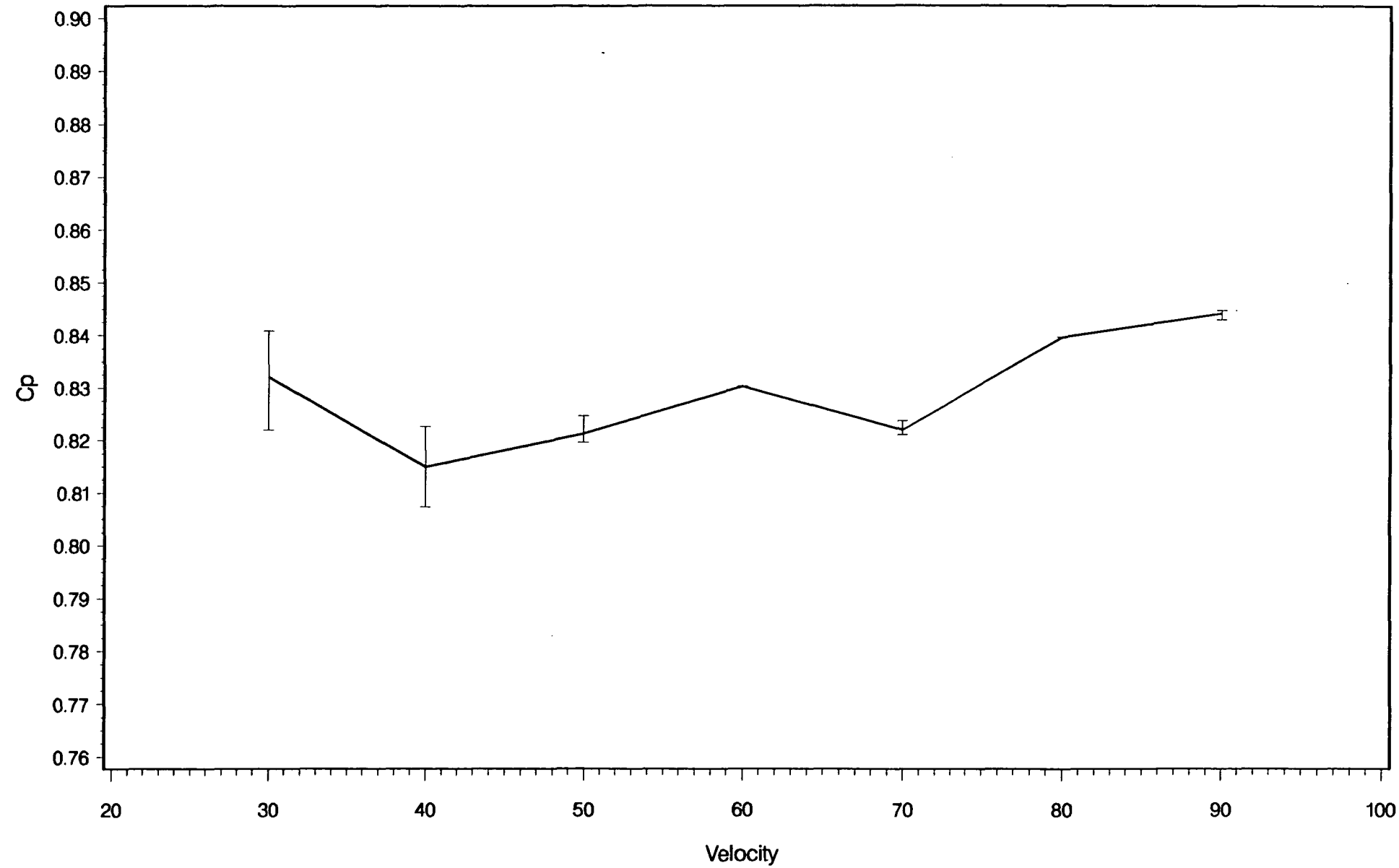

Bands Indicate the Minimum and Maximum Values

Figure 4-2. Probe: 3/8" Type S-2

Calibration Coefficients

Pitch = 0, Yaw = 0

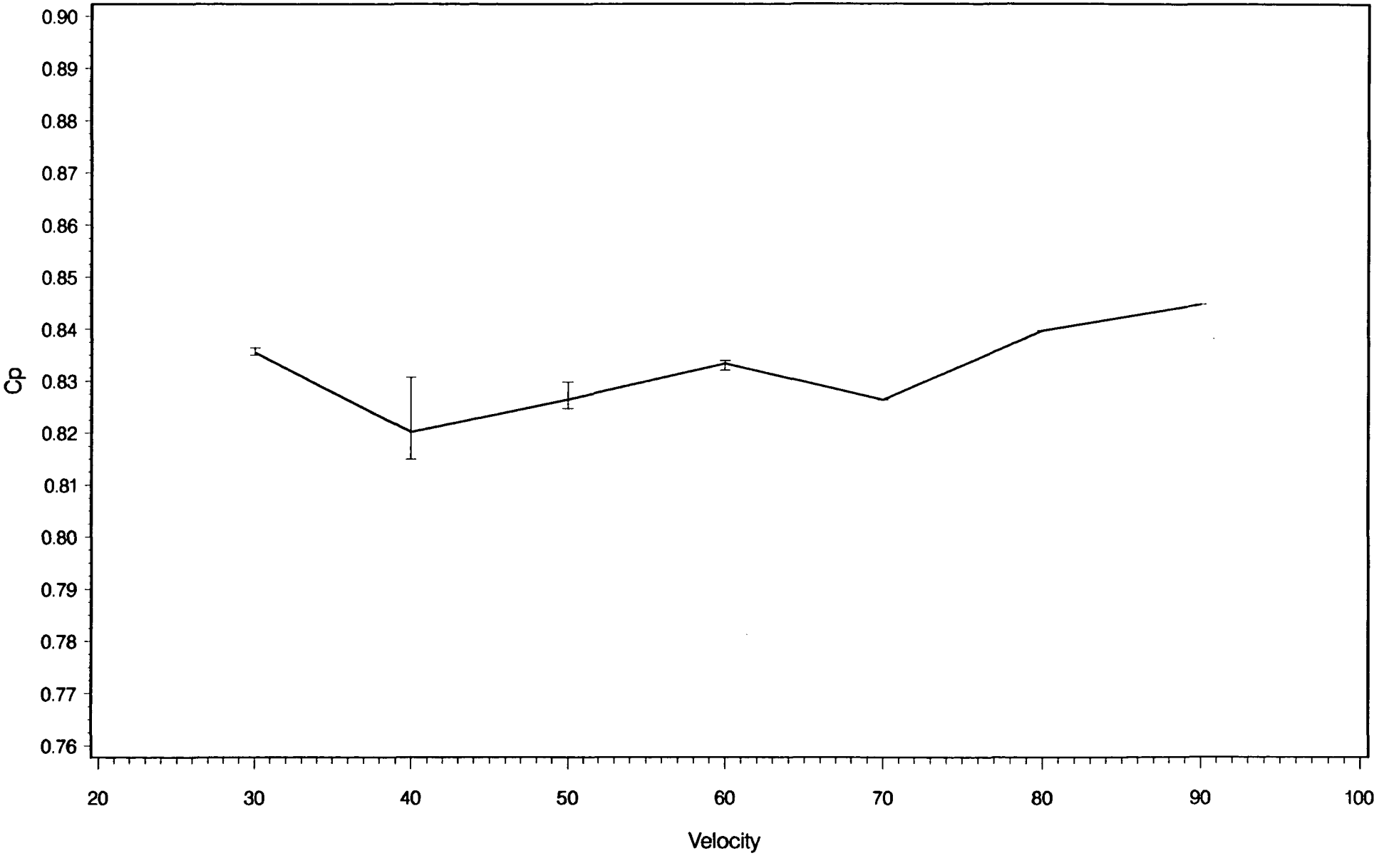

Bands Indicate the Minimum and Maximum Values

Figure 4-3. Probe: 3/8" Type S-3

Calibration Coefficients

Pitch = 0, Yaw = 0

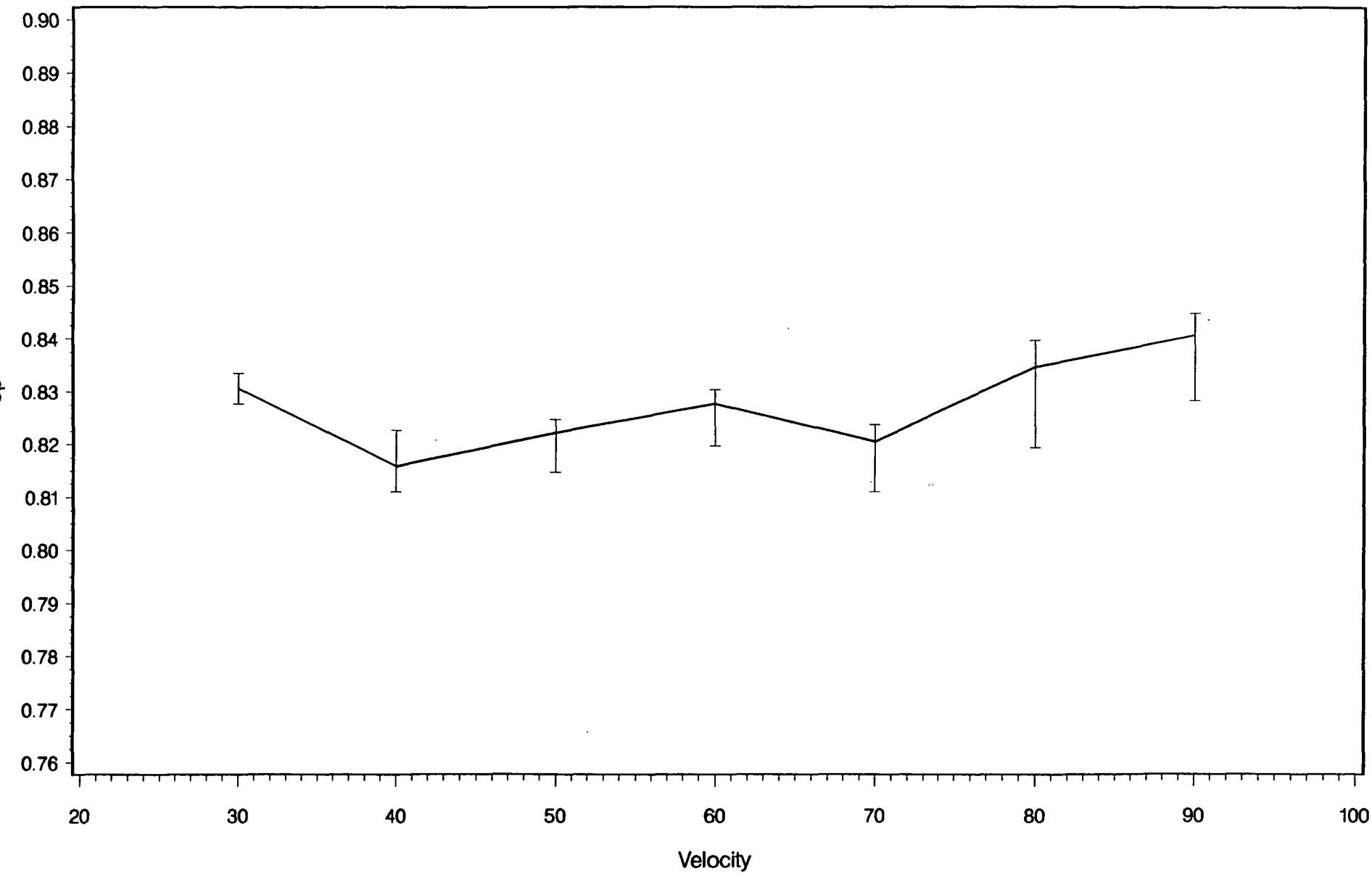

Bands Indicate the Minimum and Maximum Values

Figure 4–4. Probe: Modified Kiel With Thermocouple – MK2

Wake Port Calibration Coefficients

Wake Port = 4

Pitch = 0, Yaw = 0

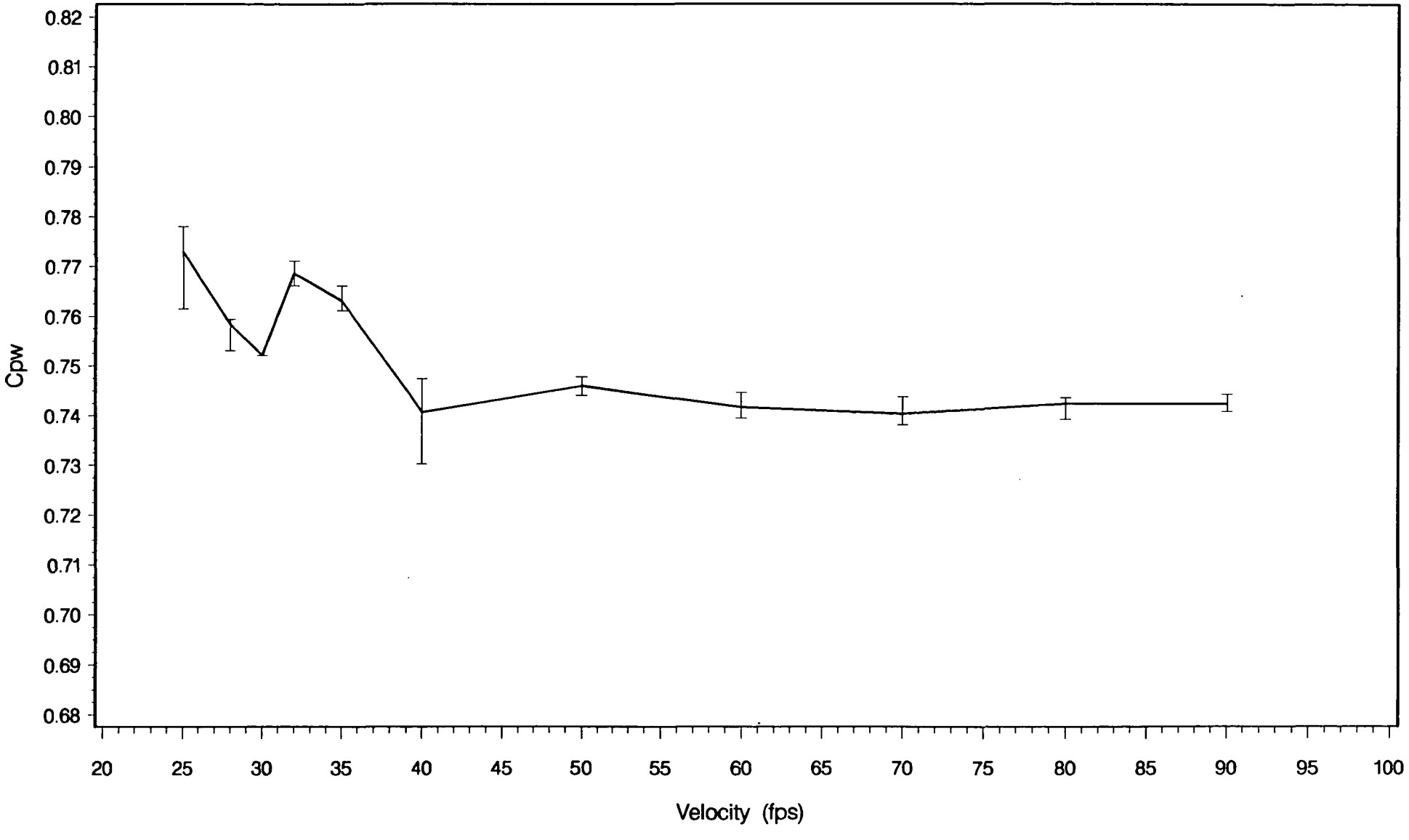

Bands Indicate the Minimum and Maximum Values

Figure 4-5. Probe: Modified S - USS-1

Calibration Coefficients

Pitch = 0, Yaw = 0

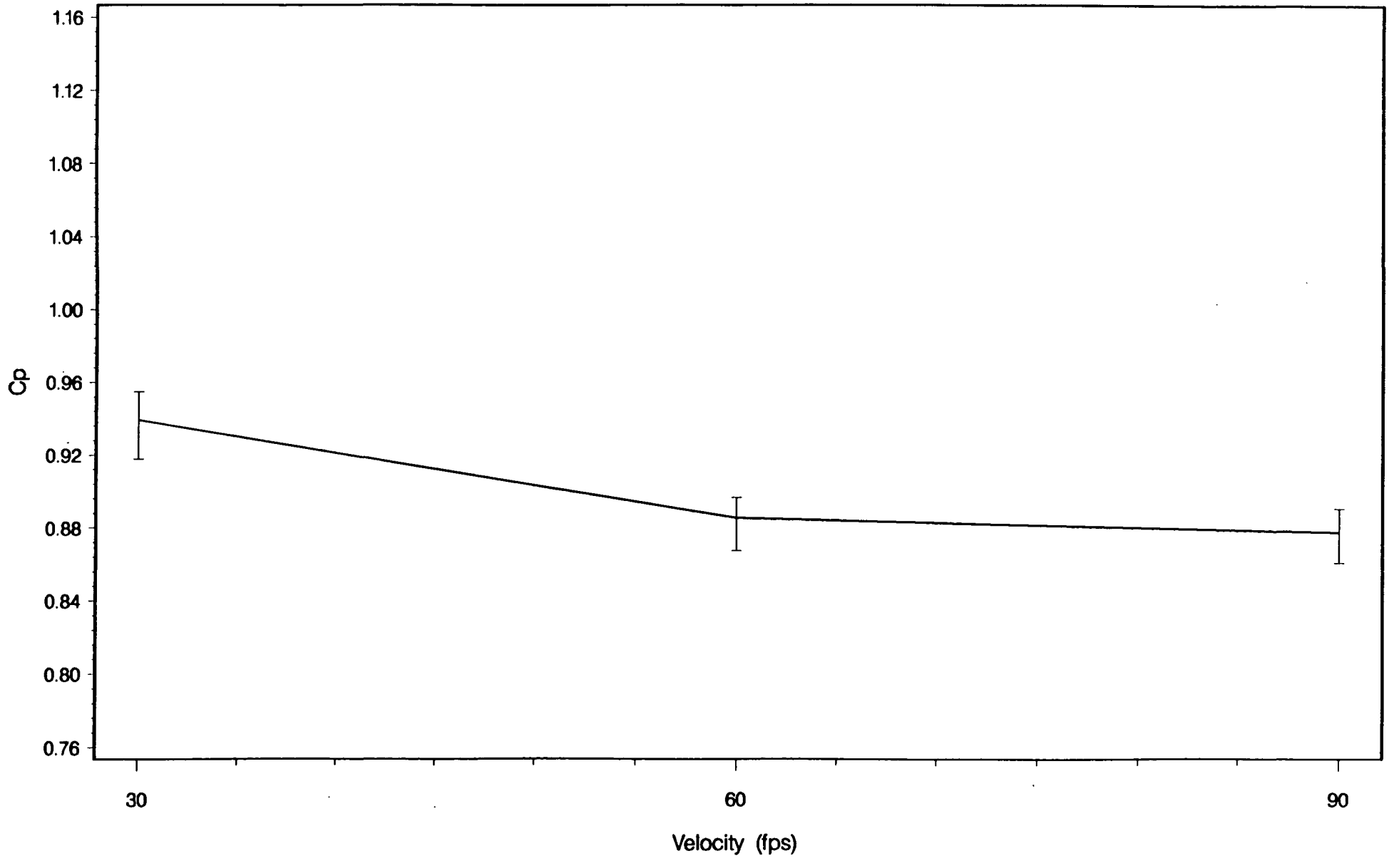

Bands Indicate the Minimum and Maximum Values

Figure 4-6. Probe: Modified S - USS-2

Calibration Coefficients

Pitch = 0, Yaw = 0

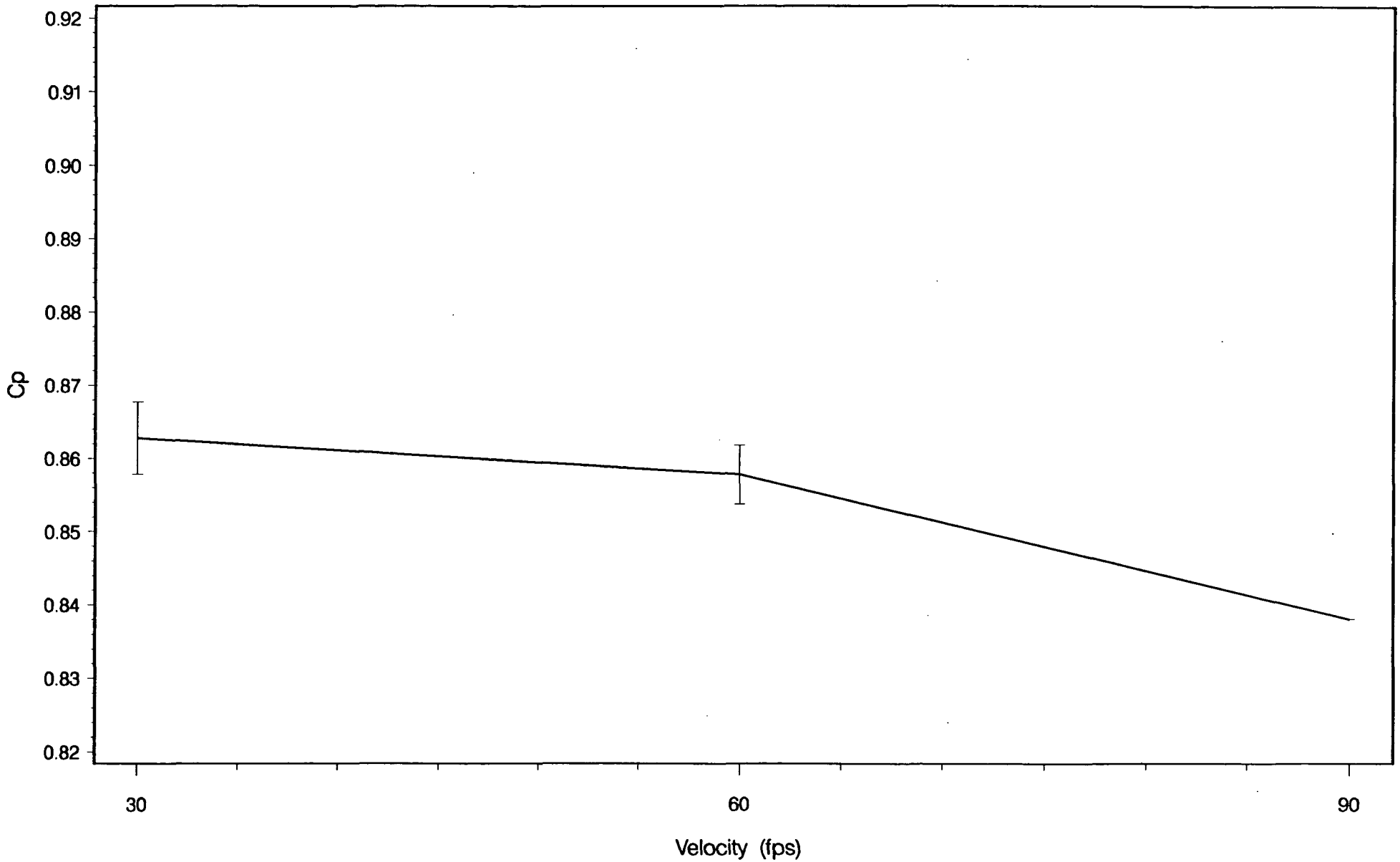

Bands Indicate the Minimum and Maximum Values

uss212ca.dat uss-2plt.sas

Figure 4-7. Probe: Modified S - USS-3

Calibration Coefficients

Pitch = 0, Yaw = 0

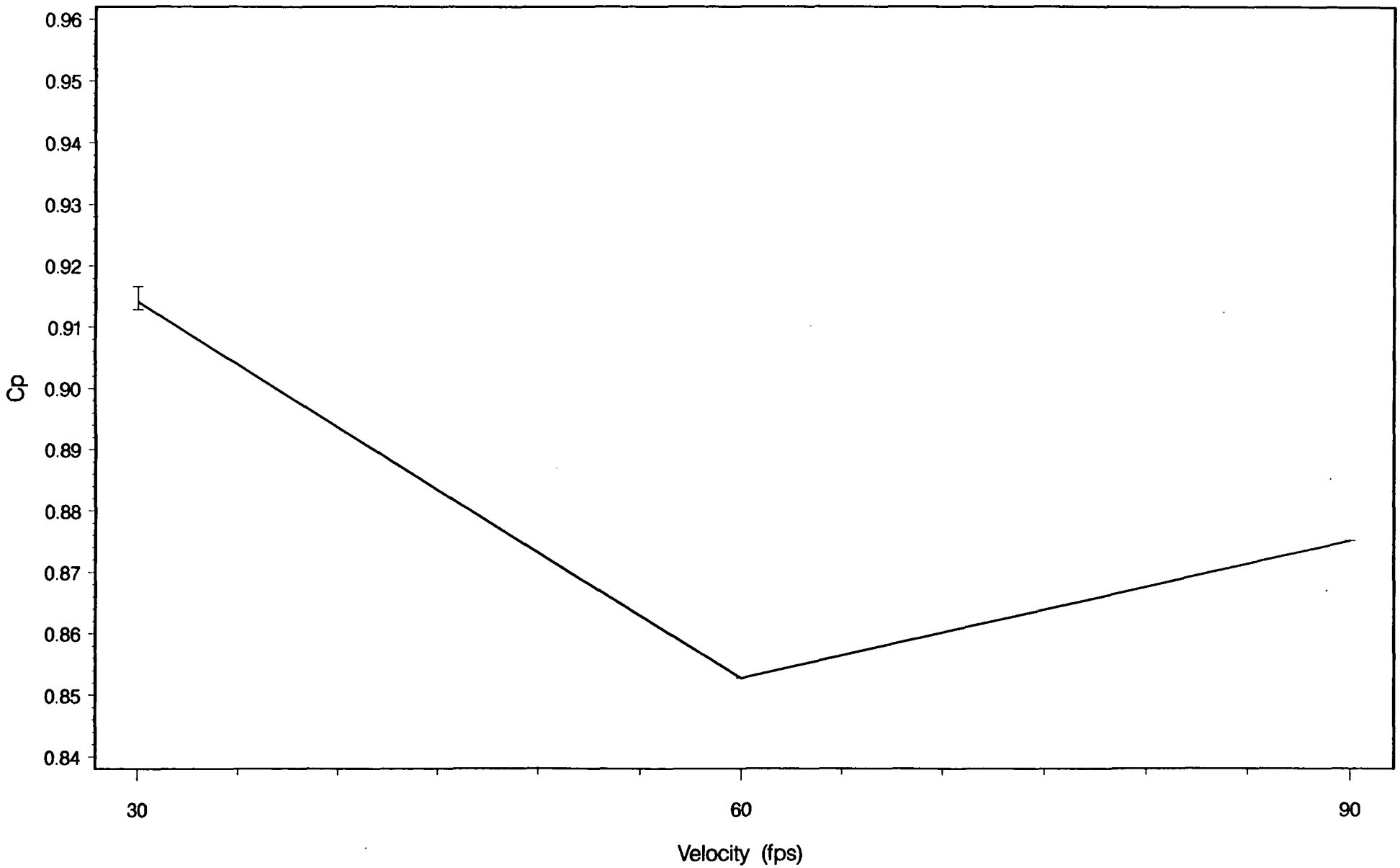

Bands Indicate the Minimum and Maximum Values

Figure 4−8. Probe: Autoprobe − Type S

Calibration Coefficient

Pitch = 0, Yaw = 0

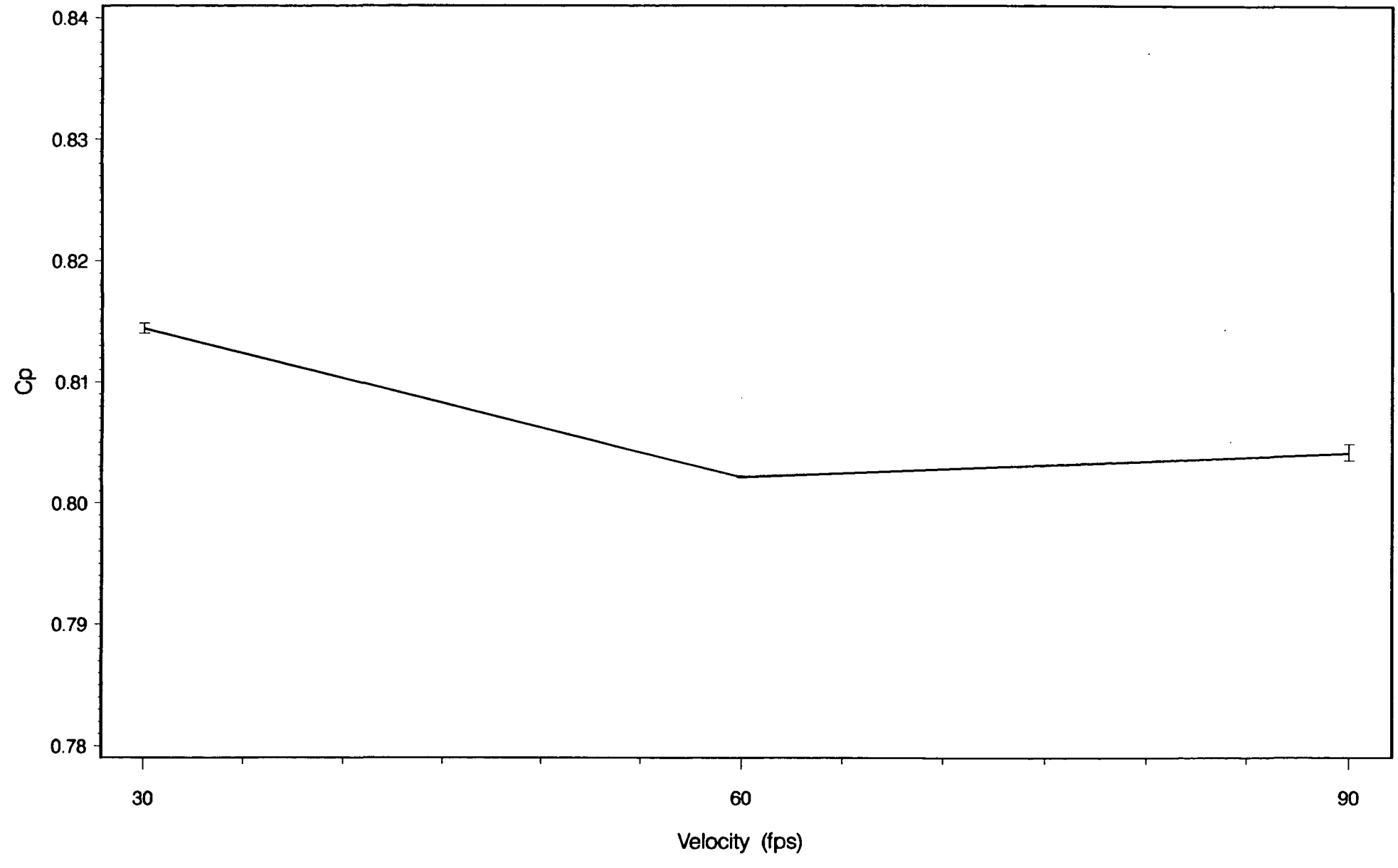

Bands Indicate the Minimum and Maximum Values

Figure 4–9. Probe: Autoprobe – Modified S

Calibration Coefficient

Pitch = 0, Yaw = 0

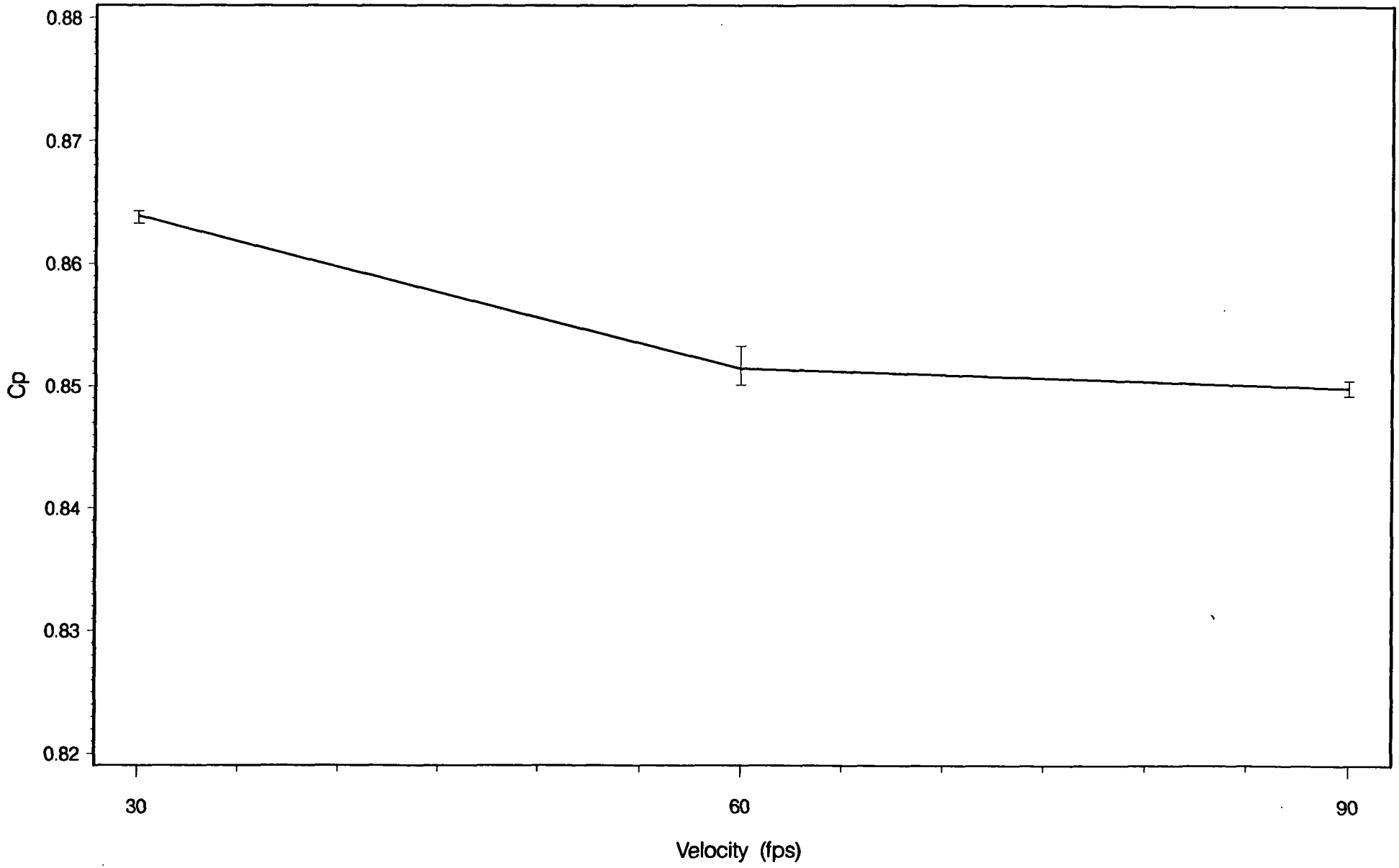

Bands Indicate the Minimum and Maximum Values

Figure 4-10. Probe: French Probe - F-2

Calibration Coefficient

Pitch = 0, Yaw = 0

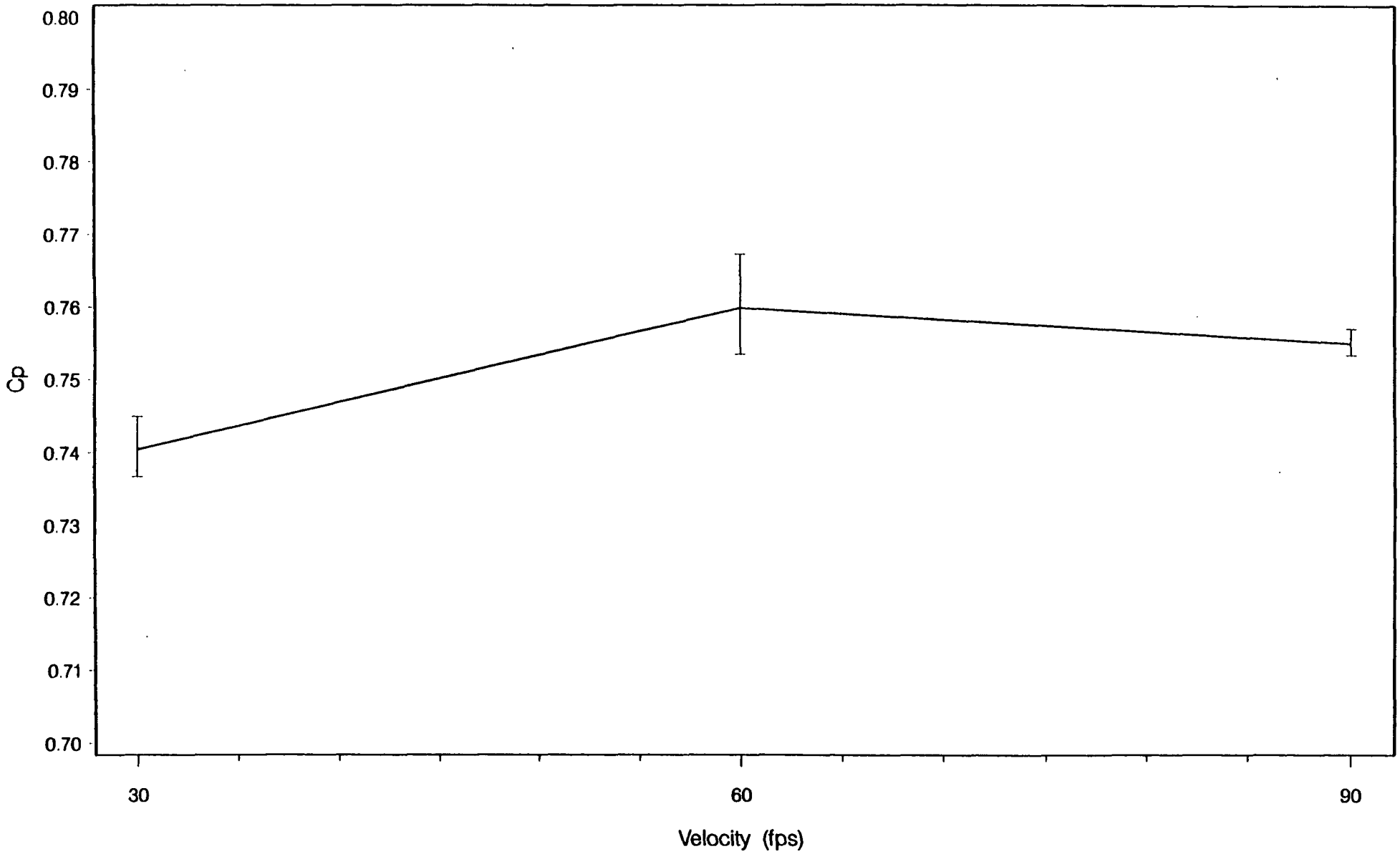

Bands Indicate the Minimum and Maximum Values

5.0 PITCH ANGLE EFFECTS ON VELOCITY MEASUREMENTS PERFORMED WITH 2D PROBES

5.1 TEST PROCEDURES

A series of tests was conducted to determine the sensitivity of velocity measurements to changes in pitch angle for each probe tested in this study. Probes included the Type S, modified S, Autoprobe fitted with a Type S probe, Autoprobe fitted with a modified Type S probe, French, and modified Kiel (see Section 3.2). Data on pitch-angle sensitivity were collected along with data on the sensitivity and accuracy of yaw-angle nulling using 2D probes. (Note that 2D probes cannot be used to determine pitch angle.)

For these experiments, each test probe (except the French probe) was yaw nulled using the procedure described in Section 2.1.1, and ΔP was measured at pitch angles between -30° and 30° in 10° increments (but including -5° and 5°) and at three velocities (30, 60, and 90 fps). The Type S, modified S, and Kiel probes were yaw nulled manually, and the Autoprobes were yaw nulled automatically. No procedure has been established for yaw nulling the French probe. Thus, all measurements with this probe were taken at a nominal yaw angle of zero. For each probe, ΔP, ΔP_P (the pressure differential across the standard pitot-static tube), yaw angle as read by the digital inclinometer, pitch angle, and temperature were recorded.

The calibration coefficient was calculated as

$$C_p = \sqrt{\frac{\Delta P_P}{\Delta P}} \qquad \textbf{(Eq. 5.1)}$$

where

ΔP = the pressure drop across the 2D probe

5.2 SENSITIVITY OF CALIBRATION COEFFICIENTS TO PITCH ANGLE

Figure 5–1 shows C_p vs. pitch angle for the Type S probe (Probe S-1) at velocities of 30, 60, and 90 fps. The construction of these curves was discussed in Section 3.2.1. Curves for the modified S probes (USS-1 and USS-3) in Figures 5–2 and 5–3, the Autoprobe Type S in Figure 5–4, and the Autoprobe modified S in Figure 5–5, are qualitatively similar to Figure 5-1 and to each other. In all cases, C_p decreases rapidly over the pitch angle range from -30° to -10° and then remains relatively constant from -10° to 20° before decreasing beyond 20°. (The Autoprobe modified S remains almost constant above 20° at 30 fps). The sharp demarcation in pitch angle sensitivity at -10° is less pronounced with the French probe, as is evident from Figure 5–6. However, the three C_p vs. pitch angle curves for the French probe differ greatly from each other. At 90 fps, the C_p vs. pitch angle curve for the French probe is similar to those for the Type S and modified S probes, with C_p showing little change in the -10° to 20° pitch range. However, the situation changes markedly at 30 to 60 fps. At 30 fps, the C_p for the French probe is highly pitch angle-dependent over the entire -30° to 30° pitch range. At 60 fps, C_p is erratically pitch angle-dependent, showing high dependency below -5°, between 5° and 10°, and above 20°. The change in C_p with pitch angle for the modified Kiel probe (MK2) is shown in Figure 3-26 in Section 3.2.2. For this probe, C_p remains essentially constant in

the -30° to -10° pitch angle range and then decreases slightly (between 3% and 4%) in the -10° to 20° pitch angle range for each of the tested velocities.

Table 5–1 summarizes the behavior of C_p with pitch angle for all 2D probes tested, including the modified Kiel probe (MK2) discussed in Section 3.2.1. The Type S and modified S probes in both manual and Autoprobe configurations, show strong sensitivity to pitch at angles between -30° and -10° and then relatively pitch-independent behavior (< 5% change) between -10° and 20°. The changes in the Autoprobe coefficients are roughly half those of the corresponding manual probes over the -10° to 20° regime. The French probe is highly pitch angle-dependent over small changes in pitch angle. The modified Kiel probe, on the other hand, is relatively robust across the pitch angle range studied (see Figure 3-26).

Table 5-1. Sensitivity of C_p to Pitch Angle for 2D Probes

Probe	% Change in C_p[a]	
	-30° to -10°	-10° to 20°
Type S (S-1)	15.9	6.3
Modified S[b]	16.8	3.2
Autoprobe Type S (AS)	18.4	3.0
Autoprobe Modified S (AMS)	21.0	2.2
French Probe (F-2)	9.1	8.6
Kiel Probe (MK2)	0.7	3.4

[a] % change is calculated as the difference between the largest and smallest mean C_p in the angular pitch range divided by the average of those means. These values are then averaged for 30, 60, and 90 fps.

[b] Average of USS-1 and USS-3.

5.3 Pitch Angle Effects on Velocity Determinations

The usefulness of a probe in determining flow depends on the probe's ability to measure total velocity and axial velocity accurately at different pitch angles. As stated earlier, 2D probes cannot be used to determine pitch angle. Instead, pitch angle determination must be made with a 3D probe such as a DAT probe or spherical probe. Pitch angle determinations with 3D probes are discussed later in this report.

The issue addressed in this section is how much measurement error is potentially associated with using a 2D probe to determine axial velocity in the absence of any information about the pitch angle of flow. To estimate this uncertainty, the data presented in the previous subsection were used to simulate the use of each probe in determining axial velocity where the unknown pitch angle of flow is constrained to lie between -30° and 30°.

The data for the simulations were developed as follows. First, actual total velocity (V_s in feet per second) was calculated from ΔP_P measured by the standard pitot-static probe using the following equation:

$$V_S = 15.9 \sqrt{\frac{\Delta P_P \ (T+460)}{P_{bar}}} \qquad \textbf{(Eq. 5.2)}$$

The simulated axial component of the actual velocity at a specific pitch angle, θ_p (yaw angle = 0°), was then calculated by multiplying V_s by the cosine of the pitch angle (set on the pitch board), i.e.,

$$V_{ax} = \cos\theta_p \ V_s \qquad \textbf{(Eq. 5.3)}$$

These values were compared to V_{null}, the velocity measured by each of the tested 2D probes at each pitch angle after yaw nulling. V_{null} was derived from the measured ΔP using the following equation:

$$V_{null} = 15.9 \, C_P \sqrt{\frac{\Delta P \ (T+460)}{P_{bar}}} \qquad \textbf{(Eq. 5.4)}$$

where C_p is the average of the calibration coefficients obtained at zero pitch and zero yaw over the applicable velocity range (i.e., 40-90 fps for the modified Kiel probe; 30-90 fps for all the other tested probes). Each of the constituent values of C_p is derived using Equation 5.1 and then averaged.

Table 5–2 compares the velocities measured by the test probes with the velocity determined from the standard probe corrected for pitch angle. The first three columns list the pitch angle, the cosine of the pitch angle ($\cos\theta_p$), and the percent of the total velocity that exceeds the angle-corrected ("pseudo" axial) velocity. This latter quantity is the percentage difference between V_{null} and V_{ax} where C_p is independent of pitch angle. In other words, because a 2D probe cannot measure pitch, a probe whose calibration coefficient is independent of pitch would provide a velocity that differs from axial velocity by $(1-\cos\theta_p)V_s$. The fourth column lists the nominal test velocity, V_{nom}.

Four columns appear in Table 5-2 under each tested probe. The first shows the values of the actual total velocity V_s as measured by the standard pitot (see Equation 5.2). The second shows the actual axial velocity V_{ax} derived from the standard pitot measurements (see Equation 5.3). The third shows the yaw-nulled velocity V_{null} obtained by the tested 2D probe (see Equation 5.4). The fourth column shows the percent deviation of V_{null} from V_{ax}, i.e.,

$$\%Dev = \left[\frac{(V_{null} - V_{ax})}{V_{ax}}\right] 100 \qquad \textbf{(Eq. 5.5)}$$

Table 5-2. Axial Velocity Evaluation for 2D Probes (a)

Pitch Angle	cos theta sub p	1-cos theta p	Vnom (b)	Modified Kiel Probe (MK2)				Type S (3/8 S-1)				Modified S							
												USS-1				USS-3			
				Vs	Vax	V null	% Dev (c)	Vs	Vax	V null	% Dev	Vs	Vax	V null	% Dev	Vs	Vax	V null	% Dev
-30	0.866	13.4%	30	30.1	26.1	28.0	7.4%	30.0	26.0	23.5	-9.6%	30.1	26.1	24.7	-5.3%	30.2	26.2	25.2	-3.7%
			60	60.3	52.2	59.2	13.4%	60.3	52.2	48.4	-7.3%	60.2	52.1	51.7	-0.8%	60.5	52.4	51.6	-1.5%
			90	90.6	78.5	89.1	13.6%	90.9	78.7	72.2	-8.3%	90.6	78.5	77.6	-1.1%	90.8	78.6	75.6	-3.9%
-20	0.94	6.0%	30	30.1	28.3	27.9	-1.4%	30.0	28.2	26.3	-6.7%	30.1	28.3	27.0	-4.5%	30.2	28.4	27.2	-4.2%
			60	60.3	56.7	58.7	3.6%	60.3	56.7	54.5	-3.8%	60.2	56.6	56.9	0.6%	60.5	56.9	56.3	-1.0%
			90	90.6	85.1	88.6	4.1%	91.0	85.5	80.8	-5.5%	90.7	85.2	85.5	0.3%	90.8	85.3	82.3	-3.5%
-10	0.985	1.5%	30	30.1	29.6	28.1	-5.2%	30.0	29.5	27.7	-6.2%	30.0	29.5	29.1	-1.5%	30.2	29.7	29.2	-1.8%
			60	60.3	59.4	58.9	-0.8%	60.3	59.4	57.3	-3.5%	60.3	59.4	61.2	3.1%	60.5	59.6	62.0	4.1%
			90	90.6	89.2	88.6	-0.7%	91.1	89.7	86.3	-3.8%	90.8	89.4	91.8	2.7%	90.9	89.5	90.9	1.5%
-5	0.996	0.4%	30	30.1	30.0	28.3	-5.6%	30.0	29.9	28.2	-5.6%	30.0	29.9	28.8	-3.6%	30.2	30.1	29.2	-2.9%
			60	60.3	60.1	59.3	-1.3%	60.4	60.2	58.7	-2.4%	60.3	60.1	61.3	2.0%	60.5	60.3	62.5	3.7%
			90	90.7	90.4	88.4	-2.2%	91.2	90.9	88.1	-3.0%	91.0	90.7	92.7	2.3%	91.0	90.7	91.6	1.0%
0	0	0.0%	30	30.1	30.1	28.5	-5.3%	30.0	30.0	28.4	-5.3%	30.0	30.0	28.8	-4.0%	30.2	30.2	29.2	-3.3%
			60	60.3	60.3	59.7	-1.0%	60.4	60.4	59.9	-0.8%	60.3	60.3	61.3	1.7%	60.5	60.5	62.5	3.3%
			90	90.7	90.7	89.6	-1.2%	91.3	91.3	89.4	-2.1%	91.0	91.0	93.3	2.5%	91.0	91.0	91.6	0.7%
5	0.996	0.4%	30	30.1	30.0	28.6	-4.6%	30.0	29.9	28.9	-3.3%	30.0	29.9	28.9	-3.3%	30.2	30.1	29.1	-3.3%
			60	60.3	60.1	60.0	-0.1%	60.4	60.2	61.3	1.9%	60.3	60.1	61.4	2.2%	60.5	60.3	62.4	3.5%
			90	90.7	90.4	90.0	-0.4%	91.3	91.0	91.5	0.6%	91.0	90.7	93.0	2.6%	91.1	90.8	90.7	-0.1%
10	0.985	1.5%	30	30.1	29.6	28.9	-2.5%	30.1	29.6	29.0	-2.2%	30.0	29.5	28.8	-2.5%	30.2	29.7	29.2	-1.8%
			60	60.3	59.4	60.5	1.9%	60.4	59.5	61.3	3.1%	60.3	59.4	62.2	4.7%	60.5	59.6	62.4	4.7%
			90	90.8	89.4	91.3	2.1%	91.4	90.0	92.6	2.9%	91.1	89.7	94.1	4.9%	91.1	89.7	90.7	1.1%
20	0.94	6.0%	30	30.1	28.3	29.3	3.6%	30.1	28.3	28.2	-0.3%	30.0	28.2	29.1	3.2%	30.2	28.4	29.6	4.3%
			60	60.3	56.7	61.1	7.8%	60.4	56.8	59.7	5.2%	60.4	56.8	63.0	11.0%	60.5	56.9	65.7	15.6%
			90	90.8	85.3	91.4	7.1%	91.5	86.0	89.9	4.6%	91.2	85.7	95.9	11.9%	91.2	85.7	94.6	10.4%
30	0.866	13.4%	30	30.1	26.1	29.6	13.5%	30.0	26.0	29.5	13.5%	30.0	26.0	30.2	16.2%	30.2	26.2	30.9	18.1%
			60	60.3	52.2	62.0	18.7%	60.4	52.3	62.5	19.5%	60.4	52.3	67.3	28.7%	60.5	52.4	67.3	28.4%
			90	90.8	78.6	93.4	18.8%	91.5	79.2	95.1	20.0%	91.2	79.0	102.9	30.3%	91.2	79.0	100.8	27.6%

[a] Pitch angle expressed in degrees. All velocities in fps.
[b] V_{nom} = nominal velocity.
[c] % Dev. = percent deviation = $[(V_{null} - V_{ax})/V_{ax}]100$.

Table 5-2 Axial Velocity Evaluation for 2D Probes (a) (cont.)

Pitch Angle	cos theta sub p	1-cos theta p	Vnom (b)	Autoprobe Type S (AS)				Autoprobe Modified S (AMS)				French (F2)			
				Vs	Vax	V null	% Dev (c)	Vs	Vax	V null	% Dev	Vs	Vax	V null	% Dev
-30	0.866	13.4%	30	30.1	26.1	24.5	-6.0%	30.1	26.1	24.0	-7.9%	30.1	26.1	25.5	-2.2%
			60	59.7	51.7	49.8	-3.7%	59.7	51.7	48.9	-5.4%	60.4	52.3	52.4	0.2%
			90	89.6	77.6	72.2	-7.0%	89.7	77.7	73.1	-5.9%	90.7	78.6	82.1	4.5%
-20	0.94	6.0%	30	30.1	28.3	27.5	-2.8%	30.1	28.3	28.3	0.1%	30.1	28.3	26.1	-7.7%
			60	59.7	56.1	53.4	-4.8%	59.7	56.1	56.2	0.2%	60.4	56.8	54.5	-4.0%
			90	89.6	84.2	80.8	-4.0%	89.6	84.2	83.3	-1.1%	90.7	85.2	82.9	-2.7%
-10	0.985	1.5%	30	30.1	29.6	29.6	-0.1%	30.1	29.6	29.5	-0.5%	30.1	29.6	28.3	-4.5%
			60	59.7	58.8	58.9	0.2%	59.7	58.8	59.9	1.9%	60.4	59.5	58.3	-2.0%
			90	89.6	88.2	87.5	-0.8%	89.6	88.2	91.3	3.5%	90.7	89.3	87.0	-2.6%
-5	0.996	0.4%	30	30.1	30.0	30.0	0.0%	30.1	30.0	30.2	0.7%	30.1	30.0	29.1	-3.0%
			60	59.7	59.5	59.8	0.5%	59.7	59.5	60.9	2.4%	60.4	60.2	59.3	-1.4%
			90	89.6	89.3	88.6	-0.7%	89.6	89.3	90.8	1.7%	90.7	90.4	89.8	-0.6%
0	0	0.0%	30	30.1	30.1	29.8	-1.0%	30.1	30.1	29.8	-1.0%	30.0	30.0	30.5	1.7%
			60	59.7	59.7	60.7	1.7%	59.7	59.7	60.5	1.3%	60.4	60.4	59.8	-1.0%
			90	89.6	89.6	90.8	1.3%	89.6	89.6	91.0	1.6%	90.7	90.7	90.3	-0.4%
5	0.996	0.4%	30	30.1	30.0	30.1	0.4%	30.1	30.0	29.6	-1.3%	30.0	29.9	31.4	5.1%
			60	59.7	59.5	60.9	2.4%	59.7	59.5	60.6	1.9%	60.4	60.2	59.9	-0.4%
			90	89.6	89.3	90.8	1.7%	89.6	89.3	89.8	0.6%	90.7	90.4	90.7	0.4%
10	0.985	1.5%	30	30.1	29.6	30.1	1.5%	30.1	29.6	29.7	0.2%	30.0	29.5	31.2	5.6%
			60	59.7	58.8	60.9	3.6%	59.7	58.8	60.2	2.4%	60.4	59.5	63.8	7.3%
			90	89.6	88.2	90.9	3.0%	89.6	88.2	89.8	1.8%	90.7	89.3	91.3	2.2%
20	0.94	6.0%	30	30.1	28.3	29.9	5.7%	30.1	28.3	29.9	5.7%	30.0	28.2	30.1	6.8%
			60	59.7	56.1	60.5	7.8%	59.7	56.1	60.4	7.7%	60.4	56.8	64.1	12.9%
			90	89.6	84.2	89.9	6.8%	89.6	84.2	91.9	9.1%	90.7	85.2	92.0	7.9%
30	0.866	13.4%	30	30.1	26.1	30.8	18.1%	30.1	26.1	30.1	15.5%	30.0	26.0	27.6	6.2%
			60	59.7	51.7	61.7	19.3%	59.7	51.7	61.9	19.7%	60.4	52.3	61.4	17.4%
			90	89.6	77.6	90.9	17.1%	89.6	77.6	92.9	19.7%	90.7	78.6	91.9	17.0%

[a] Pitch angle expressed in degrees. All velocities in fps.
[b] V_{nom} = nominal velocity.
[c] % Dev. = percent deviation = $[(V_{null} - V_{ax})/V_{ax}]100$.

To facilitate interpreting the data in Table 5-2, Tables 5-3 and 5-4 summarize the maximum deviation from axial velocity (in percent) measured for each probe over selected pitch-angle ranges at zero yaw. At pitch angles between -10° and 10°, the difference between V_{null} and V_{ax} is within the range -6.2% and 7.3%. Over all velocities in this pitch angle range, the smallest variations are seen with the two Autoprobes. Over the two higher velocities, 60 and 90 fps, the smallest variation at pitch angles from -10° to 10° is seen with the modified Kiel probe. The French probe exhibited the highest variation in both Tables 5-3 and 5-4 over this pitch-angle range.

Table 5-3. Maximum Percent Deviation of Measured Velocity from Axial Velocity Across All Velocities at Zero Yaw

Probe	Pitch Angle Ranges		
	-10 to +10	-10 to +20	-20 to +20
MK2	-5.6	+7.8	+7.8
3/8 S-1	-6.2	-6.2	-6.7
USS-1	+4.9	+11.9	+11.9
USS-3	+4.7	+15.6	+15.6
AS	+3.6	+7.8	+7.8
AMS	+3.5	+9.1	+9.1
F-2	+7.3	+12.9	+12.9

Table 5-4. Maximum Percent Deviation of Measured Velocity from Axial Velocity Across 60 and 90 fps at Zero Yaw

Probe	Pitch Angle Ranges		
	-10 to +10	-10 to +20	-20 to +20
MK2	-2.2%	+7.8%	+7.8%
3/8 S-1	-3.8%	+5.2%	-5.5%
USS-1	+4.9%	+11.9%	+11.9%
USS-3	+4.7%	+15.6%	+15.6%
AS	+3.6%	+7.8%	+7.8%
AMS	+3.5%	+9.1%	+9.1%
F-2	+7.3%	+12.9%	+12.9%

Figures 5-7 through 5-9 are plots of percent deviation from axial velocity vs. pitch angle at each nominal velocity. Each plot shows the variation of percent deviation with velocity for all six probe types (data for the two modified S probes in Table 5-2 have been averaged). From the figures it is apparent that, except for the French probe at 30 fps, the percent deviation from actual axial velocity

increases significantly between pitch angles of 10 and 30°. In the ±10° pitch-angle range, except for the French probe at 60 fps, deviations from axial velocities were all between ±5%. At 30 fps in this same pitch-angle range, except for the French probe, deviations from axial velocities were between -7% and +2%.

5.4 CONCLUSIONS

5.4.1 Calibration Coefficients

Analyzing the impact of pitch angle on calibration coefficients leads to the following findings:

- Except for the Type S and French probes, the calibration coefficients changed by less than 3.5% over the pitch angle range of -10° to 20°. The Type S and French probes' calibration coefficients changed by 6.3% and 8.6%, respectively, over this range.

- Over the -10° to 20° range, the percent change in the calibration coefficients of the Type S and modified S pitots using the Autoprobe (3.0% and 2.2%, respectively) was less than that found when these probes were used in the manual mode (6.3% and 3.2%).

- Over the pitch angle range of -30° to -10° the percent change in calibration coefficients was above 9.1% for all probes except the modified Kiel. The percent change in C_p ranged from 9.1% for the French probe to 21.0% for the Autoprobe using the modified S probe head. The extent of change indicates that the calibration coefficients of all test probes except the modified Kiel are highly pitch angle-dependent in the -30° to -10° pitch range.

- The modified Kiel probe's calibration coefficient changed by 3.4% or less across the -10° to 20° pitch range, and by less than 0.7% in the -30° to -10° range.

These findings lead to the following conclusions:

- The calibration coefficients of all probes, except for the Type S and French, were stable to within 3.5% in the -10° to 20° pitch range.

- None of the probes, except the modified Kiel, maintained a stable calibration coefficient in the -30° to -10° pitch range.

5.4.2 Velocity Determination

Analyzing the pitch effects on velocity determination leads to the following findings:

- Within the -10° to +10° pitch angle range, consistently high or consistently low velocity measurements were not evident. However, the manual Type S and modified Kiel measurements were consistently low between -10° and 0° pitch and -10° and 5° pitch, respectively.

- At positive pitch angles of 10° and greater at the higher tested velocities (60 and 90 fps), all probes measured high relative to actual axial flow. The degree of the disparity increased as the pitch angle increased.

- At pitch angles of -10° and less, all probes, except the modified Kiel, measured predominantly low relative to actual axial flow. The measurements were low by as much as 9.6%. Five out of nine velocity measurements from the modified Kiel were high by as much as +13.6%. Four out of nine velocity measurements were low by as much as 5.2%.

- Aggregating results across all three tested velocities, measurements by the Autoprobe were least affected by pitched flow in the -10° to +10° range. The maximum deviation for the Autoprobe from the actual axial velocity was 3.5% with the modified S probe head and 3.6% with the Type S probe head.

- At the higher tested velocities (60 and 90 fps), the modified Kiel probe's velocity measurements were least affected by pitched flow in the -10° to +10° range. Its maximum deviation from the actual axial flow was -2.2 % followed by the Autoprobe modified S (3.5%), Autoprobe S (3.6%), and manual Type S (-3.8%).

- In the -20° to +20° pitch angle range, the maximum deviation from actual axial velocity for all tested probes across all velocities was never better than -6.7%. The manual Type S had the lowest maximum deviation: -6.7% over all three velocities and -5.5% at the higher velocities. The maximum deviation for the other probes over all velocities ranged from +7.8% for the modified Kiel and Autoprobe with the Type S probe head to 15.6% for one of the manual modified S probes.

- Over the ±10° pitch angle range, across all velocities, there was no discernible advantage of equipping the Autoprobe with the modified S (+3.5% maximum deviation) as compared to the Type S probe (+3.6% maximum deviation).

These findings support the following conclusions:

- In the ±10° pitch angle range, no single probe excelled under all velocity conditions. Maximum deviations from axial velocity ranged from +3.5% for the Autoprobe operated with a modified S pitot head to +7.3% for the French probe.

- In the ±10° pitch angle range at the higher tested velocities (60 and 90 fps), all probes except the French measured velocities that were less than or equal to 4.9% of the axial velocity. The modified Kiel had the lowest deviation at -2.2%.

- In the ±20° pitch angle range, across all velocities tested, none of the tested 2D probes kept deviations from actual axial flow within ±5%.

- In the ±20° pitch angle range, over all velocities, the manual Type S probe had the smallest maximum deviation (-6.7%) and smallest maximum overestimation (+5.2%). At 60 and 90 fps, the maximum deviation for the manual Type S probe (-5.5%) was also lowest of all the tested probes.

- At negative pitch angles, the manual Type S probe always underestimated true axial velocity—the more negative the pitch, the larger the underestimate.

Figure 5-1. Probe: 3/8" Type S - S-1

Calibration Coefficient vs. Pitch Angle

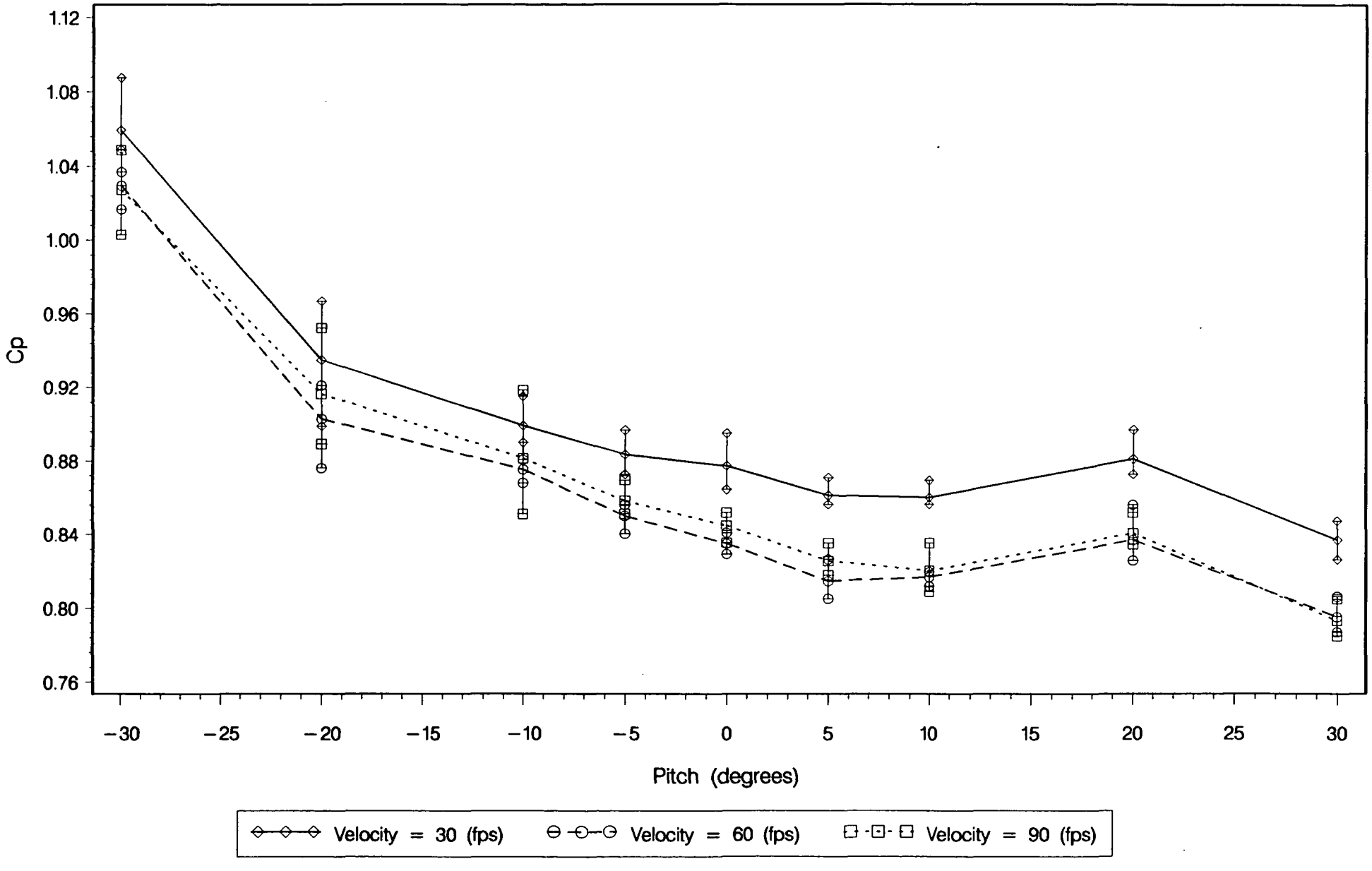

Bands Indicate the Minimum and Maximum Values

Figure 5-2. Probe: Modified S - USS-1

Calibration Coefficient vs. Pitch Angle

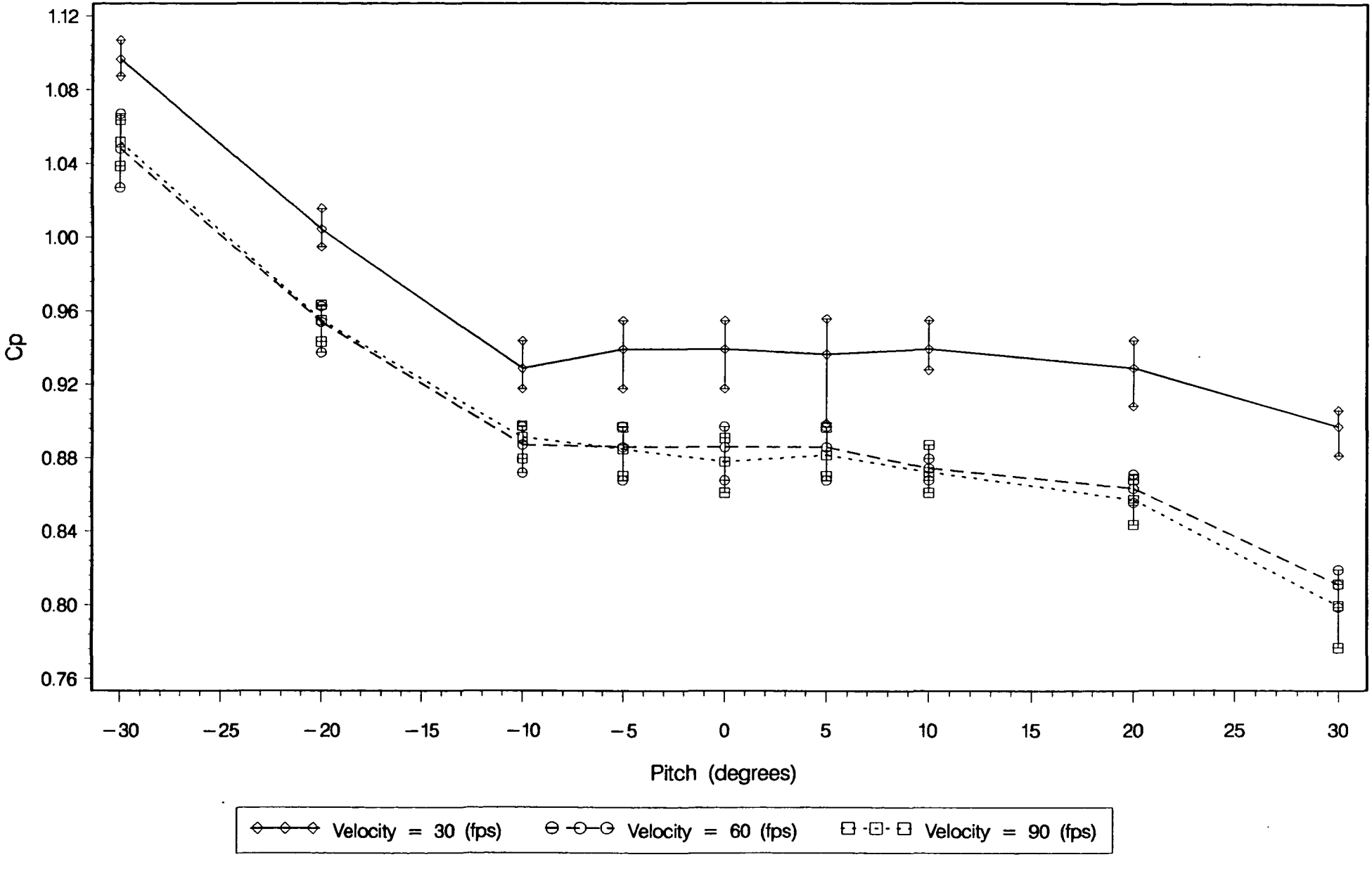

Bands Indicate the Minimum and Maximum Values

Figure 5-3. Probe: Modified S - USS-3

Calibration Coefficient vs. Pitch Angle

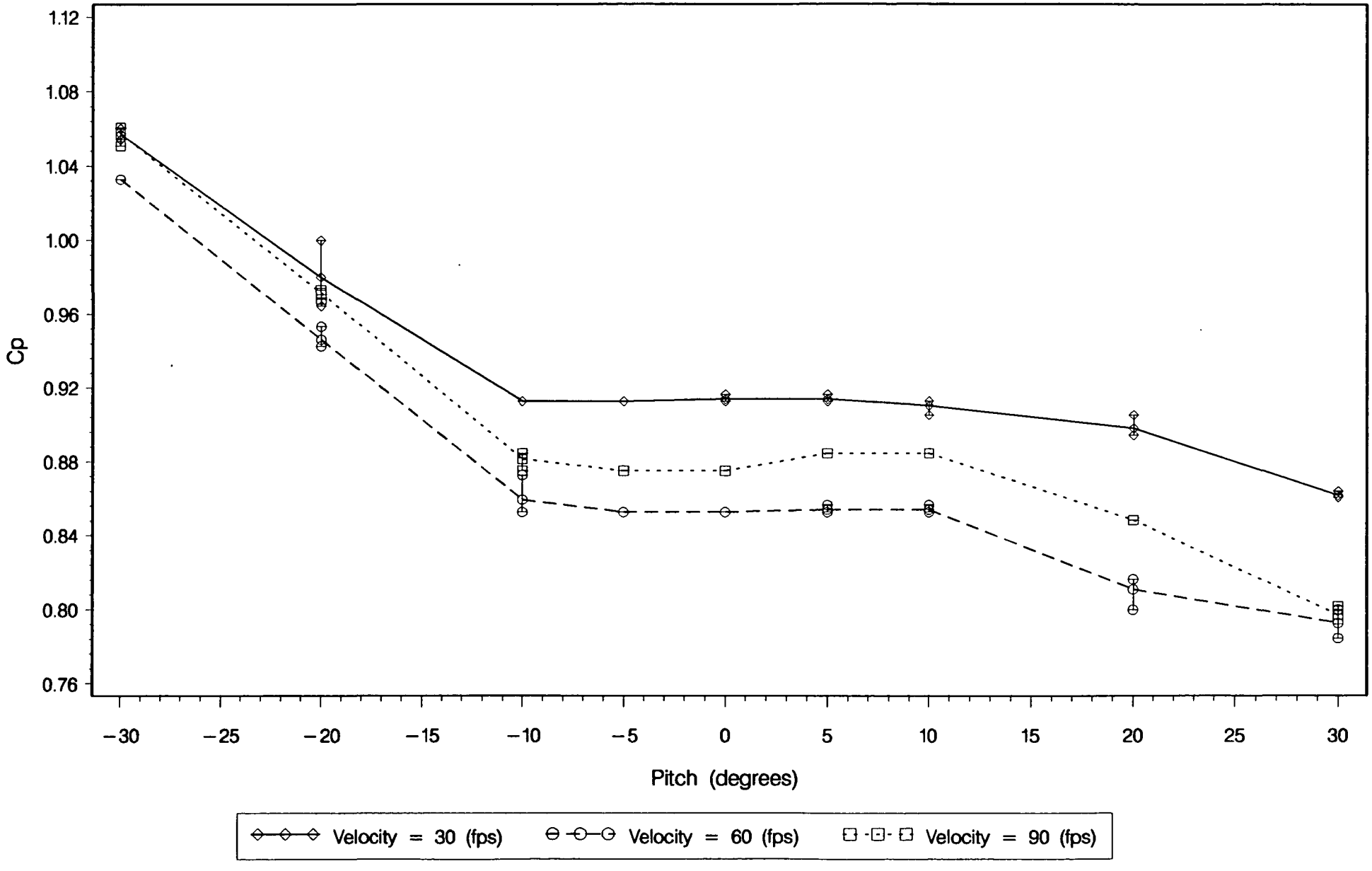

Bands Indicate the Minimum and Maximum Values

Figure 5-4. Probe: Autoprobe-Type S

Calibration Coefficient vs. Pitch Angle

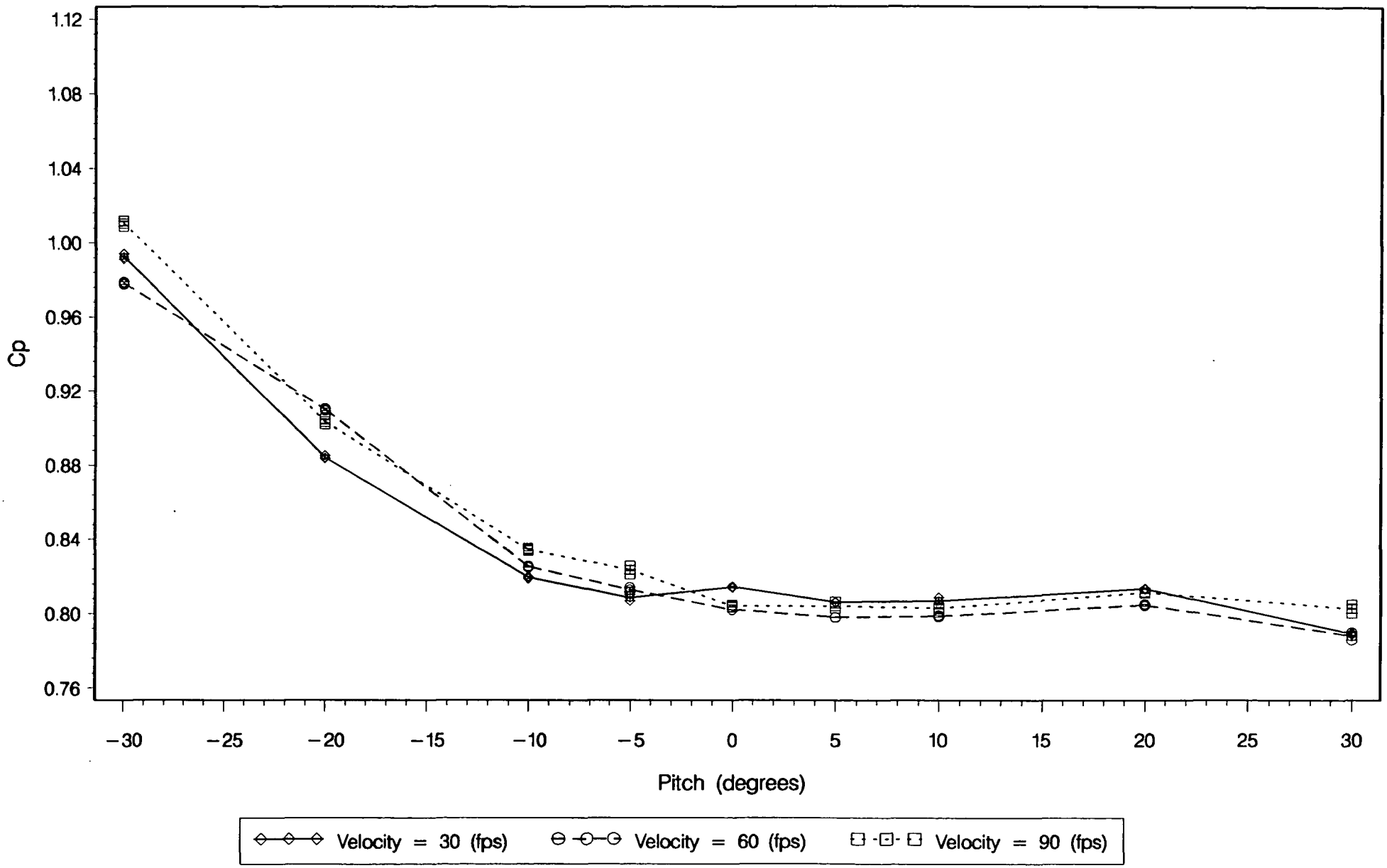

Bands Indicate the Minimum and Maximum Values

Figure 5-5. Probe: Autoprobe-Modified S

Calibration Coefficient vs. Pitch Angle

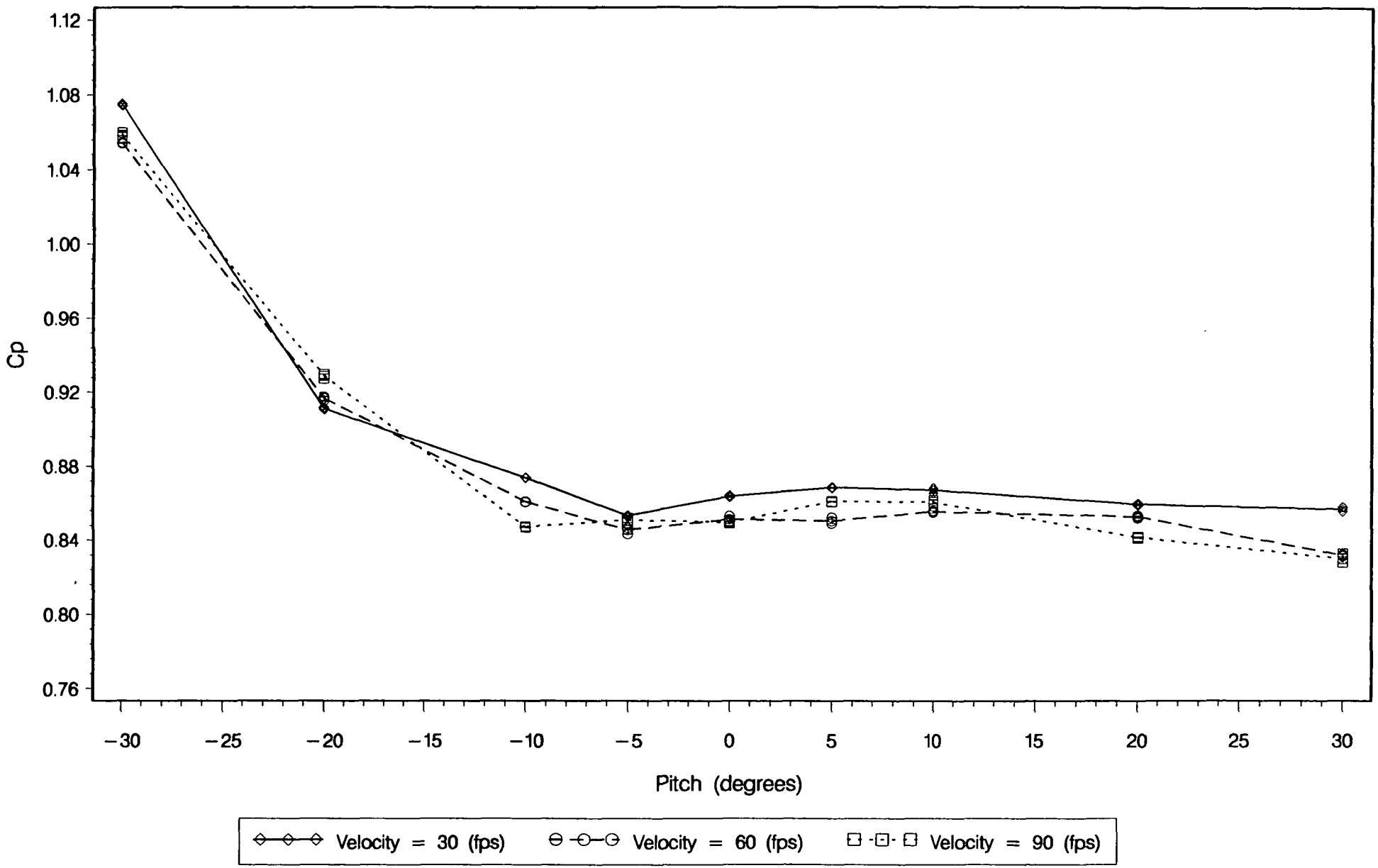

Bands Indicate the Minimum and Maximum Values

Figure 5-6. Probe: French Probe - F-2

Calibration Coefficient vs. Pitch Angle

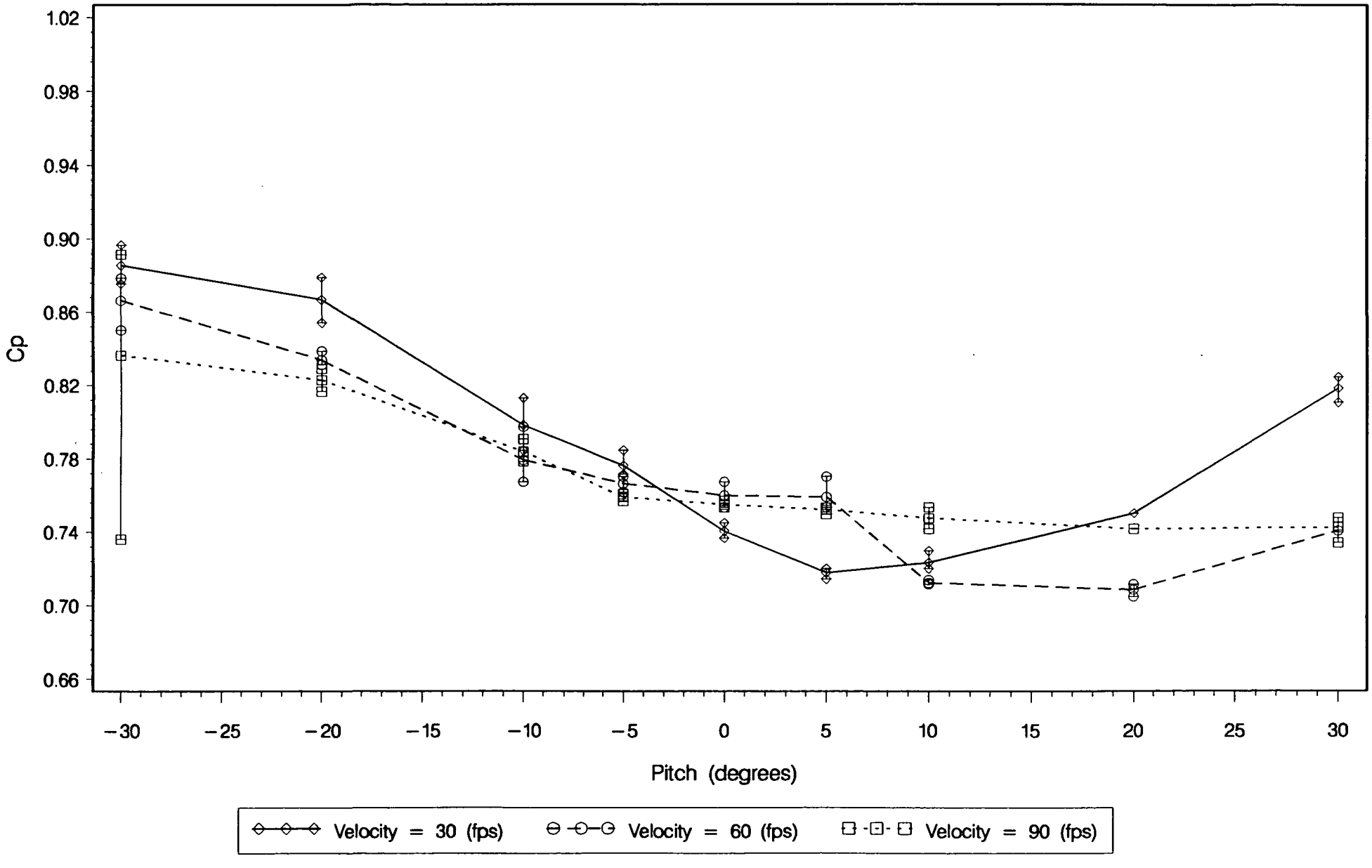

Bands Indicate the Minimum and Maximum Values

Figure 5-7.

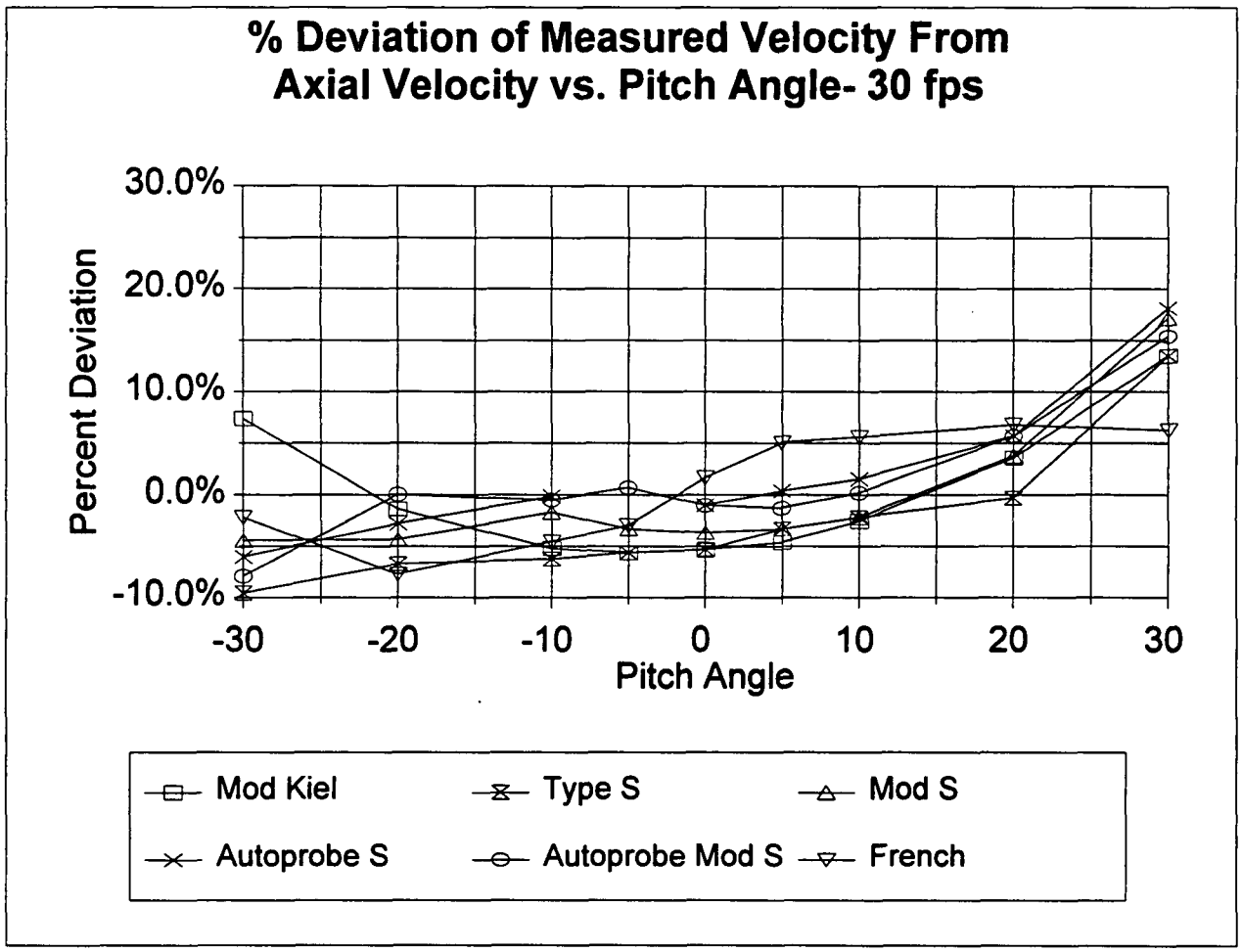
% Deviation of Measured Velocity From Axial Velocity vs. Pitch Angle- 30 fps
Percent Deviation
30.0%
20.0%
10.0%
0.0%
-10.0%
-30
-20
-10
0
10
20
30
Pitch Angle
Mod Kiel
Type S
Mod S
Autoprobe S
Autoprobe Mod S
French

Figure 5-8.

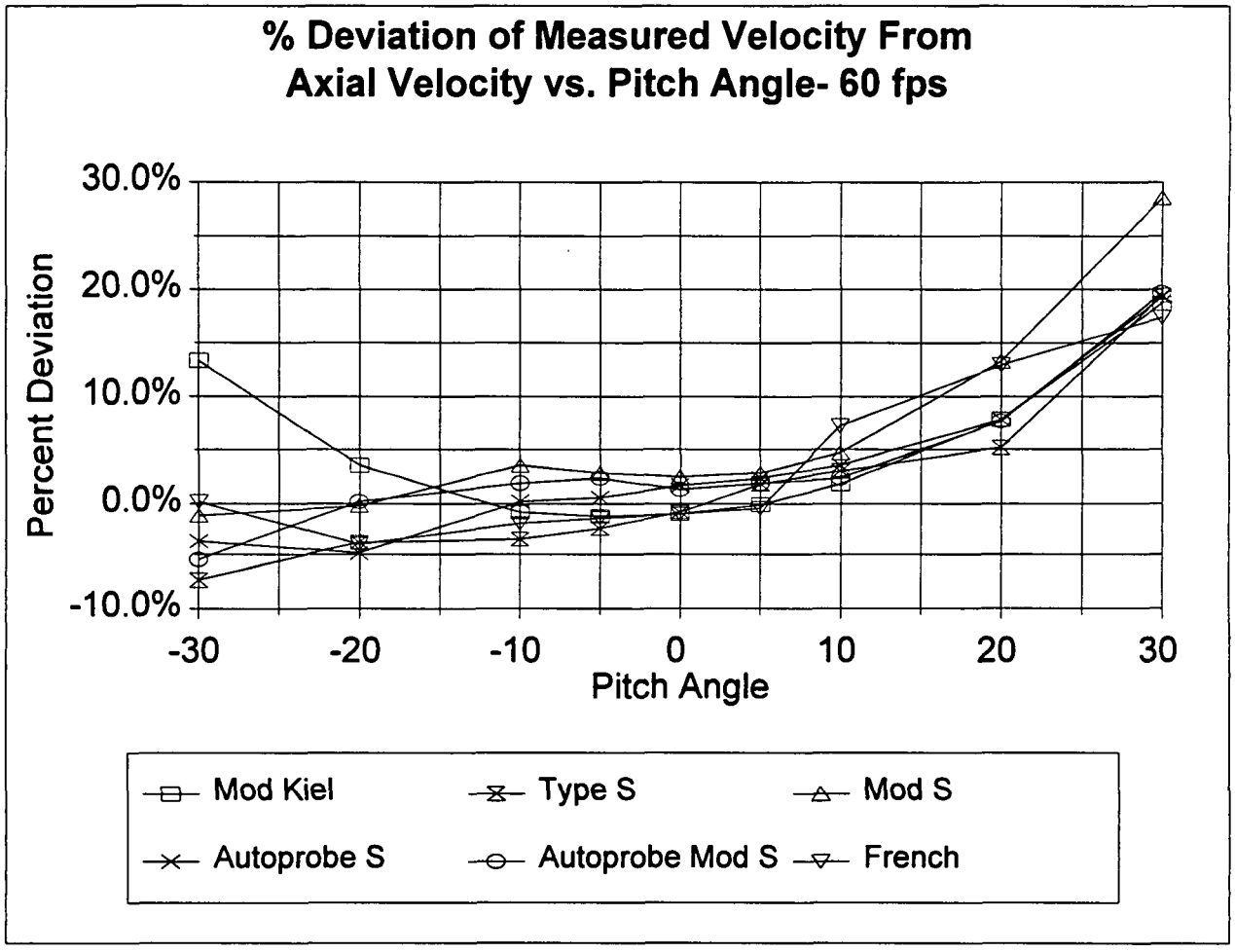
% Deviation of Measured Velocity From
Axial Velocity vs. Pitch Angle- 60 fps
30.0%
20.0%
10.0%
0.0%
-10.0%
Percent Deviation
-30
-20
-10
0
10
20
30
Pitch Angle
Mod Kiel
Type S
Mod S
Autoprobe S
Autoprobe Mod S
French

Figure 5-9.

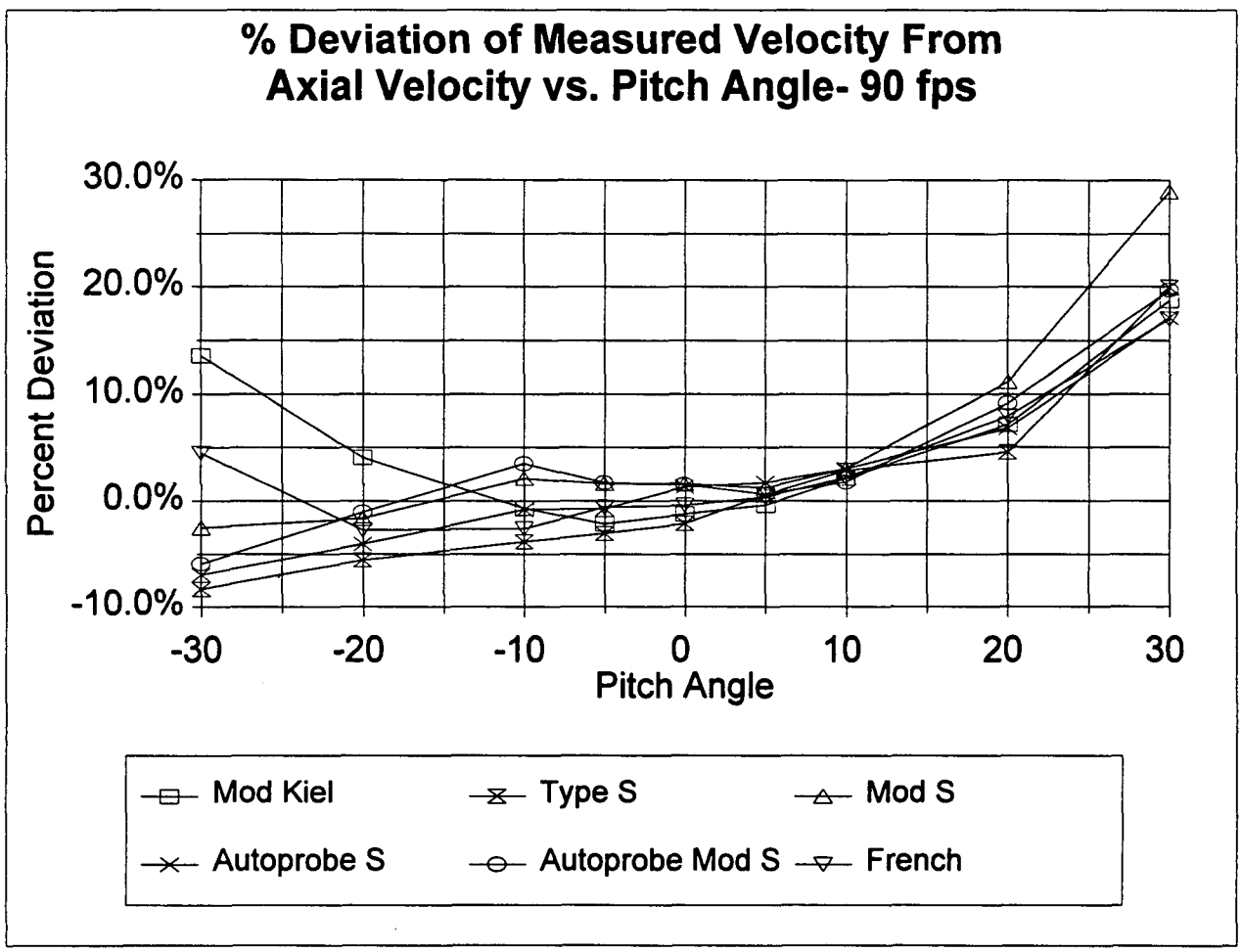
% Deviation of Measured Velocity From Axial Velocity vs. Pitch Angle- 90 fps
Percent Deviation
30.0%
20.0%
10.0%
0.0%
-10.0%
-30
-20
-10
0
10
20
30
Pitch Angle
Mod Kiel
Type S
Mod S
Autoprobe S
Autoprobe Mod S
French

6.0 ACCURACY OF YAW ANGLE MEASUREMENTS AND EFFECT ON VELOCITY MEASUREMENT

6.1 TEST PROCEDURES

The objectives of the experiments described in this section were to determine how accurately each probe could find a yaw null and to determine the effect on velocity measurement of errors in yaw nulling. Data on yaw nulling accuracy were collected during the tests described in Sections 3, 5, and 7 using the test procedures described in those sections. During the experiments, the wind tunnel was set at a velocity of 30, 60, or 90 fps, and the test probe was inserted into the wind tunnel at a preset pitch angle. The probe was yaw nulled by rotating it until ΔP across the appropriate ports (Fechheimer ports for the modified Kiel, impact and static ports for the manual and Autoprobe Type S and modified S, and P_2 and P_3 ports for the DAT and spherical probes) read 0. The angle, read by an inclinometer with a visually estimated accuracy of 0.1°, was then recorded as θ_{null}.

Because flow in the wind tunnel was at a yaw angle of zero, the measurement error is equivalent to the measured yaw angle θ_{null}. The Type S and modified S were yaw nulled manually, and the Autoprobes were yaw nulled automatically. No procedure has been established for yaw nulling the French probe, and, therefore, it was not included in this analysis.

In each replication of the experiment, the yaw null angle was read with the digital inclinometer and recorded. The 2D probes (except the modified Kiel probe) were then rotated 90° to align the measurement ports with the flow and ΔP across the probe was measured and recorded. The modified Kiel probe did not require rotation; ΔP was simply measured and recorded at the yaw null position. For the 3D probes, ΔP across ports P_1 and P_2 and across ports P_4 and P_5 were measured and recorded. Velocities at each point were then calculated using Equation 5.4 for the 2D probes and Equation 7.3 for the 3D probes. These steps were conducted three times to provide replicate runs.

6.2 ACCURACY OF YAW ANGLE DETERMINATIONS AND VELOCITY DETERMINATIONS

Figures 6–1 through 6–10 are plots of the deviation of the measured yaw null (θ_{null}) vs. pitch angle. Nine observations were made at each pitch setting, representing measurements taken at three velocities with three replicates performed at each velocity. Error bars show the maxima and minima of the nine measurements at each pitch. The means are connected by straight lines. Positive or negative deviations refer to clockwise or counterclockwise probe rotation, respectively.

Table 6–1 summarizes the data shown in Figures 6–1 through 6–10. For each probe, the table lists the maximum yaw null error ($\theta_{nullmax}$), in degrees, over the tested velocity and pitch ranges, and the associated percentage error in velocity that would have resulted if the actual yaw angle of the flow were 0° and 20°. Also shown is the pitch angle at which the maximum yaw angle and maximum deviation occurs.

Table 6-1. Summary of Yaw Angle Accuracy and Effect on Velocity Determination

Probe	$\theta_{nullmax}$ (°)	% Error in Velocity		Pitch Angle (°)
		θ_{yaw}=0°	θ_{yaw}=20°	
Modified Kiel (MK2)	1.1	0.02	0.7	30
Type S (S-1)	1.3	0.03	0.9	30
Modified S (USS-1)	6.6	0.66	4.8	-30
Modified S (USS-3)	2.8	0.12	1.9	-30
Autoprobe Type S (AS)[a]	-3.6	0.20	2.5	5
Autoprobe Mod S (AMS)[a]	5.4	0.44	3.9	20
Spherical (MS5-2)	-0.5	0.00	0.3	-30
DAT (3D-1)	1.0	0.02	0.7	30
DAT (3D-2)	-0.3	0.00	0.2	-20
DAT (3D-3)	0.7	0.01	0.5	30

[a] The Autoprobe tested in this study employed a "sweep" procedure to determine the yaw null. A curve-fitting algorithm has subsequently been implemented by the manufacturer to find the yaw null.

The errors in velocity were calculated from the following equation:

$$\% \text{ Error} = 100 \frac{\left(V_{null} \cos\left(\theta_y + \theta_{nullmax}\right)\right) - V_{null} \cos\left(\theta_y\right)}{V_{null} \cos\left(\theta_y\right)}$$

$$= 100 \left(\frac{\cos\left(\theta_y + \theta_{nullmax}\right)}{\cos\left(\theta_y\right)} - 1 \right) \qquad \textbf{(Eq. 6.1)}$$

where

V_{null} = velocity calculated from ΔP
θ_y = actual yaw angle (0° or 20°)
$\theta_{nullmax}$ = maximum error in measuring θ_y

EPA Method 2, the only method currently approved for flue gas flow measurement, is based on measuring flow with a Type S probe without yaw nulling. EPA Method 1[1] permits use of the Type S probe only if the yaw angle of flow determined by averaging yaw angle over traverse points is less than 20°. Yaw angles are measured at each traverse point by yaw nulling with the Type S probe with

[1] 40 CFR Ch. 1 (7-1-92 Edition), Pt. 60, App. A, Method 1—Sample and Velocity Traverses for Stationary Sources, pgs. 682-688.

the same technique used in this study. Examining errors in velocity attributable to yaw angles of up to 20° is thus instructive about the range of errors that can potentially be observed.

Table 6-2 shows additional summary statistics for the data displayed in Figures 6-1 through 6-10. For each probe at each velocity, the table lists the minimum, mean, and maximum deviations from θ_{null} calculated across all pitch angles tested, and the range and standard deviation across all pitch angles. The table also shows these parameters calculated across all velocities. Across all pitch angles and all velocities, the largest absolute mean yaw angle error was 1.5° for one of the modified S probes. The smallest was 0.1° for the spherical probe and one of the DAT probes. The largest standard deviation across all pitch angles and all velocities was 2.8° for one modified S probe; the smallest was 0.3° for the spherical probe and one of the DAT probes.

6.3 Flow Measurement Error Due to Yaw Null Misalignment for the Autoprobe Type S

An issue related to the accuracy of yaw nulling procedures is the magnitude of the error that would be produced in flow measurements when probes are not yaw nulled or are misaligned relative to the yaw component of flow. A previous study of Type S probes found that the estimated error was as high as 18% at a 20° yaw misalignment.[2] If the error in velocity measurements were due strictly to the inability to measure and account for yaw, the overestimation of flow due to a 20° misalignment of the probe would be (1-cos20°)/cos20°, or only 6.42%. That is, a probe that could measure total velocity perfectly would overestimate the flow velocity by 6.42% strictly due to the inability to determine the yaw angle. Thus, a deviation as high as that reported in the previous study would indicate that the error could not be fully explained by the probe's inability to measure the yaw angle and derive the axial component of velocity. It would imply that physical characteristics of the probe were causing a further overestimation of the flow velocity.

Table 6-2. Yaw Angle Error Detailed Data

Probe	Velocity (fps)	Across All Pitch Angles (-30° to +30°)					
		Sample Size	Minimum (°)	Mean (°)	Maximum (°)	Range (°)	Standard Deviation (°)
Modified Kiel (MK2)	30	27	-0.4	0.4	2.2	2.6	0.5
	60	27	-0.2	0.4	1.5	1.7	0.4
	90	27	0.1	0.5	1.3	1.4	0.3
	All	81	-0.4	0.4	2.2	2.6	0.4
Type S (S-1)	30	27	-1.0	0.1	1.7	2.7	0.7
	60	27	-1.0	0.3	1.4	2.4	0.6
	90	27	-1.0	0.4	1.5	2.5	0.7
	All	81	-1.0	0.3	1.7	2.7	0.7

[2] Williams, III, J.C., and F.R. DeJarnette. 1977. A Study on the Accuracy of Type S Pitot Tubes. EPA Report No. EPA-600/4-77-030. 70 pgs.

Table 6-2. Yaw Angle Error Detailed Data (continued)

Probe	Velocity (fps)	Across All Pitch Angles (-30° to +30°)					
		Sample Size	Minimum (°)	Mean (°)	Maximum (°)	Range (°)	Standard Deviation (°)
Modified S (USS-1)	30	27	-10.8	1.5	9.0	19.8	3.6
	60	27	-5.1	1.6	7.0	12.1	2.6
	90	27	-4.5	1.4	5.3	9.8	2.2
	All	81	-10.8	1.5	9.0	19.8	2.8
Modified S (USS-3)	30	27	-0.7	0.6	3.0	3.7	0.8
	60	27	-3.0	0.5	4.7	7.7	1.6
	90	27	-4.1	0.2	3.1	7.2	1.9
	All	81	-4.1	0.5	4.7	8.8	1.5
Autoprobe Type S (AS)	30	26	-8.1	0.6	3.9	12.0	2.5
	60	26	-7.6	-1.1	3.0	10.6	2.8
	90	27	-6.1	-2.1	1.7	7.8	2.0
	All	79	-8.1	-0.9	3.9	12.0	2.7
Autoprobe Mod S (AMS)	30	27	-0.2	1.2	4.7	4.9	1.4
	60	27	0.1	1.2	4.4	4.5	1.2
	90	29	0.5	1.7	8.1	7.6	2.2
	All	83	-0.2	1.4	8.1	8.3	1.7
Spherical (MS5-2)	30	27	-0.8	-0.1	0.6	1.4	0.3
	60	27	-0.6	-0.2	0.5	1.1	0.3
	90	27	-0.7	-0.1	0.6	1.3	0.4
	All	81	-0.8	-0.1	0.6	1.4	0.3
DAT (3D-1)	30	27	-0.3	0.0	0.2	0.5	0.1
	60	27	-0.2	0.4	1.6	1.8	0.5
	90	27	-0.3	0.7	1.8	2.1	0.5
	All	81	-0.3	0.4	1.8	2.1	0.5
DAT (3D-2)	30	27	-1.0	-0.3	0.4	1.4	0.4
	60	27	-0.8	0.0	0.7	1.5	0.3
	90	27	-0.8	0.0	0.6	1.4	0.3
	All	81	-1.0	-0.1	0.7	1.7	0.3

Table 6-2. Yaw Angle Error Detailed Data (continued)

Probe	Velocity (fps)	Across All Pitch Angles (-30° to +30°)					
		Sample Size	Minimum (°)	Mean (°)	Maximum (°)	Range (°)	Standard Deviation (°)
DAT (3D-3)	30	27	-0.9	0.0	0.6	1.5	0.4
	60	27	-0.4	0.3	1.1	1.5	0.5
	90	27	-0.8	0.3	1.1	1.9	0.5
	All	All	-0.9	0.2	1.1	2.0	0.5

To investigate this issue, the current study used the Autoprobe, because it could take measurements quickly at predefined yaw angles. Operating in the non-yaw nulled mode, the Autoprobe measured ΔP in 5° yaw increments. The measurements were successively carried out at pitch angle settings of -10°, 0°, and +10° at a nominal velocity of 60 fps. At each yaw angle θ_y, the calibration coefficient C_{p_y} was calculated using Equation 6.2.

$$C_P = \sqrt{\frac{\Delta P_P}{\Delta P_{s_y}}} \qquad \textbf{(Eq. 6.2)}$$

where

ΔP_P = differential pressure for the standard pitot tube at yaw angle = 0°

ΔP_{s_y} = differential pressure for the Type S pitot tube at yaw angle, θ_y

Figure 6-11 is a plot of C_{p_y} vs. yaw angle. The shapes of the curves at all three pitch angles are similar in the -20° to +20° range. Using the data shown in Figure 6-11, flow measurement errors due to errors in yaw angle measurement were calculated according to Equation 6.3.

$$\%\ Error = \left(\frac{C_{p_0}}{C_{p_y}} - 1 \right) 100 \qquad \textbf{(Eq. 6.3)}$$

where

C_{p_0} = calibration coefficient of Type S pitot tube at yaw angle = 0°

C_{p_y} = calibration coefficient of the Type S pitot tube at yaw angle, θ_y

These errors are plotted in Figure 6-12. In the -10° to +10° pitch-angle range typically found in stacks covered under the Acid Rain Program, the maximum flow measurement error in the ±20° yaw angle range (the range in which Method 2 is applicable) is 1.98%. This error is well below the 6.42% error resulting at 20° yaw when the yaw angle is not measured at all.

6.4 CONCLUSIONS

The data presented in this section support the following findings:

- For all probes employing Fechheimer-type ports to measure yaw (i.e., the modified Kiel, the spherical, and DAT probes), the error in the derived yaw angle was 1.1° or less (see Table 6-1). This translates into a 0.7% or less error in velocity measurements in a flow profile displaying 20° yaw.

- For the manually operated Type S probe, the yaw angle error was 1.3°, resulting in a 0.9% velocity error in a flow profile displaying 20° yaw.

- For the manual and automated modified S probes, the absolute value of the yaw angle error ranged from 2.8° to 6.6° with a corresponding 1.9% to 4.8% error in velocity measurements in a flow profile with a 20° yaw.

- Maximum error in determining yaw angle with the Autoprobe was -3.6° using the Type S head and 5.4° using the modified S head. This translates into a 2.5% and 3.9% velocity error in a flow profile displaying 20° yaw.

These findings lead to the following conclusions:

- Use of Fechheimer ports produces consistently better yaw angle measurements than other procedures for measuring yaw angles.

- In the wind tunnel, the manually operated Type S probe gave yaw null and velocity accuracy results comparable to those of the probes employing Fechheimer ports.

- The maximum yaw angle error using the Autoprobe[3] was higher than the maximum errors produced by either the manually operated Type S probe or any of the manually operated probes that employ Fechheimer ports.

- Among the manually operated probes, the largest error in yaw angle measurements was produced by the modified S probe: 6.6°. Similarly, the largest error with the Autoprobe was produced using the modified S probe head: 5.4°.

[3] As noted in Table 6-1, the Autoprobe tested in this study employed a "sweep" procedure to determine the yaw null rather than the curve-fitting algorithm subsequently implemented by the manufacturer.

Figure 6-1. Probe: Modified Kiel Probe With Thermocouple-MK2

Theta_null Deviation from True Yaw Null

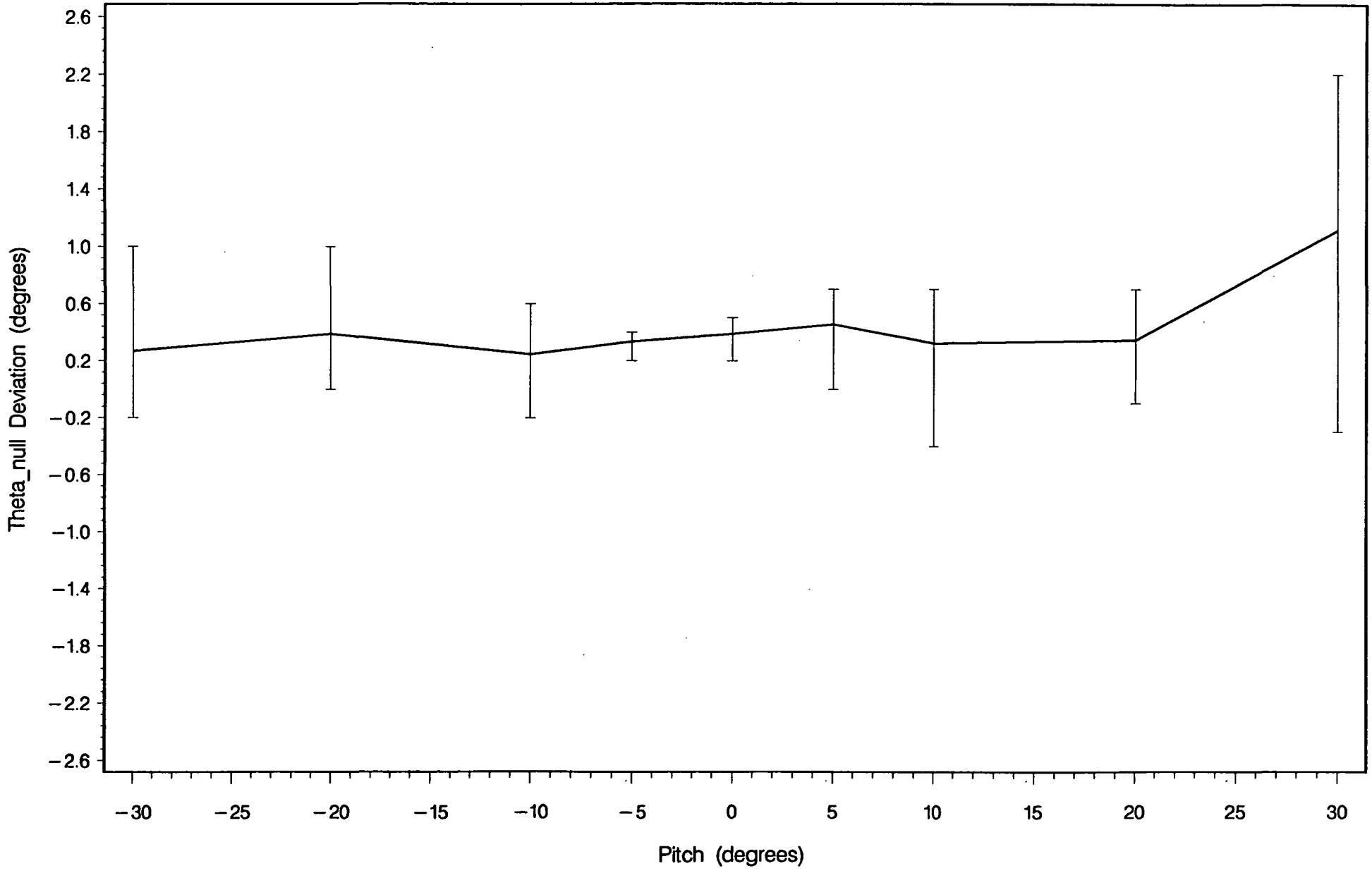

Bands Indicate the Minimum and Maximum Values

Figure 6-2. Probe: 3/8" Type S-S1

Theta_null Deviation from True Yaw Null

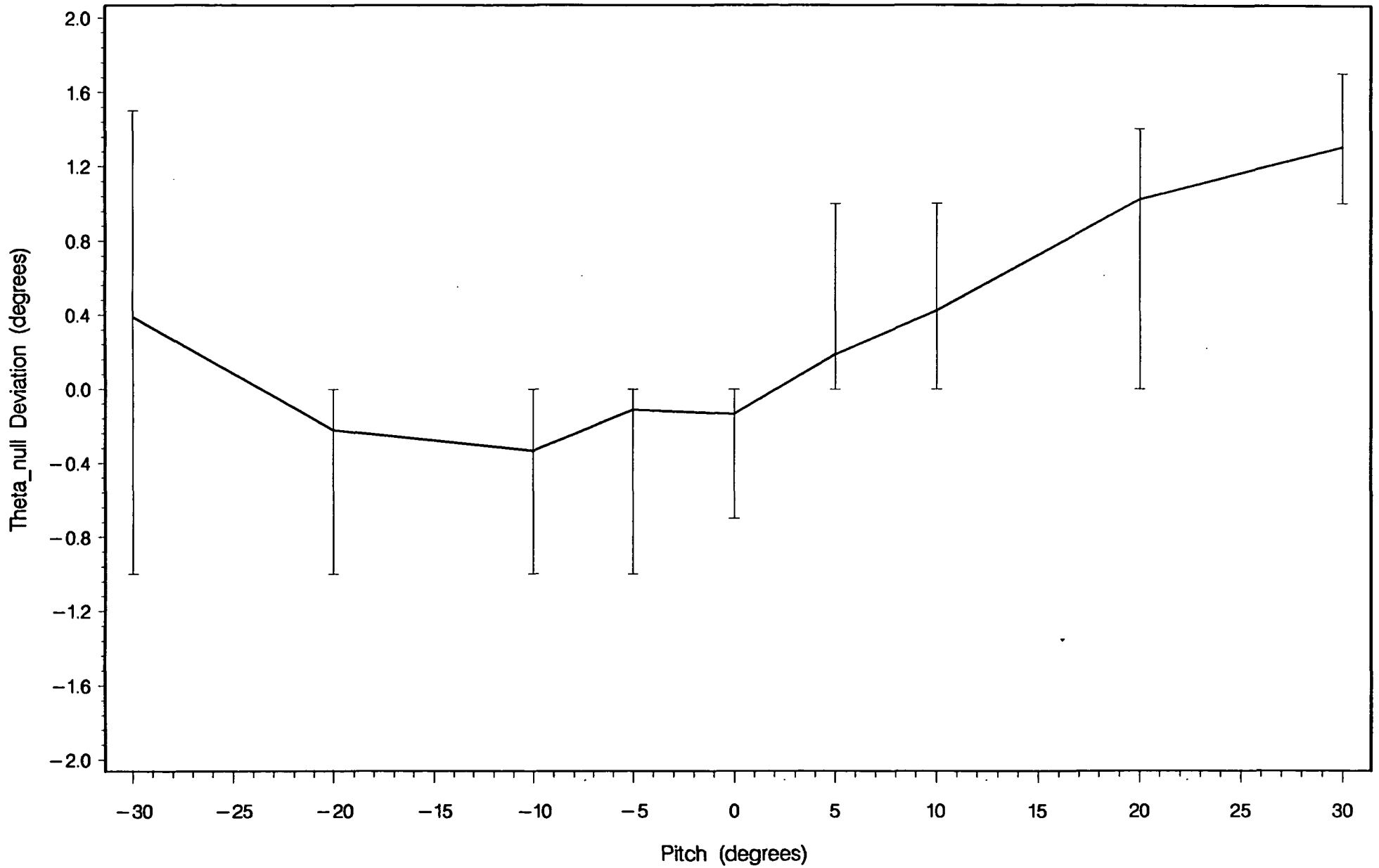

Bands Indicate the Minimum and Maximum Values

Figure 6-3. Probe: Modified S-USS-1

Theta_null Deviation from True Yaw Null

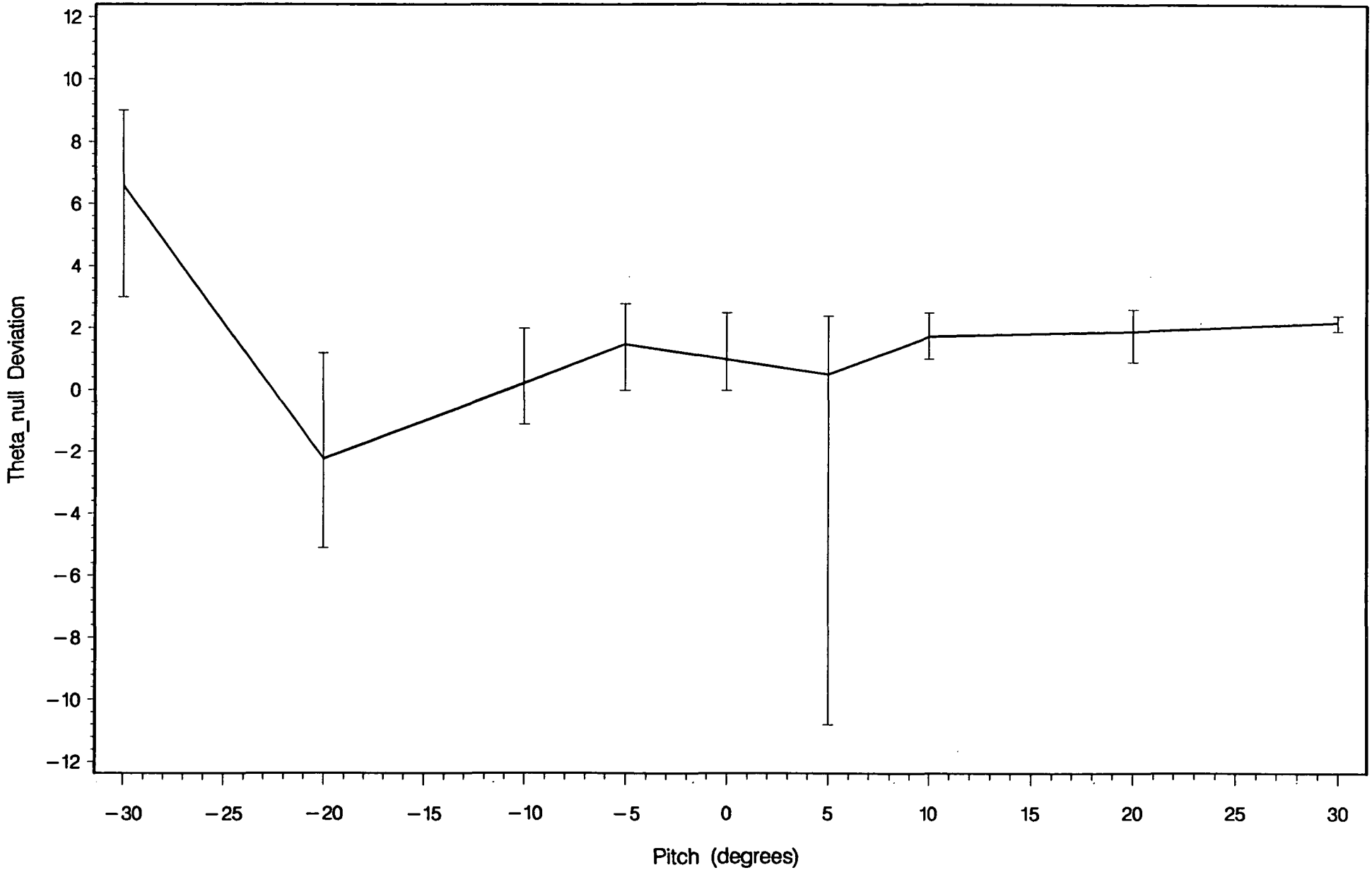

Bands Indicate the Minimum and Maximum Values

Figure 6-4. Probe: Modified S-USS-3

Theta_null Deviation from True Yaw Null

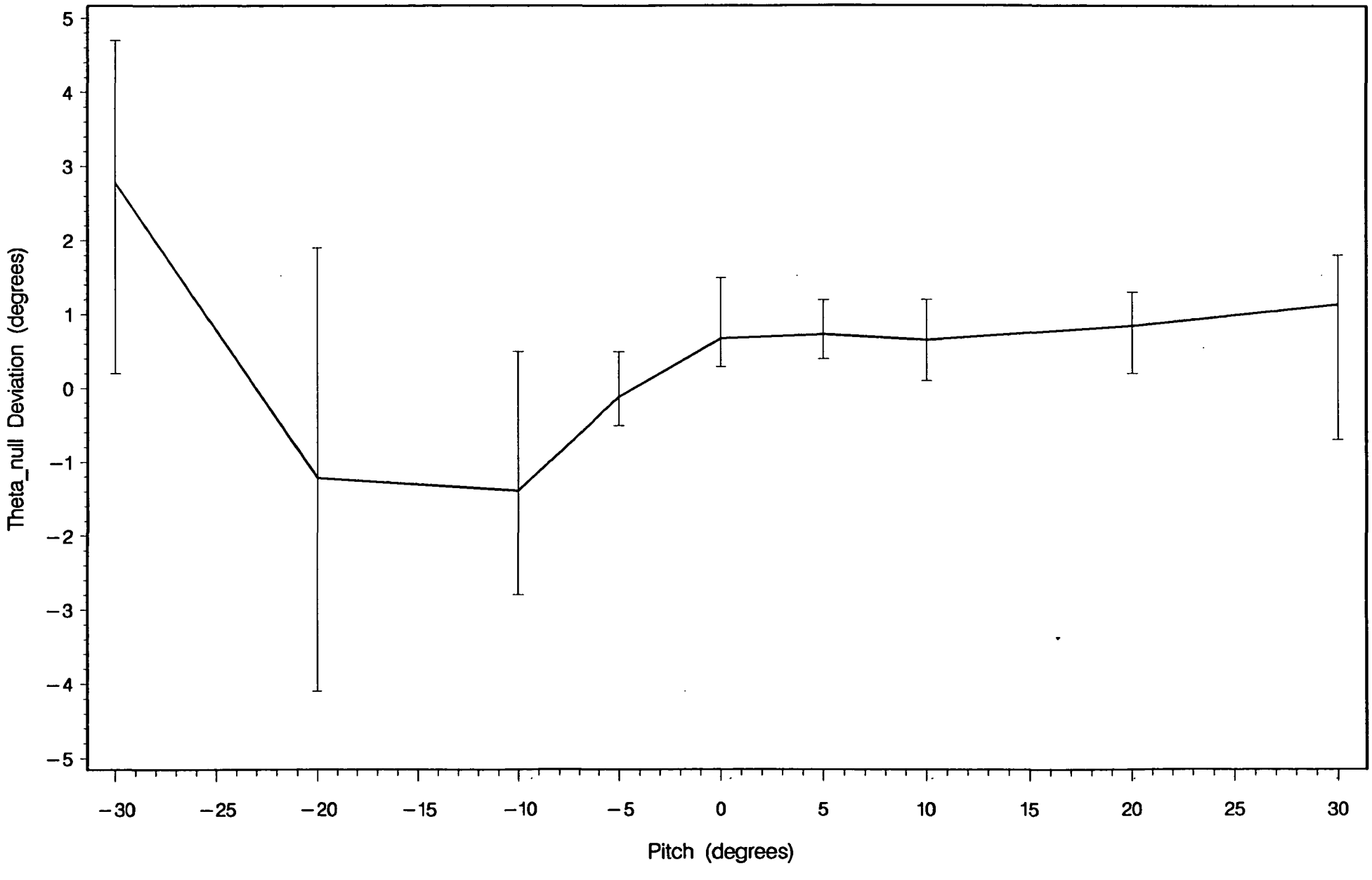

Bands Indicate the Minimum and Maximum Values

Figure 6-5. Probe: Autoprobe Type S

Theta_null Deviation from True Yaw Null

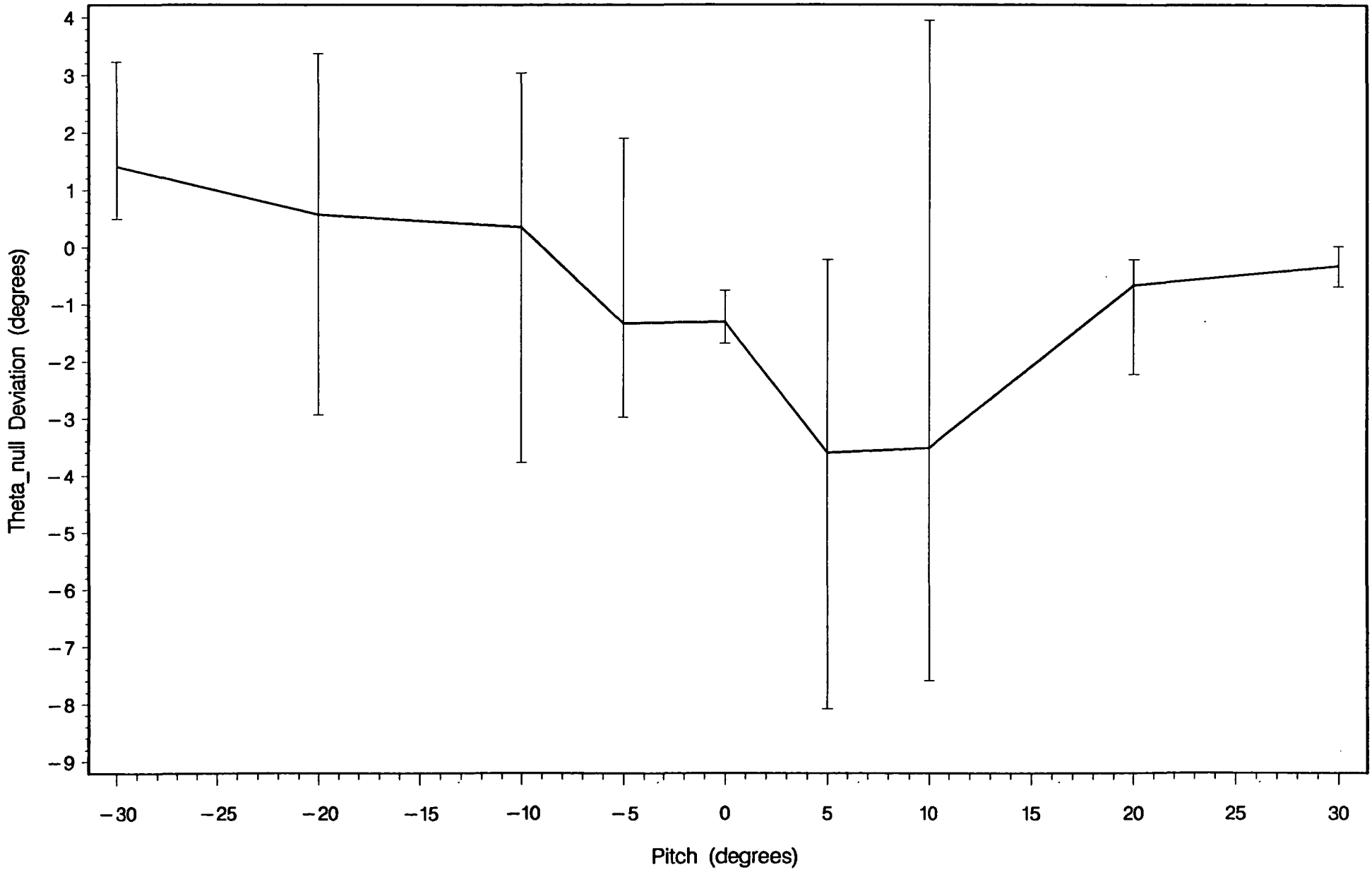

Bands Indicate the Minimum and Maximum Values

Figure 6-6. Probe: Autoprobe Mod S

Theta_null Deviation from True Yaw Null

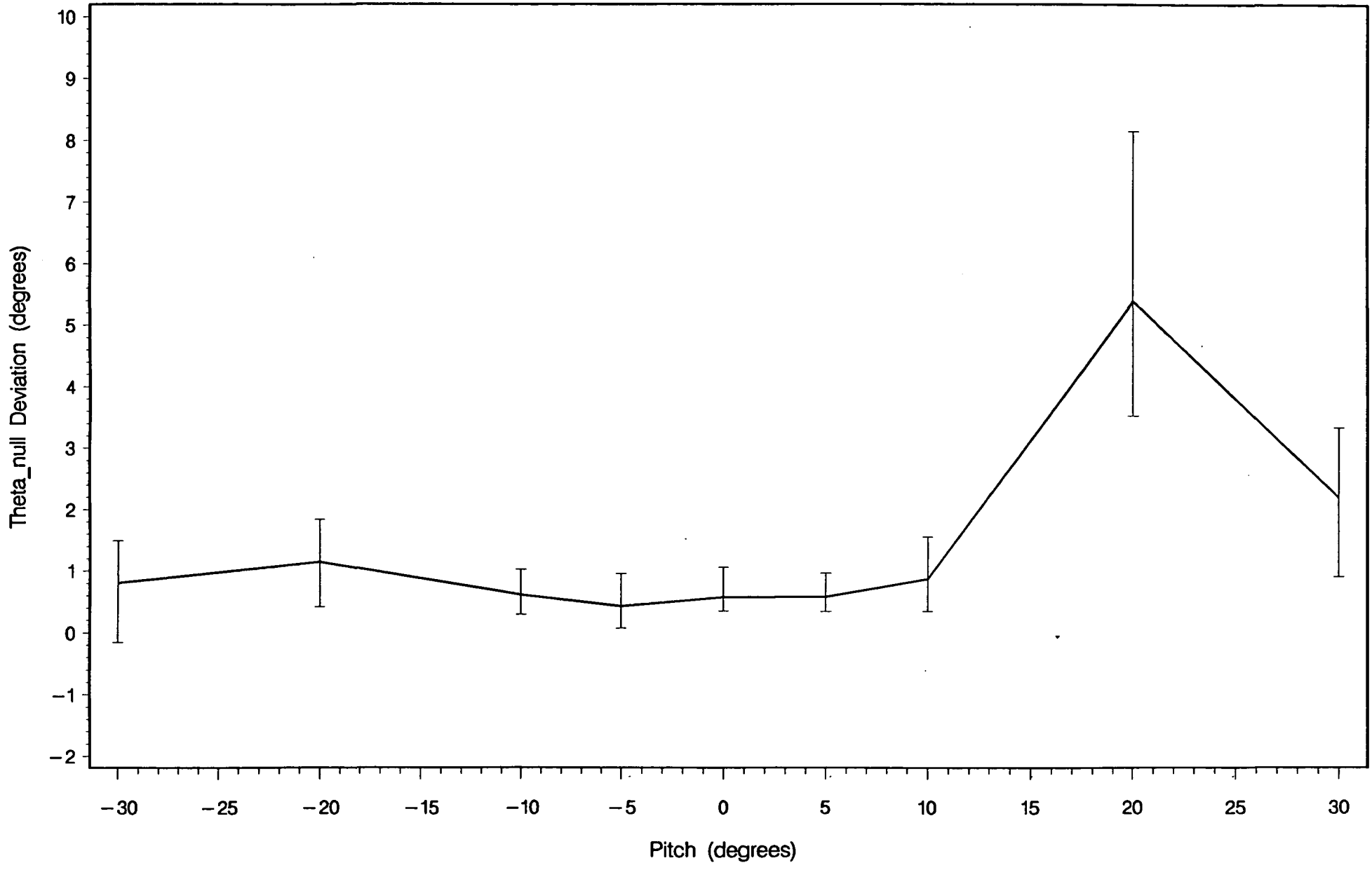

Bands Indicate the Minimum and Maximum Values

Figure 6-7. Probe: Spherical MS5-2

Theta_null Deviation from True Yaw Null

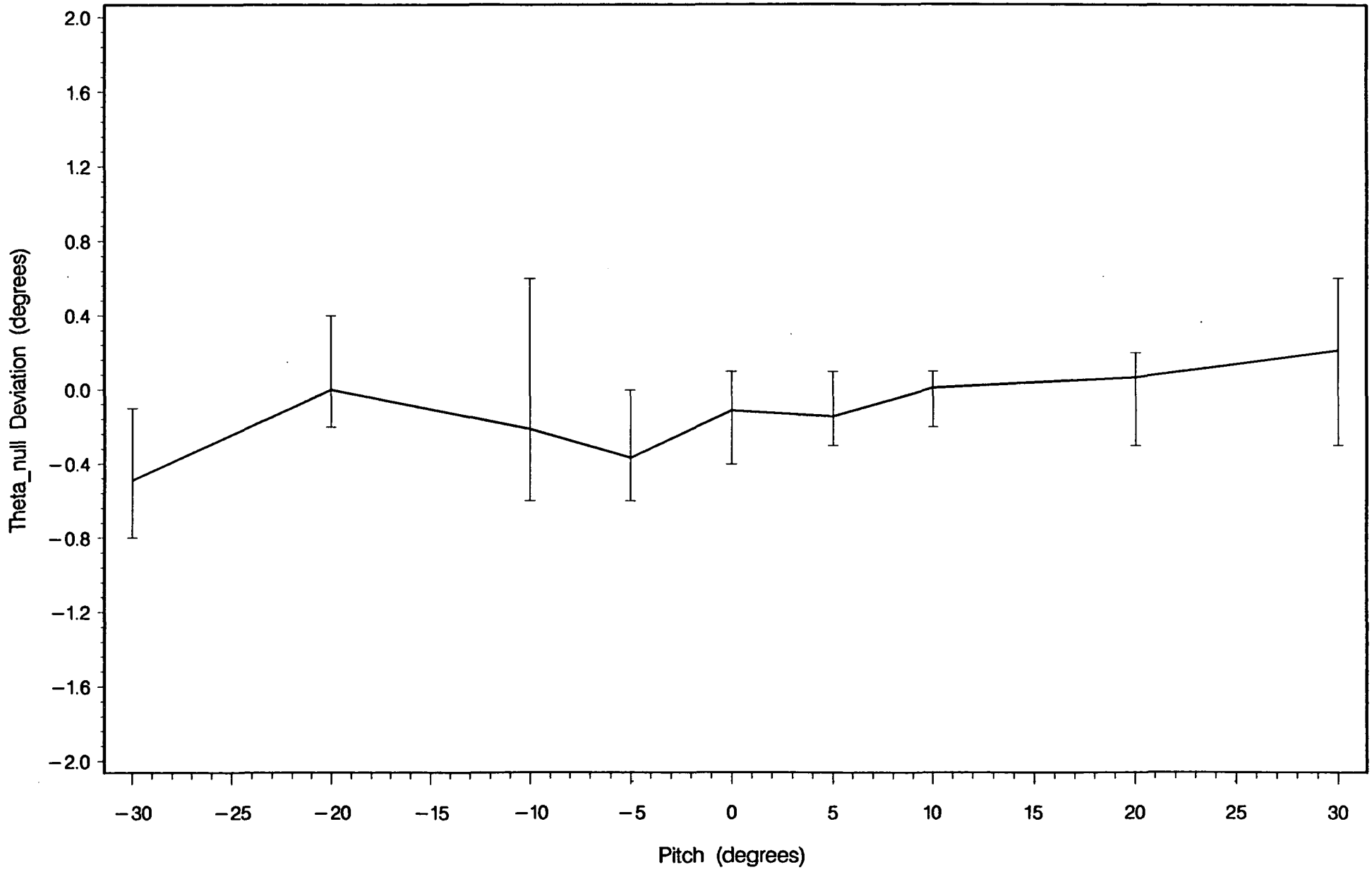

Bands Indicate the Minimum and Maximum Values

Figure 6-8. Probe: DAT-3D-1

Theta_null Deviation from True Yaw Null

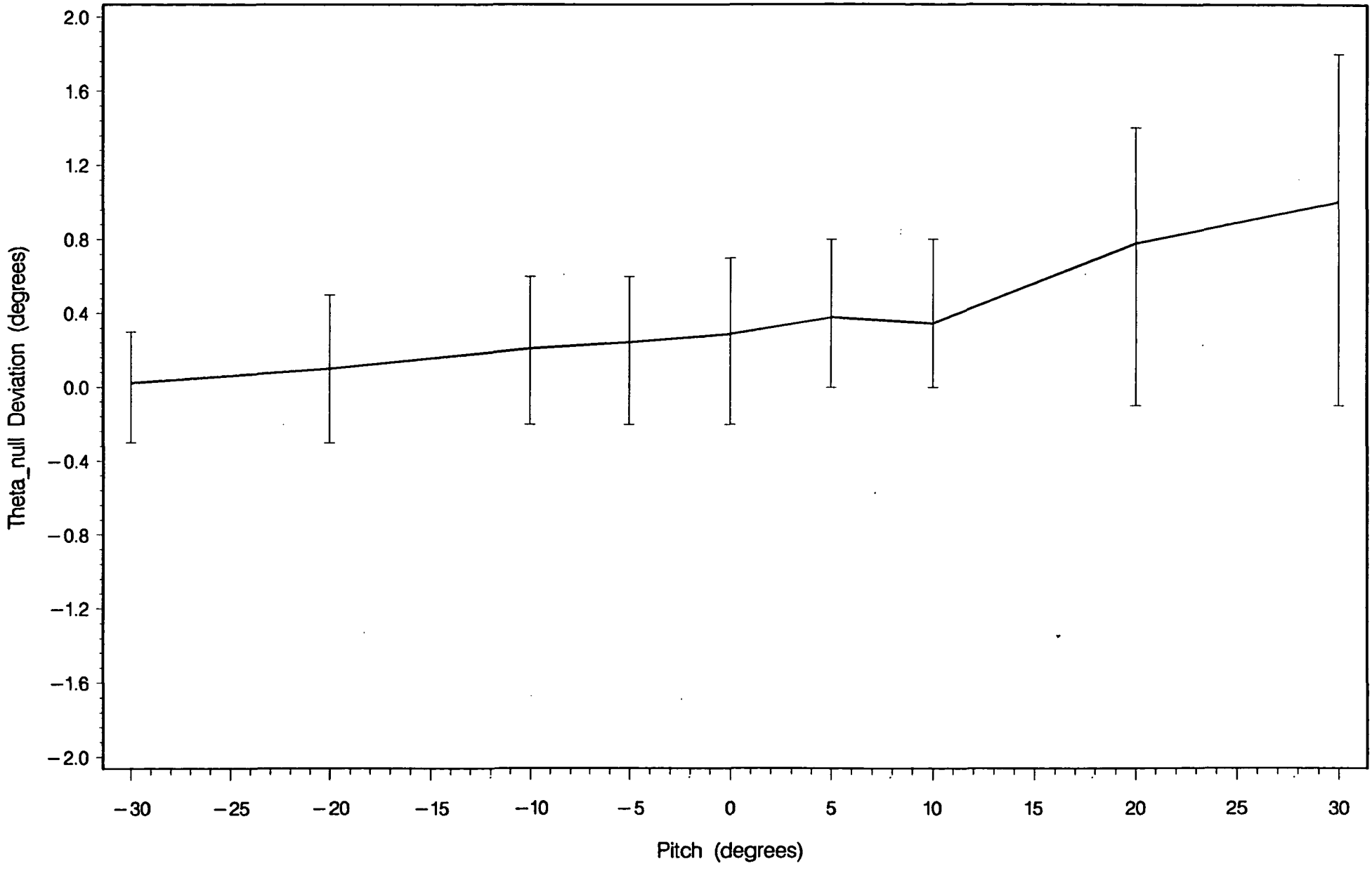

Bands Indicate the Minimum and Maximum Values

Figure 6-9. Probe: DAT-3D-2

Theta_null Deviation from True Yaw Null

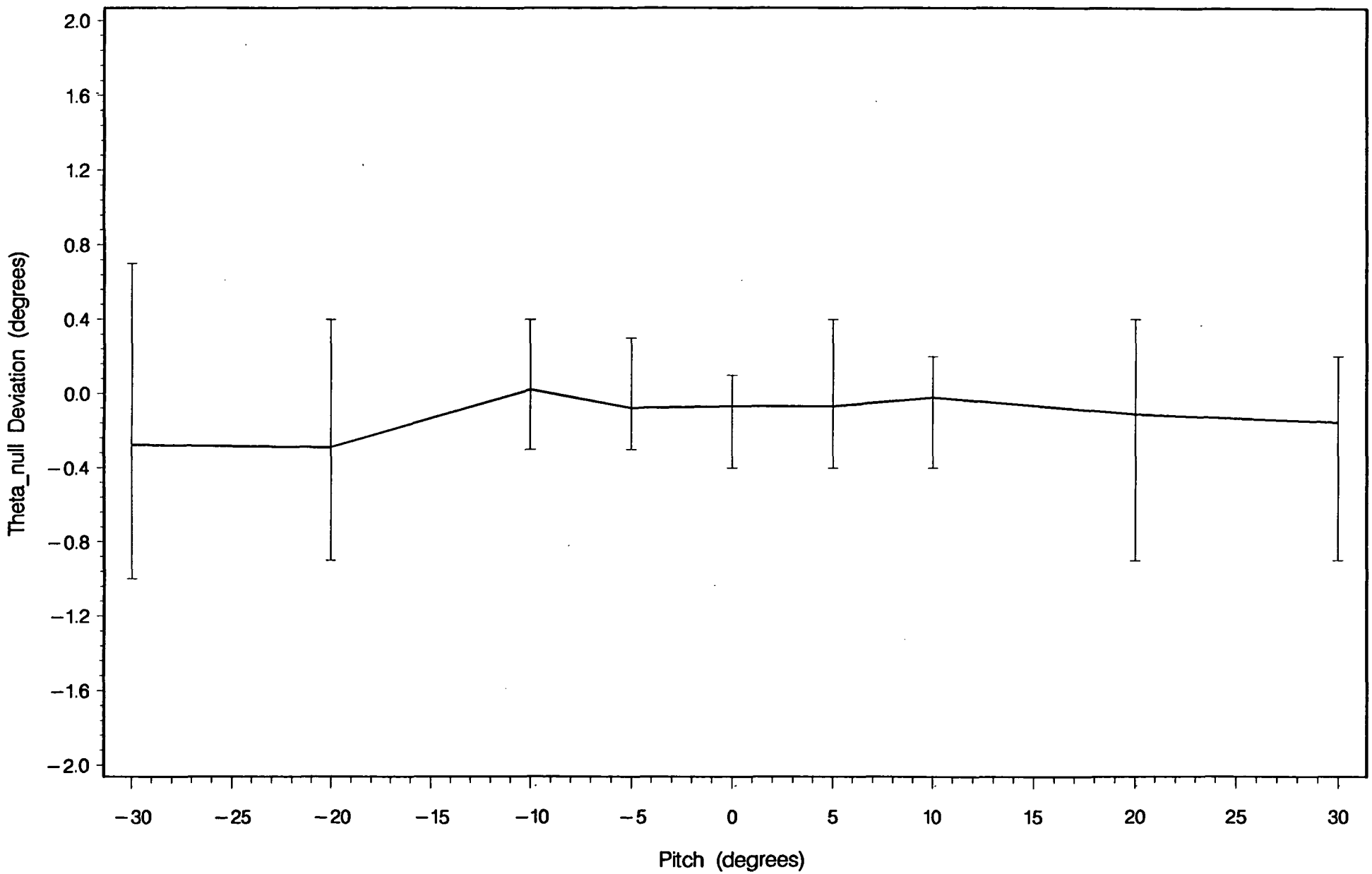

Bands Indicate the Minimum and Maximum Values

Figure 6-10. Probe: DAT-3D-3

Theta_null Deviation from True Yaw Null

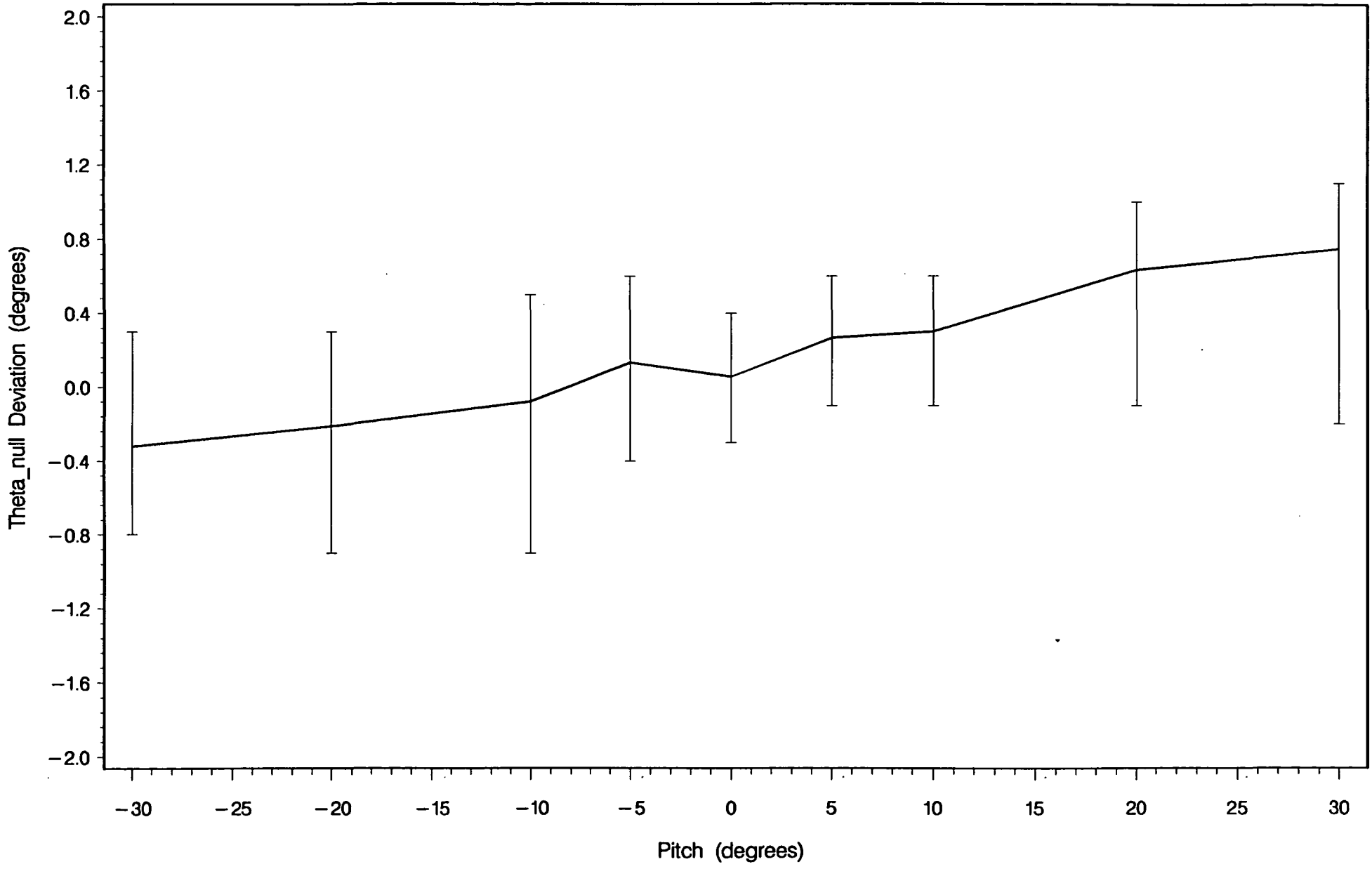

Bands Indicate the Minimum and Maximum Values

Figure 6-11.

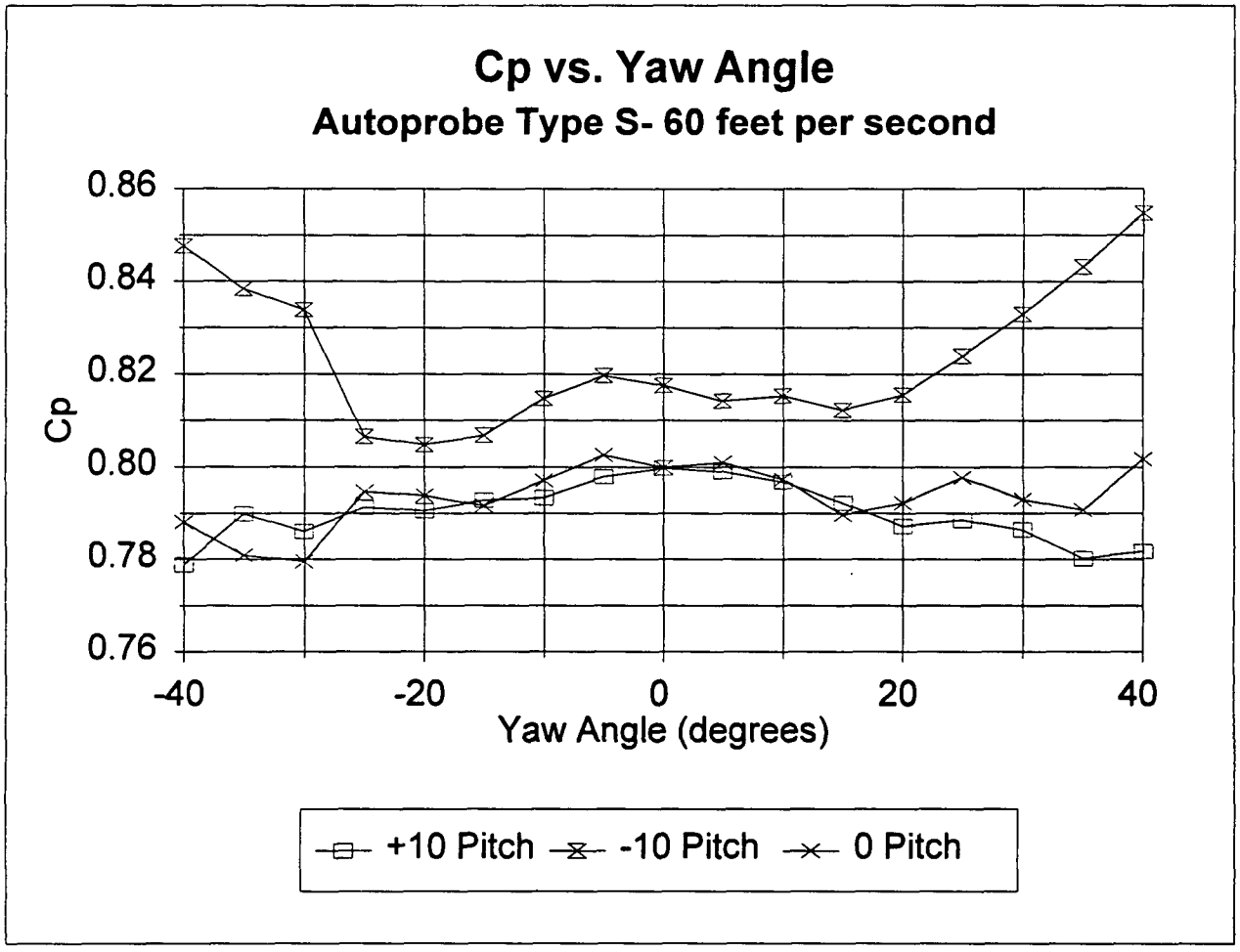
Cp vs. Yaw Angle
Autoprobe Type S- 60 feet per second
0.86
0.84
0.82
0.80
0.78
0.76
Cp
-40
-20
0
20
40
Yaw Angle (degrees)
+10 Pitch
-10 Pitch
0 Pitch

Figure 6-12.

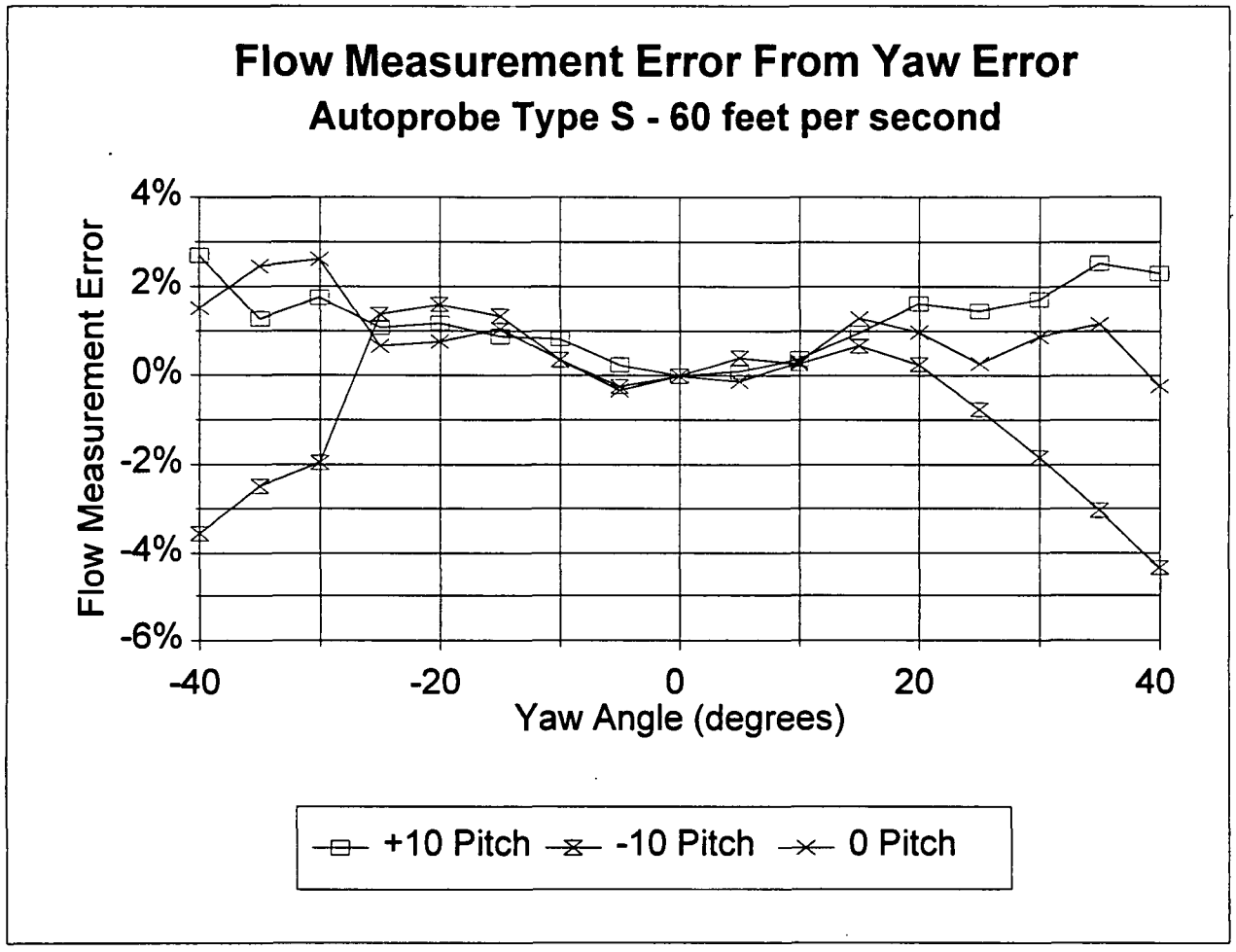
Flow Measurement Error From Yaw Error
Autoprobe Type S - 60 feet per second
Flow Measurement Error
4%
2%
0%
-2%
-4%
-6%
-40
-20
0
20
40
Yaw Angle (degrees)
+10 Pitch
-10 Pitch
0 Pitch

7.0 CALIBRATION CURVES AND ACCURACY OF VELOCITY DETERMINATIONS FOR 3D PROBES

7.1 TEST PROCEDURES

7.1.1 Calibrating 3D Probes

The three DAT probes and the spherical probe were calibrated using the procedures specified in draft Method 2F. The calibration procedure described in the draft method calls for yaw nulling by rotating the probe until ΔP across the Fechheimer ports (P_2 - P_3) equals zero. The pressure differentials, P_4-P_5 and P_1-P_2, are then measured to determine the following ratios (see Figures 1-4 and 1-5 for locations of numbered measurement ports):

$$F_1 = \frac{(P_4 - P_5)}{(P_1 - P_2)} \qquad \textbf{(Eq. 7.1)}$$

$$F_2 = C_{ps} \sqrt{\frac{\Delta P_P}{(P_1 - P_2)}} \qquad \textbf{(Eq. 7.2)}$$

where C_{ps} is the calibration coefficient of the standard pitot tube (which is equal to unity), and ΔP_P is the pressure differential across the standard pitot tube. Values of F_1 and F_2 are obtained at a predefined series of velocities and pitch angles. Then, two calibration curves are plotted: one curve (F_1 vs. pitch angle) is used to determine pitch angle; the other curve (F_2 vs. pitch angle) is used to determine the 3D probe's calibration coefficient, F_2.

Draft Method 2F calls for calibration curves of F_1 and F_2 vs. pitch angle to be developed by taking measurements of P_4-P_5 and P_1-P_2 at two velocities: one velocity between 20 and 40 fps and another velocity between 40 and 60 fps. Each calibration curve is created by calculating and then averaging the F_1 or the F_2 ratio at each pitch angle over the two velocities. For the experiments conducted here, two sets of calibration curves were created for each probe, one set by averaging data obtained at two velocities, 30 and 60 fps, and another set by averaging data at three velocities, 30, 60, and 60 fps. The three-velocity computation was performed to see if it yielded more accurate values of velocity outside the range of calibration velocities dictated by Method 2F.

The draft method calls for F_1 and F_2 to be determined at pitch angles between -60° and 60° in 5° increments. For the experiments conducted in this study, the geometry of the wind tunnel limited pitch angles to the range -30° to +30°. Pitch angles were therefore set at ±30°, ±20°, ±10°, ±5°, and 0°. All measurements were made in triplicate; the draft method calls for only one measurement at each point in this angle range.

7.1.2 Velocity Determination with 3D Probes

Once calibration curves have been derived for a 3D probe, velocity measurements can be obtained in a particular duct or stack by yaw nulling the probe until P_2-P_3 equals zero and then measuring P_4-P_5, P_1-P_2, and the corresponding yaw angle, θ_y. The measurements of P_4 -P_5 and P_1 -P_2 are used

in Equation 7.1 to calculate a value for F_1. The pitch angle, θ_p, associated with this value of F_1 is then found on the first calibration curve (F_1 vs. pitch angle). The resulting pitch angle is used to find the 3D pitot calibration coefficient (F_2) from the second calibration curve (F_2 vs. pitch angle).

Using the derived values of P_4-P_5, P_1-P_2, θ_y, θ_p, and measurements of temperature and barometric pressure, the total velocity, V_s, and axial velocity, V_{ax}, are then determined from the following equations:

$$V_s = 15.9\ F_2 \sqrt{\frac{(P_1 - P_2)(T + 460)}{P_{bar}}} \qquad \textbf{(Eq. 7.3)}$$

$$V_{ax} = V_s \cos\theta_y \cos\theta_p \qquad \textbf{(Eq. 7.4)}$$

7.2 CALIBRATION CURVES

Figures 7-1 through 7-8 are plots of the data used to construct the calibration curves for each probe. Each point is the average of three runs performed at each pitch angle and velocity. The draft method calls for a "smooth line to be drawn between points." For the curves here, a cubic spline method with continuous second derivatives was used to fit each curve. This method was chosen because it is the easiest and most appropriate for the data structure. For each set of two adjacent points, the method uses a piecewise third-degree polynomial, which passes through the data points and matches the first and second derivatives of neighboring segments at the points in order to obtain the smoothest line possible.

The three F_1 curves in each plot overlap significantly and show no velocity-dependent separation. The F_2 curves for two of the three DAT probes (3D-2 and 3D-3) shown in Figures 7–4 and 7–6 show clear velocity dependence, because they do not intersect and the spread between the curves is significant. For probe 3D-2, the spread between the F_2 ratios at 30 and 90 fps is about 5%, with the 60 fps curve between the two extremes; for probe 3D-3, the spread at 30 and 90 fps is about 4%. These differences between the 30 and 60 fps F_2 curves and between the 60 and 90 fps F_2 curves are within the range of ±3% allowed by draft Method 2F for F_2 values between 30 and 60 fps. The data for each velocity used to calculate F_1 and F_2 ratios for the spherical probe overlap, except for a divergence of the F_2 ratio measured at 30 fps and pitch angles of -30° and +30°.

The velocity dependence of F_2 for DAT probes 3D-2 and 3D-3 (across all pitch angle settings) and for the spherical probe MS5-2 (at -30° and +30° pitch angles) suggests that it may be advisable to require calibrations of 3D probes at velocities close to those prevailing in the situations where such probes will be used. The plot of F_2 vs. pitch angle for DAT 3D-1 shows much less velocity dependence than the curves for the other three probes, for which no readily apparent explanation is available.

Figures 7–9 through 7–16 are calibration curves for the three DAT probes and the spherical probe. Each curve is derived from point-by-point averages of the F_1 and F_2 ratios determined at all three velocities shown in Figures 7–1 through 7–8.

7.3 ACCURACY OF VELOCITY DETERMINATIONS

An attempt was made to estimate the extent to which the axial velocity derived from the 3D calibration curves deviated from the axial velocity derived from the standard pitot that was used to calibrate the wind tunnel. The analysis was performed twice: once using the calibration curves (shown in Figures 7-9 through 7-14) that were derived by averaging the results across three velocities (30, 60, and 90 fps), and once using the calibration curves derived using two velocities (30 and 60 fps), i.e., in accordance with draft Method 2F. Repeating the analysis using two separate sets of calibration curves was intended to provide a sense of the range in error inherent in the 3D calibration curves.

Note, however, that the data used to perform this error analysis are the same as the data used to derive the calibration curves. Therefore, the resulting analysis represents only an estimate of the error inherent in the calibration curves as originally produced, not an independent bounding of the error using new measurements. Furthermore, the data used to produce the second set of calibration curves were a subset of the data used to derive the first set of calibration curves, which may limit the variation in the error detected between the two analyses. Rather than establishing definitive bounds on the likely error to be found in the 3D calibration curves, this analysis should be viewed as indicating the extent to which error can be reduced by deriving calibration curves from an average over three velocities rather than over just two velocities as currently stipulated in draft Method 2F.

The results of the analysis are shown in Tables 7-1 through 7-4. The first four columns on the left list the pitch angle, nominal velocity, total velocity (V_s, measured with the standard pitot probe), and resulting axial velocity, V_{ax}. The axial velocity is calculated simply as $V_{ax} = V_s \cos\theta_p$, because the yaw angle component of flow within the wind tunnel was negligible, and, consequently, $\cos\theta_y = 1$ (see Equation 7.4). The middle group of five columns lists the values derived from the first set of 3D probe calibration curves, i.e., those obtained by averaging over 30, 60, and 90 fps. The first column in this group lists the pitch angle, θ_p, calculated from the F_1 vs. pitch angle calibration curve. The next column lists the average of the three pitch angles in the preceding column. The third and fourth columns show the total, V_s, and axial, V_{ax}, velocities calculated using Equations 7.3 and 7.4. The fifth column shows the percent deviation of the axial velocity calculated from the 3D probe calibration curves and the axial velocity calculated for the standard pitot. Percent deviation was computed as follows:

$$\% \text{ Dev} = \left[\frac{(V_s - V_{ax})}{V_{ax}}\right] 100 \qquad \textbf{(Eq. 7.5)}$$

The righthand group of columns is similar to the center group, except that all calculations were made from the calibration curves determined from the 30 and 60 fps curves. The columns below the table list the average percent velocity deviations over all pitch angles for each velocity for the entire pitch

angle range and for pitch angles in the ±20° and ±10° ranges. These values are based on the absolute values of the percent deviations and show how far, on average, the 3D axial velocity departed from the standard pitot axial velocity.

DAT Probes (Tables 7-1 to 7-3): Whether using the 30/60 or 30/60/90 fps calibration curves, the errors in velocity found with probe 3D-1 were less than 1.4%, except at -30° pitch, where the errors rose to a maximum of 3.0% at 90 fps when using the 30/60 calibration curves and -2.2% when using the 30/60/90 curves. The largest difference in average errors across the pitch angle ranges determined from the two calibration curves is 0.2%. Figure 7-2, showing F_2 vs. pitch angle for the 3D-1 probe, illustrates that F_2 is largely independent of velocity across the pitch angle range of -20° to +30°. This observation is in marked contrast to the results for the other two DAT probes (see Figures 7-4 and 7-6.)

With probe 3D-2, the largest errors are found at 30 fps and 20° pitch angle for both sets of calibration curves, namely, 5.5% using the 30/60/90 curves and 4.4% using the 30/60 curves. Errors in velocity measurements at 30 fps are consistently high with absolute deviations averaging 2.9% when the 30/60/90 fps calibration curves were used, and 1.7% when the 30/60 fps curves were used. Errors in velocity determinations at 90 fps are consistently low. At this velocity, deviations averaged -2.2% with the 30/60/90 fps curves and -3.4% with the 30/60 fps curves across all velocities. At 10° pitch across all three velocities, anomalous negative errors occurred between the average calculated pitch angle (Table 7-2, columns 5 and 10) and the actual pitch angle of 10° (Table 7-4, column 1). When using the 30/60/90 calibration curves, the difference between the actual and average calculated pitch angle was -2.3°. With the 30/60 curves, the difference was -2.6°. Nevertheless, the velocity errors at this pitch angle are consistent with velocity errors at other pitch angles, reflecting the small difference in cosine values between 10° and 7° (0.8%).

The velocities measured with probe 3D-3 were consistently high at 30 fps and consistently low at 90 fps (Table 7-3). The largest deviation (-3.8%) occurred at 90 fps and 10° pitch using the 30/60 fps calibration curves. This deviation is similar to those found with probe 3D-2.

Spherical Probe (Table 7-4): Over the entire pitch angle velocity range, the largest single velocity deviation is -5.2% at 30 fps and -30° pitch angle using the 30/60/90 fps calibration curves. Spherical probe velocities computed using the 30/60/90 curves were consistently higher than the standard pitot measurements at the 90 fps level (by 1.6% on average) and consistently lower at the 30 fps level (by 1.5% on average). Using the 30/60 curves, the largest velocity deviations at each pitch angle were found at 90 fps and averaged 2.4% over the entire pitch angle range. Considering the results for both the 30/60 and 30/60/90 curves together, the largest deviations at each velocity were -5.2% at 30 fps, 3.8% at 60 fps, and 4.7% at 90 fps, occurring at pitch angles of -30°, 30°, and -20°, respectively. Over each of the pitch ranges shown at the bottom of Table 7-4, the difference between the average absolute deviations produced using the 30/60/90 calibration curves and those produced using the 30/60 curves never exceeded 0.8%. For example, in the -30° to +30° pitch range, where the differences produced using the two sets of calibration curves were greatest, the differences were -0.4% at 30 fps, 0.6% at 60 fps, and 0.8% at 90 fps.

Table 7-1. DAT Probe (3D-1) Velocity Accuracy *

Reference				Calculated Values for DAT Probe (3D-1)									
				Calibrated at 30-60-90 fps					Calibrated at 30-60 fps				
Pitch Angle (deg)	Nominal Velocity (fps)	Vs Total Velocity (fps)	Vax Axial Velocity (fps)	Pitch Angle (deg)	Avg Pitch Angle (deg)	Vs Total Velocity (fps)	Vax Axial Velocity (fps)	% Dev.	Pitch Angle (deg)	Avg Pitch Angle (deg)	Vs Total Velocity (fps)	Vax Axial Velocity (fps)	% Dev.
	30	30.0	25.98	-30.0		29.34	25.41	-2.2	-30.0		29.53	25.57	-1.6
-30	60	60.1	52.05	-28.6	-29.0	60.22	52.87	1.6	-28.1	-28.6	60.45	53.32	2.5
	90	90.4	78.29	-28.5		90.88	79.87	2.0	-27.8		91.13	80.61	3.0
	30	30.0	28.19	-22.4		30.10	27.83	-1.3	-21.7		30.09	27.96	-0.8
-20	60	60.1	56.48	-18.7	-19.9	60.15	56.97	0.9	-18.0	-19.2	60.19	57.24	1.4
	90	90.4	84.95	-18.5		90.43	85.76	1.0	-17.9		90.49	86.11	1.4
	30	30.0	29.54	-9.6		29.89	29.47	-0.2	-9.4		29.91	29.51	-0.1
-10	60	60.1	59.19	-10.9	-10.0	60.26	59.17	0.0	-10.6	-9.8	60.30	59.27	0.1
	90	90.4	89.03	-9.6		90.51	89.24	0.2	-9.4		90.58	89.36	0.4
	30	30.0	29.89	-4.9		29.95	29.84	-0.2	-4.9		29.95	29.84	-0.2
-5	60	60.1	59.87	-5.1	-5.0	60.16	59.92	0.1	-5.0	-5.0	60.17	59.94	0.1
	90	90.4	90.06	-5.0		90.37	90.03	0.0	-5.0		90.38	90.04	0.0
	30	30.0	30.00	0.8		30.05	30.05	0.2	0.4		30.09	30.09	0.3
0	60	60.1	60.10	0.6	1.1	59.75	59.75	-0.6	0.9	1.3	59.79	59.78	-0.5
	90	90.4	90.40	1.9		90.52	90.47	0.1	2.5		90.52	90.43	0.0
	30	30.0	29.89	5.3		30.08	29.95	0.2	5.5		30.06	29.92	0.1
5	60	60.1	59.87	3.4	4.7	60.01	59.90	0.1	3.9	5.0	59.98	59.84	-0.1
	90	90.4	90.06	5.4		90.38	89.98	-0.1	5.5		90.32	89.90	-0.2
	30	30.0	29.54	10.5		29.92	29.42	-0.4	10.7		29.88	29.36	-0.6
10	60	60.1	59.19	9.5	10.1	60.33	59.50	0.5	9.6	10.3	60.24	59.40	0.4
	90	90.4	89.03	10.4		90.16	88.68	-0.4	10.6		90.02	88.48	-0.6
	30	30.0	28.19	18.1		29.87	28.39	0.7	19.0		29.86	28.23	0.2
20	60	60.1	56.48	20.0	19.8	60.39	56.75	0.5	20.6	20.5	60.56	56.69	0.4
	90	90.4	84.95	21.2		91.24	85.07	0.1	21.8		91.56	85.01	0.1
	30	30.0	25.98	28.6		29.82	26.18	0.8	28.9		29.87	26.15	0.7
30	60	60.1	52.05	29.6	29.4	59.94	52.12	0.1	29.7	29.5	60.00	52.12	0.1
	90	90.4	78.29	30.0		90.69	78.54	0.3	30.0		90.72	78.57	0.4

Pitch Angles	Total Velocity	Average Absolute Deviation %	%
-30	30.0	0.7	0.5
to	60.1	0.5	0.6
30	90.4	0.5	0.7
-20	30.0	0.5	0.3
to	60.1	0.4	0.4
20	90.4	0.3	0.4
-10	30.0	0.2	0.3
to	60.1	0.3	0.2
10	90.4	0.2	0.2

* Note: Data represent the average of triplicate measurements made at each pitch angle and velocity.

Table 7-2. DAT Probe (3D-2) Velocity Accuracy *

Reference				Calculated Values for DAT Probe (3D-2)									
				Calibrated at 30-60-90 fps					Calibrated at 30-60 fps				
Pitch Angle (deg)	Nominal Velocity (fps)	Vs Total Velocity (fps)	Vax Axial Velocity (fps)	Pitch Angle (deg)	Avg Pitch Angle (deg)	Vs Total Velocity (fps)	Vax Axial Velocity (fps)	% Dev.	Pitch Angle (deg)	Avg Pitch Angle (deg)	Vs Total Velocity (fps)	Vax Axial Velocity (fps)	% Dev.
	30	30.0	25.98	-29.9		30.95	26.83	3.3	-29.7		30.56	26.55	2.2
-30	60	60.1	52.05	-29.8	-29.7	59.68	51.79	-0.5	-29.7	-29.5	58.95	51.21	-1.6
	90	90.3	78.20	-29.5		87.90	76.50	-2.2	-29.2		86.76	75.73	-3.2
	30	30.0	28.19	-21.9		31.03	28.79	2.1	-21.5		30.60	28.47	1.0
-20	60	60.1	56.48	-18.0	-19.6	60.13	57.19	1.3	-17.0	-18.8	59.34	56.75	0.5
	90	90.3	84.85	-18.8		87.99	83.30	-1.8	-18.0		86.84	82.59	-2.7
	30	30.0	29.54	-13.8		30.74	29.85	1.0	-12.4		30.32	29.61	0.2
-10	60	60.1	59.19	-9.8	-10.5	60.42	59.54	0.6	-8.9	-9.5	59.64	58.92	-0.4
	90	90.3	88.93	-7.8		88.02	87.21	-1.9	-7.3		86.89	86.19	-3.1
	30	30.0	29.89	-4.5		30.60	30.51	2.1	-4.5		30.21	30.12	0.8
-5	60	60.1	59.87	-5.4	-4.9	60.45	60.18	0.5	-5.3	-4.8	59.69	59.43	-0.7
	90	90.3	89.96	-4.8		88.06	87.75	-2.5	-4.7		86.95	86.66	-3.7
	30	30.0	30.00	1.0		30.61	30.61	2.0	1.0		30.25	30.25	0.8
0	60	60.1	60.10	0.7	0.8	60.35	60.35	0.4	0.7	0.8	59.65	59.65	-0.8
	90	90.3	90.30	0.6		88.32	88.32	-2.2	0.6		87.29	87.29	-3.3
	30	30.0	29.89	4.9		30.73	30.62	2.4	5.1		30.35	30.23	1.2
5	60	60.1	59.87	5.5	5.1	60.19	59.91	0.1	5.4	5.2	59.45	59.19	-1.1
	90	90.3	89.96	5.0		88.22	87.88	-2.3	5.1		87.13	86.79	-3.5
	30	30.0	29.54	7.2		30.70	30.46	3.1	7.0		30.32	30.09	1.9
10	60	60.1	59.19	7.7	7.7	60.30	59.76	1.0	7.4	7.4	59.55	59.05	-0.2
	90	90.3	88.93	8.2		88.20	87.30	-1.8	7.8		87.10	86.29	-3.0
	30	30.0	28.19	16.9		31.07	29.73	5.5	16.5		30.70	29.44	4.4
20	60	60.1	56.48	19.4	19.2	60.18	56.76	0.5	20.5	19.6	59.36	55.60	-1.5
	90	90.3	84.85	21.2		88.55	82.56	-2.7	21.8		87.57	81.31	-4.2
	30	30.0	25.98	28.0		30.83	27.22	4.8	28.4		30.48	26.81	3.2
30	60	60.1	52.05	30.0	29.3	59.62	51.63	-0.8	30.0	29.5	58.85	50.97	-2.1
	90	90.3	78.20	30.0		88.20	76.38	-2.3	30.0		87.06	75.40	-3.6

Pitch Angles	Total Velocity	Average Absolute Deviation %	%
-30	30.0	2.9	1.7
to	60.1	0.6	1.0
30	90.3	2.2	3.4
-20	30.0	2.6	1.5
to	60.1	0.6	0.8
20	90.3	2.2	3.3
-10	30.0	2.1	1.0
to	60.1	0.5	0.7
10	90.3	2.1	3.3

* Note: Data represent the average of triplicate measurements made at each pitch angle and velocity.

Table 7-3. DAT Probe (3D-3) Velocity Accuracy *

Reference				Calculated Values for DAT Probe (3D-3)									
				Calibrated at 30-60-90 fps					Calibrated at 30-60 fps				
Pitch Angle (deg)	Nominal Velocity (fps)	Vs Total Velocity (fps)	Vax Axial Velocity (fps)	Pitch Angle (deg)	Avg Pitch Angle (deg)	Vs Total Velocity (fps)	Vax Axial Velocity (fps)	% Dev.	Pitch Angle (deg)	Avg Pitch Angle (deg)	Vs Total Velocity (fps)	Vax Axial Velocity (fps)	% Dev.
	30	30.1	26.07	-30.0		30.39	26.32	1.0	-30.0		30.23	26.18	0.4
-30	60	60.2	52.13	-28.8	-29.1	59.81	52.41	0.5	-28.7	-29.0	59.45	52.15	0.0
	90	91.0	78.81	-28.4		89.22	78.48	-0.4	-28.2		88.63	78.11	-0.9
	30	30.1	28.28	-21.7		30.68	28.51	0.8	-20.7		30.29	28.33	0.2
-20	60	60.2	56.57	-20.0	-19.6	60.70	57.04	0.8	-18.9	-18.4	60.11	56.87	0.5
	90	91.0	85.51	-17.0		88.91	85.03	-0.6	-15.7		88.09	84.80	-0.8
	30	30.1	29.64	-12.1		30.61	29.93	1.0	-11.1		30.38	29.81	0.6
-10	60	60.2	59.29	-10.1	-10.2	59.95	59.02	-0.4	-9.3	-9.4	59.54	58.76	-0.9
	90	91.0	89.62	-8.3		89.65	88.71	-1.0	-7.8		89.07	88.25	-1.5
	30	30.1	29.99	-6.2		30.52	30.34	1.2	-6.0		30.33	30.16	0.6
-5	60	60.2	59.97	-3.0	-4.7	59.92	59.84	-0.2	-2.8	-4.5	59.53	59.46	-0.9
	90	91.0	90.65	-4.9		89.75	89.42	-1.4	-4.8		89.18	88.87	-2.0
	30	30.1	30.10	2.3		30.51	30.49	1.3	2.0		30.31	30.29	0.6
0	60	60.2	60.20	1.6	1.6	60.03	60.01	-0.3	2.1	1.8	59.57	59.53	-1.1
	90	91.0	91.00	1.0		89.62	89.61	-1.5	1.4		88.96	88.93	-2.3
	30	30.1	29.99	4.3		30.71	30.62	2.1	4.6		30.47	30.37	1.3
5	60	60.2	59.97	4.7	4.9	59.89	59.69	-0.5	5.1	5.2	59.41	59.17	-1.3
	90	91.0	90.65	5.6		89.56	89.13	-1.7	6.0		88.84	88.35	-2.5
	30	30.1	29.64	10.0		30.57	30.11	1.6	11.0		30.29	29.73	0.3
10	60	60.2	59.29	7.7	9.9	60.16	59.62	0.6	8.6	10.8	59.64	58.97	-0.5
	90	91.0	89.62	12.0		89.32	87.37	-2.5	12.9		88.44	86.21	-3.8
	30	30.1	28.28	18.1		30.46	28.95	2.4	18.9		30.14	28.52	0.8
20	60	60.2	56.57	20.4	19.9	60.74	56.93	0.6	21.0	20.6	60.27	56.27	-0.5
	90	91.0	85.51	21.3		89.72	83.59	-2.2	21.8		89.02	82.65	-3.3
	30	30.1	26.07	28.5		30.72	27.00	3.6	29.0		30.44	26.62	2.1
30	60	60.2	52.13	30.0	29.5	59.85	51.83	-0.6	30.0	29.7	59.19	51.26	-1.7
	90	91.0	78.81	30.0		89.17	77.22	-2.0	30.0		88.19	76.37	-3.1

Pitch Angles	Total Velocity	Average Absolute Deviation %	%
-30	30.1	1.6	0.8
to	60.2	0.5	0.8
30	91.0	1.5	2.3
-20	30.1	1.5	0.6
to	60.2	0.5	0.8
20	91.0	1.6	2.3
-10	30.1	1.4	0.7
to	60.2	0.4	0.9
10	91.0	1.6	2.4

* Note: Data represent the average of triplicate measurements made at each pitch angle and velocity.

Table 7-4. Spherical Probe (MS5-2) Velocity Accuracy *

Reference				Calculated Values for Spherical Probe (MS5-2)								
				Calibrated at 30-60-90 fps					Calibrated at 30-60 fps			
Pitch Angle (deg)	Nominal Velocity (fps)	Vs Total Velocity (fps)	Vax Axial Velocity (fps)	Pitch Angle (deg)	Avg Pitch Angle (deg)	Vs Total Velocity (fps)	Vax Axial Velocity (fps)	% Dev.	Pitch Angle (deg)	Avg Pitch Angle (deg)	Vs Total Velocity (fps)	Vax Axial Velocity (fps)	% Dev.
	30	30.2	26.15	-27.5		27.96	24.80	-5.2	-27.8		28.48	25.19	-3.7
-30	60	60.4	52.31	-26.0	-27.7	57.99	52.12	-0.4	-26.5	-28.0	59.13	52.92	1.2
	90	91.0	78.81	-29.7		93.34	81.08	2.9	-29.7		94.91	82.44	4.6
	30	30.2	28.38	-18.4		30.08	28.54	0.6	-19.2		30.40	28.71	1.2
-20	60	60.4	56.76	-20.0	-20.1	60.72	57.06	0.5	-20.8	-20.8	61.76	57.73	1.7
	90	91.0	85.51	-21.8		94.88	88.09	3.0	-22.5		96.89	89.51	4.7
	30	30.2	29.74	-9.2		29.87	29.49	-0.9	-9.9		30.06	29.61	-0.4
-10	60	60.4	59.48	-9.5	-10.1	60.56	59.73	0.4	-10.2	-10.8	60.90	59.94	0.8
	90	91.0	89.62	-11.6		92.39	90.50	1.0	-12.4		93.14	90.97	1.5
	30	30.2	30.09	-4.7		29.86	29.76	-1.1	-5.0		30.01	29.90	-0.6
-5	60	60.4	60.17	-4.7	-5.0	60.63	60.43	0.4	-5.0	-5.3	60.94	60.71	0.9
	90	91.0	90.65	-5.5		91.97	91.55	1.0	-5.9		92.45	91.96	1.4
	30	30.2	30.20	0.6		29.97	29.97	-0.8	0.6		30.10	30.10	-0.3
0	60	60.4	60.40	0.5	0.5	60.47	60.47	0.1	0.6	0.5	60.73	60.73	0.5
	90	91.0	91.00	0.3		91.82	91.82	0.9	0.4		92.22	92.22	1.3
	30	30.2	30.09	5.1		29.97	29.85	-0.8	5.1		30.09	29.97	-0.4
5	60	60.4	60.17	4.8	5.0	60.47	60.26	0.1	4.8	5.0	60.72	60.51	0.6
	90	91.0	90.65	5.2		91.86	91.48	0.9	5.2		92.25	91.87	1.3
	30	30.2	29.74	10.4		30.06	29.57	-0.6	10.2		30.16	29.68	-0.2
10	60	60.4	59.48	10.1	10.0	60.35	59.41	-0.1	9.8	9.8	60.58	59.70	0.4
	90	91.0	89.62	9.5		91.79	90.53	1.0	9.4		92.14	90.90	1.4
	30	30.2	28.38	20.0		30.04	28.23	-0.5	20.1		30.16	28.32	-0.2
20	60	60.4	56.76	19.7	19.9	60.52	56.98	0.4	19.8	20.0	60.73	57.14	0.7
	90	91.0	85.51	20.1		91.80	86.21	0.8	20.2		92.16	86.49	1.1
	30	30.2	26.15	28.3		28.65	25.23	-3.5	28.8		29.09	25.49	-2.5
30	60	60.4	52.31	28.0	28.8	60.91	53.78	2.8	28.8	29.2	61.98	54.31	3.8
	90	91.0	78.81	30.0		93.42	80.90	2.7	30.0		94.54	81.87	3.9

Pitch Angles	Total Velocity	Average Absolute Deviation %	%
-30	30.2	1.5	1.1
to	60.4	0.6	1.2
30	91.0	1.6	2.4
-20	30.2	0.7	0.5
to	60.4	0.3	0.8
20	91.0	1.2	1.8
-10	30.2	0.8	0.4
to	60.4	0.2	0.6
10	91.0	1.0	1.4

* Note: Data represent the average of triplicate measurements made at each pitch angle and velocity.

7.4 ACCURACY OF PITCH ANGLE DETERMINATIONS

The wind tunnel test data include pitch angle measurements made by each 3D probe. These angles are determined from the F_1 vs. pitch angle calibration curves established for each probe. Table 7-5 presents the pitch angle measurements and calculated differences from the reference pitch angle (determined by comparing the secured probe orientation with a protractor during the wind tunnel tests). Performance of each probe in determining pitch was similar. The largest difference in pitch angle was 4.3°, which occurred for the 3D-3 probe at -20° pitch and 90 fps using the 30/60 fps calibration curves. An error of this magnitude in the angle measurement produces an error of only 0.3% error in the axial velocity.

While these wind tunnel tests showed the pitch angle accuracy of the spherical probe to be comparable to that of the DAT probes, a previous study[1] indicated that scratches on the probe head can significantly alter the pitch angle calibration characteristics of the spherical probe design. No attempt was made in this study to evaluate this property. This characteristic of spherical probes, however, may merit investigation before such probes are approved for use under field conditions.

7.5 CONCLUSIONS

Cross-probe velocity accuracy results are summarized in Table 7-6. Recognizing the methodological limitations of the approach employed in this study (as described in Section 7.3 above), the results support the following findings on velocity accuracy:

- *Overall performance:* Across all pitch angles and all velocities, whether using the 30/60 or 30/60/90 fps calibration curves, the average absolute deviations from the actual axial velocities never exceeded 3.4% for the spherical probe and the three DAT probes. For one of the DAT probes (3D-1), the average absolute deviations were 0.7% or less.

- *Comparative results using 30/60 and 30/60/90 fps calibration curves:* For all probes over all tested velocities, the difference between the average absolute deviations obtained with the 30/60 and that obtained with the 30/60/90 calibration curves never exceeded ±1.2%.

- *Patterns in velocity deviations (I):* When using the 30/60 fps calibration curves, the greatest average absolute velocity deviations for all probes over all pitch angles (-30° to + 30°) and velocities always occurred at the 90 fps velocity setting.

- *Patterns in velocity deviations (II)*: Except for one occurrence with DAT probe 3D-3 at +10° using the 30/60 fps curves, the largest velocity errors occurred at the pitch angle settings of -30°, -20°, 20°, and 30°.

---

[1] Klinge, M. D. 1987. *Detailed Near-Wake Flowfield Surveys and Comparison to an Euler Method of an Aspect Ratio 4 Rectangular Wing.* M .S. Thesis, Mechanical and Aerospace Engineering Department, North Carolina State University, Raleigh.

Table 7-5. 3D Probe Pitch Angle Accuracy

Reference		3D-1 Probe				3D-2 Probe				3D-3 Probe				Spherical Probe			
		30/60/90 Cal		30/60 Cal		30/60/90 Cal		30/60 Cal		30/60/90 Cal		30/60 Cal		30/60/90 Cal		30/60 Cal	
Pitch Angle (deg)	Nominal Velocity (fps)	Pitch Angle (deg)	Difference (deg)	Pitch Angle (deg)	Difference (deg)	Pitch Angle (deg)	Difference (deg)	Pitch Angle (deg)	Difference (deg)	Pitch Angle (deg)	Difference (deg)	Pitch Angle (deg)	Difference (deg)	Pitch Angle (deg)	Difference (deg)	Pitch Angle (deg)	Difference (deg)
-30	30	-30.0	0.0	-30.0	0.0	-29.9	0.1	-29.7	0.3	-30.0	0.0	-30.0	0.0	-27.5	2.5	-27.8	2.2
	60	-28.6	1.4	-28.1	1.9	-29.8	0.2	-29.7	0.3	-28.8	1.2	-28.7	1.3	-26.0	4.0	-26.5	3.5
	90	-28.5	1.5	-27.8	2.2	-29.5	0.5	-29.2	0.8	-28.4	1.6	-28.2	1.8	-29.7	0.3	-29.7	0.3
-20	30	-22.4	-2.4	-21.7	-1.7	-21.9	-1.9	-21.5	-1.5	-21.7	-1.7	-20.7	-0.7	-18.4	1.6	-19.2	0.8
	60	-18.7	1.3	-18.0	2.0	-18.0	2.0	-17.0	3.0	-20.0	0.0	-18.9	1.1	-20.0	0.0	-20.8	-0.8
	90	-18.5	1.5	-17.9	2.1	-18.8	1.2	-18.0	2.0	-17.0	3.0	-15.7	4.3	-21.8	-1.8	-22.5	-2.5
-10	30	-9.6	0.4	-9.4	0.6	-13.8	-3.8	-12.4	-2.4	-12.1	-2.1	-11.1	-1.1	-9.2	0.8	-9.9	0.1
	60	-10.9	-0.9	-10.6	-0.6	-9.8	0.2	-8.9	1.1	-10.1	-0.1	-9.3	0.7	-9.5	0.5	-10.2	-0.2
	90	-9.6	0.4	-9.4	0.6	-7.8	2.2	-7.3	2.7	-8.3	1.7	-7.8	2.2	-11.6	-1.6	-12.4	-2.4
-5	30	-4.9	0.1	-4.9	0.1	-4.5	0.5	-4.5	0.5	-6.2	-1.2	-6.0	-1.0	-4.7	0.3	-5.0	0.0
	60	-5.1	-0.1	-5.0	0.0	-5.4	-0.4	-5.3	-0.3	-3.0	2.0	-2.8	2.2	-4.7	0.3	-5.0	0.0
	90	-5.0	0.0	-5.0	0.0	-4.8	0.2	-4.7	0.3	-4.9	0.1	-4.8	0.2	-5.5	-0.5	-5.9	-0.9
0	30	0.8	0.8	0.4	0.4	1.0	1.0	1.0	1.0	2.3	2.3	2.0	2.0	0.6	0.6	0.6	0.6
	60	0.6	0.6	0.9	0.9	0.7	0.7	0.7	0.7	1.6	1.6	2.1	2.1	0.5	0.5	0.6	0.6
	90	1.9	1.9	2.5	2.5	0.6	0.6	0.6	0.6	1.0	1.0	1.4	1.4	0.3	0.3	0.4	0.4
5	30	5.3	0.3	5.5	0.5	4.9	-0.1	5.1	0.1	4.3	-0.7	4.6	-0.4	5.1	0.1	5.1	0.1
	60	3.4	-1.6	3.9	-1.1	5.5	0.5	5.4	0.4	4.7	-0.3	5.1	0.1	4.8	-0.2	4.8	-0.2
	90	5.4	0.4	5.5	0.5	5.0	0.0	5.1	0.1	5.6	0.6	6.0	1.0	5.2	0.2	5.2	0.2
10	30	10.5	0.5	10.7	0.7	7.2	-2.8	7.0	-3.0	10.0	0.0	11.0	1.0	10.4	0.4	10.2	0.2
	60	9.5	-0.5	9.6	-0.4	7.7	-2.3	7.4	-2.6	7.7	-2.3	8.6	-1.4	10.1	0.1	9.8	-0.2
	90	10.4	0.4	10.6	0.6	8.2	-1.8	7.8	-2.2	12.0	2.0	12.9	2.9	9.5	-0.5	9.4	-0.6
20	30	18.1	-1.9	19.0	-1.0	16.9	-3.1	16.5	-3.5	18.1	-1.9	18.9	-1.1	20.0	0.0	20.1	0.1
	60	20.0	0.0	20.6	0.6	19.4	-0.6	20.5	0.5	20.4	0.4	21.0	1.0	19.7	-0.3	19.8	-0.2
	90	21.2	1.2	21.8	1.8	21.2	1.2	21.8	1.8	21.3	1.3	21.8	1.8	20.1	0.1	20.2	0.2
30	30	28.6	-1.4	28.9	-1.1	28.0	-2.0	28.4	-1.6	28.5	-1.5	29.0	-1.0	28.3	-1.7	28.8	-1.2
	60	29.6	-0.4	29.7	-0.3	30.0	0.0	30.0	0.0	30.0	0.0	30.0	0.0	28.0	-2.0	28.8	-1.2
	90	30.0	0.0	30.0	0.0	30.0	0.0	30.0	0.0	30.0	0.0	30.0	0.0	30.0	0.0	30.0	0.0

Angle Range	Nominal Velocity	Average Absolute Difference (degrees)	Average Absolute Difference (degrees)	Average Absolute Difference (degrees)	Average Absolute Difference (degrees)	Average Absolute Difference (degrees)	Average Absolute Difference (degrees)	Average Absolute Difference (degrees)	Average Absolute Difference (degrees)
-30	30	0.9	0.7	1.7	1.5	1.3	0.9	0.9	0.6
to	60	0.8	0.9	0.8	1.0	0.9	1.1	0.9	0.8
30	90	0.8	1.1	0.9	1.2	1.3	1.7	0.6	0.8

Table 7-6. Summary of 3D Probes Velocity Accuracy Results

Probe ID	Calibration Curve	Average Absolute Deviation (over the ±30° pitch range)			Maximum Deviation and Conditions When it Occurs		
		30 fps	60 fps	90 fps	Deviation	Pitch Angle	Nominal Velocity
DAT Probe (3D-1)	30/60	0.5%	0.6%	0.7%	+3.0%	-30°	90 fps
	30/60/90	0.7%	0.5%	0.5%	-2.2%	-30°	30 fps
	Difference	0.2%	0.1%	0.2%			
DAT Probe (3D-2)	30/60	1.7%	1.0%	3.4%	+4.4%	+20°	30 fps
	30/60/90	2.9%	0.6%	2.2%	+5.5%	+20°	30 fps
	Difference	1.2%	0.4%	1.2%			
DAT Probe (3D-3)	30/60	0.8%	0.8%	2.3%	-3.8%	+10°	90 fps
	30/60/90	1.6%	0.5%	1.5%	+3.6%	+30°	30 fps
	Difference	0.8%	0.3%	0.8%			
Spherical (MS5-2)	30/60	1.1%	1.2%	2.4%	+4.7%	-20°	90 fps
	30/60/90	1.5%	0.6%	1.6%	-5.2%	-30°	30 fps
	Difference	0.4%	0.6%	0.8%			

Key findings for the examination of pitch angle accuracy are:

- *Overall performance:* Across all probes, all velocities, and all pitch angle settings, the largest error in measuring pitch angle was 4.3°. The average absolute difference between derived and actual pitch angles never exceeded 1.7°.

- *Other considerations:* The potential impact of probe head scratches on the accuracy of pitch angle determinations using the spherical design probe (which were reported in a previous study) were not evaluated in the current study.

These findings point to the following conclusions:

- Over the pitch angle ranges ±30° and ±20°, the velocity accuracy of all tested 3D probes was within 5.5% of the true axial velocity. In the ±10° pitch-angle range, the velocity accuracy of all tested 3D probes was within 3.8% of the true axial velocity.

- No significant gain in accuracy is attained by developing calibration curves at three velocities rather than at the two specified in draft Method 2F.

- In order to minimize error in the flue gas velocity measurement, calibration curves for 3D probes should be developed at velocity settings close to, or possibly bracketing, the prevailing velocity where the probe will be used.

- The largest error in measuring pitch angle for all four probes was 4.3°, which occurred at 90 fps and -20° pitch and produced a velocity error of 0.3%.

Figure 7-1. Probe: DAT 3D-1

F1 vs. Pitch Angle

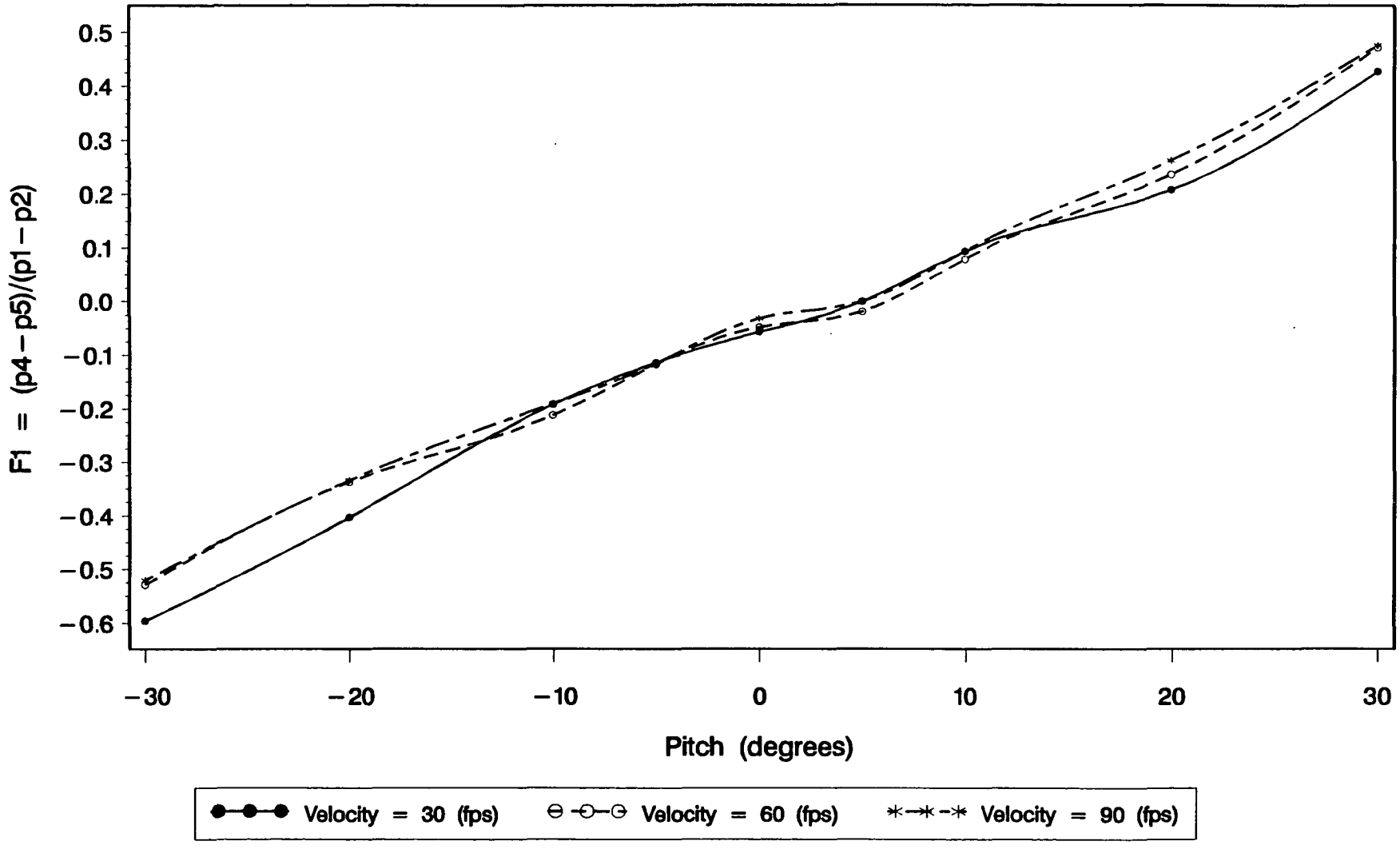

Figure 7−2. Probe: DAT 3D−1

F2 vs. Pitch Angle

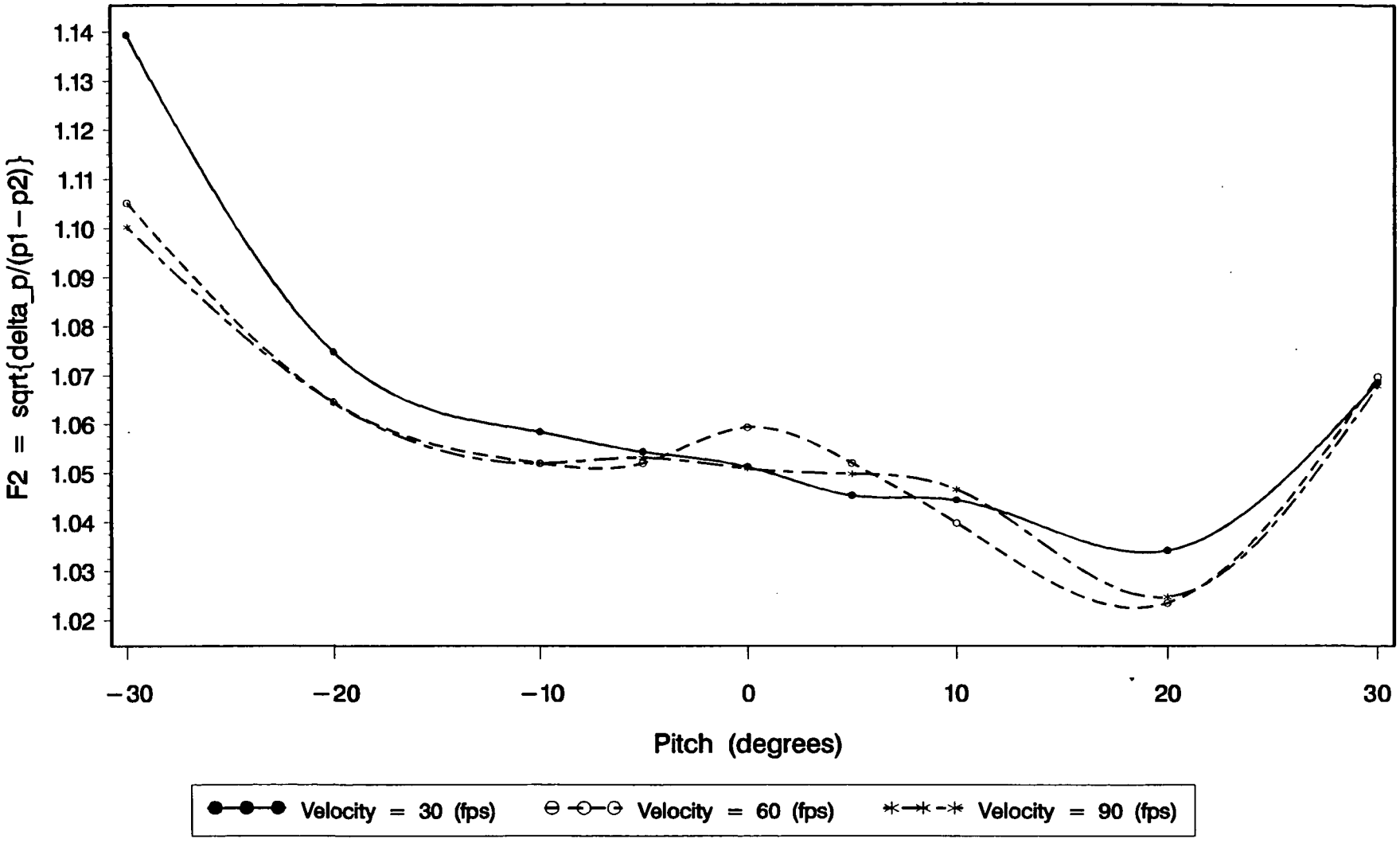

Figure 7-3. Probe: DAT 3D-2

F1 vs. Pitch Angle

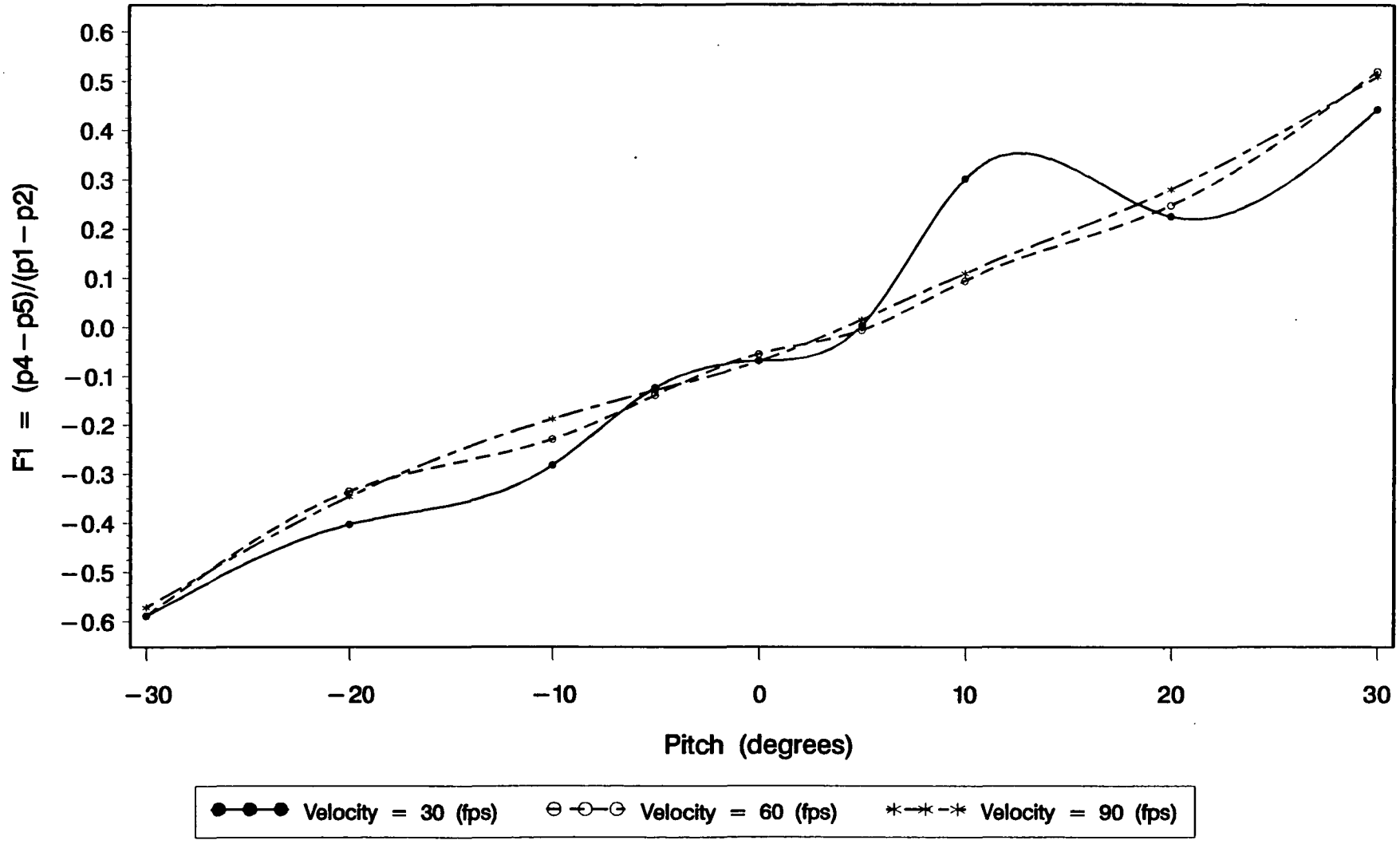

Figure 7−4. Probe: DAT 3D−2

F2 vs. Pitch Angle

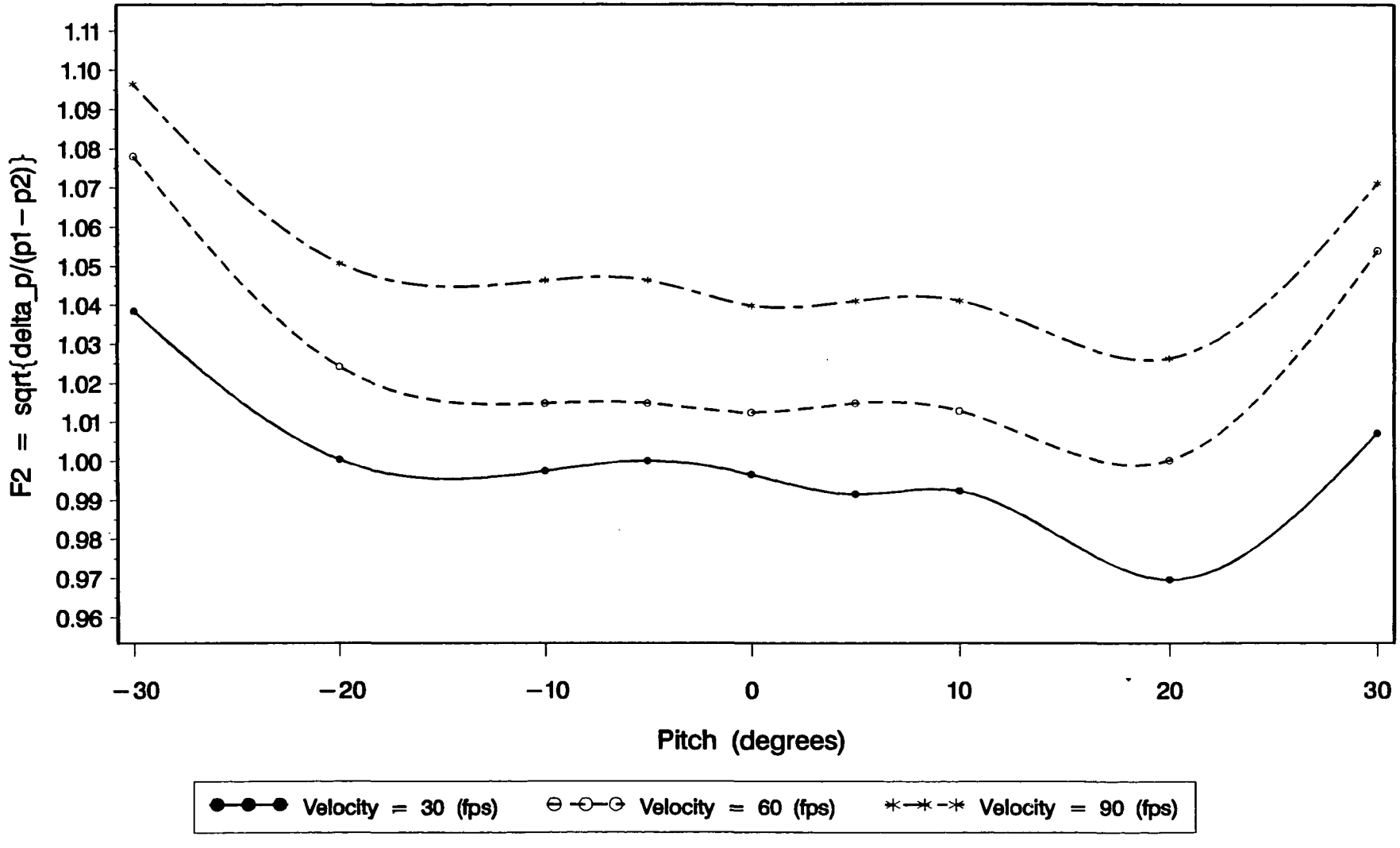

Figure 7-5. Probe: DAT 3D-3

F1 vs. Pitch Angle

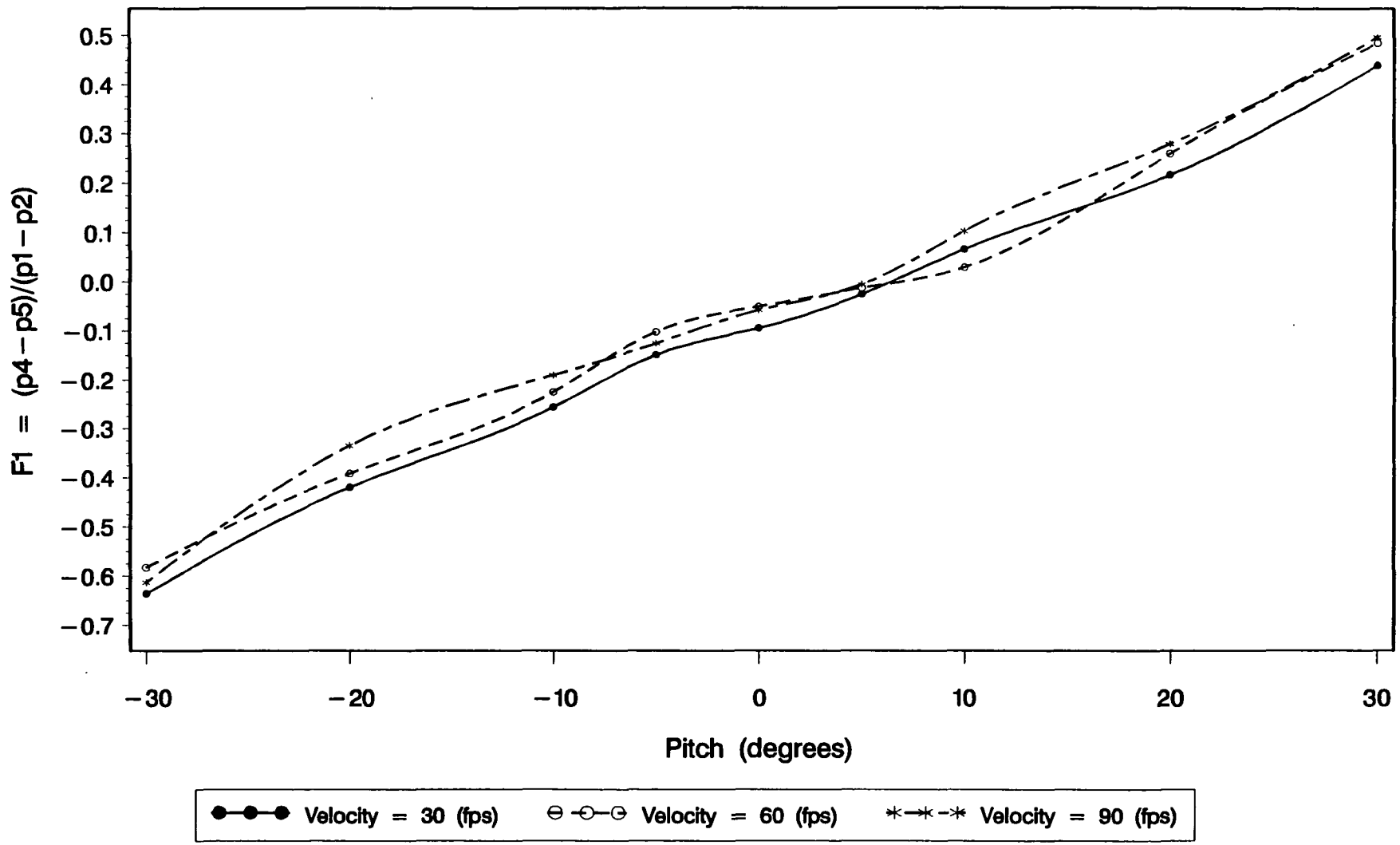

Figure 7-6. Probe: DAT 3D-3

F2 vs. Pitch Angle

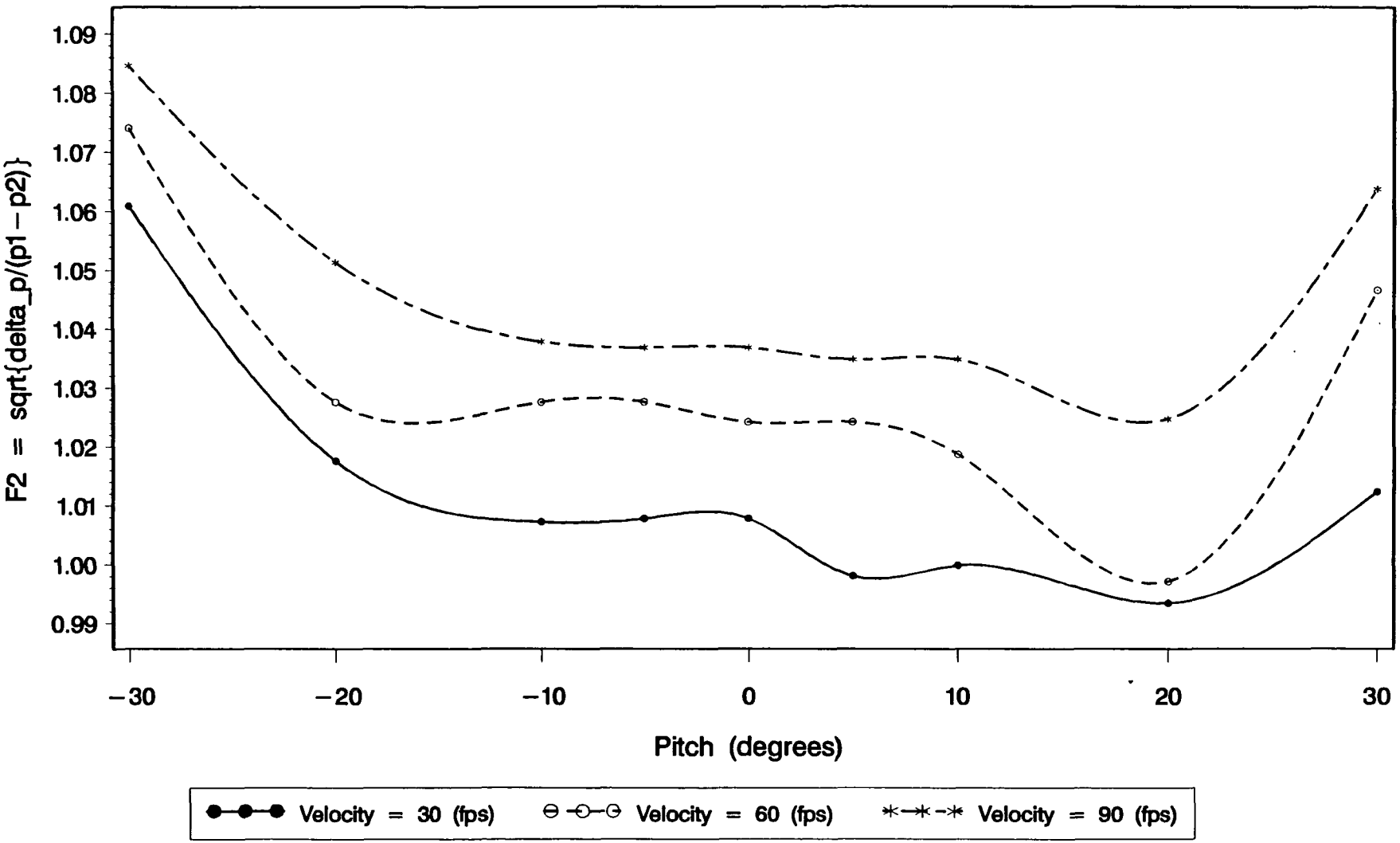

Figure 7-7. Probe: Spherical MS5-2
F1 vs. Pitch Angle

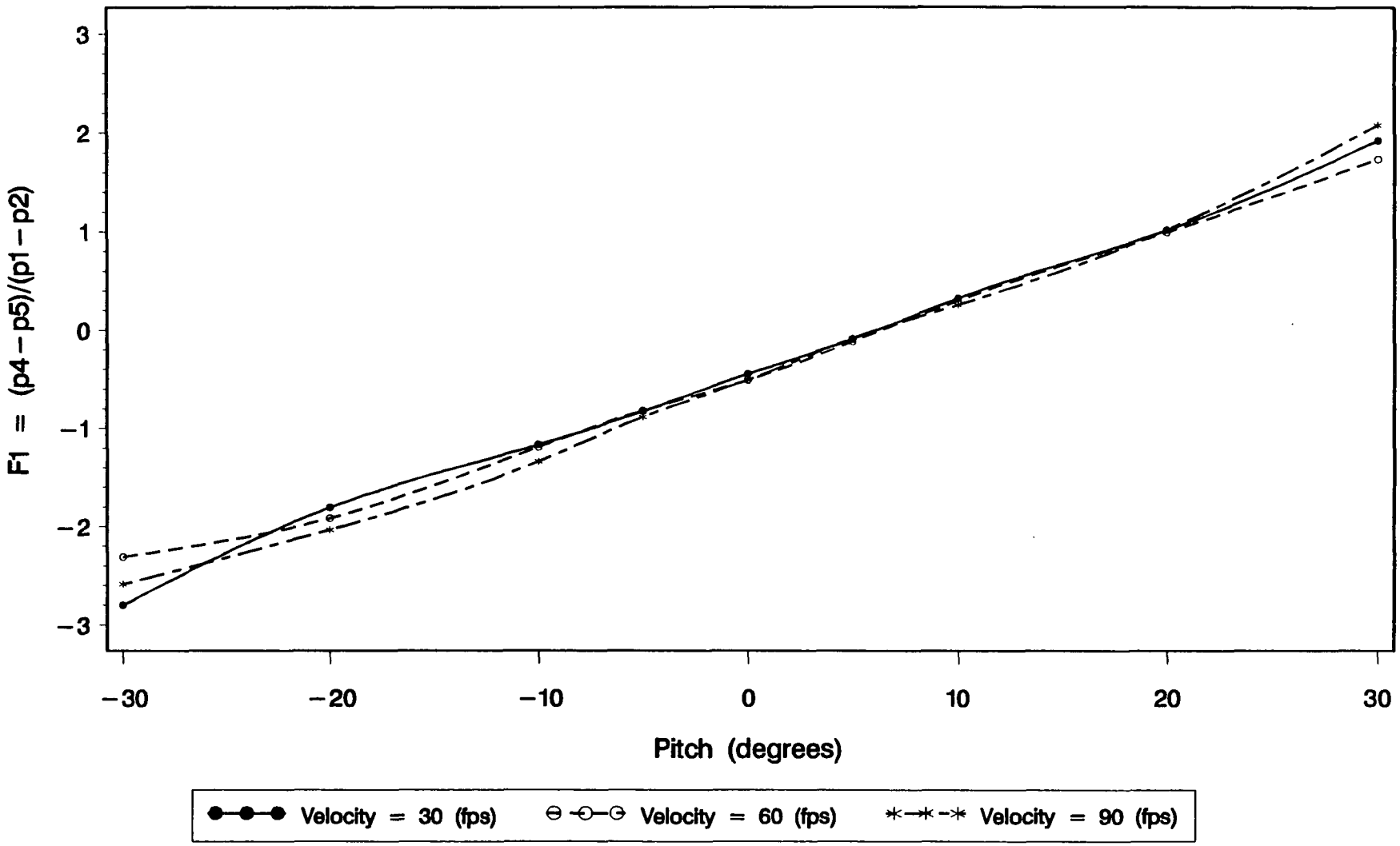

Figure 7-8. Probe: Spherical MS5-2
F2 vs. Pitch Angle

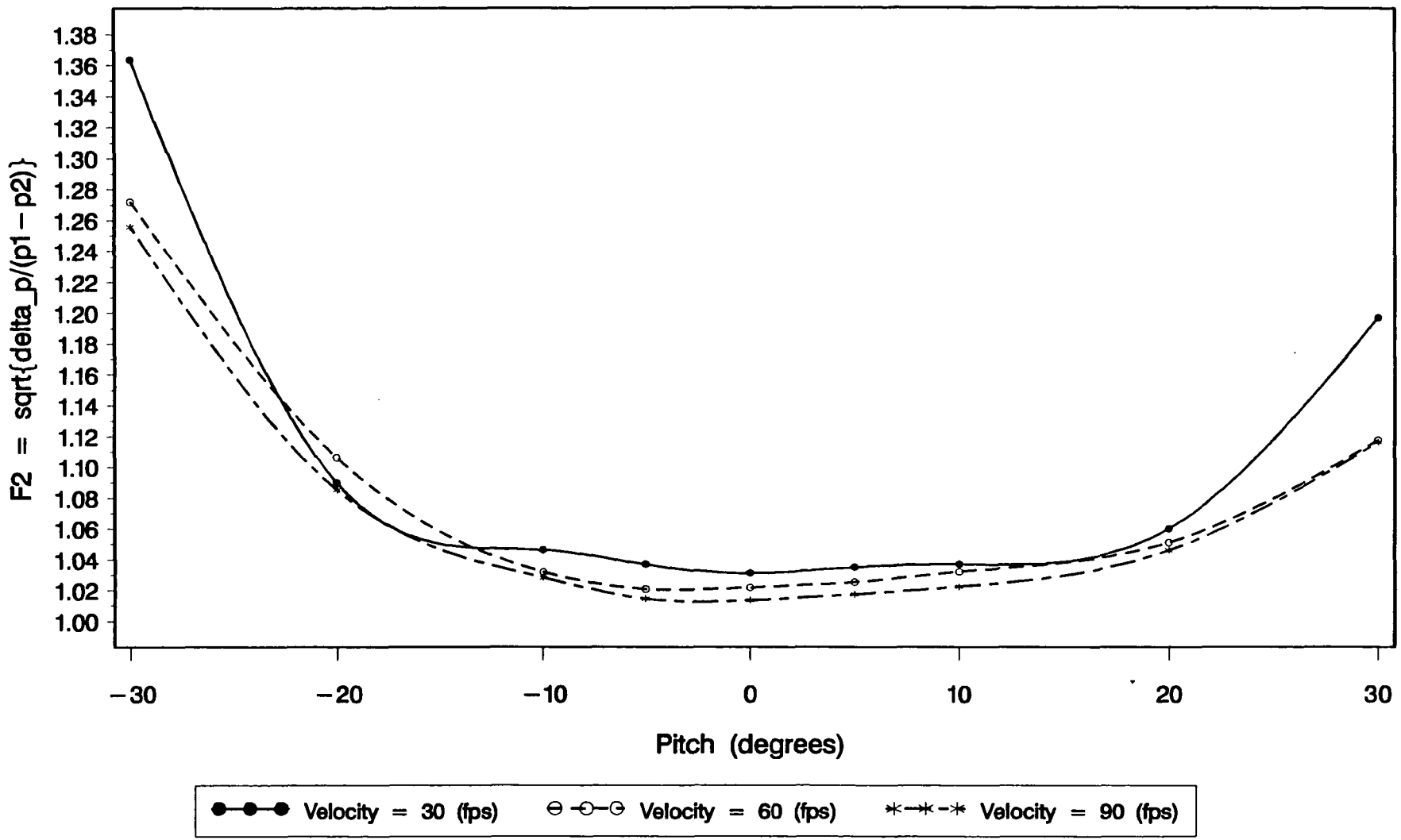

Figure 7−9. Probe: DAT 3D−1

F1 vs. Pitch Angle

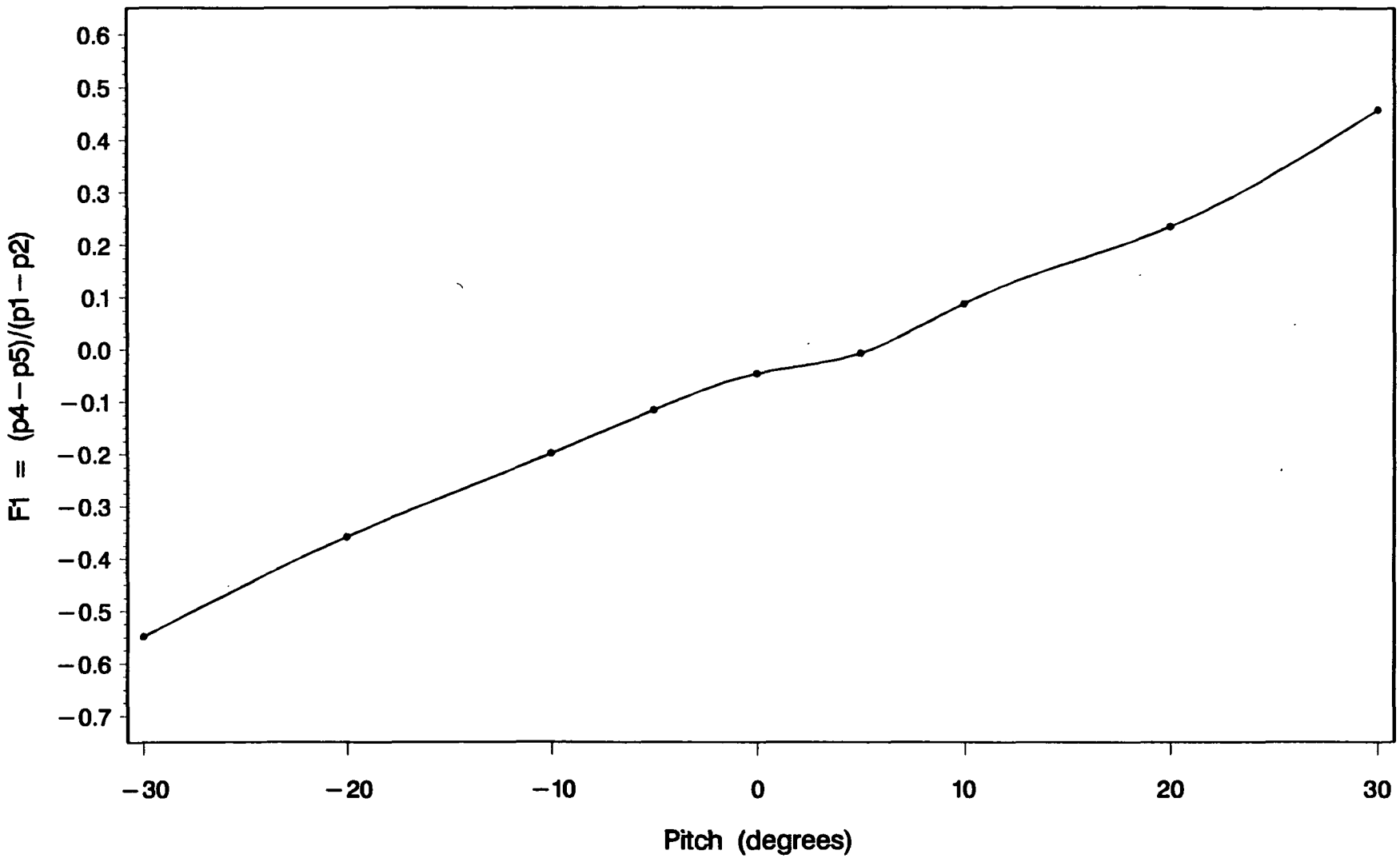

Figure 7−10. Probe: DAT 3D−1

F2 vs. Pitch Angle

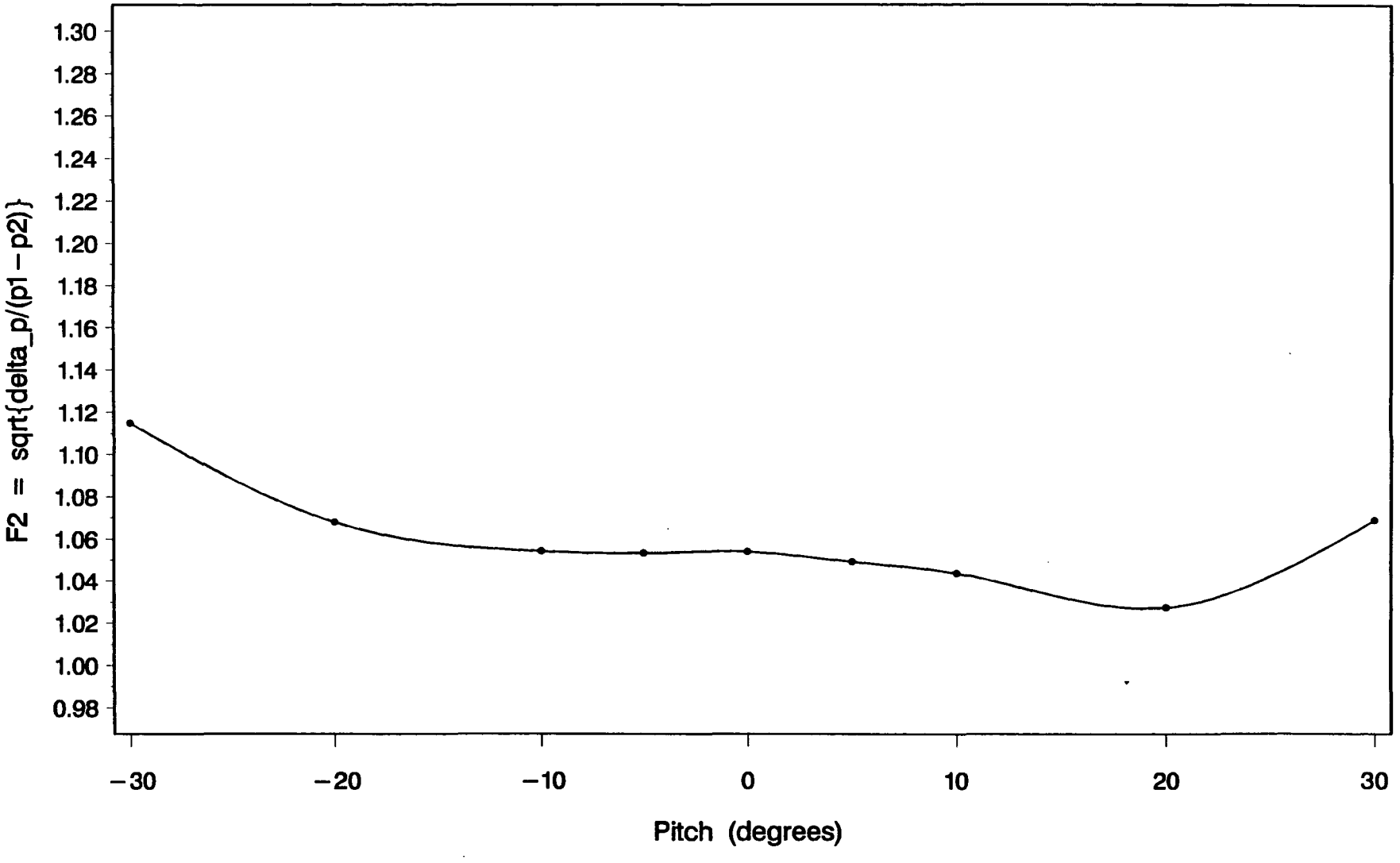

Figure 7-11. Probe: DAT 3D-2

F1 vs. Pitch Angle

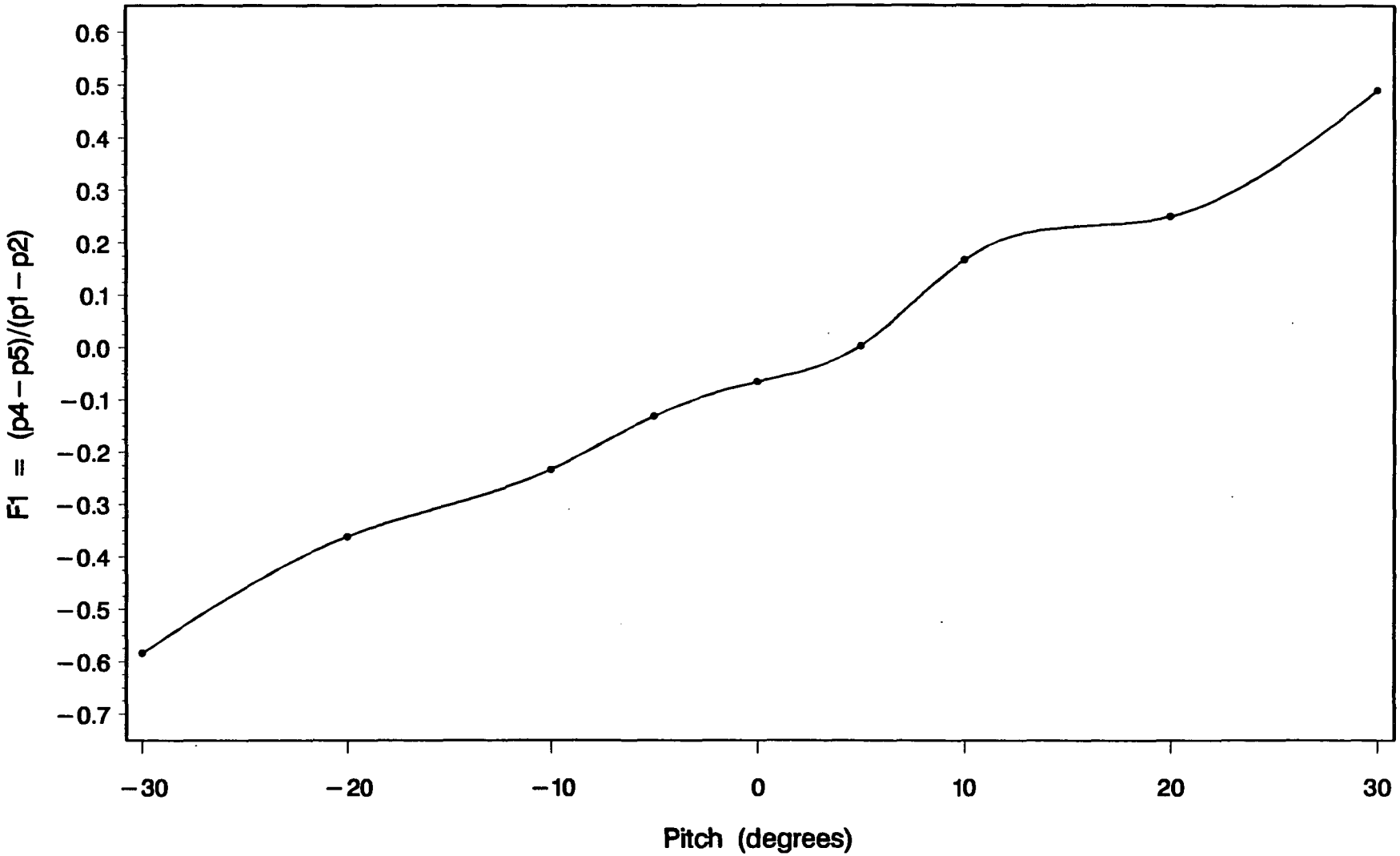

Figure 7−12. Probe: DAT 3D−2

F2 vs. Pitch Angle

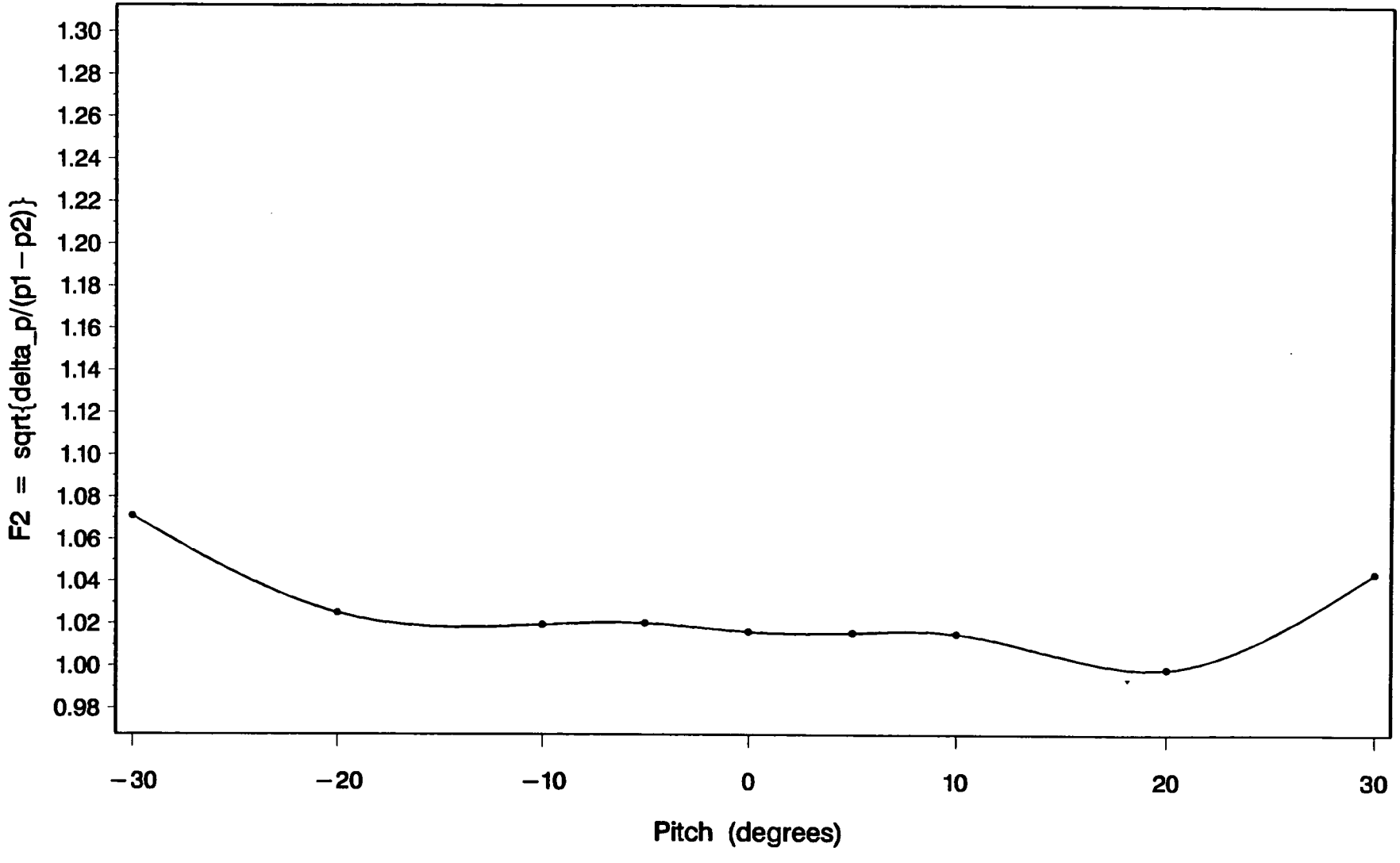

Figure 7-13. Probe: DAT 3D-3
F1 vs. Pitch Angle

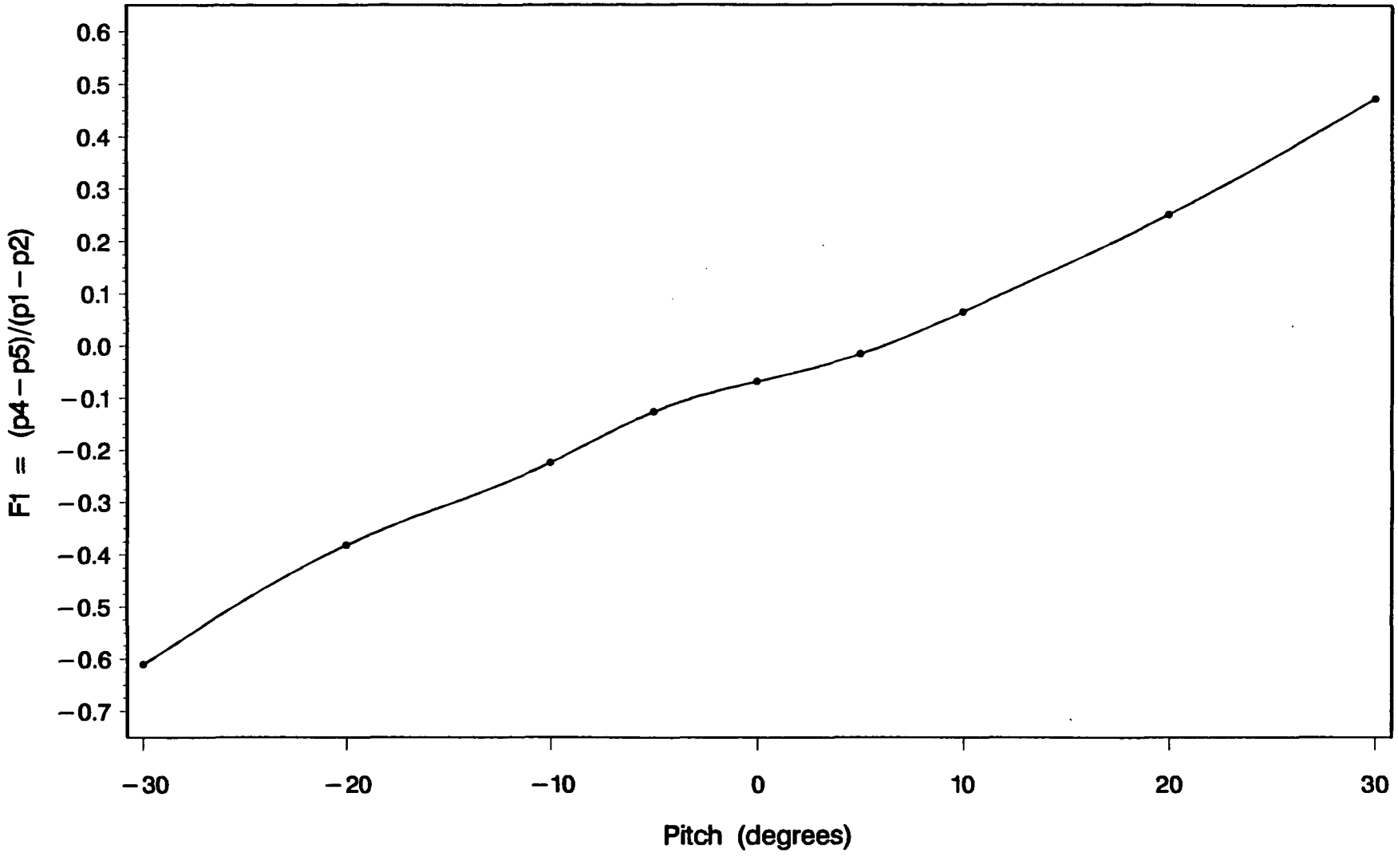

Figure 7-14. Probe: DAT 3D-3
F2 vs. Pitch Angle

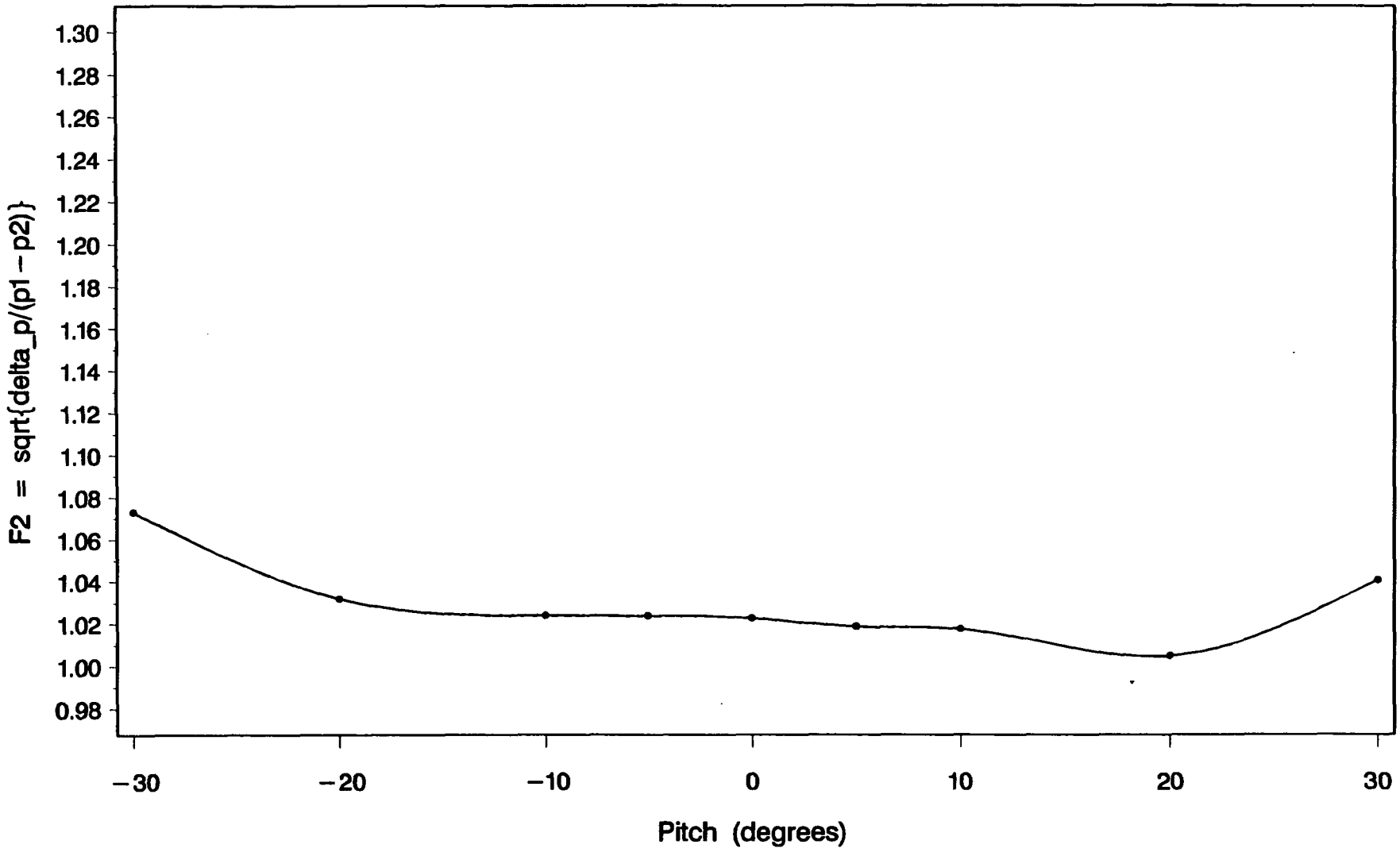

Figure 7-15. Probe: Spherical MS5-2
F1 vs. Pitch Angle

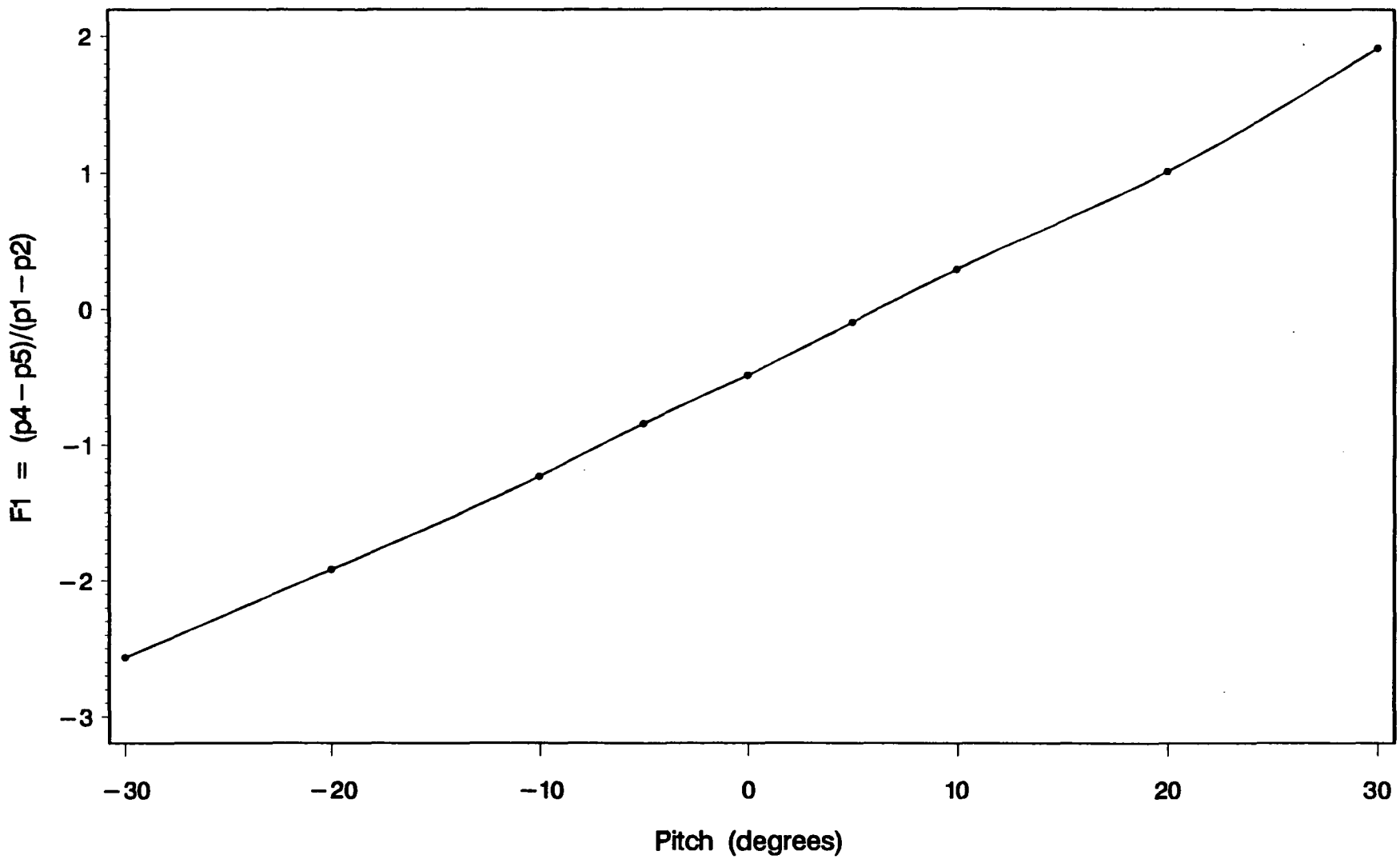

Figure 7-16. Probe: Spherical MS5-2
F2 vs. Pitch Angle

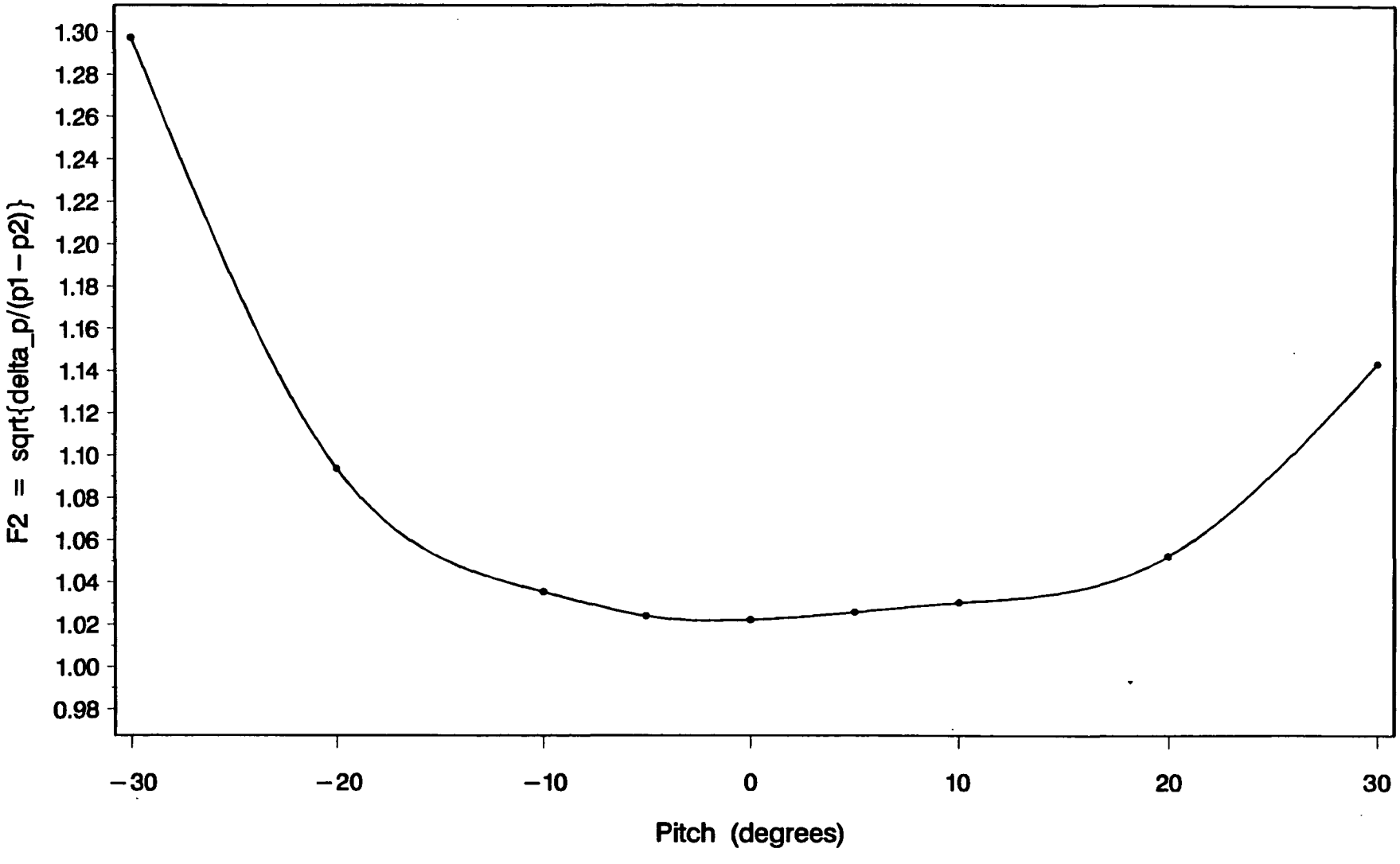

8.0 ENTRY WALL EFFECTS ON YAW NULLING

The experiments described in this section were conducted to confirm swirl tunnel findings obtained by Fossil Energy Research Corporation (FERCo) in an unpublished study funded by the Electric Power Research Institute (EPRI) in 1996. FERCo found that a Type S probe yielded multiple yaw nulls within several inches of the wall through which the probe was inserted into the tunnel. This effect is called an "entry wall" effect, because it appears to be associated with flow disturbance caused by a combination of the probe shaft and proximity to the entry wall.

8.1 TEST PROCEDURES

All experiments were conducted at 60 fps and at pitch angles of -10°, 0°, or 10°. The distance from the entry wall is the shortest (perpendicular) distance between the end of the probe head and the entry wall. Distances were measured with a ruler. For manual probes, multiple yaw nulls were sought using the standard yaw nulling techniques for each probe. Manual probes tested were the Type S, modified Kiel (MK2), DAT, and spherical probes. To look for multiple yaw nulls, ΔP was measured and plotted as a function of yaw angle in 5° increments from -20° to 20°. Yaw angles were measured with the digital inclinometer. Points were connected by straight lines. A yaw null was defined as the angle at which any line crossed the $\Delta P = 0°$ line. Multiple yaw nulls occurred when $\Delta P = 0$ at more than one yaw. When multiple yaw nulls were observed, three $\Delta P = 0$ values typically occurred. In some cases, ΔP remained at 0 for 5° or more. In this case, the yaw angle determination was said to be flat and the end points were recorded.

The vast majority of measurements were taken with the Autoprobe fitted with the Type S probe. Advantage was taken of the Autoprobe's ability to scan automatically over a yaw angle range and record ΔP at specified angles. All Autoprobe runs represent two replicate scans, each of which was made from -10° to 190°. Each run consisted of two replicate scans made consecutively. Data were collected on disk and downloaded to Quattro Pro®, and ΔP vs. yaw angle was plotted. Plots over three different yaw angle ranges were generated: a complete scan of ΔP vs. yaw from -10° to 190°; a plot of ΔP vs. yaw centered at 0°; and a plot of ΔP vs. yaw from 165° to 190°.

8.2 RESULTS OF ENTRY WALL EFFECTS TESTS

Before conducting quantitative tests of entry wall-related multiple yaw nulls, a qualitative test was performed to examine whether rotation of a Type S probe near an entry wall would cause a flow disturbance. To make this observation, strings were taped to the entry wall surrounding the probe shaft. With no flow in the tunnel, the strings were limp. The fan motor was increased slowly until a flow velocity of about 40 fps was reached, at which time all strings were lifted into a horizontal position in the direction of flow. At this point, the Autoprobe Type S probe was extended into the wind tunnel for a distance of about 1 inch. The probe was then rotated to a yaw angle of about -45°. As shown in Figure 8–1, the string immediately downstream of the probe at this angle (the flow direction is right to left) is horizontal, indicating that flow moves around the probe symmetrically at this yaw angle. Figure 8–2 shows the same configuration after the probe has been rotated to a yaw angle of about 20°. At this yaw angle, the direction of flow immediately downstream of the probe is indicated by the string to the left of the probe, which is deflected by about 45° from the flow direction. No quantitative analyses were conducted from these photographs.

Figure 8–3 shows plots of ΔP vs. yaw angle determined with the manual Type S probe at 0° pitch at 1", 3", 6", 9", 12", and 42" from the entry wall. Each curve is the average of three replicate runs. Figures 8–4 through 8–9 are plots for each distance showing the three replicate runs. The largest distance, 42", is 3" from the far wall of the wind tunnel. The figures clearly show pronounced multiple yaw nulls at distances of 1" through 6" from the entry wall. At 12" and 42", unique yaw nulls are found. The transition from multiple to unique yaw nulls is apparent at 9".

Figures 8–10 through 8–12 contain plots for the Autoprobe Type S at 0° pitch and distances from 1" to 44.5" from the wall. Figure 8–10 includes data for yaw angles from -10° to 15°, Figure 8–11 data from 165° to 190°, and Figure 8–12 for the complete yaw angle scan. For yaw angles around 0°, the thermocouple is on the upstream side of the probe, while at 180° the thermocouple is downstream. These data show more than one crossing of the $\Delta P = 0$ line or cases where ΔP remains near 0 over a substantial yaw angle range.

Figures 8–13 through 8–15 and Figures 8–16 through 8–18 are similar plots at pitch angles of 10° and -10°. A similar trend is apparent here. The only exception is the sharp yaw null at 1" and 10° pitch observed at both 0° and 180°. Individual plots for each distance/pitch angle plot are presented in Appendix B.

The observation reported in the EPRI-sponsored study is confirmed by this work. With the manual Type S probe, multiple yaw nulls are clearly observed at distances from the entry wall of up to about 9". Thereafter, unique yaw nulls are found. Multiple yaw nulls are not found near the far wall, indicating that the effect is related to an interaction between the probe shaft and the entry wall. Multiple yaw nulls are observed with the Autoprobe Type S at essentially all distances from the entry wall. The unique design of the Autoprobe may be responsible for the occurrence of multiple yaw nulls at all distances from the wall. Whereas the manual Type S probe is attached to a 1" shaft and has only a thermocouple in addition to the pitot head, the Autoprobe has a 2" diameter clamp located within 2" of the pitot head and has a dilution probe parallel to the thermocouple on the opposite side of the probe. The clamp may in fact be causing a "pseudo-entry wall effect", which is evident at all distances from the entry wall.

To determine whether multiple yaw nulls at distances near the entry wall are uniquely associated with Type S probes, ΔP vs. yaw angle curves were obtained for the modified Kiel probe and the two 3D probes (i.e., DAT and spherical). Each probe uses Fechheimer-type ports to locate the yaw null point. Figures 8–19 and 8–20 are plots of ΔP_f (across the Fechheimer ports) vs. yaw angle over the range -20° to 20° for the modified Kiel probe (MK2). Each plot presents curves, determined in triplicate, at pitch angles of -10°, 0°, and 10°, for a total of 9 curves. The data shown in Figure 8–19 were taken at 1" from the entry wall, and the data in Figure 8–20 were taken at 5" from the wall. Both plots clearly indicate that the Fechheimer ports on the modified Kiel probe locate a unique yaw null at each distance independent of pitch. In fact, the curves at both distances from the wall are very similar. At 1", a yaw null is found at about 3.5°; at 5" from the wall, the yaw null is found at about 2°.

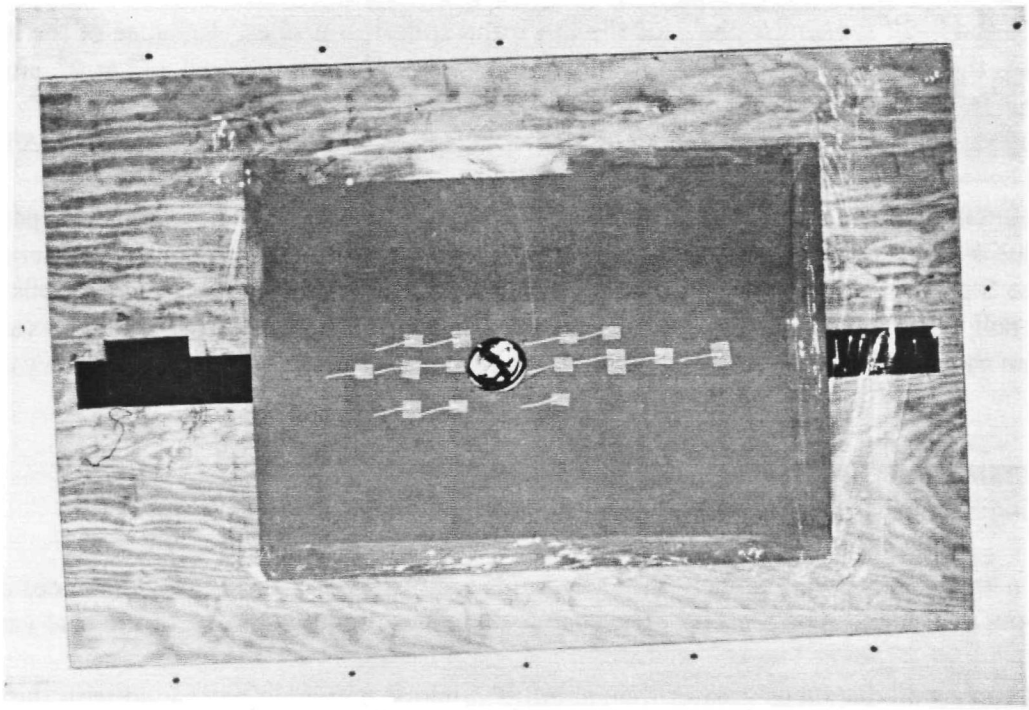

Figure 8-1. Flow pattern at yaw angle of -45°.

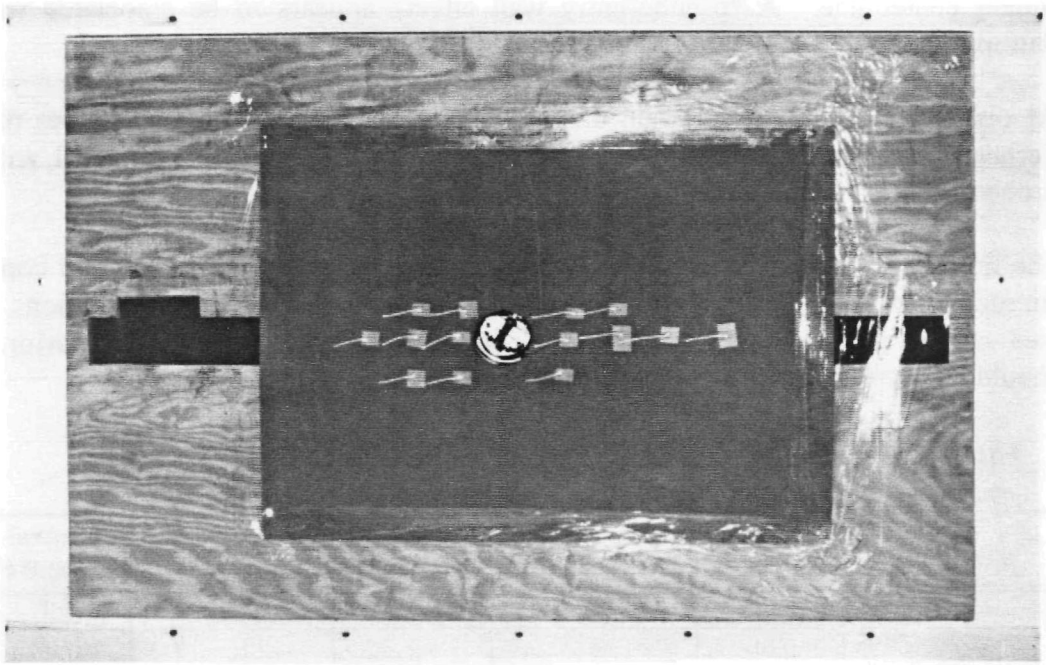

Figure 8-2. Flow pattern at yaw angle of +20°.

Figures 8–21 and 8–22 are similar plots for the DAT and spherical probes. Because of the length of these probes, the data for the spherical probe were taken at 4" from the wall and at 0° pitch only. Data for the DAT probe were taken at 3" from the wall at pitch angles of -10° and 10°. In both cases, unique yaw nulls are found—at about 0.5° for the spherical probe and 2° for the DAT probe.

Table 8–1 summarizes data collected from all probes that were tested. (The modified S probe was not tested due to time constraints.) As noted from the figures, multiple yaw nulls are observed only for the Type S probes. Data in the last column of Table 8-1 indicate that unique yaw nulls and the middle yaw null, when three yaw nulls are present, are within 4° of the true yaw zero. The yaw angle range column shows that the range in which multiple yaw nulls is found is symmetric about yaw angle zero.

8.3 CONCLUSIONS

The following conclusions can be drawn from the data presented in this section:

- In a laminar-flow wind tunnel, three yaw nulls are observed at wall entry distances of up to about 9" using a Type S probe. The center yaw null is found within 1° of the true yaw zero.
- At entry wall distances greater than about 9", unique yaw nulls are found with the manual Type S probe.
- Multiple yaw nulls are found with the Autoprobe Type S at all distances from the wind tunnel center line. A "pseudo-entry wall effect" appears to be associated with the Autoprobe.
- At distances near the entry wall, unique yaw nulls are found with all probes that use Fechheimer-type ports to determine the yaw angle: the modified Kiel, spherical, and DAT probes.

It should be noted that probes that detect multiple yaw nulls near the entry wall in a controlled environment such as a wind tunnel may not exhibit the same behavior under field conditions, where the increased variability of the gas stream flow may prevent the occurrence of this behavior. Field test data should be observed to see whether this is the case.

Table 8–1. Summary Table of the Effect of Distance from Wall Entry on the Number of Yaw Nulls Observed

Probe	Pitch Angle (°)	Distance from entry wall (in.)	Number of yaw nulls	Yaw angle null range (°)	Central yaw null (°)
Type S (3/8 S-3)	0.00	1	3	-10 to +15	+1
	0.00	3	3	-12 to +17	0.00
	0.00	6	3	- 8 to 12.5	0.00
	0.00	9	3	- 5 to +10	0.00
	0.00	12	1		+1
	0.00	42	1		+2.5

Table 8–1. Summary Table of the Effect of Distance from Wall Entry on the Number of Yaw Nulls Observed (continued)

Probe	Pitch Angle (°)	Distance from entry wall (in.)	Number of yaw nulls	Yaw angle null range (°)	Central yaw null (°)
Autoprobe Type S (AS)[a]	0.00	1	3	- 6 to + 9	+4
	0.00	1.5	3	-7.5 to +10	0.00
	0.00	3	3	- 5 to +10	0.00
	0.00	6	3	- 5 to + 7	+2
	0.00	11.25	2	- 2.5 to + 7.5	
	0.00	12	2	- 2 to + 5	
	0.00	22.5	2	0 to + 5	
	0.00	33.75	1		-2
	0.00	44.5	2	- 1 to + 5	
Autoprobe Type S (AS)[b]	0.00	1	3	+174 to +188	182.5
	0.00	1.5	2	+175 to +190	
	0.00	3	2	+175 to +190	
	0.00	6	3	+174 to +187.5	182.5
	0.00	11.25	2	+175 to +185	
	0.00	12	2	+175 to +185	
	0.00	22.5	1		176
	0.00	33.75	1		176
	0.00	44.5	1		177
Autoprobe Type S (AS)[a]	-10	1	2	- 6 to + 5	
	-10	2	2	- 5 to + 7.5	
	-10	6	2	0 to + 7.5	
	-10	22.5	2	- 3 to + 5	
Autoprobe Type S (AS)[b]	-10	1	2	+174 to +185	
	-10	2	1		190
	-10	6	3	+175 to +187.5	181
	-10	22.5	2	+174 to +185	
Autoprobe Type S (AS)[a]	+10	1	1		+1.5
	+10	2	3	- 5.5 to + 8.5	+3
	+10	6	3	- 5.5 to + 7	+3
	+10	12	3	- 6 to + 6	+2
	+10	22.5	3	- 6.5 to + 6	+4
	+10	38.8	3	- 5.5 to + 6.5	+3.5

Table 8–1. Summary Table of the Effect of Distance from Wall Entry on the Number of Yaw Nulls Observed (continued)

Probe	Pitch Angle (°)	Distance from entry wall (in.)	Number of yaw nulls	Yaw angle null range (°)	Central yaw null (°)
Autoprobe Type S (AS)[b]	+10	1	1		182
	+10	2	3	+174 to +190	182
	+10	6	3	+174 to +187.5	183
	+10	12	3	+174 to +187.5	181.5
	+10	22.5	3	+174 to +187	182
	+10	38.8	3	+174 to +187.5	180
Modified Kiel (MK2)	-10	1	1		3.50
	-10	5	1		+2.5
	0.00	1	1		3.50
	0.00	5	1		+2.5
	+10	1	1		3.50
	+10	5	1		+2.5
DAT (3D-1)	-10	3	1		+2.5
	+10	3	1		+3
Spherical (MS502)	0.00	4	1		+1

[a] Thermocouple facing upwind.

[b] Thermocouple facing downwind.

Figure 8-3.

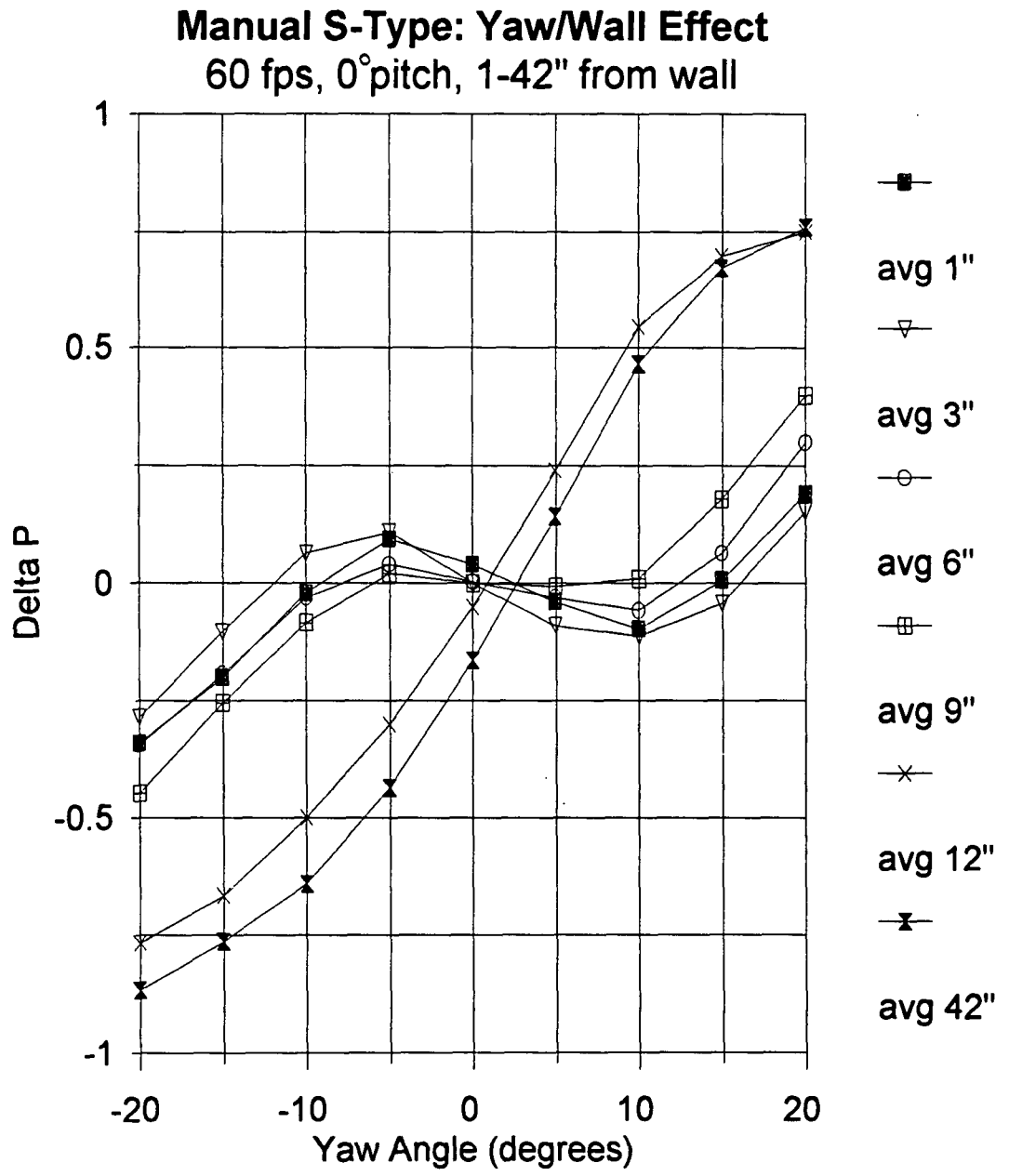
Manual S-Type: Yaw/Wall Effect
60 fps, 0°pitch, 1-42" from wall
Delta P
1
0.5
0
-0.5
-1
-20
-10
0
10
20
Yaw Angle (degrees)
avg 1"
avg 3"
avg 6"
avg 9"
avg 12"
avg 42"

Figure 8-4.

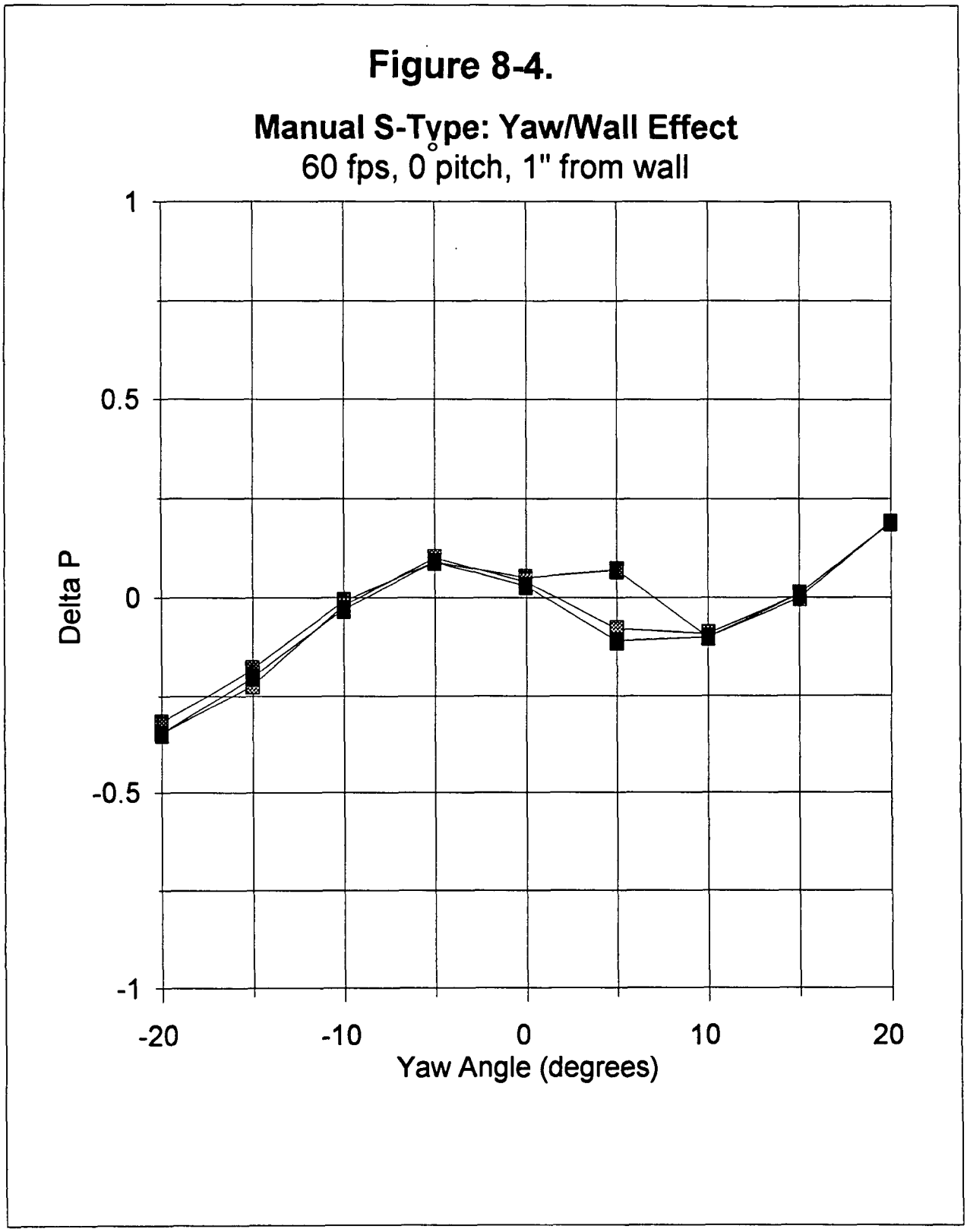
Manual S-Type: Yaw/Wall Effect
60 fps, 0° pitch, 1" from wall
Delta P
1
0.5
0
-0.5
-1
-20
-10
0
10
20
Yaw Angle (degrees)

Figure 8-5.

Manual S-Type: Yaw/Wall Effect

60 fps, 0°pitch, 3" from wall

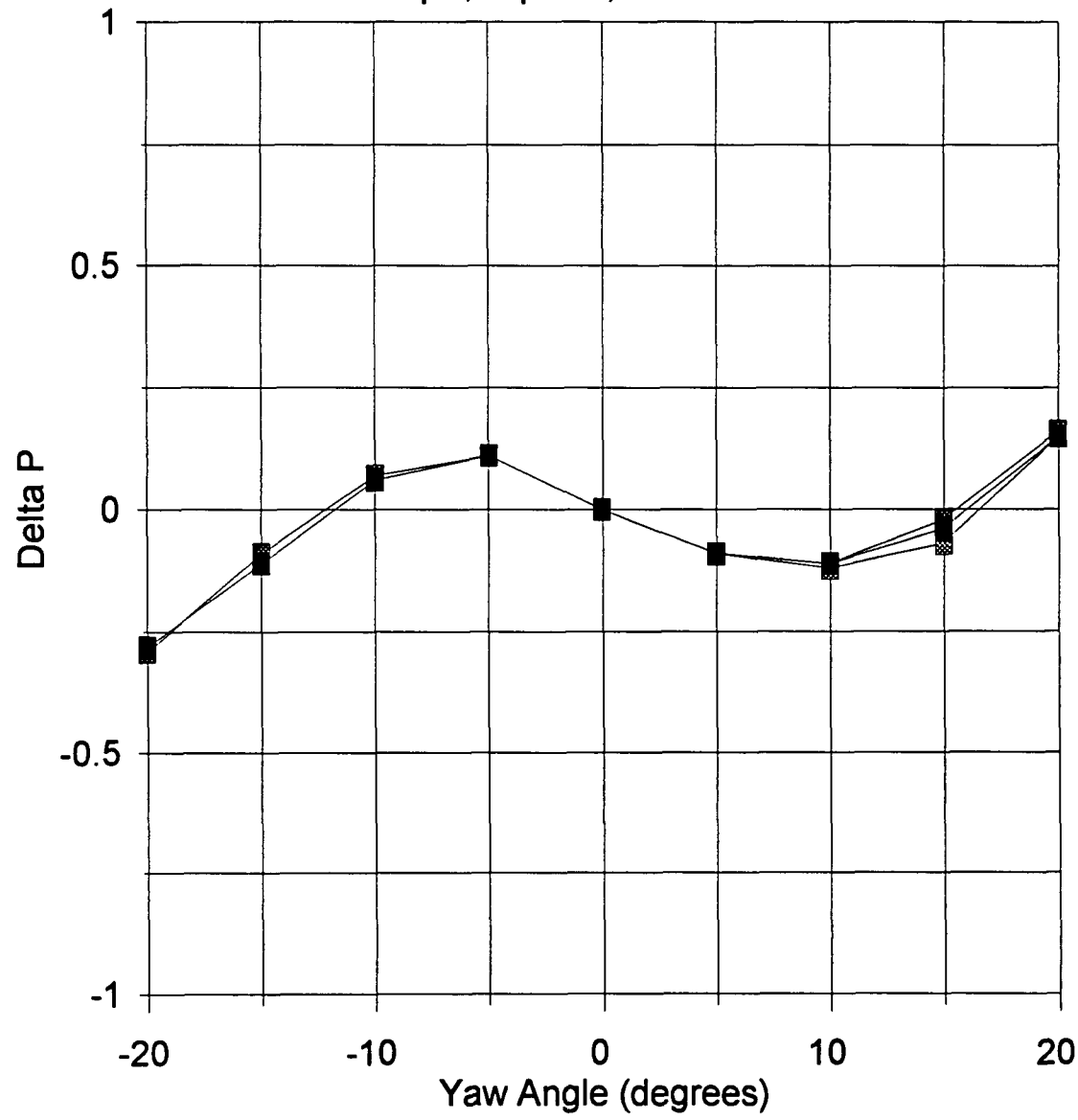

Figure 8-6.

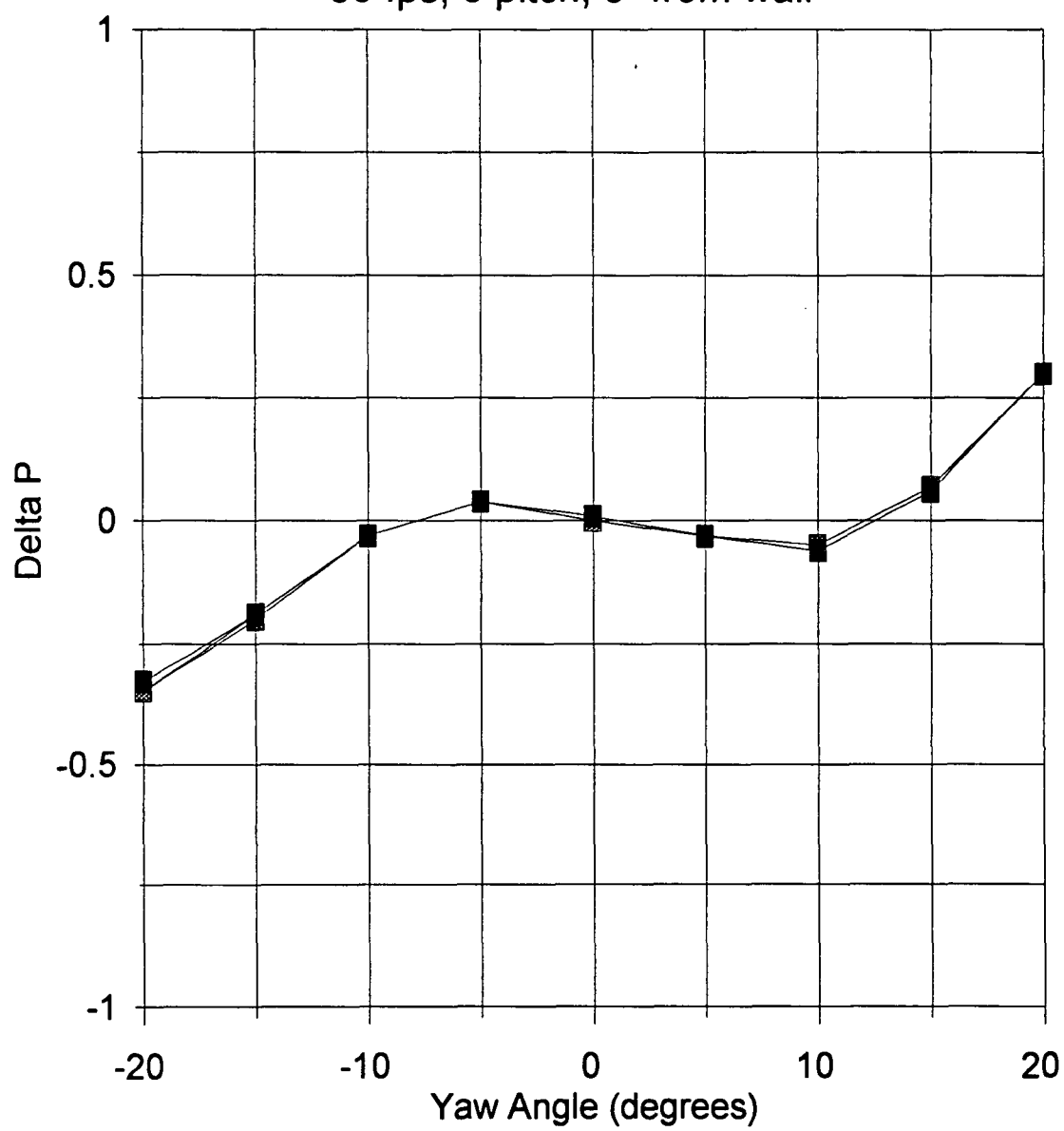
Manual S-Type: Yaw/Wall Effect
60 fps, 0° pitch, 6" from wall
1
0.5
0
-0.5
-1
Delta P
-20
-10
0
10
20
Yaw Angle (degrees)

Figure 8-7.
Manual S-Type: Yaw/Wall Effect
60 fps, 0°pitch, 9" from wall

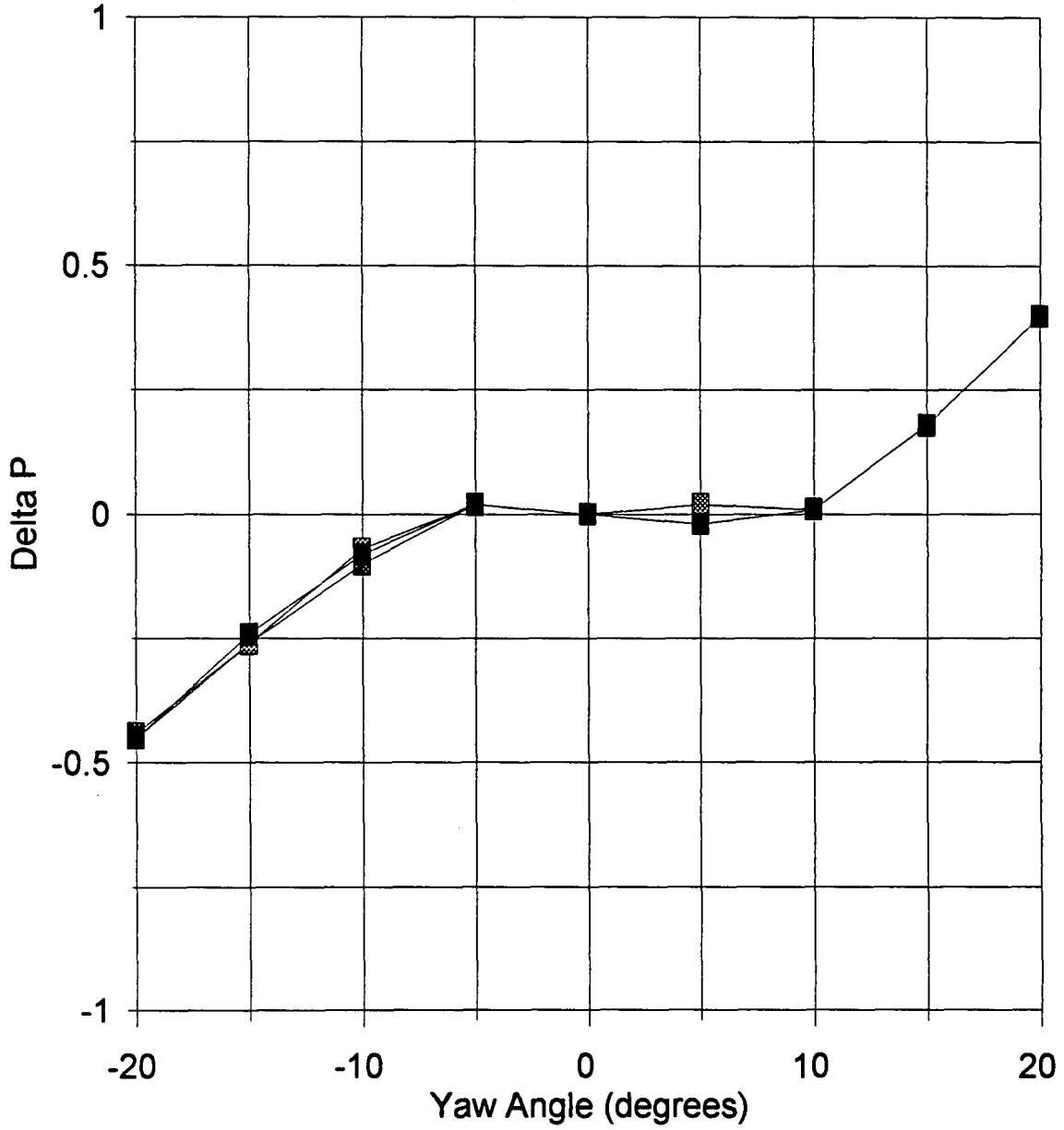

Figure 8-8.

Manual S-Type: Yaw/Wall Effect

60 fps, 0° pitch, 12" from wall

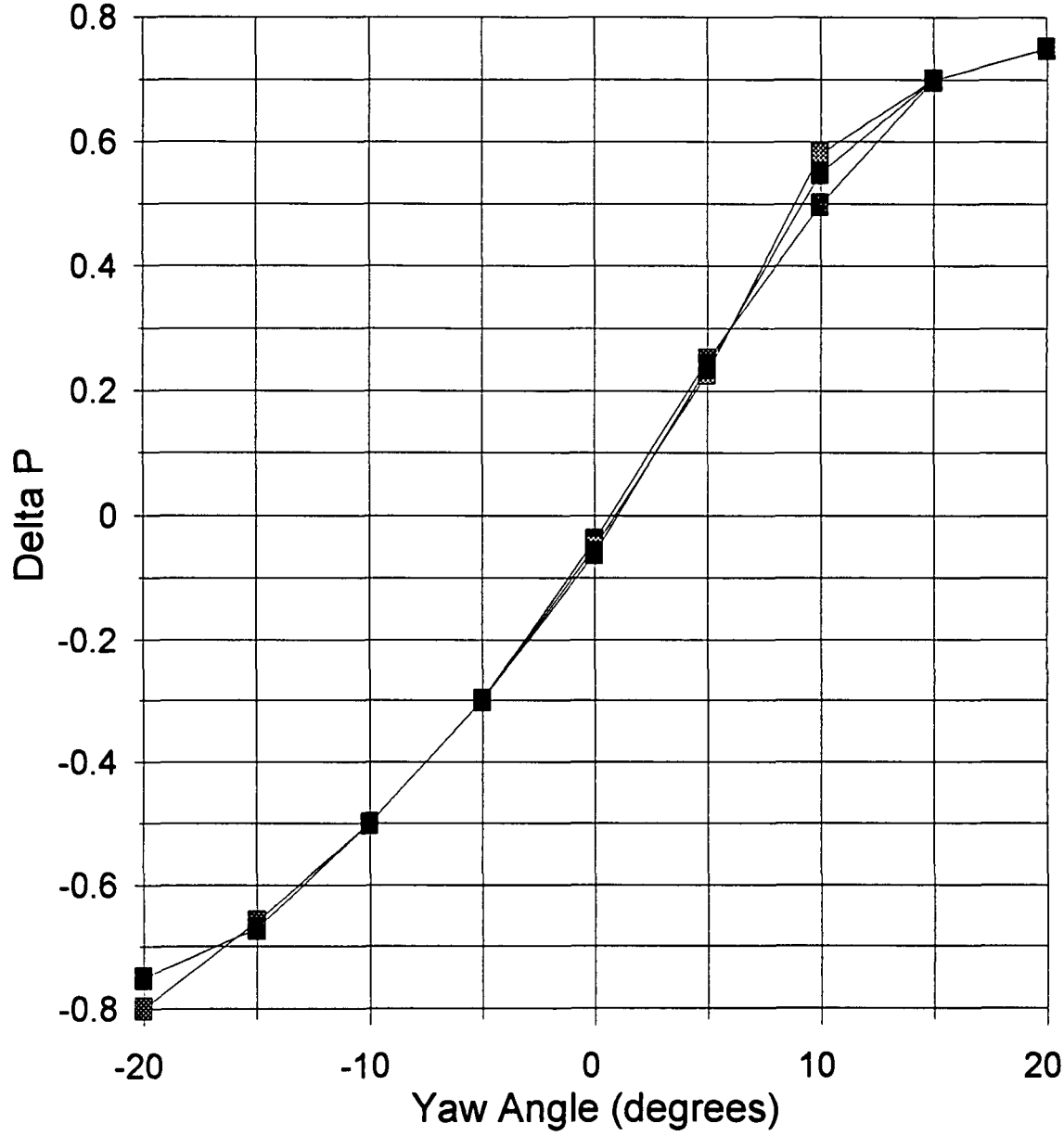

Figure 8-9.

Manual S-Type: Yaw/Wall Effect

60 fps, 0°pitch, 42" from wall

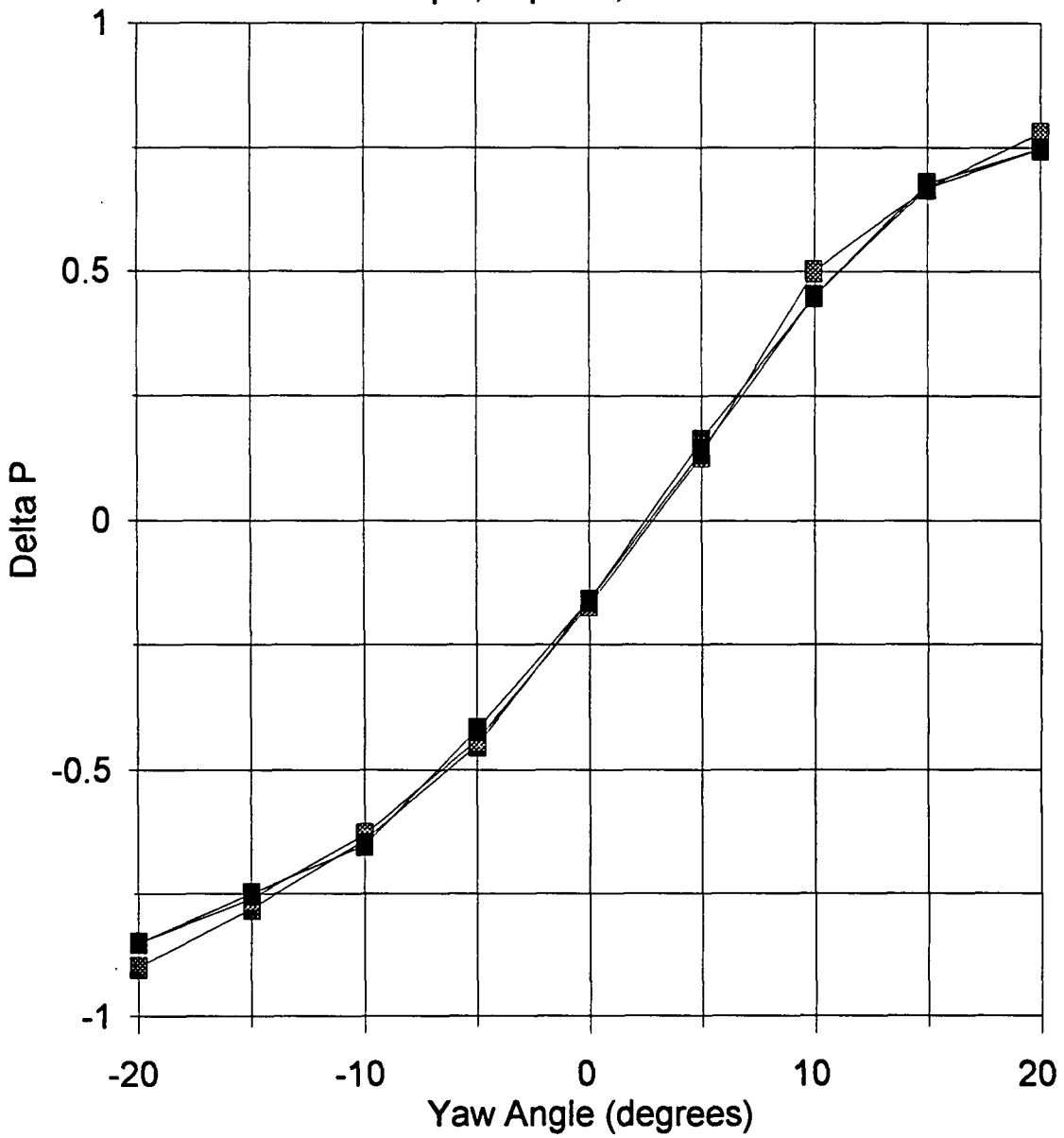

Figure 8-10.

Autoprobe S-Type: Yaw/Wall Effect

60 fps, 0° pitch

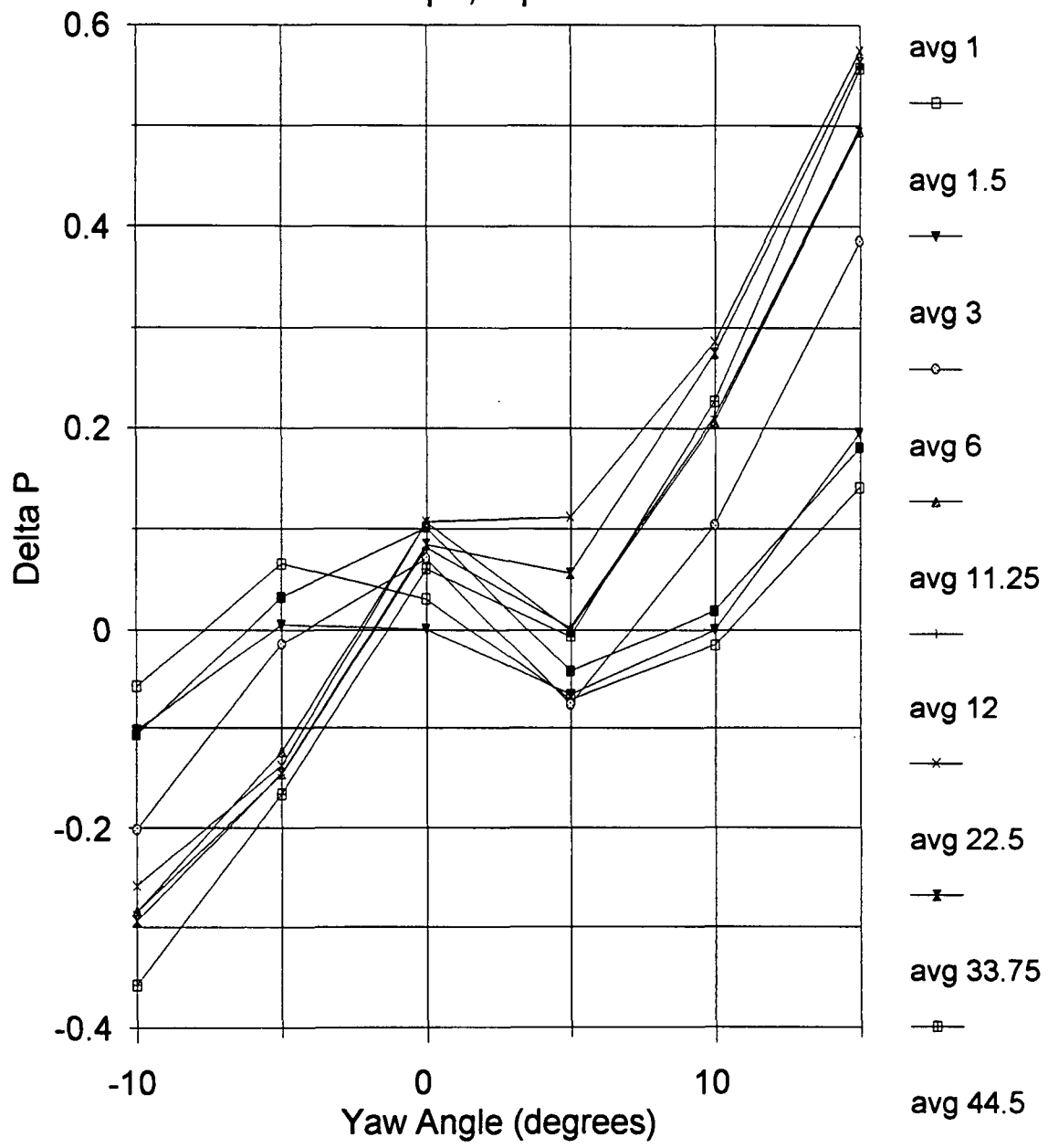

Figure 8-11.

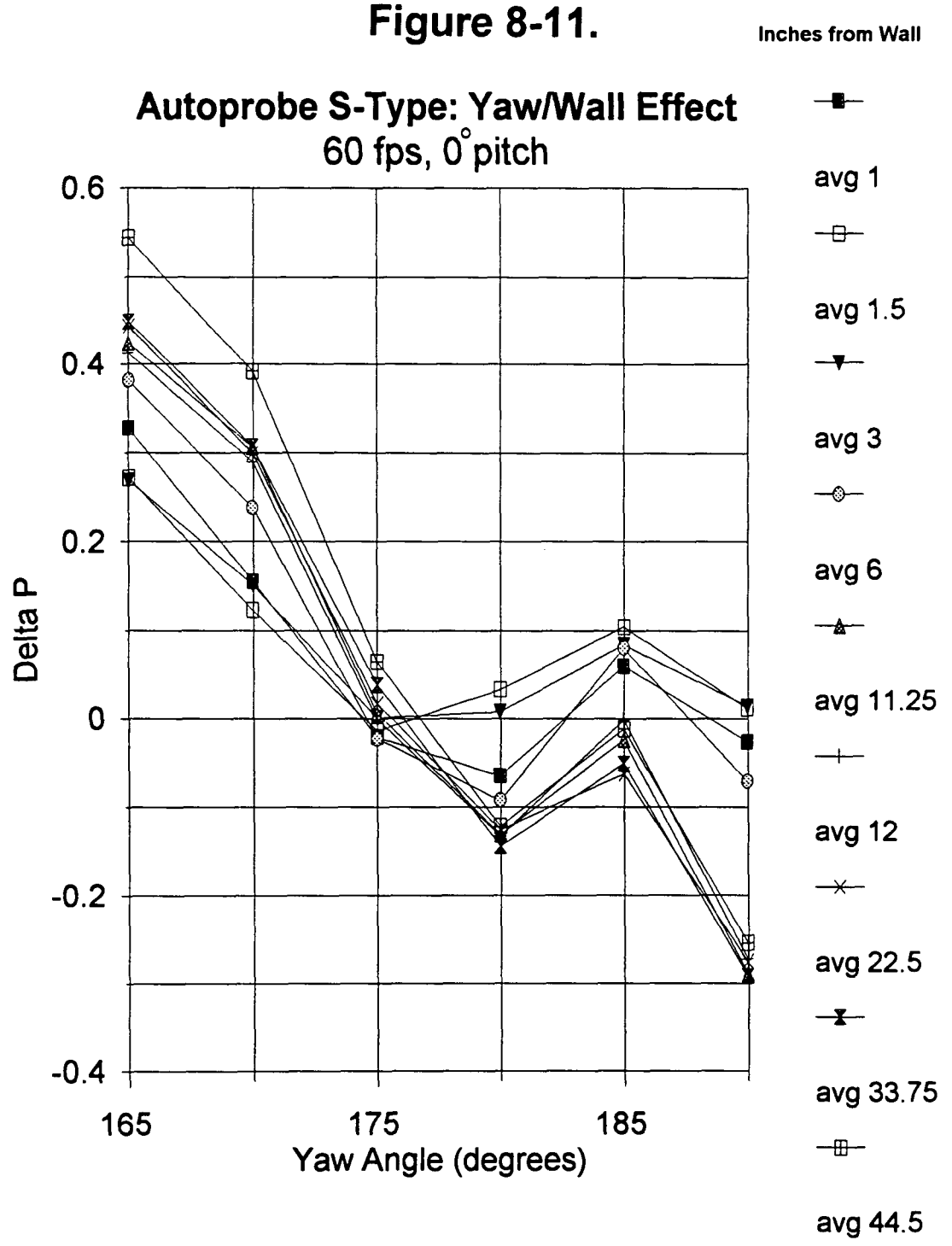
Autoprobe S-Type: Yaw/Wall Effect
60 fps, 0° pitch
Delta P
0.6
0.4
0.2
0
-0.2
-0.4
165
175
185
Yaw Angle (degrees)
Inches from Wall
avg 1
avg 1.5
avg 3
avg 6
avg 11.25
avg 12
avg 22.5
avg 33.75
avg 44.5

Figure 8-12.

Autoprobe S-Type: Yaw/Wall Effect

60 fps, 0° pitch

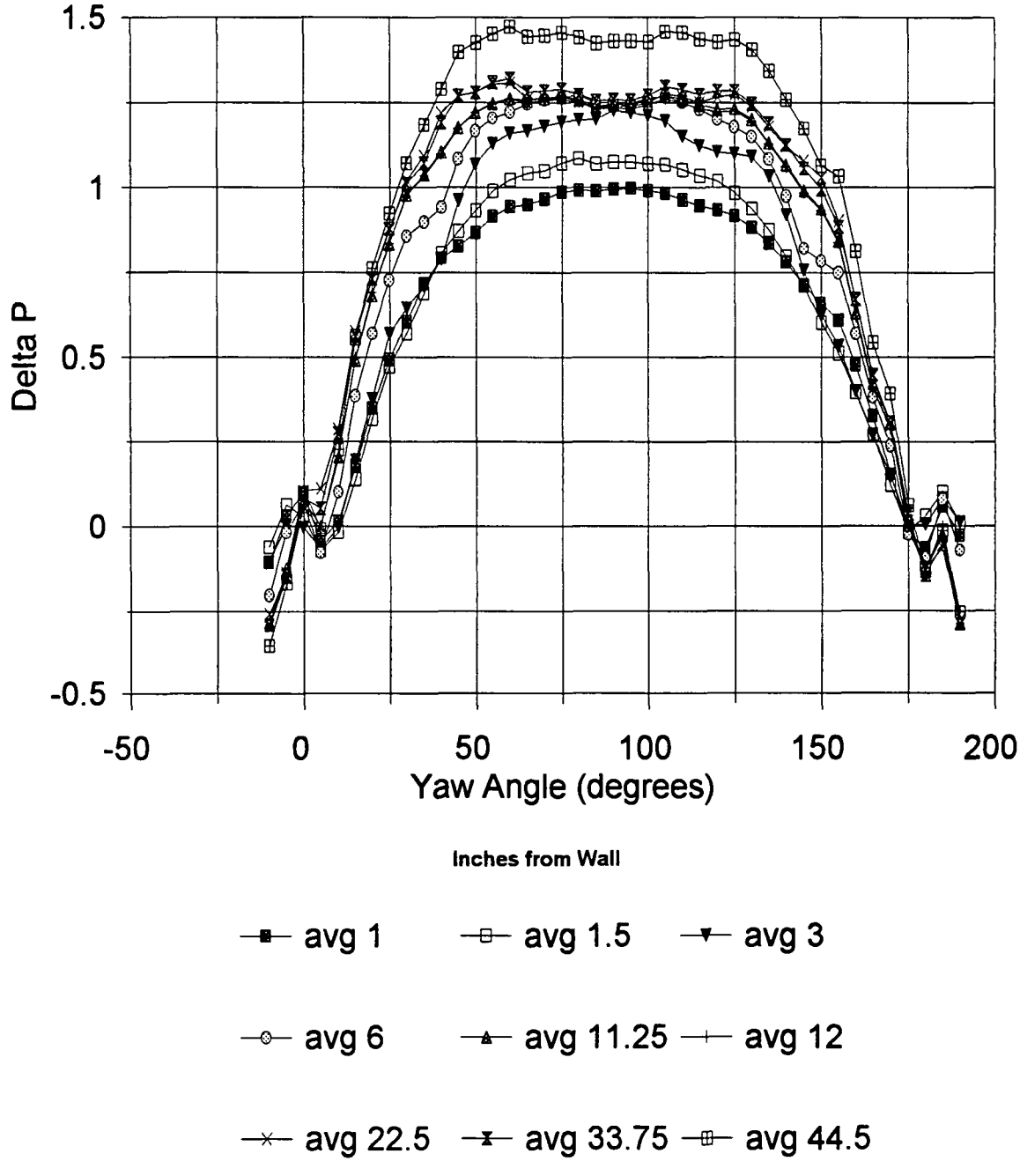

Figure 8-13.

Autoprobe S-Type: Yaw/Wall Effect

60 fps, +10° pitch

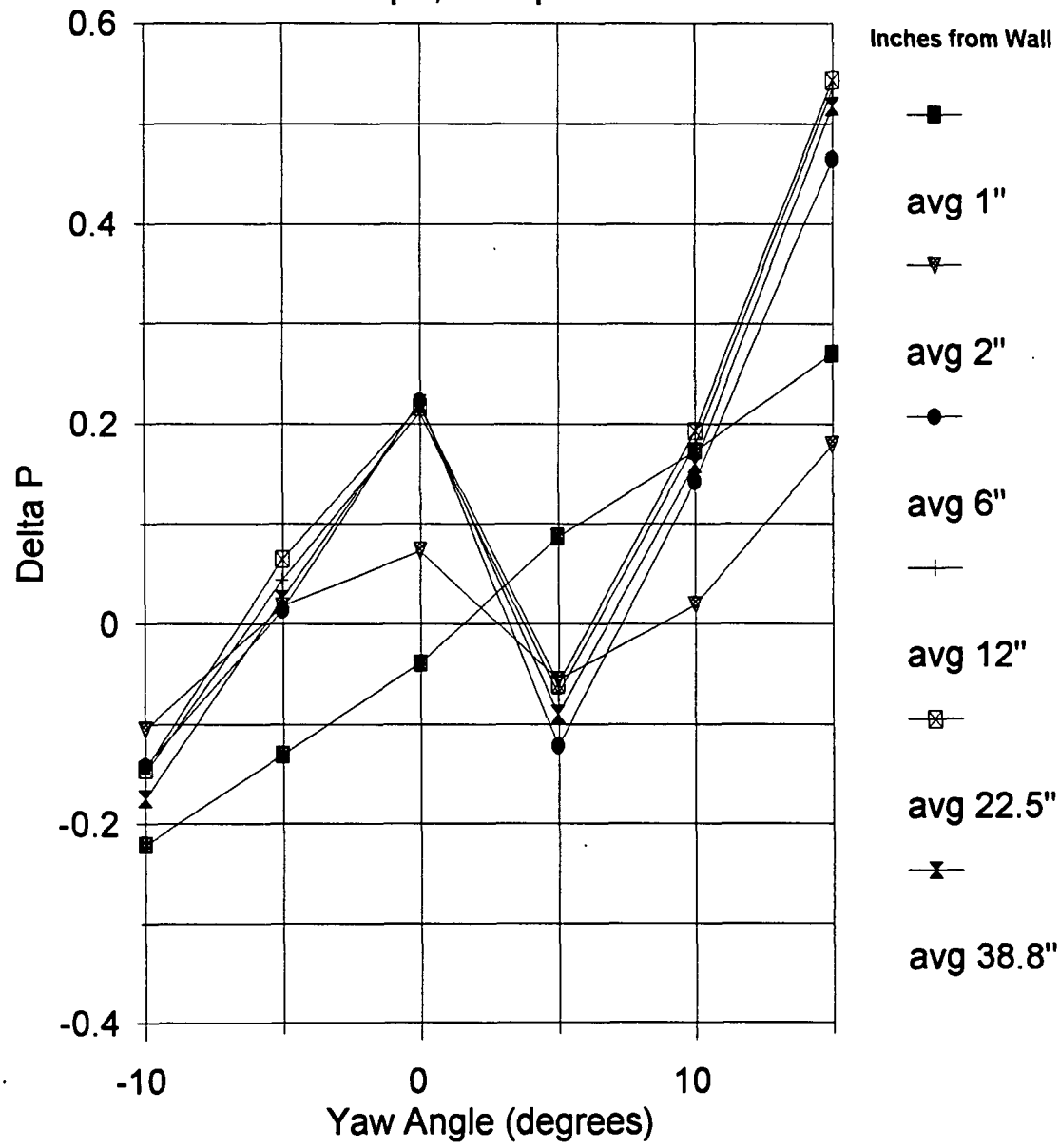

Figure 8-14.

Autoprobe S-Type: Yaw/Wall Effect

60 fps, +10 pitch °

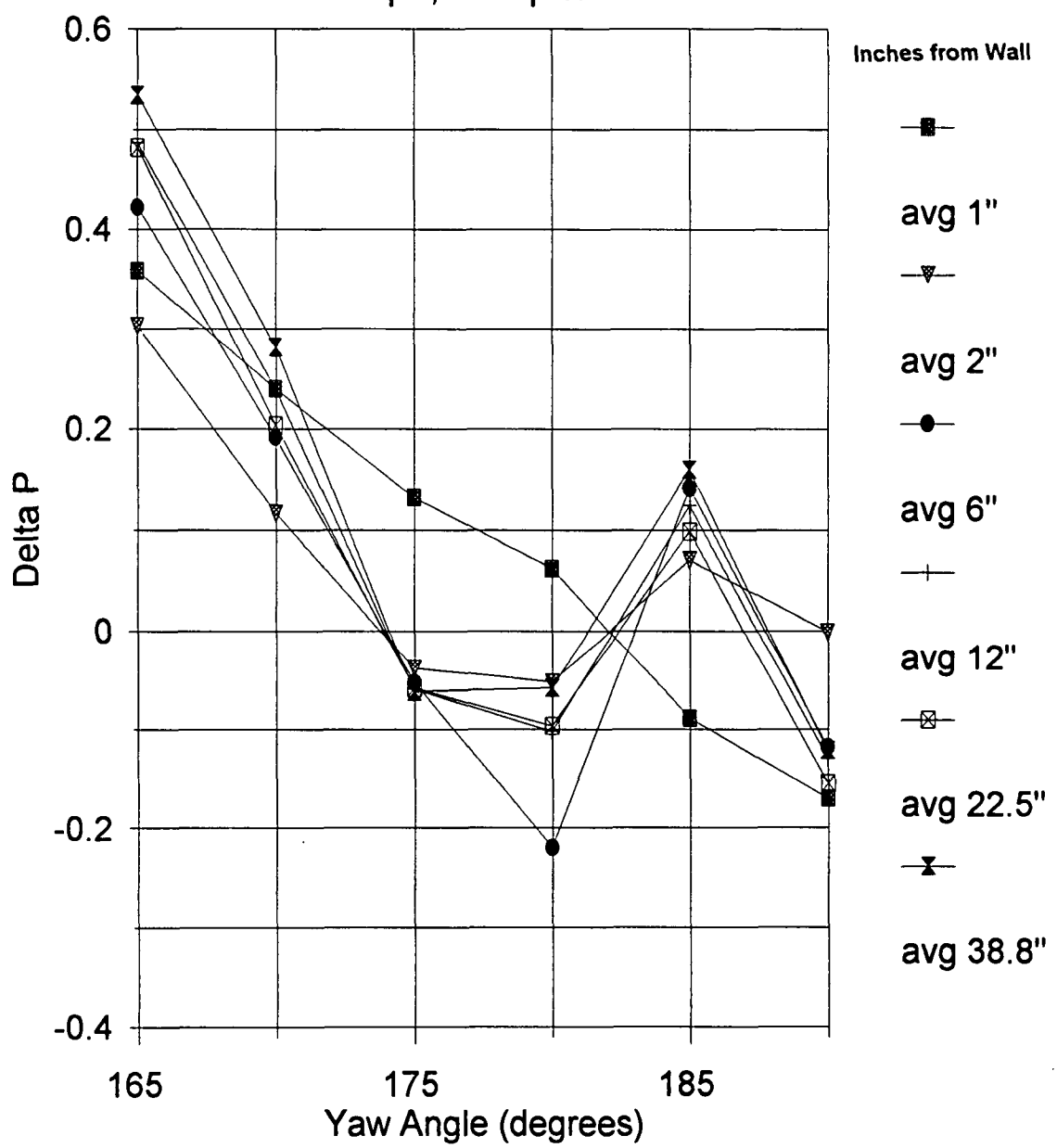

Figure 8-15.

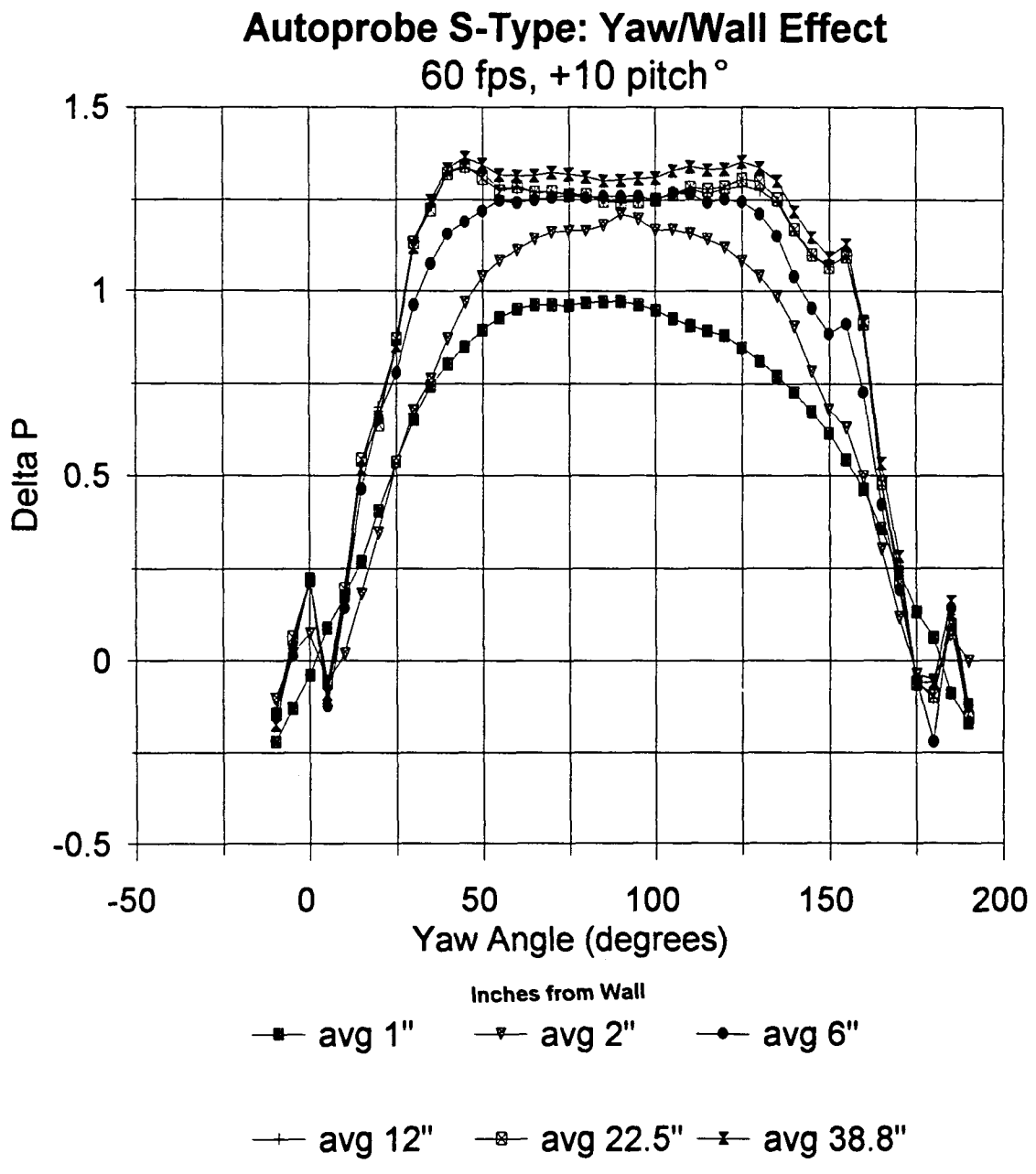
Autoprobe S-Type: Yaw/Wall Effect
60 fps, +10 pitch °
Delta P
1.5
1
0.5
0
-0.5
-50
0
50
100
150
200
Yaw Angle (degrees)
Inches from Wall
avg 1"
avg 2"
avg 6"
avg 12"
avg 22.5"
avg 38.8"

Figure 8-16.

Autoprobe S-Type: Yaw/Wall Effect

60 fps, -10 pitch °

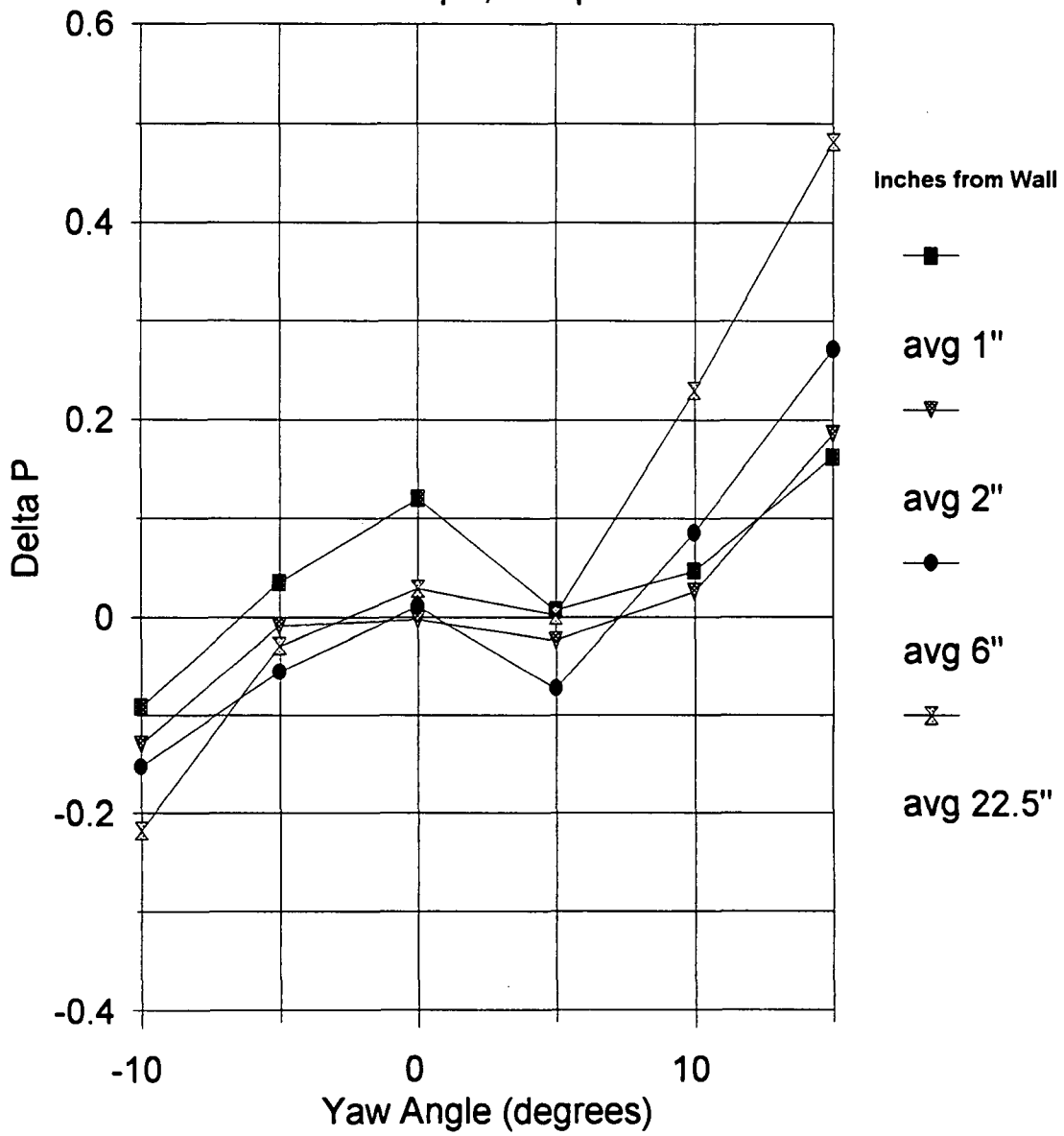

Figure 8-17.

Autoprobe S-Type: Yaw/Wall Effect

60 fps, -10 pitch °

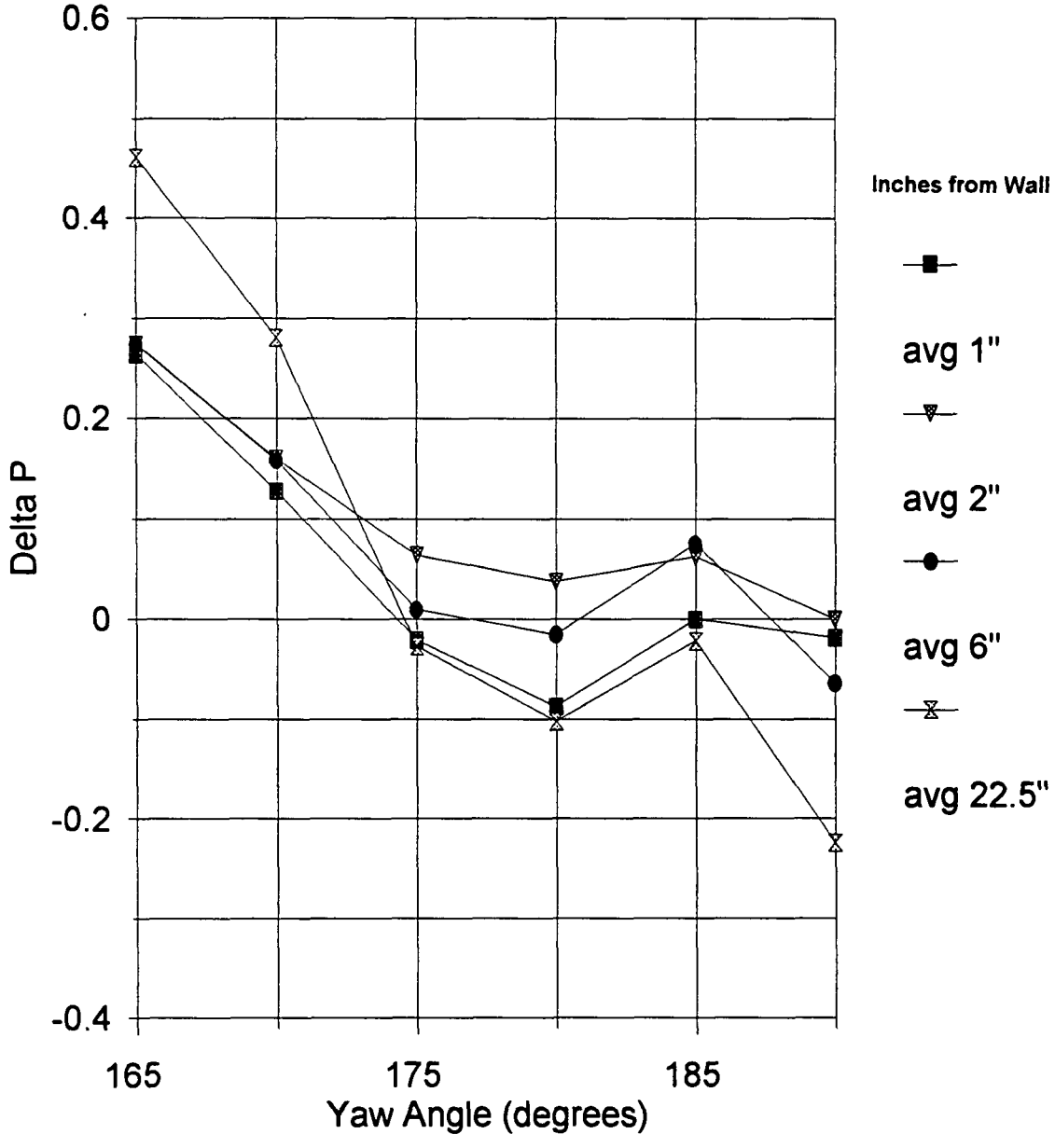

Figure 8-18.

Autoprobe S-Type: Yaw/Wall Effect

60 fps, -10 pitch °

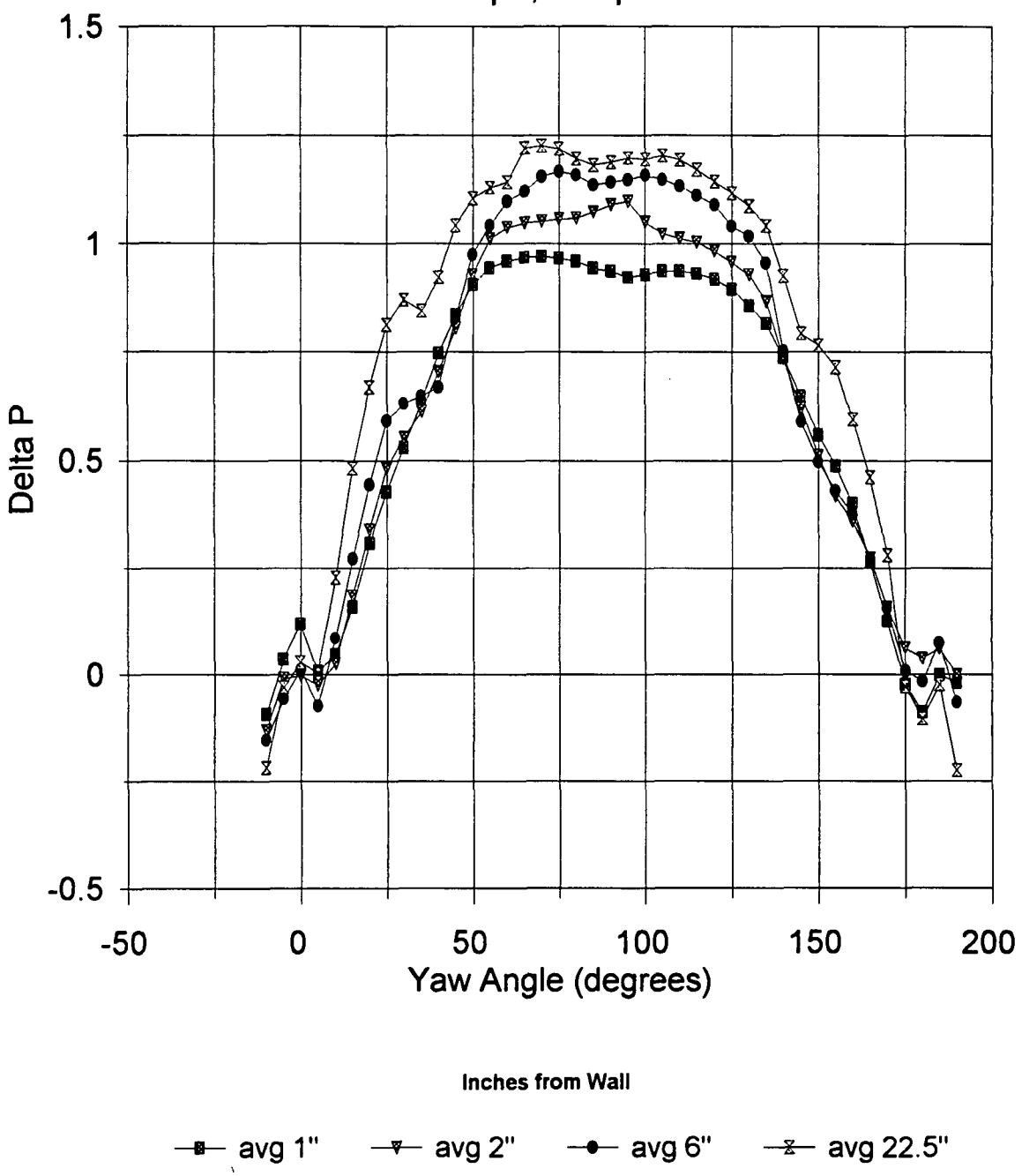

Figure 8-19.

Mod Kiel w/ Therm.: Yaw/Wall Effect

60 fps, 1" from wall, pitch= +10,0,-10 °

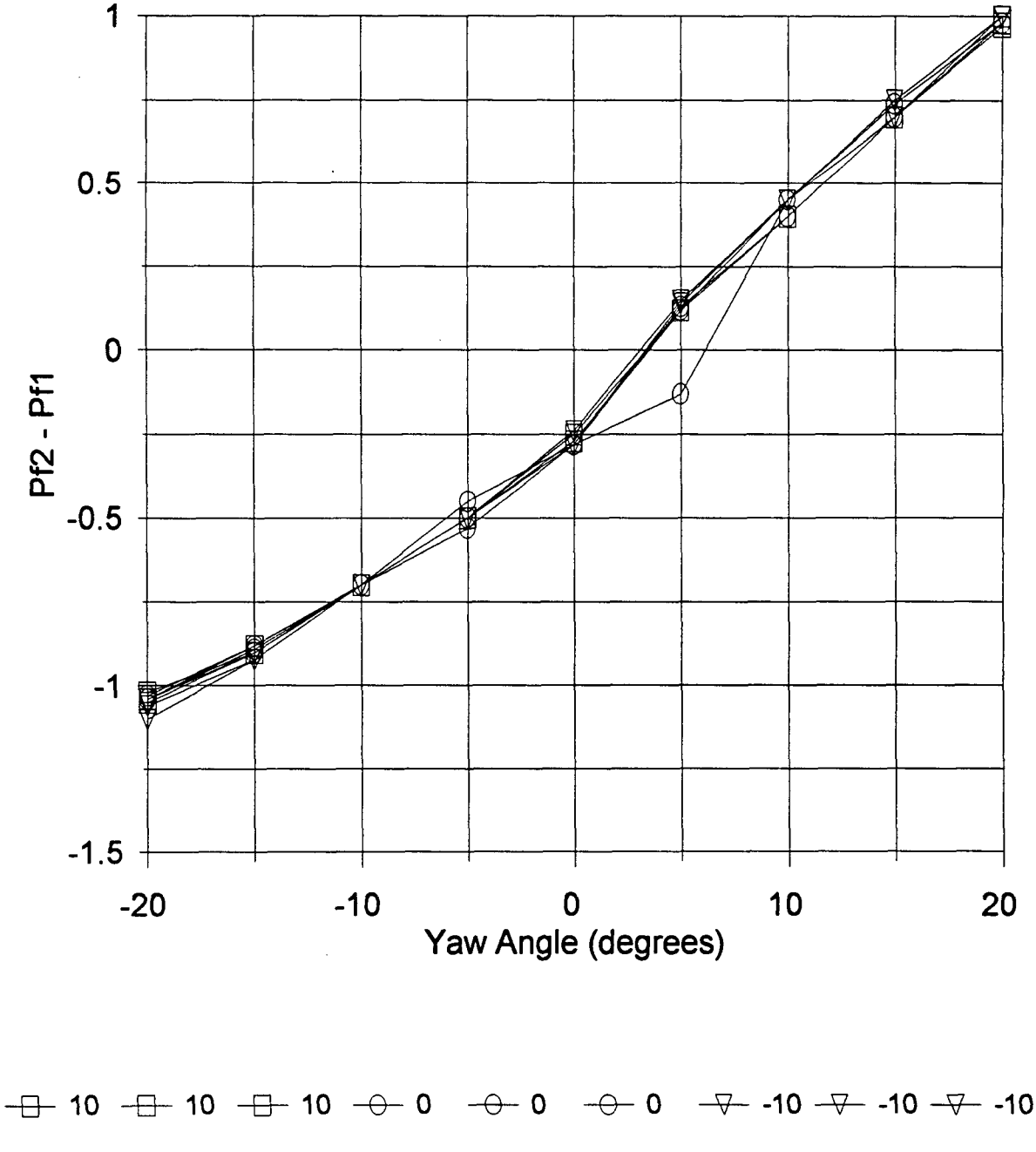

Figure 8-20.

Mod Kiel w/ Therm.: Yaw/Wall Effect

60 fps, 5" from wall, pitch= +10,0,-10 °

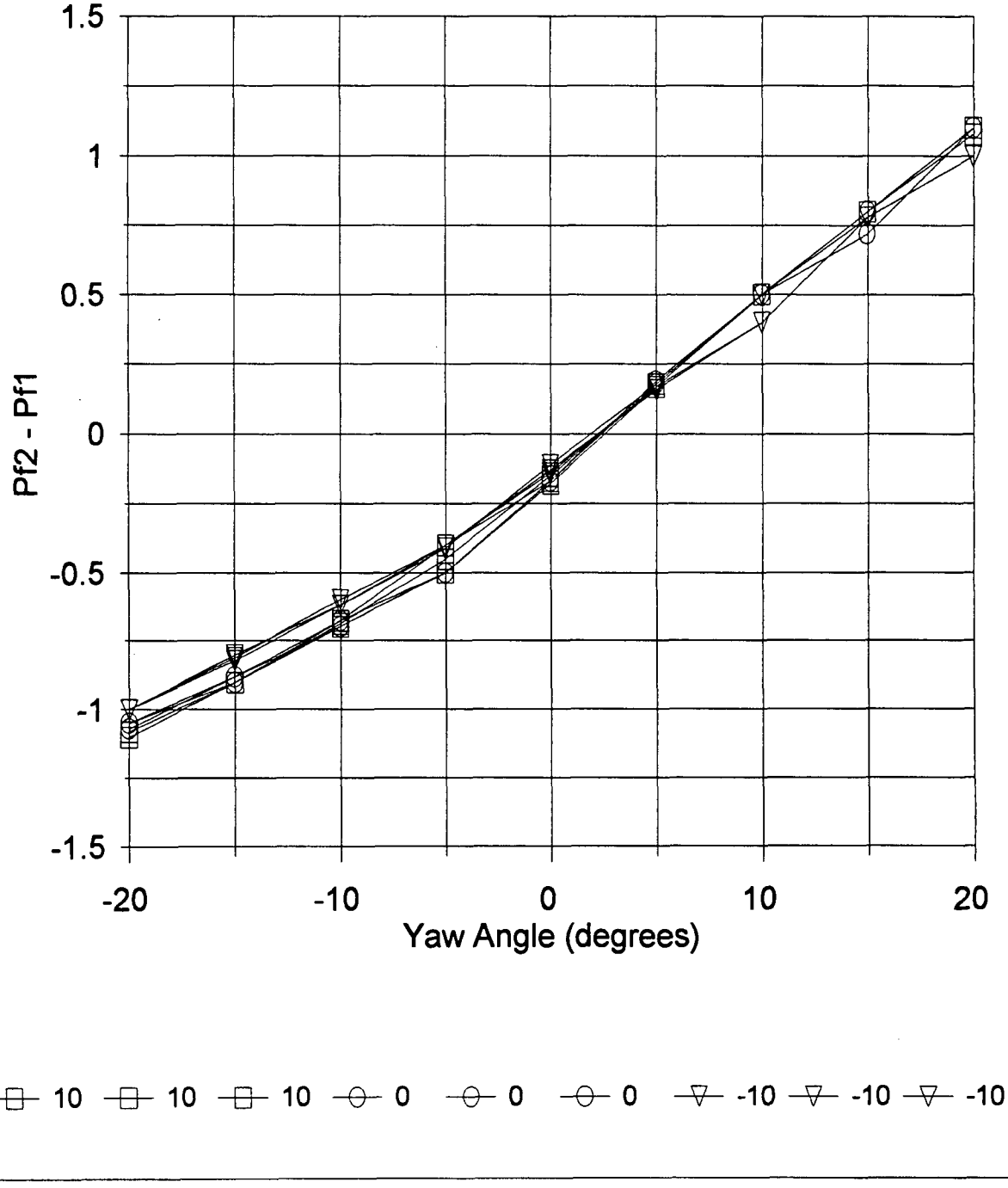

Figure 8-21.

Spherical Probe: Yaw/Wall Effect

60 fps, 0°pitch, port #1, 4" from wall

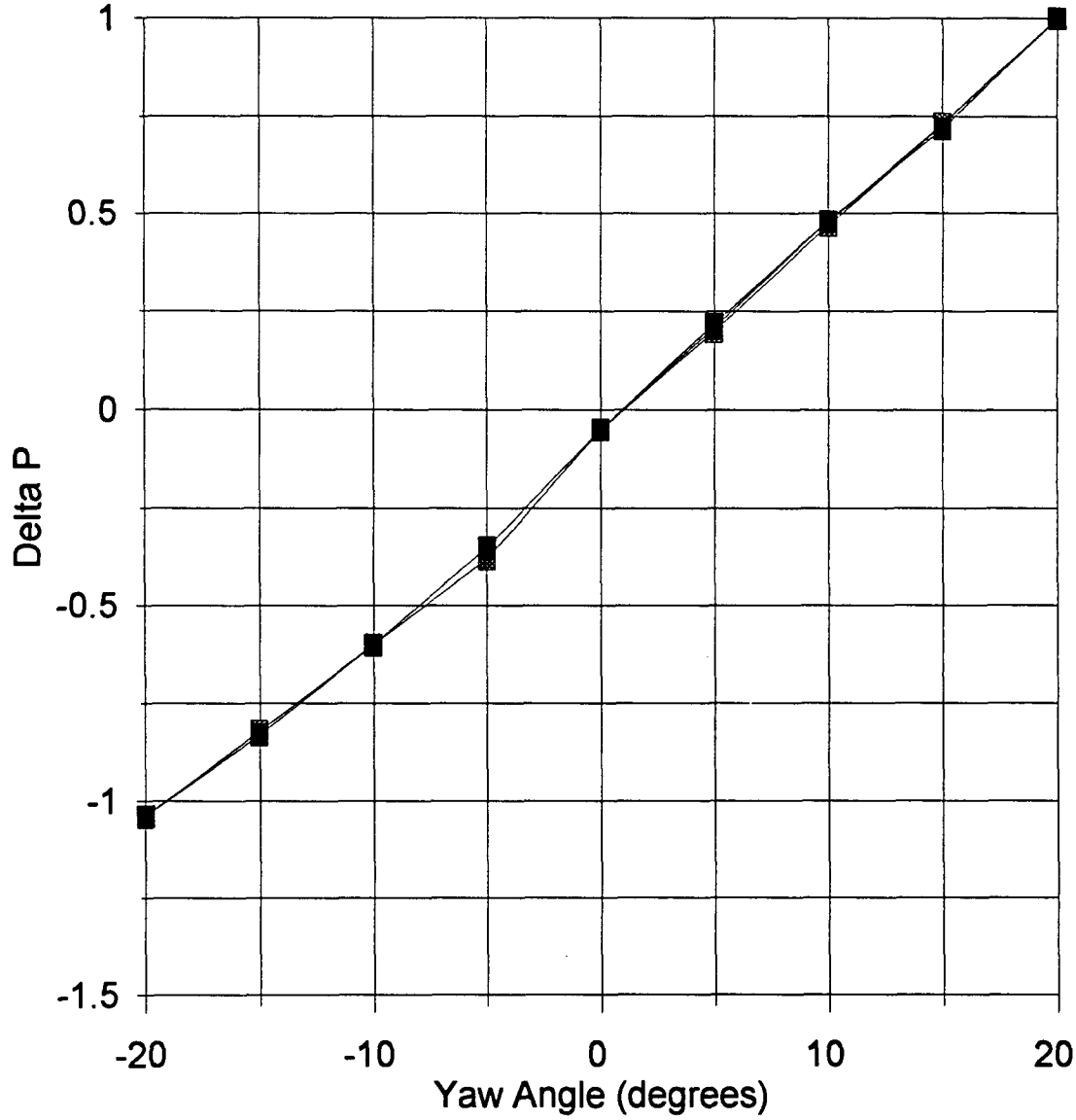

Figure 8-22.

DAT Probe: Yaw/Wall Effect

60 fps, 3" from wall, pitch= +10,-10 °

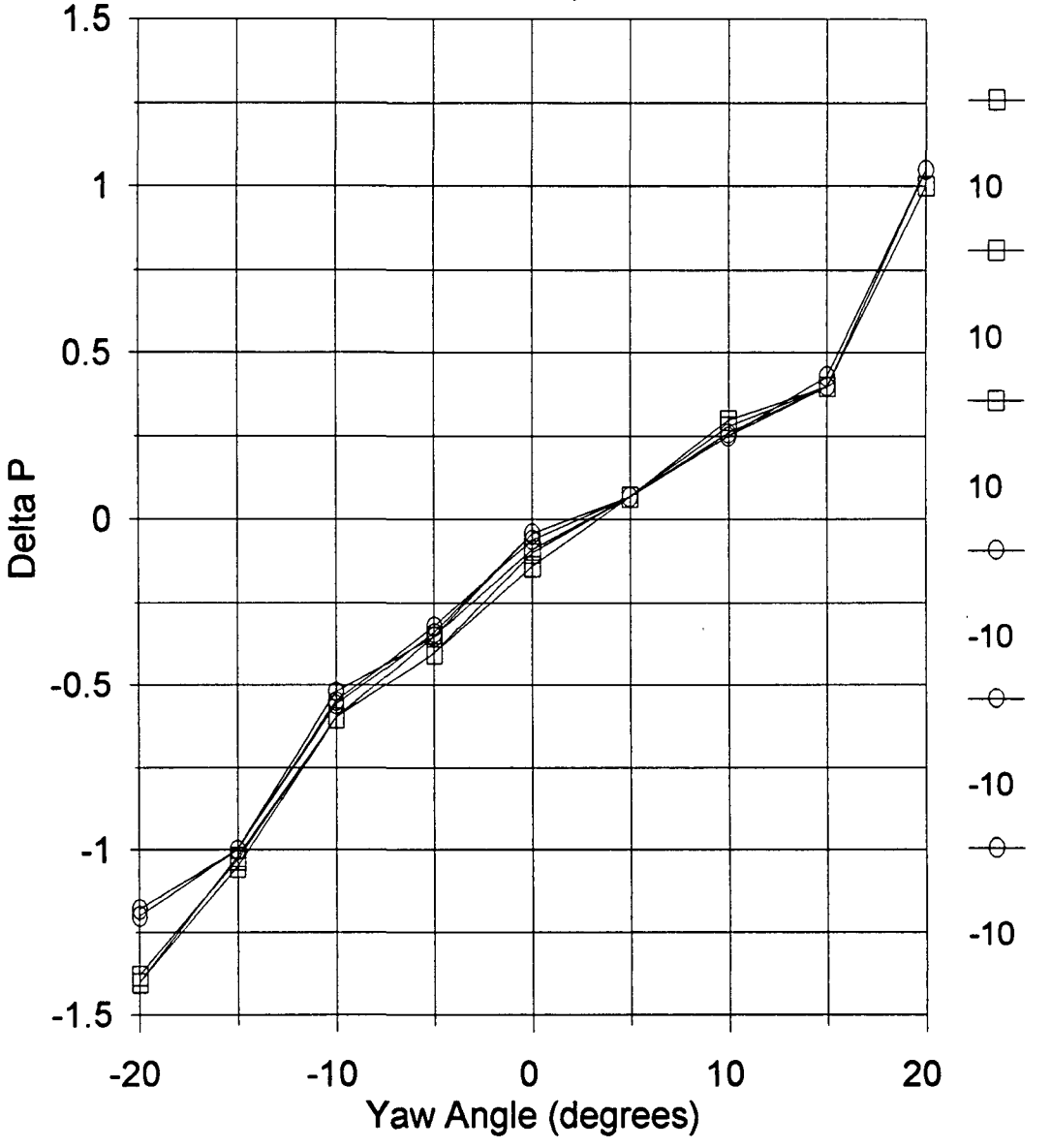

9.0 CONCLUSIONS AND RECOMMENDED FOLLOW-UP

The conclusions found in previous sections of this report are presented below, along with Cadmus' recommendations for follow-up actions that are technically justifiable based on the wind tunnel findings. The recommendations relate to both the upcoming collaborative field tests and possible revisions of EPA's test methods for volumetric flow.

MODIFIED KIEL PROBE EXPERIMENTS—SECTION 3

CONCLUSIONS

- Wake ports are too insensitive to be used for yaw nulling.
- Fechheimer ports can be used to yaw null with an accuracy of better than 1° at velocities between 40 and 90 fps and at all pitch angles in the range ±30°.
- At pitch and yaw angles equal to zero, a wake port placed between 1-3/8 inches and 3-5/8 inches from the Kiel head can be used to measure static pressure. For velocities between 40 and 90 fps, each port can be used to derive a constant calibration coefficient.
- For a wake port located 3-5/8 inches from the Kiel port, pressure drop measured by the probe is independent of pitch angle in the range ±30°; for wake ports placed closer to the Kiel head, measured pressure drop is dependent on pitch angle.
- The modified Kiel probe using wake port 4 can be used to determine total stack flow and yaw angle in the velocity range 40 to 90 fps for pitch angles in the range ±30°. The probe cannot be used to determine pitch angle.

RECOMMENDATIONS

The wind tunnel test results provide a sufficient technical basis for including the modified Kiel probe in EPA's planned collaborative study. Before including this probe in the collaborative study, however, EPA should consider performing a pre-test of the probe in a power plant stack to confirm the probe's field readiness based on a comparison of its velocity measurements with those obtained using DAT and Type S probes. If the modified Kiel probe gives plausible results relative to the DAT and Type S probes (e.g., velocity measurements lower than those of the non-nulled Type S, but higher than the DAT's), it should be included in the collaborative field study. In that case, EPA should review the results of the collaborative study to determine whether revising Test Method 2 to allow use of this probe is technically justified.

VARIABILITY OF 2D PROBE CALIBRATION COEFFICIENTS WITH VELOCITY CHANGES—SECTION 4

CONCLUSIONS

- For all probes except the manual modified S, variability in the calibration coefficients derived at individual velocity settings was low. The variability was especially low for the Autoprobes.
- As reflected in the percentage change in mean C_p and in the low coefficients of variation, the calibration coefficients for all the tested 2D probes, except for the modified S probes, are stable in the 30 to 90 fps range (40 to 90 fps for the modified Kiel probe).
- Across all velocities, the greatest variation in calibration coefficients was exhibited by the manual modified S probes, reaching as high as 7.15% across the tested range. It may be advisable to require this probe to be calibrated at a wind tunnel velocity close to the prevailing velocity where the probe will be used.
- The modified Kiel probe should not be used at velocities less than 40 fps because its calibration coefficient appears to be very sensitive to velocity changes below this level. This specific velocity cutoff applies only to the modified Kiel probe dimensions tested here; modified Kiel probes of the same design but with a different diameter and port sizes may have different velocity cutoffs.

RECOMMENDATIONS

EPA should consider revising the calibration requirements currently found in Method 2 (40 CFR Part 60, Appendix A) §4.1.2.3 to define conditions under which a probe would be required to use calibration coefficients obtained at multiple velocities. For example, such a requirement might take the following form:

Step 1: Testers would be asked to declare the
Minimum velocity (V_{min}) where the probe will be used: _____ fps
Maximum velocity (V_{max}) where the probe will be used: _____ fps

Step 2: Following the procedures in Method 2, §4.1, the tester would derive C_p^{min} and C_p^{max}, the calibration coefficient at the declared minimum and maximum velocities respectively.

Step 3: Users would then calculate the percent change in calibration coefficient (PCCC), where:

$$PCCC = \frac{C_p^{max} - C_p^{min}}{C_p^{min}} \times 100\%$$

Step 4: Users would apply the following criteria to determine the required number of cali-bration coefficients to be used:

PCCC≤ 3.0% ⇒ Use a single calibration factor determined by averaging C_p^{min} and C_p^{max}.

PCCC > 3.0% ⇒ Determine C_{p1} at the velocity (V_1) mid-way between V_{max} and V_{min}.

Determine the percent change in calibration (PCCC') between C_{p1} and C_p^{max}. If PCCC'≤ 3.0%, record C_{p1} and C_p^{max}. If PCCC' > 3.0%, determine C_{p2} for the velocity V_2 mid-way between the V_{max} and V_1. Determine the percent change in calibration (PCCC") between C_{p2} and C_p^{max} and PCCC'" between C_{p2} and C_{p1}. If either percent change is ≤ 3.0%, record the calibration coefficients and velocities. If either percent change is > 3.0%, continue generating the calibration curve until the percent change in calibration coefficients between adjacent velocities is ≤ 3.0%. Repeat these steps for the velocity interval between V_1 and V_{min}. Once the calibration table is established, the tester should use the calibration coefficient for the velocity closest to the velocity measured in the field.

Wind tunnel tests have demonstrated that calibration coefficients for the manual modified Type S probe have significantly higher variation with velocity than other 2D probes. For this reason, we recommend against including the manual modified Type S probe in the field tests. We do, however, recommend including the Autoprobe modified S probe in the field tests.

If the results of the preliminary field tests conducted with the modified Kiel probe lead to the inclusion of this probe in the planned collaborative tests, the four modified Kiel probes that will be used should be calibrated in the wind tunnel at velocities between 10 and 90 fps, to determine if there should be a low-velocity cutoff for use of this probe.

PITCH ANGLE EFFECTS ON VELOCITY MEASUREMENTS PERFORMED WITH 2D PROBES—SECTION 5

CONCLUSIONS

Calibration Coefficients

- The calibration coefficients of all probes, except the Type S and French, were stable to within 3.5% in the -10° to 20° pitch range.
- None of the probes, except the modified Kiel, maintained a stable calibration coefficient in the -30° to -10° pitch range.

Velocity Determinations

- In the ±10° pitch-angle range, no single probe excelled under all velocity conditions. Maximum deviations from axial velocity ranged from +3.5% for the Autoprobe operated with a modified S pitot head to +7.3% for the French probe.
- In the ±10° pitch-angle range at the higher tested velocities (60 and 90 fps), all probes except the French measured velocities that were less than or equal to 4.9% of the axial velocity. The modified Kiel had the lowest deviation at -2.2%.
- In the ±20° pitch angle range, across all velocities tested, none of the tested 2D probes kept deviations from actual axial flow within ±5%.
- In the ±20° pitch angle range over all velocities, the manual Type S had the smallest maximum deviation (-6.7%) and the smallest maximum overestimation (+5.2%). At 60 and 90 fps, the maximum deviation for the manual Type S probe (-5.5%) was also lowest of all tested probes.
- At negative pitch angles, the manual Type S probe always underestimated true axial velocity—the more negative the pitch, the larger the underestimate.

RECOMMENDATIONS

In revisions to Method 2, EPA should consider limiting the use of 2D probes to specific pitch ranges, even if yaw nulling procedures for 2D probes are included in the revised test method. Pitch-angle range restrictions would require sources either to (a) explicitly determine the extent of pitch in a stack (e.g., by performing a pre-test 3D traverse) or (b) demonstrate by some other means that flow is within stipulated pitch-angle limits.

The wind-tunnel tests suggest that, for all 2D probes except the French probe, the acceptable pitch-angle range should be restricted to 0° to +10°. The manual Type S and modified Kiel probes gave consistently low velocity measurements between 0° and -10° pitch. At pitch angles of 10° and greater and velocities of 60 and 90 fps, all probes gave consistently high measurements. If allowed at all, use of the French probe should be restricted to situations where pitch angles are essentially 0°.

The collaborative field tests should be designed to provide additional data on how pitch angle affects the accuracy of velocity measurements.

ACCURACY OF YAW ANGLE MEASUREMENTS AND EFFECT ON VELOCITY MEASUREMENT—SECTION 6

CONCLUSIONS

- Use of Fechheimer ports produces consistently better yaw angle measurements than other procedures for measuring yaw angles.
- In the wind tunnel, the manually operated Type S probe gave yaw null and velocity accuracy results comparable to those of the probes employing Fechheimer ports.
- The maximum yaw angle error using the Autoprobe[1] was higher than the maximum errors produced by either the manually operated Type S probe or any of the manually operated probes that employ Fechheimer ports.
- Among the manually operated probes, the largest error in yaw angle measurements was produced by the modified S probe: 6.6°. Similarly, the largest error with the Autoprobe was produced using the modified S probe head: 5.4°.

RECOMMENDATIONS

In revising Method 2, EPA should consider allowing yaw nulling of 2D probes for determining axial velocities. The method should stipulate that a probe to be used in the field with yaw nulling must be calibrated in a wind tunnel. Such a calibration procedure should involve rotating the probe to find a yaw null ($\Delta P = 0$) and recording angle relative to true yaw = 0°. The absolute difference between the rotational position reached after yaw nulling and true 0° yaw would have to be less than or equal to some standard (e.g., 5°). This standard would have to be met over the range of allowable pitch angles in 5° increments. If the absolute difference exceeded the standard (e.g., 5°) at any pitch setting, the yaw nulling procedure would not be usable with the tested probe.

EPA should consider re-testing the yaw nulling capabilities of the Autoprobe Type S and Autoprobe Modified S with the curve-fitting algorithm currently employed by the manufacturer.

[1] As noted in Section 6, the Autoprobe in this study employed a "sweep" procedure to determine the yaw null rather than the curve-fitting algorithm subsequently implemented by the manufacturer.

CALIBRATION CURVES AND ACCURACY OF VELOCITY DETERMINATIONS FOR 3D PROBES— SECTION 7

CONCLUSIONS

- Over the pitch angle ranges ±30° and ±20°, the velocity accuracy of all tested 3D probes was within 5.5% of the true axial velocity. In the ±10° pitch angle range, the velocity accuracy of all tested 3D probes was within 3.8% of the true axial velocity.
- No significant gain in accuracy is attained by developing calibration curves at three velocities rather than at the two specified in draft Method 2F.
- In order to minimize error in the flue gas velocity measurement, calibration curves for 3D probes should be developed at velocity settings close to, or possibly bracketing, the prevailing velocity where the probe will be used.
- The largest error in measuring pitch angle for all four probes was 4.3°, which occurred at 90 fps and -20° pitch and produced a velocity error of 0.3%.

RECOMMENDATIONS

To investigate the third conclusion (above) further, EPA should consider deriving two alternative sets of calibration curves for each DAT and spherical probe used in the collaborative field tests. The first set of calibration curves would be derived for the velocity ranges specified in draft Test Method 2F; the second set would be derived at wind tunnel velocities that bracket the velocity(ies) found in the field. (EPA may want to define bracketing ranges to be within ± 20 fps of the prevailing velocity.) The resulting velocities and volumetric flow rates using each set of curves would then be compared.

A previous study [2] noted that scratches on the head of a spherical probe can significantly alter the pitch angle calibration characteristics of that probe. EPA should consider designing and conducting wind-tunnel tests to assess the impact of scratches on spherical probe heads on the accuracy of pitch angle and velocity measurements.

[2] Klinge, M.D. 1987. *Detailed Near-Wake Flowfield Surveys and Comparison to an Euler Method of an Aspect Ratio 4 Rectangular Wing*. M.S. Thesis, Mechanical and Aerospace Engineering Department, North Carolina State University, Raleigh..

ENTRY WALL EFFECTS ON YAW NULLING—SECTION 8

CONCLUSIONS

- In a laminar-flow wind tunnel, three yaw nulls are observed at wall entry distances of up to about 9" using a Type S probe. The center yaw null is found within 1° of the true yaw zero.
- At entry wall distances greater than about 9", unique yaw nulls are found with the manual Type S probe.
- Multiple yaw nulls are found with the Autoprobe Type S at all distances from the wind tunnel center line. A "pseudo-entry wall effect" appears to be associated with the Autoprobe.
- At distances near the entry wall, unique yaw nulls are found with all probes that use Fechheimer-type ports to determine the yaw angle: the modified Kiel, spherical, and DAT.

RECOMMENDATIONS

In should be noted that probes that detect multiple yaw nulls near the entry wall in a controlled environment such as a wind tunnel may not exhibit the same behavior under field conditions, where the increased variability of the gas stream may prevent the occurrence of this behavior. Field test data should be observed to see whether this is the case. Therefore, we recommend the following:

- In the collaborative field tests, EPA should observe whether multiple yaw nulls occur near the entry wall when using 2D probes.
- In the collaborative field tests, EPA should observe whether the Autoprobe Type S and Autoprobe modified S produce multiple yaw nulls away from the entry wall due to the postulated "pseudo-entry wall effect."